

MOLECULAR REGULATION OF ZEBRAFISH CARDIAC MATURATION

Leigh Ann Samsa

A dissertation submitted to the faculty at the University of North Carolina at Chapel Hill in partial fulfillment of the requirements for the degree of Doctor of Philosophy in the Department of Cell Biology and Physiology in the School of Medicine (Cell and Molecular Physiology).

Chapel Hill
2016

Approved by:

Jiandong Liu

Kathleen M. Caron

Andrew C. Dudley

James E. Faber

Victoria L. Bautch

Franklin L. Conlon

© 2016
Leigh Ann Samsa
ALL RIGHTS RESERVED

ABSTRACT

Leigh Ann Samsa: Molecular Regulation of Zebrafish Cardiac Maturation
(Under the direction of Jiandong Liu)

Congenital heart diseases (CHDs) are the most common type of human birth defect and often feature structural abnormalities that arise during development and maturation. Many CHDs have a genetic component which provides a molecular basis for the cellular defects underlying structural malformations. During embryonic development, the vertebrate heart expands and remodels to meet the cardiovascular needs of the developing embryo in a process called cardiac maturation. In particular, the ventricular chamber matures to optimize the internal architecture for efficient conduction and contraction. Chamber maturation features formation of luminal muscular protrusions, called trabeculae, which increase myocardial mass and are often malformed in CHD. Here, zebrafish (*Danio rerio*) are used as an optically accessible, genetically tractable, vertebrate model to explore the conserved, molecular basis of chamber maturation

Accumulating evidence indicates a critical role for cardiac contraction and the resulting fluid forces in shaping the developing heart, yet the molecular basis of this function is largely unknown. Data reported in Chapter 2 describe an essential role for cardiac contraction-responsive transcriptional changes in endocardial cells for regulating trabeculation. Cardiac contraction causes blood flow, which is likely mechanotransduced into intracellular signaling cues by endocardial primary cilia. Contraction stimulates *notch1b* transcription, and Notch1 activation induces expression of downstream genes *ephrinb2a* (*efnb2a*) and *neuregulin-1* (*nrg1*) in the endocardium. Forced Notch activation rescues *efnb2a* and *nrg1* expression in non-contractile hearts, and *efnb2a* is essential for trabeculation.

Although ErbB2 receptor tyrosine-protein (ErbB2), an essential receptor partner in the Nrg1-ErbB2/ErbB4 signaling pathway, is necessary to stimulate trabeculation in mice and zebrafish, requirement for *nrg1* has not been explored in zebrafish. In Chapter 3, CRISPR/Cas9 targeted gene editing was used to generate novel, isoform-specific mutations in *nrg1*. Phenotypic analysis of *nrg1* mutants revealed that *nrg1* is dispensable for cardiac trabeculation. However, one isoform, *nrg1-III* is

essential for establishing the cardiac nerve plexus. Likely as a consequence of impaired cardiac innervation, *nrg1* mutants have cardiac malformations and experience early mortality.

In sum, this study reveals previously uncharacterized cellular and molecular relationships regulating chamber maturation.

ACKNOWLEDGEMENTS

This dissertation would not be possible without the institutional support provided by UNC-Chapel Hill and the countless efforts of my mentors, committee, collaborators, colleagues, family, and friends.

There is simply not enough space to convey the depth and breadth of my gratitude to the people and organizations who have contributed to my success. I considered making a chart to categorize these contributions, but that seemed a little dispassionate, even for me. Instead, I sketched a schematic illustrating the interrelationships between the groups and individuals who have lent me support. Unfortunately, formatting constraints restricted its inclusion of such a schematic. That said, and with apologies for the inadequacy of this list, I would like to acknowledge my funding sources through the NIH to the BBSP and IVB training programs. I am grateful to the University of North Carolina at Chapel Hill for providing the infrastructure and core facilities essential for the work described in this dissertation including the Michael Hooker and Olympus Imaging Centers and the Zebrafish Aquaculture Core. I am incredibly grateful to the Department of Cell Biology and Physiology (CBP) for being my home for the past 5 years. It has been a wonderfully supportive place to train and grow, and I am particularly grateful to Michael Goy and Carol Otey for their guidance and perspectives. I would like to thank my first graduate mentor, Arjun Deb, for providing a firm foundation in conducting logical, rigorous science. I am grateful to my current mentor, Jiandong Liu for his constant support and opportunities for growth, and I have truly enjoyed working with incredible labmates on the Jiandong Liu and Li Qian team. Furthermore, would like to thank my current and former committee members, Kathleen Caron, Vicki Bautch, Drew Dudley, Eleni Tzima, James Faber, and Frank Conlon for their guidance throughout the progression of this dissertation.

None of this would be possible without the constant support of my friends, both for selflessly lending their academic expertise and for being amazing people to get to know. I would like to thank my wonderful partner, JR Roland for his unwavering support over the last decade...and for never acting happy when I stay that extra hour (or two) in lab! Above it all, I am particularly grateful to my family for their constant support and an upbringing encouraging curiosity, questioning, and an ambitious mindset.

PREFACE

Chapter 1

The contents of Chapter 1 are derived from two review articles that I wrote while completing graduate studies in Dr. Jiandong Liu's laboratory. Please note that figures and text have been reproduced and reformatted with permission from the publishers.

"Embryonic Chamber Maturation," was published online May 29, 2013 in the American Journal of Medical Genetics Part C: Seminars in Medical Genetics (Samsa et al., 2013). This article provides a broad overview of the gross morphological changes that occur during chamber maturation and the molecular mechanisms that regulate these events in vertebrates. As lead author, I wrote and revised the document and generated figures. Betsy Yang contributed to writing the manuscript. Jiandong Liu, Ph.D revised the manuscript.

"Advances in the study of heart development and disease using zebrafish," was published online April 9, 2016 in the Journal of Cardiovascular Development and Disease (JCDD) (Brown et al., 2016). This article is a detailed report on how zebrafish are used, historically and currently, as a model system to study heart development and disease. Daniel Brown, Ph.D conceptualized and wrote the manuscript. As second author, I contributed sections of written content, generated figures and revised the text. Li Qian, Ph.D and Jiandong Liu, Ph.D conceptualized and revised the manuscript. Though the majority of this review is not germane to this dissertation, the full text is accessible in an open access format, and the sections included in Chapter 1 are primarily my work. These sections provide important background information for Chapters 2 and 3 and are reproduced as Chapter 1.2, below.

Chapter 2

Chapter 2.2 was published in *Development* on December 1, 2015 (Samsa et al., 2015), where it was highlighted by the editor as a featured article. In this study, we explored the relationship between hemodynamic forces caused by cardiac contraction, cell signaling, and cardiac trabeculation. Our data supports a model in which the beating heart initiates blood flow, which is in turn detected by primary cilia

on endocardial cells, stimulating *notch1b* and downstream signaling components essential for initiating cardiac trabeculation. Prior to this work, little was known about these relationships in the zebrafish heart, and this work represents the most comprehensive assessment of molecular epistasis regulating zebrafish trabeculation.

The study was a combined effort in which I designed and performed the majority of experiments, analyzed data and wrote the manuscript. Chris Givens designed and assisted with the *in vitro* flow experiment. Eleni Tzima, Ph.D, Didier Stainier, Ph.D, and Li Qian, Ph.D provided intellectual input and supervised the work. Jiandong Liu, Ph.D additionally designed and performed experiments, analyzed data and revised the manuscript. All authors commented on the manuscript.

Chapter 2.2 has been modified from its original version to conform to formatting standards. All figures that were previously reported in online-only supplemental materials have been reproduced in this work. Additionally, the in-text and online-only methods have been combined into a single section. Chapter 2.3 highlights the significance of Chapter 2.2 and discusses future directions.

Chapter 3

Previous work by Dr. Liu, while in Dr. Didier Stainier's lab at the University of California at San Francisco, revealed an essential role for ErbB2 in zebrafish cardiac trabeculation (Liu et al., 2010), but the cardiac function of its primary ligand, Neuregulin 1 (Nrg1) has not been explored. Based on our pilot studies and historical reports from in mammalian systems (Kramer et al., 1996; Lee et al., 1995; Meyer and Birchmeier, 1995), we anticipated that Nrg1 would play a clear role in regulating cardiovascular development, including mediating formation and spatial distribution of cardiac trabeculae. Zebrafish *nrg1* is alternative spliced to form three main isoforms, *nrg1-I*, *nrg1-II*, and *nrg1-III*, which differ primarily in their N-terminal domains. Our studies strongly suggested *nrg1-I* is the only isoform expressed in the heart during trabeculation, and blocking *nrg1-I* splicing with a morpholino led to dramatic cardiovascular phenotypes. So, we used CRISPR/Cas9 gene editing to target *nrg1* and produce alleles coding for frame-shifts mutations in all *nrg1* isoforms or *nrg1-I* and *nrg1-II* isoforms only. In Chapter 3.2, we characterize the phenotypes of our novel mutants in comparison to a previously published mutant that lacks functional *nrg1-III* (Perlin et al., 2011). Our study reveals that Nrg1 is completely dispensable for trabeculation.

However, it plays an essential role in development of the cardiac nerve plexus, which has later life consequences in zebrafish.

Chapter 3.2 is a manuscript in preparation and a combined effort of myself and co-authors. I generated and validated all the novel mutant lines included in the study, designed experiments, analyzed data, and have drafted the manuscript. While I produced the majority of data reported in this document, this study is being completed by Daniel Brown, Ph.D as a co-first author, whose contributions include designing experiments (included in this work and in progress), analyzing data, and manuscript revisions. Other author contributions include data collection and technical assistance from Cade Ito, expected data collection and analysis from Hong Ma, as well as intellectual input, supervision, and manuscript commentaries from Li Qian, Ph.D and Jiandong Liu, Ph.D. We expect to submit for publication in late 2016 or early 2017.

Please note that, due to high redundancy between chapters, all literature cited has been compiled into a single Reference list.

TABLE OF CONTENTS

LIST OF TABLES	xi
LIST OF FIGURES.....	xii
LIST OF ABBREVIATIONS.....	xiv
CHAPTER 1 INTRODUCTION	1
1.1 Embryonic Cardiac Chamber Maturation: Trabeculation, Conduction and Cardiomyocyte Proliferation	1
Introduction	1
Embryonic chamber maturation	3
Biomechanical forces in cardiac wall maturation	12
New areas for investigation.....	13
Chapter 1.1 Figures	15
1.2 Advances in the Study of Heart Development and Disease Using Zebrafish.....	19
Introduction	19
Modeling cardiovascular development and disease in zebrafish	19
Cardiovascular development in zebrafish	20
Zebrafish cardiac morphogenesis.....	20
Chapter 1.2 Figures	24
CHAPTER 2 CARDIAC CONTRACTION ACTIVATES ENDOCARDIAL NOTCH SIGNALING TO MODULATE CHAMBER MATURATION	27
2.1 Historical Context	27
2.2 Cardiac Contraction Activates Endocardial Notch Signaling to Modulate Chamber Maturation	28
Introduction	28
Results	30
Discussion.....	37

Materials and methods.....	40
Chapter 2.2 Figures	45
2.3 Significance and Future Directions	73
Significance.....	73
Future directions	73
CHAPTER 3 ISOFORM-SPECIFIC MUTAGENESIS INDICATES MULTIPLE ROLES FOR NEUREGULIN 1 IN ZEBRAFISH CARDIAC MATURATION	80
3.1 Historical Context	80
3.2 Isoform-Specific Mutagenesis Indicates Multiple Roles for Neuregulin-1 in Zebrafish Cardiac Maturation	82
Introduction	82
Results	83
Discussion and future directions	89
Conclusions.....	94
Materials and methods.....	95
Chapter 3.2 Figures	99
3.3 Significance and Additional Interpretations.....	121
Significance.....	121
Additional interpretations.....	121
CHAPTER 4 CONCLUSIONS.....	125
Insights into zebrafish chamber maturation	125
Insights into congenital heart disease modeling	126
REFERENCES.....	129

LIST OF TABLES

Table 1 Chapter 2 Morpholino validation	71
Table 2 Chapter 2 Oligonucleotide sequences	72
Table 3 Chapter 3 Oligonucleotide Sequences	120

LIST OF FIGURES

Figure 1 Cardiac chamber maturation	15
Figure 2 Signaling pathways in cardiac chamber maturation	17
Figure 3 Biomechanical forces in cardiac wall maturation.....	18
Figure 4 Zebrafish model system.....	24
Figure 5 Zebrafish heart development	26
Figure 6 Cardiac contraction is required for myocardial trabeculation	45
Figure 7 Verapamil treated embryos do not form trabeculae	46
Figure 8 Cardiac contraction is required for endocardial Notch activation and <i>notch1b</i> transcription.....	47
Figure 9 Notch signaling is not active in the hearts of blebbistatin treated embryos.....	48
Figure 10 Notch activation in the ventricular endocardium.....	49
Figure 11 Notch activation at 4 weeks post-fertilization.....	50
Figure 12 Notch activation in the developing endocardium is not inhibited by PTK787	51
Figure 13 <i>Notch1b</i> and <i>efnb2a</i> splice blocking MO gene expression quantification	53
Figure 14 Cardiac contraction promotes trabeculation through <i>notch1b/efnb2a/nrg1</i> epistasis	54
Figure 15 Trabeculation in <i>mib1</i> mutant embryos.....	55
Figure 16 Gene expression at 48hpf.....	56
Figure 17 Notch activation pattern in <i>efnb2a</i> morphants	57
Figure 18 Notch1 activation rescues <i>efnb2a</i> and <i>nrg1</i> expression in non-contractile hearts	58
Figure 19 Primary cilia are detectable in myocardium and endocardium	60
Figure 20 Shear stress promotes <i>notch1</i> expression in a primary-cilia dependent manner	61
Figure 21 Control and <i>tnnt2a</i> morphants have endocardial primary cilia	63
Figure 22 Ciliobrevin D treatment within a short time window prevents Notch activation	64
Figure 23 Cyclopamine treatment does not inhibit Notch activation in the endocardium	65
Figure 24 Reducing shear stress or retrograde flow fraction via <i>gata1a</i> , <i>gata2a</i> , and <i>gata1a/2a</i> knockdown does not prevent Notch activation or trabeculation	66
Figure 25 <i>Klf2</i> expression in MLECs after 1 and 4 hrs flow.....	68

Figure 26 Notch activation requires <i>klf2a</i>	69
Figure 27 Cardiac contraction activates endocardial Notch signaling in a primary cilia-dependent manner to regulate trabeculation.....	70
Figure 28 Zebrafish neuregulin 1	99
Figure 29 Cross-species comparison Nrg1.....	102
Figure 30 Nrg1 alleles	104
Figure 31 Predicted translations Nrg1-I mutant alleles.....	105
Figure 32 Supernumerary neuromasts in Nrg1-III deficient mutants.....	106
Figure 33 Nrg1 mutants require ErbB2 tyrosine kinase activity to form trabeculae.....	107
Figure 34 Adult <i>nrg1^{nc28}</i> mutant phenotype.....	108
Figure 35 Survival and gross phenotype of <i>nrg1</i> mutants	109
Figure 36 Gross phenotype of <i>nrg1-III</i> -deficient mutants	110
Figure 37 Ventricle surface innervation defect emerges in juvenile stage	111
Figure 38 Reduced surface innervation in Nrg1-III-deficient hearts	113
Figure 39 Innervation in the myocardial wall.....	115
Figure 40 Peri-mortem cardiac morphology of <i>nrg1^{nc26}</i> fish.....	116
Figure 41 Altered cardiac morphology in <i>nrg1^{nc26}</i> mutants	117
Figure 42 Compact myocardial wall derangements.....	118
Figure 43 Model	119

LIST OF ABBREVIATIONS

A	Atrium
AVC	Atrio-Ventricular Canal
BA	Bulbous Arteriosus
<i>btc</i>	<i>betacellulin</i>
CBD	Ciliobrevin D
CHD	Congenital Heart Disease
CRD	Cysteine Rich Domain
CRISPR/Cas9	Clustered regularly interspaced short palindromic repeats associated / CRISPR associated protein 9
dpf	Days post-fertilization
<i>efnb2</i>	<i>ephrin-B2</i>
EGF	Epidermal Growth Factor
<i>erb2</i>	<i>erb-b2 receptor tyrosine kinase 2</i>
ERBB2/4	ERBB2 and ERBB4 heterodimer
<i>erb4</i>	<i>erb-b2 receptor tyrosine kinase 4</i>
FACS	Fluorescence Activated cell Sorting
H&E	Hematoxylin and Eosin
hpf	Hours post-fertilization
<i>ift88</i>	<i>intraflagellar transport protein 88</i>
IgG	Immunoglobulin-like domain
<i>kdr</i>	<i>vascular endothelial growth factor receptor kdr-like; vegfr2</i>
<i>klf2a</i>	<i>krüppel-like factor 2</i>
MO	Morpholino
mpf	Months post-fertilization
<i>myl7</i>	<i>myosin light chain 7, regulatory</i>
NICD	Notch1 Intracellular Domain
<i>nrg1</i>	<i>neuregulin-1</i>
SL	Standard Length (mm) from snout to caudal peduncle

TM	Transmembrane
<i>tnnt2a</i>	<i>troponin T type 2a (cardiac)</i>
V	Ventricle
wpf	Weeks post fertilization

CHAPTER 1 INTRODUCTION

1.1 Embryonic Cardiac Chamber Maturation: Trabeculation, Conduction and Cardiomyocyte Proliferation¹

Introduction

Cardiovascular malformation is one of the leading causes of human birth defects (Parker et al., 2010), and cardiovascular diseases are the number one cause of adult morbidity and mortality in the developed world (Go et al., 2013). During development, in order to increase cardiac output, the vertebrate embryonic heart undergoes a series of complex morphogenic processes known collectively as cardiac chamber maturation. Alterations in these processes are linked to many cardiac diseases such as non-compaction cardiomyopathy (also known as hypertrabeculation), diastolic dysfunction, and arrhythmias (Teekakirikul et al., 2013). Monogenic alterations that lead to human congenital heart defects have been valuable in identifying key regulators of heart development (Teekakirikul et al., 2013). Yet, these rare mutations do not explain the heterogeneity in cardiovascular defects observed clinically in both children and adults. Clearly, genetic mutations that completely impair heart development do not appear clinically. Advancements in our understanding of the mechanisms that govern cardiac chamber maturation and patient-specific genetic information are necessary for developing improved and personalized therapeutics for these congenital defects. In this review, we present evidence that collectively suggest a wide range of signaling pathways are involved in orchestrating cardiac chamber maturation.

Left ventricular non-compaction

One of the most widely recognized disorders of cardiac maturation is left ventricular non-compaction (LVNC) (Jenni et al., 2007). LVNC is characterized by prominent trabeculae and large recesses/sinuses between trabeculae (Jenni et al., 2001; Stollberger and Finsterer, 2004). Patients with LVNC may be symptomatic or asymptomatic, and LVNC leads to heart failure, thromboembolic events,

¹ This chapter previously appeared in the American Journal of Medical Genetics Part C: Seminars in Medical Genetics. The original citation is as follows: Samsa, L. A., Yang, B., and Liu, J. (2013) Embryonic cardiac chamber maturation: Trabeculation, conduction, and cardiomyocyte proliferation. *Am. J. Med. Genet. C. Semin. Med. Genet.* 163C, 157-168.

arrhythmias and/or sudden cardiac death (Bhatia et al., 2011; Ichida et al., 1999; Paterick and Tajik, 2012). LVNC can occur as an isolated disease (called isolated left ventricular non-compaction or ILVNC) or in conjunction with other congenital defects (Peters et al., 2012; Stanton et al., 2009), suggesting multiple etiologies for LVNC. Due in large part to variable diagnostic criteria (Paterick and Tajik, 2012; Thavendiranathan et al., 2013), the true burden of LVNC is unknown, but is estimated to be 0.014–1.3% of children referred to echocardiography laboratories (Oechslin et al., 2000).

The morphology of LVNC hearts closely resembles early embryonic hearts. Because of this resemblance, frequent comorbidity with other congenital cardiac malformations, and prevalence in infants, LVNC is widely considered to be caused by the embryonic arrest of cardiac wall maturation (Angelini et al., 1999; Chin et al., 1990; Sedmera et al., 2000). However, this hypothesis has been challenged recently (Ichida et al., 1999) given the identification of LVNC in adults (Murphy et al., 2005; Oechslin et al., 2000; Stollberger and Finsterer, 2004) and observation that some of the morphological features of LVNC are distinct from the embryonic heart (Stanton et al., 2009; Wessels and Sedmera, 2003). Nevertheless, whether LVNC is strictly congenital, acquired, or some combination of the two, there is a clear genetic component to LVNC (Oechslin and Jenni, 2011; Teekakirikul et al., 2013). Indeed, the American Heart Association classifies LVNC as a genetic cardiomyopathy (Maron et al., 2006). LVNC is associated with mutations in sarcomere-encoding genes, calcium handling genes, genes that encode proteins of the dystrophin-associated glycoprotein complex (DTNA), nuclear lamina, Nkx2.5 and with mutations that cause compromised mitochondrial function [reviewed in (Teekakirikul et al., 2013)]. Although the genetic studies of LVNC and other trabecular disorders have identified some genes associated with LVNC, we know little about how mutations in these genes lead to altered cardiac morphogenesis.

Basic research in cardiac chamber maturation biology

Over the past 2 decades, though we have seen substantial progress in our understanding of the formation of the cardiovascular system, improvements in this understanding are necessary to develop therapies for non-compaction/trabecular diseases. Much of our understanding of cardiac ontology is derived from study of human, mouse, and chicken embryos. However, direct observation of heart development is limited in these organisms. The zebrafish (*Danio rerio*) has recently emerged as a

powerful vertebrate model organism for studying early heart development (Beis and Stainier, 2006; Liu and Stainier, 2012). The zebrafish heart is simpler than that of higher vertebrates, but recapitulates early cardiac development. Moreover, accumulating evidence suggests that genes responsible for essential steps of cardiovascular development and morphogenesis are conserved throughout vertebrates (Moorman and Christoffels, 2003). Unlike the mouse or chicken, the zebrafish embryo develops entirely externally, and the transparency of the embryos enables direct, non-invasive observation of heart development at a cellular resolution. External development also makes it highly accessible for forward genetic approaches and for screening drug targets. Zebrafish embryos are particularly useful for studying developmental cardiac defects because they do not initially require a functioning cardiovascular system. Since their early oxygen needs can be met by passive diffusion, phenotypes that are lethal in other model systems can be studied in greater detail in zebrafish. In addition, technologies for creating zebrafish knockout, transgenic, and reporter lines are readily available.

Embryonic chamber maturation

During development, in order to increase cardiac output, the vertebrate embryonic heart undergoes a series of complex morphogenic changes known collectively as cardiac chamber maturation. The early embryonic heart is a smooth, two-layered linear heart tube composed of a luminal endocardial endothelial layer and an immature myocardial layer (Fig. 1A). This tube later undergoes extensive growth and topological remodeling to generate the mature vertebrate heart. Though the ultimate cardiac wall topology is somewhat different between cardiac chambers and between species, the patterning and processes of wall maturation is well conserved (Sedmera et al., 2000). Alterations in these processes are linked to many cardiac diseases such as non-compaction cardiomyopathy, diastolic dysfunction, and arrhythmias. A basic understanding of these processes is necessary to appreciate the morphological defects observed in non-compaction and trabecular disease and to identify how mutations in genes regulating these processes can lead to non-compaction phenotypes.

Cardiac chamber maturation can be separated into three interrelated processes—formation of myocardial projections called trabeculae, establishment of the conduction system, and thickening of the compact myocardium. Each of these processes has been well described historically, and our description is reflective of the published current views of leaders in the field. In the following sections, we will briefly

describe the anatomical changes in the cardiac chamber associated these processes. In the sections following these descriptions, we will then discuss known regulators of chamber maturation and propose future directions for research in chamber maturation.

Trabeculation

We direct interested readers to the reviews by and references in Sedmera et al. (2000) and (Moorman and Christoffels, 2003) for in depth presentation of the morphological changes associated with trabeculation. Cardiac trabeculation begins after the cardiac looping stage to form a network of luminal projections called trabeculae which consist of myocardial cells covered by the endocardial layer. Trabeculae increase cardiac output and permit nutrition and oxygen uptake in the embryonic myocardium prior to coronary vascularization without increasing heart size (Liu and Stainier, 2010; Minot, 1901; Rychter and Ostadal, 1971). As the cardiac wall matures, trabeculae undergo extensive remodeling concomitant with compact myocardial proliferation, formation of the coronary vasculature and maturation of the conduction system. In humans, infants born with either hypotrabeclated or hypertrabeclated ventricles have impaired function (Breckenridge et al., 2007; Weiford et al., 2004). The anatomical changes associated with trabeculation can be divided into three distinct steps—emergence, trabeculation, and remodeling.

Emergence. In the human at Carnegie stage 12, chicken at stage 16/16, mouse at E9.5 and zebrafish around 60 hpf (hour post-fertilization), myocardial protrusions begin to appear extending into the lumen (Moorman and Christoffels, 2003; Peshkovsky et al., 2011; Sedmera et al., 2000) (Fig.1B). Recent work using zebrafish embryos have described this process in greater detail (Peshkovsky et al., 2011). Trabeculae begin to develop in the outer curvature of the ventricle in a stereotypical manner starting on the outer curvature ventrally across from the AV nodes. It is not clear whether these protrusions form by buckling of the myocardial wall, active invagination of cardiomyocytes into the lumen, active evagination of the endocardium into the myocardial layer, or some combination of these actions (Icardo and Fernandez-Teran, 1987; Marchionni, 1995; Sedmera and Thomas, 1996) though Peshkovsky et al.'s work would suggest active invagination of the myocardium as the primary mechanism (2011). In support of this idea, Liu et al. (2010) demonstrated that cardiac trabeculation is primarily driven by delamination of the cardiomyocytes from the compact myocardium.

Trabeculation. After the initial trabecular ridges form, trabecular projections propagate radially to form a network of trabeculae and also increase in length (Peshkovsky et al., 2011; Sedmera et al., 2000). During this stage, the majority of the myocyte mass is contained within trabeculae rather than within the compact wall (Fig. 1C). Cells along the longitudinal axis of each trabecula are more differentiated at the luminal side and less differentiated at the mural side (Sedmera and Thompson, 2011). Defects at this stage manifest as either over or under trabeculated myocardial walls populated by thin trabeculae, and this stage is considered complete when the first signs of trabecular remodeling begin.

Remodeling. The final stage of trabecular growth is a period of remodeling also known as consolidation or compaction (independent of expansion of the compact myocardial layer, discussed below). Species and cardiac chamber-specific differences in adult trabecular morphology are generally attributed to differences in remodeling. This stage is characterized by trabeculae ceasing growth in the luminal direction and thickening radially (Fig. 1D). The bases of the trabeculae thicken and/or collapse to the point that they are indistinguishable from the myocardial wall proper. As the trabeculae compact, the spaces between trabeculae are transformed into capillaries. This compaction stage is considered complete when a “mature” trabeculated network is evident at Carnegie stage 22, chicken stage 34, and mouse at E14.5 (Sedmera et al., 2000). Defects at this stage manifest as overly long, thin trabecular projections that are separated by deep invaginations in the wall.

Compact myocardium proliferation

Though consolidation and compaction of trabeculae increases myocytes mass, the compact myocardium ultimately provides most of the myocardial mass in the mature heart (Fig. 1D). We direct interested readers to the reviews by and references in Risebro and Riley (2006) and Sedmera and Thompson (2011) for review of compact layer cardiomyocyte proliferation and related formation of coronary circulation. Initially, the linear heart tube is comprised of the endocardial and myocardial layers. Around the same time as the initiation of trabeculation, cells of the proepicardial organ migrate to the post-looped heart to form its outermost layer, the epicardium (Fig. 1C). As the endocardium and part of the myocardium generate trabeculae, the more distal portion of the myocardial layer proliferates slowly. Interestingly, it is well accepted that these cells are less differentiated than the trabecular myocardium, and by that reasoning should have a greater proliferative capacity than the trabecular myocytes.

Temporally, around the remodeling/compaction step of trabeculation (above), the epicardium invades the myocardial wall, forming the coronary vasculature and contributing cardiac fibroblasts to the myocardial wall. The appearance of coronary vasculature is accompanied by rapid proliferation of the compact layer. As the compact layer grows in size and complexity, it supplants trabecular myocardium as the major contractile force (Wessels and Sedmera, 2003). This proliferation is concomitant with trabecular remodeling, so it is often difficult to distinguish whether altered myocardial wall structure is from maladaptive trabecular compaction or compact myocardium proliferation. Factors modulating the spatial and temporal growth of the compact layer are reviewed in Sedmera and Thompson (2011) and include FGFs, Wnts, Retinoic acid (RA), and erythropoietin (Chen et al., 2002; Merki et al., 2005; Pennisi et al., 2003; Stuckmann et al., 2003). Further growth and rearrangement of the compact myocardium occur in post-natal development.

Conduction system

Non-compaction and trabecular diseases are often associated with arrhythmias, suggesting a role for altered cardiac action potential (AP) conduction in these disorders (Ichida et al., 1999). Morphological development of the cardiac conduction system and the gene networks involved have been recently reviewed (Chin et al., 2012; Merki et al., 2005; Miquerol et al., 2011; Moorman and Christoffels, 2003; Munshi, 2012). In the normal adult, vertebrate heart, the cardiac AP is initiated in the atrial sinoatrial node then spreads through the atria, inducing atrial contraction. The AP is delayed in the atrioventricular node which allows for completion of atrial contraction before initiation of ventricular contraction. The AP then travels through the atrioventricular bundle and bundle branches and ultimately terminates in the Purkinje fibers (PFs) of the arborized peripheral ventricular conduction system (PVCS). The PVCS, also called the His-Purkinje network, is responsible for depolarizing ventricular cardiomyocytes in a rapid, coordinated fashion. Clearly, the proper development of the cardiac conduction system is very complex and involves coordinated growth and differentiation processes. Due to its physical proximity within the cardiac wall and early embryonic function, the Purkinje fiber network (PFN)/PVSC is directly impacted by altered wall maturation observed in non-compaction and trabecular diseases. Thus, we will restrict our discussion of the conduction system to the anatomical development of the PFN in this section and the signaling networks involved in a later section.

The mature PVCS consist of PFs of myogenic origin, insulating fibers, and nervous input and is located within trabeculae in the subendocardial space between the endocardial cells and underlying differentiated cardiomyocytes. PFs do not require the insulating fibers and or external innervation as they can propagate the cardiac AP when trabeculae have just been formed (Christoffels and Moorman, 2009). The morphological appearance of the PFs varies somewhat across vertebrates, but are generally characterized by underdeveloped sarcomeres, sarcoplasmic reticulum, and mitochondrial network; insulation by connective tissue (mature fibers only); and connected as an electrically excitable network detectable by retrograde tracing (Munshi, 2012). Based on lineage tracing data using different markers in different species, conduction cells are derived from cardiac progenitor cells and not from endocardial or epicardial cells (Miquerol et al., 2011). There is some debate as to whether conduction cells arise from direct progenitor differentiation into conduction cells, from cardiomyocyte differentiation into conduction cells, or if both derivations are possible (Munshi, 2012; Yelon et al., 1999). Christoffels and Moorman (2009) have suggested a model of PF development in which differentiation of cardiomyocytes on the epicardial side of trabeculae into working cardiomyocytes is opposed by differentiation of cardiomyocytes on the endocardial side into working PF cells.

Vertebrate small animal models including mouse, chicken, and zebrafish have been used to study the basic cell signaling involved in cardiac wall maturation. Much of what we do know is from genetic loss of function approaches in which removal of a gene results in a cardiac chamber maturation phenotype. While gene networks governing general cell survival and proliferation are essential for cardiac development, at the molecular level, cardiac maturation requires specific signaling networks including Notch, Neuregulin, Ephrin, BMP, FGF, Semaphorin, RA, Endothelin, and extracellular matrix signaling (ECM). As of yet, no comprehensive model has emerged describing the specific molecular regulators of chamber maturation. In the following section, we will review the evidence implicating each of these pathways in wall maturation.

Notch

The Notch signaling pathway plays multiple roles during vertebrate cardiac differentiation and development, including regulation of valve formation, outflow tract development and cardiac chamber maturation. Upon binding of DELTA or JAGGED family ligands, the extracellular portion of NOTCH is

cleaved by ADAM17 (ADAM metalloproteinase domain 17) and the intracellular portion is cleaved by a γ -secretase. This releases the NOTCH intracellular domain (NICD) into the cytoplasm where it translocates into the nucleus and associates with transcription factors to activate downstream target genes (MacGrogan et al., 2010) (Fig. 2A). Notch activation is upstream of Ephrin and Neuregulin-based modulation of trabeculation and BMP10 modulation of cardiomyocyte proliferation (Fig. 2A).

Consistent with the involvement of Notch signaling in multiple aspects of cardiac development, components of the Notch pathway show dynamic spatial and temporal expression patterns in the developing vertebrate heart and both endocardial and myocardial expression have been described (MacGrogan et al., 2010). The endocardium expresses DELTA4, NOTCH1, and NOTCH4 (Del Amo et al., 1992; Krebs et al., 2000; Uyttendaele et al., 1996) while the myocardium expresses JAGGED1 and NOTCH2 (Loomes et al., 1999; McCright et al., 2002). NOTCH1 is expressed in the endocardium and its activated form shows strongest expression at the base of the ventricular trabeculae. In addition, *Notch1* or *RBPjk* (effector transcription factor) deficient mice display deficient cardiac wall maturation including failure of cardiac trabeculation, reduced marker genes expression, and decreased cardiomyocyte proliferation (Grego-Bessa et al., 2007). The myocardially expressed NOTCH2 has also been shown to play a role in chamber maturation. NOTCH2 is down-regulated in the compact myocardium layer during mouse cardiac development. Overexpression of Notch2 in the myocardium leads to hypertrabeculation, reduced compaction, and septal defects (Yang et al., 2012). Double knockout of *Numb* and *Numblike* (suppressors of NOTCH2) leads to a comparable phenotype as NOTCH2 overexpression and increases BMP10 expression which modulates trabeculation (discussed below) (Yang et al., 2012).

Neuregulin/ERBB

Neuregulin-1 (NRG1) is a Type 1 transmembrane protein and a member of the epidermal growth factor (EGF) family of ligands. It is highly expressed in the cardiovascular system and has been implicated in heart development and disease (Odiete et al., 2012). Transmembrane NRG1 acts as a paracrine ligand. In the heart, binding of NRG-1 to the ERBB family receptor ERBB4 promotes formation of ERBB4/ERBB2 heterodimeric signaling complex. ERBB2 tyrosine kinase activity phosphorylates the C-

terminal domains, leading to downstream signaling modulation of gene expression through (Fig. 2A) (Yarden and Slivkowski, 2001).

In the heart, endocardial derived Neuregulin signaling through ERBB2/4 heterodimers in the myocardium is essential for proper chamber maturation (Fuller et al., 2008). Mice lacking NRG1 (Meyer and Birchmeier, 1995) or functional NRG1 Ig-like domain 1 (Kramer et al., 1996), die before birth due to defective cardiac trabeculation. Likewise, mice lacking either ERBB2 (Lee et al., 1995) or ERBB4 (Gassmann et al., 1995) also die in early gestation due to defective trabeculation. Similar to mice, zebrafish devoid of functional ERBB2 protein (Liu et al., 2010) or with ERBB activity pharmacologically inhibited (Peshkovsky et al., 2011) do not form trabeculae (Liu et al., 2010). Detailed lineage tracing and transplantation studies in zebrafish embryo has suggested that initiation of trabeculation is driven by directional migration of cardiomyocytes regulated by ERBB2 signaling (Liu et al., 2010).

Since NRG1, ERBB2, and ERBB4 deficiency results in embryonic lethality in multiple model organisms, it is unlikely that complete loss-of-function mutations are present in the human populace with congenital heart malformations. However, it is possible that partial loss of function in these genes or in the up or downstream mediators of Neuregulin signaling could manifest within the cardiac wall malformation disease etiology.

Ephrin B2/B4

Ephrin signaling is essential for normal endothelial cell function and thus heart development. In the heart, Ephrin-B2 (EFNB2) and one of its receptors, EPHB4, are expressed in the endothelial cells lining trabeculae (Wang et al., 1998). Eph4 tyrosine kinase activity leads to downstream signaling that modulates cell shape, migration, and adhesion (Salvucci and Tosato, 2012) (Fig. 2A). In mice, trabeculae fail to form in the absence of EFNB2 (Wang et al., 1998) or EPHB4 (Gerety et al., 1999).

BMP

Bone morphogenic protein-10 (BMP10) signaling plays an important role in modulating heart development (Lowery and de Caestecker, 2010). BMP10 expression is restricted to cardiomyocytes in the developing and post-natal heart (Neuhaus et al., 1999). BMP10 is part of the TGF- β superfamily of ligands with specificity for ALK1, ALK6, and BMPR2 receptors. Ligand-receptor binding initiates SMAD signal transduction to modulate gene transcription (Lowery and de Caestecker, 2010) (Fig. 2A). Global

deletion of BMP10 is embryonic lethal with severely reduced cardiomyocyte proliferative capacity (Chen et al., 2004). BMP10 appears to modulate cardiomyocyte differentiation through activation of transcription factors NKX2.5, MEF2C (Chen et al., 2004), and TBX20 (Zhang et al., 2011).

FGF

Fibroblast growth factor (FGF) family of secreted ligands binds to fibroblast growth factor receptors (FGFR) in either a cell autonomous or non-cell autonomous manner, leading to complex, cell- and context-specific intracellular signaling (Fig. 2A). Proliferation of the compact myocardium requires FGF signaling (Mikawa, 1995; Mima et al., 1995). In mouse embryos, the FGF9 family members FGF9, FGF16, and FGF20 are expressed in both the endocardium and epicardium and are important regulators of regulate cardiomyocyte proliferation (Lavine et al., 2005; Lu et al., 2008).

Semaphorins

Semaphorin signaling through Plexin receptors modulate cell behavior and gene transcription through complex intracellular signaling cascades (Zhou et al., 2008b) (Fig. 2B). Though Semaphorins are more typically known for their role in axonal migration, members of the semaphorin family, such as SEMA6D (Semaphorin-6D) have been shown to play a role cardiac patterning, and SEMA6D loss-of-function leads to trabeculation phenotypes (Toyofuku et al., 2004a; Toyofuku et al., 2004b). In mouse and chicken embryos, knockdown of SEMA6D or its receptor PLXNA1 (PlexinA1) in mouse and chicken embryos leads to the typical non-compaction phenotype with a thin compact myocardium and expansive spongy trabeculated myocardium (Toyofuku et al., 2004a; Toyofuku et al., 2004b).

Retinoic acid

RA is derived from Vitamin A. Both Vitamin A deficiency (Wilson et al., 1953; Wilson and Warkany, 1949) and exposure of embryos to excess Vitamin A leads to cardiac defects (Morriss-Kay, 1992). Canonically, lipophilic RA diffuses into cells and binds to the RA receptor RXRs on the nuclear membrane (Fig. 2B). RXRs directly bind DNA to regulate gene transcription (Duester, 2008). Genetic ablation of the RA receptor RXR α is embryonic lethal in mice due to failed proliferation of the compact myocardium (Sucov et al., 1994). This arrest of cardiomyocyte proliferation is not directly attributable to

RA signaling on cardiomyocytes. Rather, RA appears to induce the epicardium to secrete trophic factor(s) that mediate cardiomyocyte proliferation (Chen et al., 2002; Stuckmann et al., 2003).

Endothelin

In the developing heart, cardiomyocyte differentiation into PFs is regulated in part by endothelin signaling (Takebayashi-Suzuki et al., 2000). Pro-endothelin (Pro-ET), the precursor of active endothelin-1 (ET1), is produced by endothelial cells in response to shear stress (the force of fluid flow parallel to the endocardial surface). Presumably due to higher levels of shear stress, in the heart endocardial and arterial endothelial cells, but not venous endothelial cells or cardiomyocytes, produce the endothelin-converting enzyme-1 (ECE1) necessary to convert Pro-ET into ET1. ET1 interacts with the G-protein coupled receptor EDNRA (endothelin receptor type A) to induce cardiomyocytes to differentiate into PFs (Gourdie et al., 1998; Takebayashi-Suzuki et al., 2000) (Fig. 2B). ECE1 is required for normal PF formation (Hall et al., 2004).

Extracellular matrix molecule signaling

Each of the cardiac layers—endocardial, myocardial, and epicardial—are separated by layers of extracellular matrix (ECM). ECM–cell interactions are coupled cell signaling through transmembrane proteins called integrins which, upon binding undergo conformational changes that lead to complex cell and context-dependent cell signaling (Fig. 2B). Integrins modulate intracellular signaling cascades to modulate many cellular processes including growth, migration, survival, and differentiation. Integrins exist as heterodimers, and ligand specificity is conferred by different combinations α and β subunit isoforms. The $\alpha 4$ integrin is essential for cell adhesion during cardiac development (Yang et al., 1995). The exact composition of cardiac ECM is important for normal cardiac development. Though there are many ECM proteins present in the developing heart, collagen (Tahkola et al., 2008), versican (Cooley et al., 2012), and nephronectin (Patra et al., 2011) have emerged as important ECM components. During cardiac morphogenesis, the ECM is broken down by matrix metalloproteases to facilitate cell migration. ECM composition is regulated at least in part by the matrix metalloprotease ADAMTS1, which is necessary for trabeculation (Stankunas et al., 2008).

Biomechanical forces in cardiac wall maturation

Though genes regulating cell signaling are clearly essential for cardiac chamber maturation, epigenetic factors such as the biomechanical forces influence heart development. We direct interested readers to a recent review for an analysis of mechanical forces in heart development (Granados-Riveron and Brook, 2012). During development, the heart is exposed to many biomechanical forces including those exerted on the wall by blood flow (shear stress), by fluid pressure (cyclic strain), within the wall by cell–cell attachments, and on the wall by extracardiac pressures (Fig. 3). The signaling mechanisms through which cells translate biomechanical forces into changes in the signaling events that modulate cardiac wall patterning are poorly understood.

Flow

Fluid flow plays an important role in trabeculation, cardiomyocyte proliferation, and establishment of the cardiac conduction system. While flow exerts a force parallel to the vessel wall called shear stress, fluid pressure exerts force on the developing heart to the vessel wall. This pressure, also known as mechanical load, can be manipulated *ex vivo* in developing hearts. Reduced mechanical load is mimicked by maintaining hearts in normal atmospheric pressure, while increased mechanical load is mimicked by filling the ventricles to end diastolic volume by injection of silicon oils. In chick, changing the mechanical load leads to altered development of the conduction system, impaired growth, and disorganized trabeculae (Sankova et al., 2010). Likewise, zebrafish carrying an atrial sarcomere mutation, the *wea* mutant, have weak blood flow in the ventricles (Berdougo et al., 2003). *Wea* mutants exhibit reduced trabeculation (Peshkovsky et al., 2011). One way that cells sense flow is through the bending of primary cilia. Primary cilia are sensory organelles that protrude from the normal plane of the cell membrane and are found on nearly every cell type, including endothelial cells. Interestingly, mice that do not have primary cilia have decreased cardiac trabeculation and abnormal outflow tract development (Clement et al., 2009), suggesting a role for shear stress sensing in chamber maturation.

Stretch

During the cardiac cycle, individual cardiomyocytes are subjected to stretch. When stretched, endothelial cells produce Pro-ET which is converted by ECE1 into ET1, and ET1 signaling is essential for PF differentiation (Takebayashi-Suzuki et al., 2000) Pharmacological inhibition of stretch responsive

channels leads to decreased expression of ECE1 in the endocardium and decreased expression of the PF specific marker connexin40 in the developing chick ventricle (Hall et al., 2004). Conversely, pressure overload by truncal banding increases PF formation (Hall et al., 2004). Thus, mechanical forces play a role in PF development at least in part through modulation of ET1 signaling.

Inward forces

The developing heart in its entirety is contained within the splanchnopleural cavity. Advances in four-dimensional optical coherence tomography (OCT) have permitted study of the complex interrelationship between cardiac layers during the cardiac cycle. (Garita et al., 2011) used OCT imaging in chick and mouse embryos to demonstrate that the splanchnopleural membrane interacts with the myocardial wall. This study is the first to demonstrate a direction interaction of the developing heart interacts with its boundaries, suggesting that inward transduction of this mechanical interaction could play a role in final positioning of the heart.

New areas for investigation

Though a few genes have been implicated as necessary for trabeculation, much work remains to fully characterize cardiac trabeculation. Greater understanding of the normal morphogenesis of the heart will inform treatment efforts and could play a role in developing personalized therapeutics. The first question which remains to be addressed is how the spatial pattern of cardiac trabeculation is generated. NRG-1 and its receptors appear to be expressed uniformly in the ventricular endocardium and myocardium respectively; however, it is not clear whether Neuregulin/ErbB signaling is spatially activated to select certain cardiomyocytes to initiate cardiac trabeculation. Alternatively the spatial regulation of cardiac trabecular initiation can be achieved by the interplay of multiple signaling pathways, such as the Neuregulin/ErbB and Semaphorin/Plexin pathways. In addition, the initiation of cardiac trabeculation appears to be driven by cardiomyocytes delamination, but little is known about the cellular basis of cardiomyocyte delamination. It is also conceivable that once certain cardiomyocytes are selected to initiate cardiac trabeculation, they might inhibit their neighbors from adopting a trabecular cardiomyocyte fate. It will be interesting to determine whether and how such lateral inhibition mechanism is employed to maintain the homeostasis of the compact myocardium. Mechanical force also plays an important role in trabeculation. Cardiac trabeculation is significantly reduced in zebrafish *wea* mutant embryos with

reduced blood flow in the ventricle. Likewise, in human, mutations in sarcomere-encoding genes can cause trabecular non-compaction in the left ventricles, suggesting in humans mechanical force associated with cardiac contraction can also have an effect on embryonic heart development as well. Thus, it will be important to study how the heart senses and responds to mechanical force to regulate cardiac chamber maturation.

Chapter 1.1 Figures

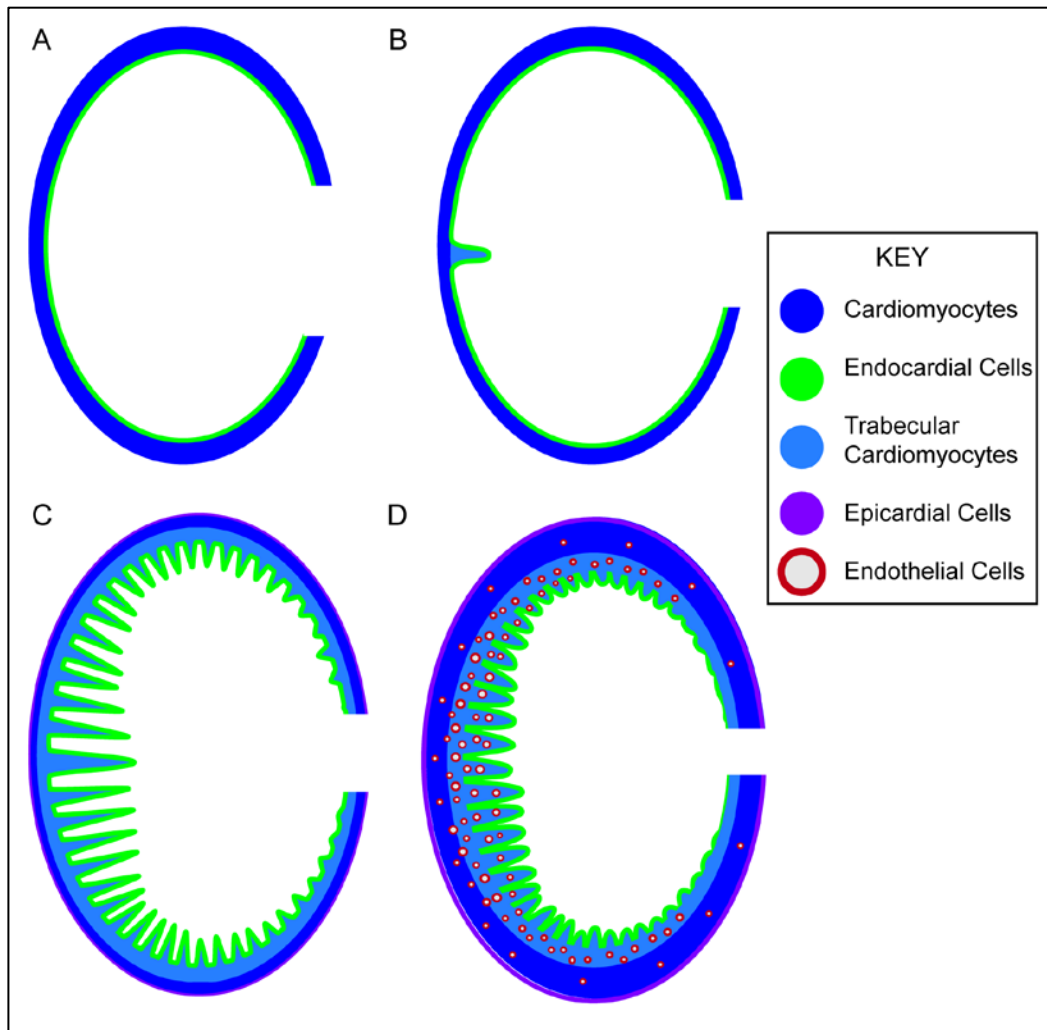


Figure 1 Cardiac chamber maturation

A–D features a schematized cross-section of a theoretical ventricle wall with the developing atrio-ventricular canal represented as the open break in the ventricle wall, such that the outer curvature is on the left and the inner curvature is on the right. A: Early in development, the cardiac chamber wall is smooth and consists of endocardial cells and myocardial cells. B: *Emergence*: Myocardial protrusions called trabeculae begin to appear in the outer curvature of the ventricle, projecting into the lumen. The trabeculae are lined by a continuous layer of endocardium. C: *Trabeculation*: Trabeculae increase in length and the chamber wall becomes topologically more complex as additional trabeculae form throughout the outer curvature, creating a meshwork network of interconnected trabeculae. The compact myocardium does not thicken appreciably. A third layer of cells, the epicardium, surrounds the developing heart. D: *Compaction/Remodeling*: Trabeculae cease luminal growth, thicken radially, and their base coalesces to form part of the solid myocardial wall. The compact myocardium increases in mass concomitant with the coronary vessel formation in the myocardial wall. The compact myocardium is shown in dark blue, trabecular cardiomyocytes in cerulean, endocardial cells in green, and epicardial cells in purple. The developing cardiac vasculature is represented by gray circles outlined in green.

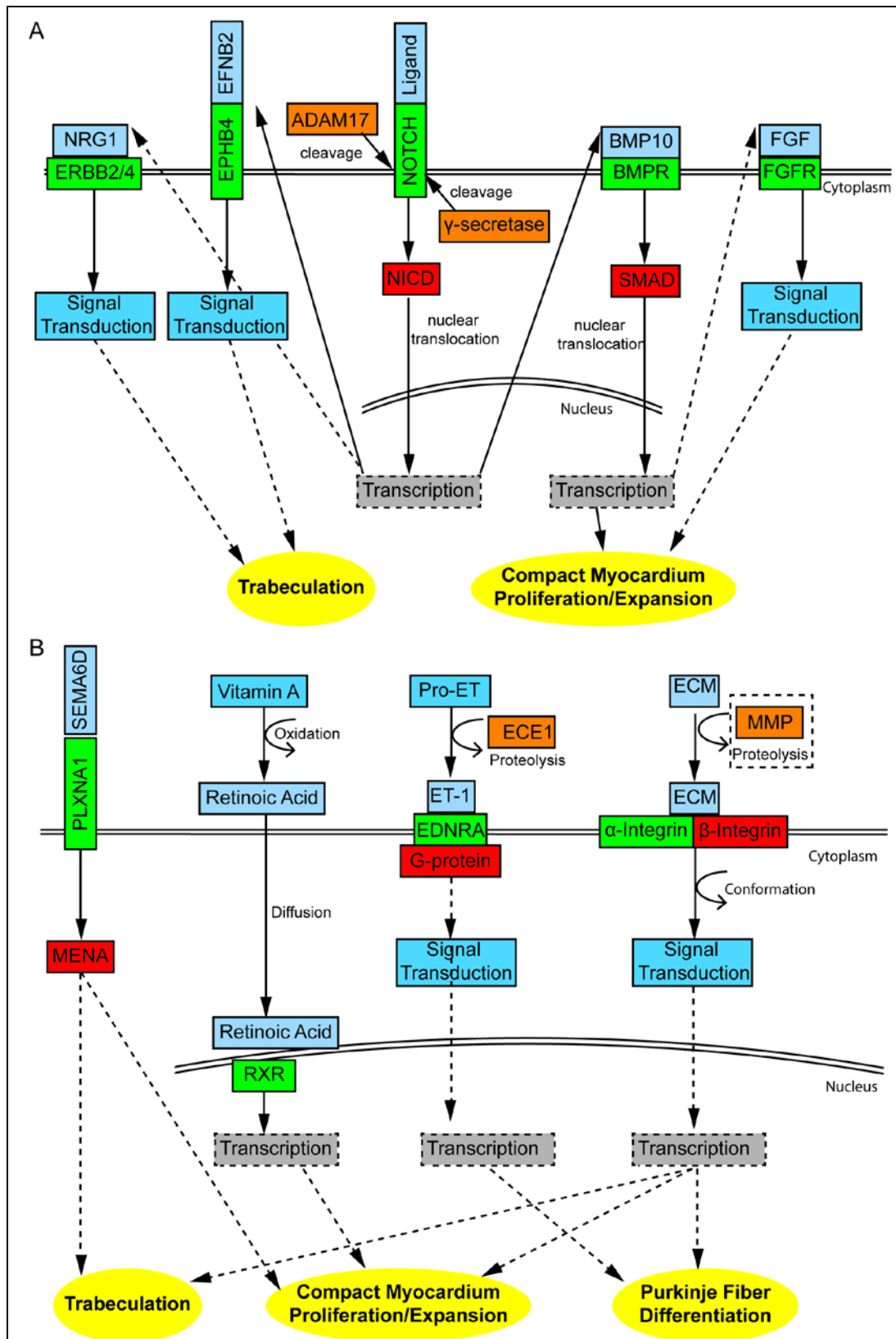


Figure 2 Signaling pathways in cardiac chamber maturation

Several signaling pathways have been identified as key regulators of cardiac chamber morphogenesis. Please see below for abbreviations. A: Canonical NOTCH ligands including Delta and Jagged family members bind to NOTCH family receptors. Upon binding, ADAM17 cleaves the extracellular domain of NOTCH and γ -secretase cleaves the intracellular domain of NOTCH, releasing the NICD into the cytoplasm. NICD translocates into the nucleus and modulates gene transcription. NOTCH activation leads to stimulation of EphrinB2 signaling through EPH4 and NRG1 signaling through ERBB2/4, both of which are essential for trabeculation. NOTCH activation also leads to activation of BMP signaling through BMP10/BMPR interactions and FGF signaling through FGFR. BMP and FGF signaling are essential for cardiomyocyte proliferation and expansion of the compact myocardium. B: Other signaling pathways essential for cardiac chamber maturation. SEMA6D signaling through PLXNA1 activates the enabled homolog MENA, modulating both trabeculation and compact myocardium proliferation/expansion. Vitamin A is oxidized into retinoic acid. Retinoic acid family members, RXRs, bind retinoic acid and translocate into the nucleus where they influence gene transcription involved in compact cardiomyocyte proliferation. Pro-endothelin secreted into extracellular space is converted into ET-1 by ECE1. ET-1 binding activates the G-protein coupled receptor EDNRA, leading to downstream signaling and gene transcription essential for Purkinje fiber formation. Diverse extracellular matrix molecules collectively referred to as ECM, either whole or after proteolysis by MMPs, interact with α/β integrin heterodimers. This induces conformation changes in the integrin heterodimer that activate downstream signal transduction that ultimately modulates all elements cardiac chamber maturation. Abbreviations: NRG1, Neuregulin-1; ERBB2/4, heterodimer of ERBB2 (v-erb-b2 erythroblastic leukemia viral oncogene homolog 2) and ERBB4 (v-erb-a erythroblastic leukemia viral oncogene homolog 4); EFNB2, Ephrin-B2; EPHB4, EPH receptor B4; ADAM17, ADAM metalloproteinase domain 17; NOTCH, NOTCH family receptors; γ -secretase, gamma-secretase; NICD, NOTCH intracellular domain; BMP10, bone morphogenic protein 10; BMPR2, bone morphogenic protein receptor, type II; SMAD, SMAD family transcription factors; FGF, fibroblast growth factors; FGFR, fibroblast growth factor receptors; SEMA6D, Semaphorin 6D; PLXNA1, Plexin A1; MENA, enabled homolog (mammalian); RXR, retinoic acid receptor family; Pro-ET, pro-endothelin; ECE1, endothelin-converting enzyme 1; ET-1, endothelin 1; EDNRA, endothelin receptor type A; ECM, extra cellular matrix components; MMP, matrix metalloproteinase.

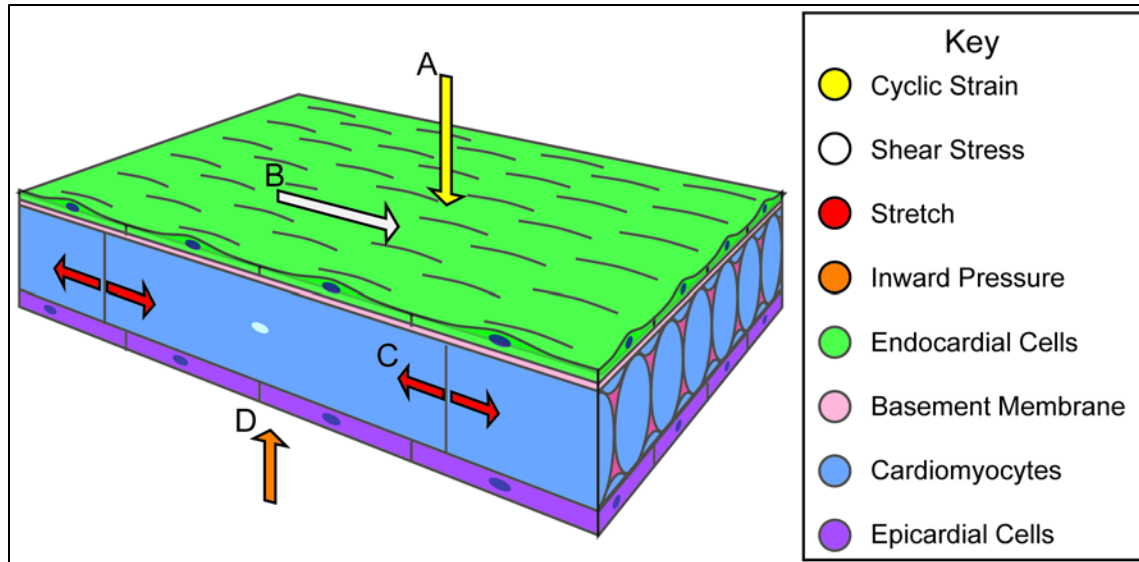


Figure 3 Biomechanical forces in cardiac wall maturation

Biomechanical forces are important for normal developmental patterning. Forces exerted on the wall from blood flow include (A) cyclic strain, a force perpendicular to the vessel wall, and (B) shear stress, the frictional force parallel to the vessel wall. C: Force from cardiac contraction exerts strain on myocardial and endothelial cell–cell junctions. D: The splanchnopleural membrane interacts with the myocardial wall during development and may exert an inward pressure on the myocardial wall. Arrows indicate force vectors.

1.2 Advances in the Study of Heart Development and Disease Using Zebrafish²

Introduction

Congenital heart diseases (CHDs) are the most common type of human birth defect and frequently exhibit structural abnormalities that arise from defective cardiac development and maturation (Moran et al., 2014; Mozaffarian et al., 2015; Vos et al., 2015). These defects compromise cardiac output and lead to poor clinical outcomes. Though Mendelian genetics can explain some CHDs, differential penetrance of CHD phenotypes in affected families underscores the need for a better understanding of the cellular and molecular events of cardiac development (Teekakirikul et al., 2013). The genetic networks that regulate vertebrate heart development are highly conserved across species enabling modeling of human heart developmental disorders in zebrafish (Fahed et al., 2013; Moorman and Christoffels, 2003). Additionally, the zebrafish model system is relatively inexpensive and can be used in high-throughput compound screens to identify novel therapeutics for personalized medicine (Asnani and Peterson, 2014; Barros et al., 2008; Delvecchio et al., 2011; Kitambi et al., 2012; Stewart et al., 2015; Vos et al., 2015; Yozzo et al., 2013).

Modeling cardiovascular development and disease in zebrafish

The zebrafish, *Danio rerio*, has emerged as a premier vertebrate model system for investigating the molecular basis of heart development and assessing therapeutic potential of small molecules (Kessler et al., 2015; Liu and Stainier, 2012; Ruzicka et al., 2015). Zebrafish have several key advantages over other vertebrate model systems that are inherent to their biology (Fig. 4A) (Westerfield, 2000). A single breeding pair produces hundreds of eggs weekly, facilitating genetic and statistical analysis. These externally fertilized eggs develop rapidly, and by 24 hours post fertilization (hpf), the embryonic heart has initiated cardiac contraction. Though the zebrafish heart has a simpler structure than the human counterpart (two chambers instead of four chambers), it possesses analogs of the major components of the human heart and utilizes similar cellular and molecular strategies to assemble the heart (Moorman and Christoffels, 2003; Stainier et al., 1993). Due to the transparency of the embryos, the morphology and function of the developing hearts can be directly observed by light microscopy. This optical

² This chapter previously appeared in part in the Journal of Cardiovascular Development and Disease. The original citation is Brown, D.R.; Samsa, L.A.; Qian, L.; Liu, J. Advances in the Study of Heart Development and Disease Using Zebrafish. *J. Cardiovasc. Dev. Dis.* 2016, 3, 13.

transparency can also be leveraged by the use of transgenic reporters in which cardiac cells are labeled with fluorescent markers (Huang et al., 2003; Jinn et al., 2005; Long et al., 1997; Perner et al., 2007). Importantly, zebrafish embryogenesis does not require a functional cardiovascular system during the first week of life because the zebrafish embryo is small enough to meet oxygenation needs by diffusion (Bang et al., 2004; Chen et al., 1996; Sehnert et al., 2002; Stainier et al., 1996; Strecker et al., 2011). This allows for examination of severe cardiovascular defects that usually cause embryonic lethality in other model organisms such as mice. These advantages allow for robust forward and reverse genetic approaches to study the genetic and molecular basis of heart development and disease (Fig. 4B-C).

In this review, we will provide an overview of zebrafish heart development, and discuss how zebrafish are leveraged to study cardiovascular development and disease.

Cardiovascular development in zebrafish

The heart is the first organ to form and function during vertebrate embryo development. The key steps of heart development are conserved across vertebrates, and the gross morphological changes associated with cardiac morphogenesis have been well described in detail in previous reviews (Kirby, 2007; Liu and Stainier, 2012; Moorman and Christoffels, 2003; Samsa et al., 2013; Sedmera et al., 2000). Additionally, we refer the interested reader to the online Zebrafish Atlas (<http://zfatlas.psu.edu>) for histological details of zebrafish development from embryo to adult. Histology methods are also readily available for zebrafish (Sabaliauskas et al., 2006; Tsao-Wu et al., 1998). Below, we will overview zebrafish cardiac morphogenesis and disease phenotypes placing an emphasis on parallels to human heart disease.

Zebrafish cardiac morphogenesis

When the zebrafish heart initiates contraction around 24 hours post fertilization (hpf), it is composed of three cell types—atrial cardiomyocytes (CMs), ventricular CMs, and endocardial cells (Stainier et al., 1993). These differentiated cell types can be traced to cardiac progenitor cells (CPCs), which originate at 5 hpf in the lateral marginal zone of the blastula stage embryos (Fig. 5A) (Keegan et al., 2004; Milgrom-Hoffman et al., 2011; Misfeldt et al., 2009; Stainier et al., 1993). The ventricular pool resides more dorsally and closer to the margin than the atrial pool, while the blastomeres that give rise to endocardial cells appear to be located across the lateral margin without any specific spatial organization

(Bussmann et al., 2007; de la Pompa et al., 1998; Keegan et al., 2004). These progenitors migrate during gastrulation to reside in the posterior half of anterior lateral plate mesoderm (ALPM) by 15 hpf (Fig. 5B) (Bussmann et al., 2007; Holtzman et al., 2007; Palencia-Desai et al., 2015; Trinh and Stainier, 2004; Yelon et al., 1999). Subsequently, these bilateral CPCs initiate differentiation program and fuse into a disk with endocardial cells in the center lined by ventricular and atrial myocytes (Fig. 5C). The disk elongates into a linear tube with distinct expression profiles for atrial CMs, ventricular CMs and endocardial cells (Fig. 5D) (Bussmann et al., 2007; Garavito-Aguilar et al., 2010; Holtzman et al., 2007; Palencia-Desai et al., 2015; Rohr et al., 2008; Yelon et al., 1999).

The linear heart tube is originally composed of cells from the first heart field (FHF). Additional cardiac cells are recruited to the heart tube in a second wave of differentiation as late-differentiating CPC populations called the second heart field (SHF) extend the linear heart at its arterial and venous poles starting at around 28 hpf (de Pater et al., 2009; Hami et al., 2011; Lazic and Scott, 2011; Zhou et al., 2011). Concurrent with addition of the SHF-derived cardiac cells, the linear heart tube migrates leftward and begins looping (Fig. 5E) (Baker et al., 2008; Chen et al., 1997; Rohr et al., 2008; Stainier et al., 1993). By 48 hpf, the looped heart is located in the pericardial cavity and is clearly divided into a two-chambered heart by constriction of the atrio-ventricular (AV) canal (Fig. 5F) (Beis et al., 2005; Stainier et al., 1993). Although at 48 hpf, the major components of the heart have formed, the heart is still immature and lacks auxiliary cell types and additional structures that are important for function as the organism grows (Martin and Bartman, 2009). These structures include the bulbous arteriosus, valve cushions and leaflets, myocardial protrusions called trabeculae, and epicardium (Figure 5G-H). These are discussed in detail, below.

Cardiac outflow tract

The zebrafish outflow tract is composed of the bulbous arteriosus and aorta. The bulbous arteriosus is analogous to the mammalian conotruncus and is composed of an inner layer of endothelial cells lined by a thick layer of smooth muscle cells (Fig. 5H). This pseudo-chamber serves as a resistor to regulate flow through the aorta, which delivers blood directly to the gills for oxygenation (Grimes and Kirby, 2009).

Epicardium

The epicardium develops from an extra-cardiac population of cells called the pro-epicardium. The pro-epicardium can be distinguished morphologically at 48 hpf as a group of spherical cells located in close proximity to the ventral wall of the looped heart at the level of AV junction (Hofsteen et al., 2013; Liu et al., 2010; Serluca, 2008; Zhou et al., 2008a). At approximately 72 hpf, the pro-epicardium expands and starts to spread over the myocardial surface to form the epicardium (Fig. 5H) (Peralta et al., 2014; Plavicki et al., 2014). The epicardium is an important source of signals to the underlying myocardium (Kikuchi et al., 2011). It also is a source of epicardial-derived, cardiac resident cells such as cardiac fibroblasts (Gonzalez-Rosa et al., 2012; Peralta et al., 2014).

Trabeculation

Cardiac trabeculae are highly organized, luminal, muscular ridges lined by endocardial cells in the ventricular lumen. Trabeculae increase myocardial surface area for blood oxygenation and are critical for cardiac function (Icardo and Fernandez-Teran, 1987; Liu et al., 2010; Samsa et al., 2013; Sedmera et al., 2000). Following cardiac looping and chamber ballooning, CMs delaminate from the ventricle wall to initiate cardiac trabecular formation, and the ventricle has obvious, stereotyped trabecular ridges by 72 hpf (Liu and Stainier, 2010; Samsa et al., 2015; Staudt et al., 2014). The trabecular myocardium rapidly expands in the developing heart and as the cardiac wall matures, the trabeculae undergo extensive remodeling in association with compact myocardial proliferation, formation of the coronary vasculature and maturation of the conduction system (Samsa et al., 2013). Remodeling, also known as consolidation or compaction, marks the final stage of trabecular growth such that species-specific differences in adult trabecular morphology are generally attributed to differences in remodeling (Sedmera et al., 2000).

Valvulogenesis

Cardiac valves are a critical component of the vertebrate heart. Valves function to ensure unidirectional blood flow and prevent retrograde flow. Valve malformation underlies many forms of human congenital and adult-onset heart diseases, such as aortic or pulmonary valve stenosis, bicuspid aortic valve, mitral valve prolapse, and Epstein's anomaly (Beis et al., 2005; Martin and Bartman, 2009; Mozaffarian et al., 2015). The AV canal forms at the border between the atrium and ventricle and is

readily detectable during looping morphogenesis. Around 40 hpf, AV CMs expand their luminal surface while constricting their abluminal surface (Beis et al., 2005). The underlying AV endocardial cells undergo an epithelial-to-mesenchymal transition to form the endocardial cushion, which subsequently remodels to create primitive valve leaflets allowing for complete block of retrograde blood flow at 76 hpf (Beis et al., 2005; Scherz et al., 2008; Timmerman et al., 2004). These leaflets continue to thicken and lengthen to form the mature valve (Martin and Bartman, 2009).

Late maturation

In zebrafish, cardiac chamber maturation continues through juvenile and early adult life stages. During larval and early juvenile stages, the ventricle remodels from a grossly pyramidal shape to a more-rectangular morphology and the heart rotates such that the ventricle is positioned ventrally to the atrium (Fig. 5I) (Singleman and Holtzman, 2012). In cross section, the myocardium of the ventricle wall is composed of a compact layer myocardium called the primordial layer and a spongy trabecular layer (Fig. 5I) (Gupta and Poss, 2012). In late juvenile development leading into adulthood, the ventricle becomes more rounded and coronary arteries form at the subepicardial space to vascularize the underlying myocardium (Harrison et al., 2015; Singleman and Holtzman, 2012). Additionally, a small population of inner trabecular cells breaks through the primordial layer and rapidly expands on the surface of the myocardium to form the cortical layer (Gupta et al., 2013; Gupta and Poss, 2012). In cross section, the ventricle wall comprises two layers, a compact myocardium layer with cortical and primordial cells and the trabecular myocardium (Fig. 5J).

Chapter 1.2 Figures

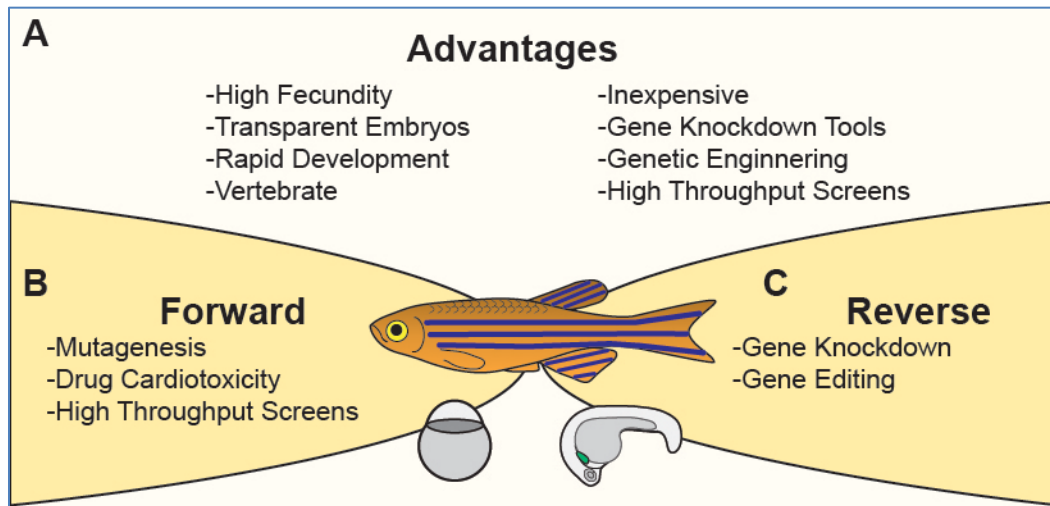


Figure 4 Zebrafish model system

Schematic illustrating (A) the advantages of zebrafish as a model system, (B) forward genetic and (C) reverse genetic approaches to studying heart development and disease in zebrafish.

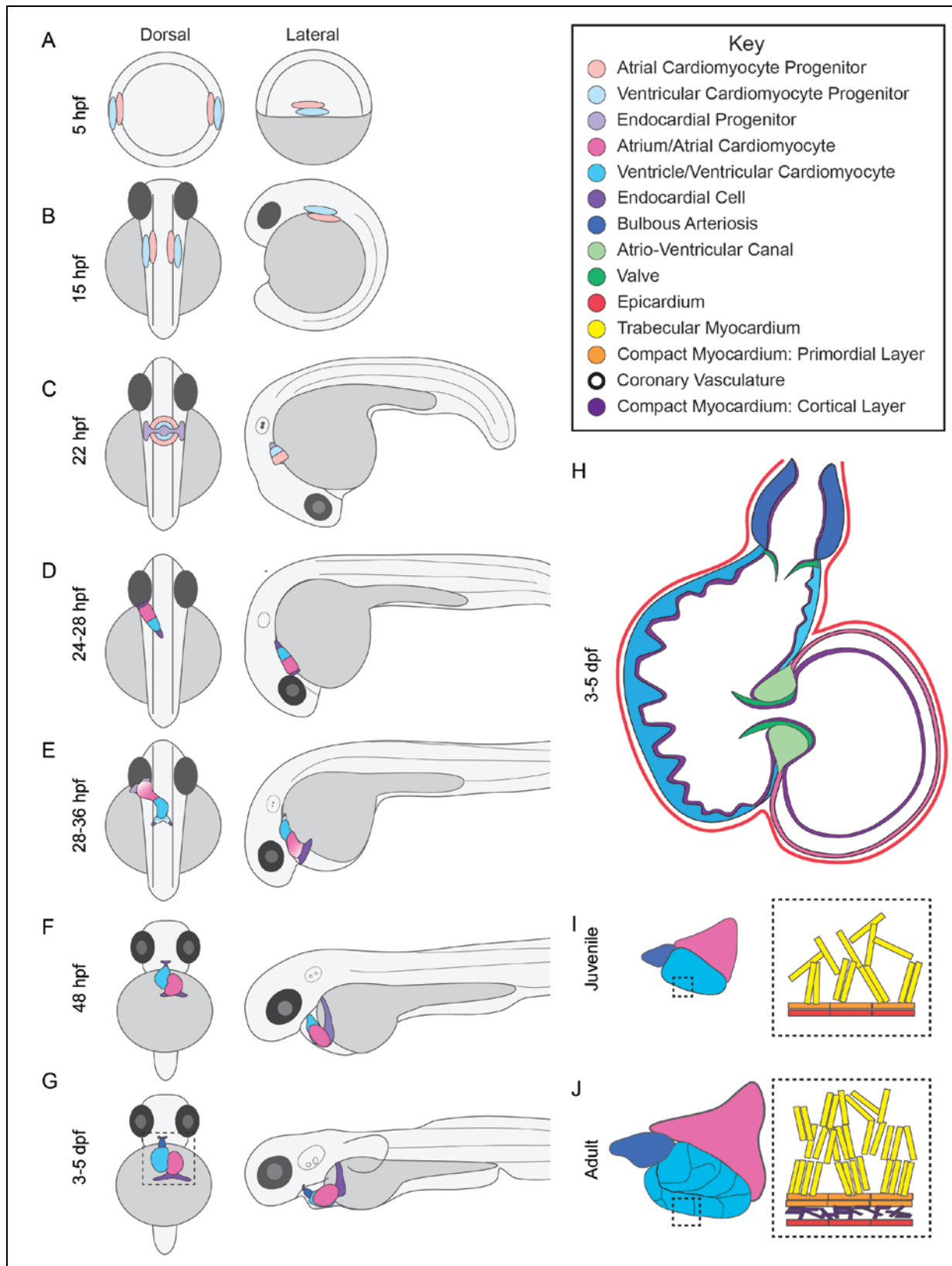


Figure 5 Zebrafish heart development

(A-G) Lateral and dorsal views of heart development from 5 hours post fertilization (hpf) embryos to 5 days post fertilization (dpf) larvae. (A) Cardiac progenitors are located at the lateral margin with the ventricular progenitors more closer to the margin than the atrial progenitors at 5 hpf. (B) Cardiac progenitors migrate bilaterally to the anterior lateral plate mesoderm by 15 hpf. (C) By 22 hpf, cardiac progenitors and developing endocardial cells have fused to form the cardiac disk which begins regular contractions between 22-24 hpf. (D) From 24-28 hpf, the disk elongates into the linear heart tube and begins leftward migration. (E) The linear heart tube continues migrating leftward and begins looping. Concurrently, from 28-36hpf, second heart field cells are added to the arterial and venous poles, illustrated by shading. (F) By 48 hpf, the two chambered heart has formed. (G) The bulbous arteriosus forms at the outflow tract. (H) Cross-sectional view of the heart from 3-5 featuring trabeculae located primarily in the outer ventricle wall, cardiac valves, and covering of the heart by the epicardium. (I) Between larval and juvenile stages, the atrium and ventricle rotate such that the atrium is dorsal to the ventricle. The inner topology is complex and features a spongy trabecular myocardium and outer compact myocardium called the primordial layer. (J) Additional features of the adult heart are coronary arteries which feed the ventricle and expansion of the compact myocardium by addition of a cortical layer of cardiomyocytes.

CHAPTER 2 CARDIAC CONTRACTION ACTIVATES ENDOCARDIAL NOTCH SIGNALING TO MODULATE CHAMBER MATURATION

2.1 Historical Context

An increasing body of evidence highlights the importance of an active interplay between the biomechanical forces generated by the functioning embryonic heart and cardiac structure in regulating cardiac maturation. Mutations in genes that influence force production or detection in the heart are associated with a wide range of CHDs, underscoring the importance of this interplay [reviewed in Granados-Riveron and Brook (2012)]. However, the underlying mechanisms connecting cardiac function and form are largely unknown.

Early studies in chicken embryos were foundational in establishing a role for biomechanical forces in regulating chamber maturation. Partial ligation of the right lateral vitelline vein disrupts intracardiac fluid dynamics and leads to later chamber maturation defects (Hogers et al., 1997). Similarly, altering ventricular afterload by conotruncal banding or changing preload and afterload dynamics through atrial ligation or clipping, respectively, leads to dramatic alterations in the ventricular myocardial architecture (Sedmera et al., 1999).

In zebrafish, implanting a small bead to occlude blood flow at the inflow or outflow tract leads to valve and chamber maturation defects, demonstrating that biomechanical forces are also important for zebrafish cardiac morphogenesis (Hove et al., 2003). In non-contractile, *silent heart* mutants, the basic structure of the heart is intact, despite lack of contraction and blood flow (Sehnert et al., 2002). Recent zebrafish work using sophisticated genetic tools has just begun to characterize how flow and contractile forces regulate the cell shape and gene expression changes that underlie chamber maturation (Auman et al., 2007; Bartman et al., 2004; Dietrich et al., 2014; Heckel et al., 2015; Kalogirou et al., 2014; Lin et al., 2012; Peralta et al., 2013; Staudt et al., 2014; Vermot et al., 2009; Yang et al., 2014). Data presented in Chapter 2.2, below, adds to this body of knowledge by connecting flow detection and gene expression in endocardial cells to myocardial cellular changes observed chamber maturation.

2.2 Cardiac Contraction Activates Endocardial Notch Signaling to Modulate Chamber Maturation³

Introduction

Congenital heart diseases often feature structural abnormalities that arise from defects in the development of the heart during embryogenesis (Chin et al., 2012; Samsa et al., 2013). The heart is the first organ to function, yet the details of its formation are only partially understood. In vertebrates, cardiac morphogenesis commences as the two bilateral cardiac primordia fuse at the ventral midline to form the linear heart tube, which is composed of a luminal endocardial layer and an immature myocardial layer (Fishman and Chien, 1997; Harvey, 2002; Olson and Srivastava, 1996; Staudt and Stainier, 2012; Yelon, 2001). Concomitant with cardiac contraction, the primitive heart tube develops into a multi-chambered functional organ that grows and matures through a series of complex morphogenic processes collectively known as cardiac chamber maturation (Moorman and Christoffels, 2003; Samsa et al., 2013).

As a part of chamber maturation, cardiac trabeculation is a tightly regulated process by which ventricular cardiomyocytes protrude and expand into the lumen of the ventricular chambers to form ridge-like muscular structures called cardiac trabeculae (Liu et al., 2010; Peshkovsky et al., 2011). Trabeculae increase cardiac output and allow for nutrition and oxygenation of the myocardium prior to coronary vascularization, and are required for establishment of the mature conduction system of the developing ventricle (Lai et al., 2010; Liu and Stainier, 2010). Thus, failure to form cardiac trabeculae causes embryonic lethality, and subtle perturbations of this process could lead to congenital cardiomyopathy (Jenni et al., 1999).

Crosstalk between endocardial and myocardial cells is important for cardiac maturation. Zebrafish *cloche* mutants that do not form endocardial cells fail to develop trabeculae and ultimately die, presumably from heart failure (Peshkovsky et al., 2011; Stainier et al., 1995). Mice deficient in the epidermal growth factor (EGF) receptor ligand Neuregulin 1 (Nrg1), which is expressed in the endocardium and signals through the myocardial ErbB4/ErbB2 receptors complex, fail to form trabeculae (Gassmann et al., 1995; Lee et al., 1995; Meyer and Birchmeier, 1995). Likewise, inhibition of Nrg1/ErbB signaling in zebrafish embryos completely blocks trabeculation (Liu et al., 2010; Peshkovsky et al., 2011;

³ This part of chapter 2 previously appeared in the journal *Development*. The original citation is Samsa, L. A., Givens, C., Tzima, E., Stainier, D. Y., Qian, L., and Liu, J. (2015) Cardiac contraction activates endocardial notch signaling to modulate chamber maturation in zebrafish. *Development*. 142, 4080-4091.

Samsa et al., 2013; Staudt et al., 2014). Notch ligands and receptors are expressed in endocardial cells during development, and Notch signaling regulates many aspects of endothelial biology including artery-vein specification, angiogenesis, and proliferation (Benedito and Hellström, 2013; Corada et al., 2014; de la Pompa and Epstein, 2012; Gridley, 2010). Upon ligand binding, the cleaved Notch receptor intracellular domain (NICD) translocates to the nucleus, where it acts as a cofactor to promote transcription of Notch effectors including EphrinB2, an essential upstream regulator of Nrg1 signaling (Grego-Bessa et al., 2007). Despite this knowledge, questions remain on whether this epistasis is a requirement for all vertebrate cardiac trabeculation, the precise spatiotemporal roles of these genes, and the roles of mediators upstream of Notch.

An increasing body of evidence suggests that the biomechanical forces generated by the functioning embryonic heart could influence cardiac chamber maturation, underscoring the importance of a dynamic relationship between cardiac form and cardiac function (Auman et al., 2007; Bartman et al., 2004; Dietrich et al., 2014; Hove et al., 2003; Kalogirou et al., 2014; Lee et al., 1995; Lin et al., 2012; Peralta et al., 2013; Stainier et al., 2002; Vermot et al., 2009; Yang et al., 2014). Interestingly, in zebrafish and chick embryos, reducing blood flow through the ventricle significantly impairs cardiac trabeculation (Auman et al., 2007; Bartman et al., 2004; Chen et al., 1996; Dietrich et al., 2014; Hove et al., 2003; Kalogirou et al., 2014; Lin et al., 2012; Peralta et al., 2013; Stainier et al., 2002; Vermot et al., 2009; Yang et al., 2014). But, how mechanical stimulus is sensed and translated into spatial and temporal signals to regulate cardiac trabeculation through regulatory interaction with other myocardial signals remains largely unexplored.

Here, we show that cardiac contraction is required for trabeculation through its role in initiating *notch1b* transcription in the ventricular endocardium. Active Notch1 signaling is detectable throughout the ventricular endocardium within 4 hours of initiation of contraction, and is restricted to the endocardial cushions during trabeculation. We further demonstrate that Notch1 activation induces the expression of its downstream effectors *ephrinb2a* (*efnb2a*) and *neuregulin-1* (*nrg1*) in the endocardium to regulate initiation of trabeculation. This endocardial-specific *notch1b* expression, and subsequent activation, requires functional primary cilia and the flow responsive transcription factor Klf2a. Also, cultured endothelial cells respond to shear stress in a cilia-dependent manner to upregulate Notch1 and its

downstream effectors, suggesting a role for primary cilia flow detection in endocardial Notch activation. Together, our findings suggest that in early cardiac morphogenesis, endocardial cells respond to cardiac contraction by detecting flow with primary cilia to regulate trabeculation by epistasis of *notch1b/efnb2a/nrg1*.

Results

Cardiac contraction is required for myocardial trabeculation

One of the earliest signs of cardiac chamber maturation is the formation of muscular, luminal protrusions called cardiac trabeculae. In zebrafish, cardiac trabeculae begin to form around 55 hpf (hours post fertilization) and are easily detectable at 3 dpf (days post fertilization) by examining cross sections of ventricle outer curvature (Liu et al., 2010; Peshkovsky et al., 2011; Staudt et al., 2014). Though the basic structure of the heart can form in the absence of myocardial function, some morphogenic events require cardiac contraction. To determine if cardiac contraction is required for trabeculation, we examined embryos deficient in *cardiac troponin T type 2a (tnnt2a)*, which encodes an essential component of the contractile apparatus (Sehnert et al., 2002). We injected *Tg(myf7:dsRed); Tg(kdrl:GFP)* double transgenic embryos (labeling cardiomyocytes and endothelial cells, respectively) with standard control or *tnnt2a* morpholinos and assessed the presence of trabeculae at 3 dpf (Fig 6A). Like *tnnt2a*^{-/-} hearts, the non-contractile *tnnt2a* morphant hearts underwent relatively unaltered looping morphogenesis and chamber formation at 3 dpf, but notably, failed to form trabeculae (Chi et al., 2008; Staudt et al., 2014) (Fig. 6B-C'').

To determine if failure to form trabeculae is due to a direct role of Tnnt2a or is more generally associated with contraction deficiency, we tested if the trabeculation defects observed in *tnnt2a* morphants could be recapitulated by chemical inhibition of cardiac contraction. We thus treated *Tg(myf7:dsRed); Tg(kdrl:GFP)* embryos with vehicle or a pharmacological inhibitor of contraction from 22 hpf to 3 dpf (Fig. 6D). The hearts of embryos treated with blebbistatin, a myosin II ATPase inhibitor, were non-contractile on day 3 and strongly resembled *tnnt2a* morphants in that both myocardial and endocardial layers formed, but trabeculae were absent in the ventricle (Fig.6E-E''). We further tested the effect of inhibition of cardiac contraction with verapamil, an L-type calcium channel blocker and observed similar results (Fig. S7A-C'). Together, these data suggest that cardiac contraction is an important regulator of cardiac trabeculation.

Cardiac contraction is required for endocardial Notch activation and *notch1b* transcription

Cardiac contraction exerts mechanical forces on both myocardium and endocardium, and trabeculation requires crosstalk between these two layers (Tian and Morrisey, 2012; Wagner and Siddiqui, 2007). Thus, we next sought to determine if any signaling pathways are activated in the ventricle in response to cardiac contraction. Using *Tg(Tp1:EGFP)* Notch reporter embryos in which the Notch1 responsive TP1 module drives EGFP as a fluorescent readout for active Notch1 signaling (Parsons et al., 2009), we assessed Notch activation in control and *tnnt2a* morphants (Fig. 8A). At 48-50 hpf, Notch activation in control morphants hearts was robust in the ventricular endocardium and atrioventricular canal (AVC) with occasional weak signal detectable in the atrium (Fig. 8B-C"). Interestingly, Notch activation was below detection in *tnnt2a* morphant hearts of embryos examined in whole mount or in confocal images (Fig. 8D-E"). In contrast, Notch signaling was robust in the brains of control and *tnnt2a* morphants, indicating a specific role for cardiac contraction in regulating endocardial Notch signaling (Fig. 8B,D). Similar results were observed with DMSO and blebbistatin-treated embryos compared to control and *tnnt2a* morphants, respectively (Fig. 9A-C"). These data indicate that cardiac contraction is required for Notch activation in the endocardium at 2 dpf.

We next sought to identify the primary Notch receptor mediating Notch activation in the endocardium. Using a previously described morpholino to knockdown *notch1b* (Milan et al., 2006; Wang et al., 2010) in *Tg(Tp1:EGFP); Tg(myf7:dsRed)* double transgenic embryos, cardiac Notch activation was below detection in *notch1b* morphants hearts at 48-50 hpf (Fig. 8F-G"). To determine whether cardiac contraction regulates Notch1 activation by controlling *notch1b* gene transcription, we performed *in situ* hybridization at 48-50 hpf. *notch1b* expression mirrors *Tg(Tp1:EGFP)* Notch reporter expression in the heart at 48 hpf, but was below detection in *tnnt2a*^{-/-} hearts (Fig. 8H,I). Thus, cardiac contraction controls Notch1 signaling by regulating *notch1b* expression. Together, these findings indicate that cardiac contraction regulates *notch1b* at the transcript level in the heart. Our studies do not exclude the possibility that the mechanical forces associated with contraction may also regulate Notch receptor activation.

Spatiotemporal pattern of Notch activation

To better understand how Notch activation might stimulate trabeculation, we characterized the spatiotemporal pattern of Notch activation in the developing zebrafish heart using the *Tg(Tp1:VenusPest)*

Notch reporter transgenic line which express, under control of the Tp1 Notch response element, a partially-destabilized fluorescent protein with a half-life around 2 hours as compared to 24 hours half-life of GFP protein (Aulehla et al., 2008; Ninov et al., 2012). The use of this reagent afforded us greater spatial and temporal resolution to determine the time window of Notch activation in the ventricular endocardium. VenusPest expression was first detectable in the endocardium at 28 hpf, just 4 hours after initiation of contraction, with substantial spatial bias towards the end of the heart tube containing ventricular cardiomyocytes (Fig. 10A). VenusPest expression in the ventricular endocardium persisted until 55 hpf, after which it declined in parts of ventricular endocardium lining the outer curvature (Fig. 10B-D). By 72 hpf, VenusPest expression was primarily restricted to AVC endocardium, and was retained in the AVC through at least 4 weeks post fertilization (Fig. 10E,F, Fig. 11A-A'). Thus, within the limits of reporter expression, Notch signaling is activated throughout the ventricular endocardium shortly after initiation of contraction, but becomes inactive shortly after the initiation of cardiac trabeculation and is completely restricted to the AVC by 3 dpf.

Cardiac contraction promotes trabeculation through notch1b/efnb2a/nrg1 epistasis

Our data demonstrate that, while Notch is required for trabeculation, it is not active in the ventricular endocardium during trabeculation, indicating that it controls trabeculation through intermediate signaling pathways. A recent report by Dietrich et al., demonstrated that blood flow and Bmp signaling regulate zebrafish endocardial chamber morphogenesis in a Vegf signaling-independent manner (Dietrich et al., 2014). Interestingly, endocardial Notch activation and myocardial trabeculation appear to be independent of canonical Vegf signaling (Fig. 12A-M). However, the arterial endothelial marker gene *EphrinB2* (*Efnb2*) is required for trabeculation in mice directly downstream of the Notch1 transcriptional complex and upstream of Neuregulin1 (*Nrg1*) (Grego-Bessa et al., 2007). We evaluated the role of these genes in cardiac trabeculation by assessing trabeculation at 3 dpf in *notch1b* and *efnb2a* morphants. Using previously described splice-blocking morpholinos for *notch1b* and *efnb2a* (Milan et al., 2006; Wang et al., 2010), we knocked down their expression by at least 75% in the heart (Fig. 13A-D). At 3 dpf, *notch1b* and *efnb2a* morphants lacked trabeculae, while control morphants had trabeculae in the outer curvature (Fig. 14A-C'). To test further whether that Notch signaling is required for trabeculation in zebrafish, we examined *mindbomb1* (*mib1*) mutants that are defective in Notch signaling due to a loss of

function point mutation in the gene *mindbomb E3 ubiquitin protein ligase 1*. *mib1* encodes an E3 ubiquitin ligase required for canonical trafficking of Notch ligands (Itoh et al., 2003). At 3 dpf, trabeculae were completely lacking in the ventricle of these mutant embryos (Fig 15A-B).

To test if *ephrinb2a* and *nrg1* could act downstream of Notch signaling to control cardiac trabeculation, and to establish the epistasis of these genes in zebrafish cardiac maturation, we assessed their expression in the zebrafish heart and found that *notch1b*, *efnb2a*, *nrg1* and their principle ligand or receptor partners are expressed at 48-50 hpf (Fig. 16). We isolated hearts at 48-50 hpf and found that *tnnt2a* morphants had significant reduction in *notch1b*, *efnb2a*, and *nrg1* expression, while *notch1b* morphants had significant reduction in *efnb2a* and *nrg1* transcripts levels (Fig. 14D,E). In contrast, *notch1b* expression and Notch activation pattern was not affected in *efnb2a* morphants, but *nrg1* expression was significantly reduced (Fig. 14F, Fig.17A-D). Notably, these defects in gene expression do not reflect failure of the endocardium to form, as both endocardium and myocardium are present at 3 dpf (Fig. 14A-C'). Combined, these data suggest that cardiac contraction is required for trabeculation by activating a regulatory *notch1b/efnb2a/nrg1* pathway.

Next, we asked if forced activation of Notch signaling could bypass the requirement for cardiac contraction in trabeculation. To this end, we overexpressed the Notch intracellular domain to activate Notch signaling using the *Tg(hsp701:gal4); Tg(UAS:NICD)* system in control and *tnnt2a* morphants carrying the *Tg(tp1:EGFP)* and *Tg(myf7:dsRed)* transgenes (Fig. 18A). All embryos were exposed to 37°C heat shock to activate Gal4 expression and, as an indication of forced Notch activation, we observed a dramatic increase in *tp1:EGFP* across all somatic tissues in approximately 25% of control and *tnnt2a* morphants at 48 hpf (Fig. 18B). We isolated hearts from control and *tnnt2a* morphants and found significant upregulation of *efnb2a* and *nrg1* expression in *tnnt2a* morphants hearts with NICD overexpression at 2-3 dpf (Fig. 18C-D). However, this upregulation was not sufficient to induce cardiac trabeculation in *tnnt2a* morphants (Fig. 18E-H).

Primary cilia are required for Notch activation in endocardial cells

We next asked how endocardial cells detect cardiac contraction to modulate Notch in the ventricle. Cardiac contraction exposes endocardial cells to mechanical forces across many different length and time scales (Bartman et al., 2004; Boselli et al., 2015; Lee et al., 2013; Vermot et al., 2009).

Endocardial cells are particularly well positioned to detect hemodynamic forces including shear stress (the frictional force of parallel flow). Endothelial primary cilia—microtubule based sensory organelles that, in certain hemodynamic environments, protrude into the lumen of blood vessels—have a well-established role in detecting low levels of flow (Culver and Dickinson, 2010; Hahn and Schwartz, 2009; Slough et al., 2008; Van der Heiden et al., 2006). Recently, Goetz et al., demonstrated that endothelial primary cilia in the zebrafish vasculature are highly sensitive to low magnitude shear forces from 24-28 hpf to regulate vascular development (Goetz et al., 2014). Thus, we hypothesized that primary cilia play a key role in flow detection, leading to *notch1b* upregulation and Notch1 activation in endocardial cells.

We validated the presence of primary cilia on endocardial cells around the time of Notch1 activation using *Tg(actb2:Arl13b-GFP)* transgenic embryos where Arl13b-GFP localizes to primary cilia (Borovina et al., 2010). Though promoter activity for this transgene is higher in myocardial than endocardial cells, primary cilia can be detected in both cell layers (Fig. 19A-B). Owing to their potential role in flow detection, we focused on characterizing endocardial primary cilia. At 30 hpf, individual endocardial cells of un-injected embryos, control morphants, and *tnnt2* morphants possess a single, primary cilium projecting into the lumen of the heart (Fig. 20A-B', Fig. 21A-B"). This indicates that endocardial cells possess primary cilia, and that ciliation is independent of cardiac contraction.

Mutations in *intraflagellar transport 88 (ift88)* cause ciliopathies in zebrafish (Kramer-Zucker et al., 2005; Lunt et al., 2009; Neugebauer and Yost, 2014; Tsujikawa and Malicki, 2004) and *ift88* morphants have deficiencies in endothelial primary cilia formation (Goetz et al., 2014). Similarly, we observed mislocalization of Arl13b-GFP in *ift88* morphants (arrowheads, Fig. 21A-C). To test if endocardial primary cilia are involved in zebrafish ventricular endocardial Notch1 activation, we knocked down *ift88* in *Tg(Tp1:VenusPest); Tg(myf7:dsRed)* double transgenic embryos and evaluated Notch1 activation in the morphants. Compared to control morphants, VenusPest expression was either undetectable or restricted to a few cells in the heart in cilia-deficient *ift88* morphants (Fig. 20C-D'). Importantly, these morphants also exhibited reduced trabeculation (Fig. 20E-F'). Using images from whole-mount embryos, we compared mean fluorescence intensity of VenusPest in the ventricle and found a significant reduction in VenusPest expression in *ift88* morphants compared to control morphants (Fig. 20G). Additionally, we

isolated hearts from *ift88* morphants and found a significant reduction in *notch1b* and *nrg1* expression (Fig. 20H,I).

Primary cilia are required at the onset of flow for Notch1 activity

Though our data supports a model in which primary cilia respond to luminal flow to activate Notch transcription, the loss of endocardial Notch activation in *ift88* morphants could be secondary to a role for primary cilia in early embryogenesis (Gerdes et al., 2009; Sasai and Briscoe, 2012). To address this possibility, we used a pharmacological approach to define when primary cilia are necessary for endocardial Notch activation. Ciliobrevin D (CBD) inhibits the AAA+ ATPase motor cytoplasmic dynein and significantly reduces the microtubule cycling necessary to construct and maintain primary cilia (Firestone et al., 2012). We treated *Tg(Tp1:VenusPest)* positive embryos with DMSO or CBD starting at 18-24 hpf and assessed VenusPest expression at 42-48 hpf (Fig. 22A-D). DMSO injection at any of these times had no effect on VenusPest expression level (Fig. 22A,B,E). Embryos injected with CBD at 18 or 20 hpf had reduced VenusPest expression (Fig. 22C,E), while embryos injected with CBD from 22 or 24 hpf were indistinguishable from DMSO injected controls (Fig. 22D,E). Given a time delay between initiation of treatment and sufficient accumulation for biological effects, these data suggest that Notch1 expression in the endocardium requires primary cilia in a short time window coinciding with the onset of flow.

Primary cilia likely detect low magnitude shear stress to upregulate Notch in ventricular endocardial cells

Primary cilia have two well-defined, independent functions—facilitating Hedgehog (Hh) signaling and detecting low magnitude shear stress (Anderson, 2006; Egorova et al., 2012; Goetz et al., 2014; Hierck et al., 2008; Roy, 2012; Van der Heiden et al., 2011; Wilson and Stainier, 2010). To determine whether Hh signaling is necessary for endocardial Notch activation, we treated *Tg(Tp1:VenusPest)*; *Tg(myI7:dsRed)* Notch reporter embryos with cyclopamine to antagonize Hh signaling downstream of primary cilia (Chen et al., 2002; Stanton and Peng, 2010). Embryos treated with cyclopamine from 4-48 hpf exhibited severe body axis deformities indicative of successful inhibition of Hh signaling (Fig. 23A,B). Embryos treated with cyclopamine from 18-48 hpf and 24-48 hpf did not exhibit defects in Notch activation (Fig. 23C-J). This argues against a role of canonical Hh signaling in controlling endocardial

Notch activation, and implicates primary cilia flow detection in endocardial Notch activation and cardiac trabeculation.

Flow magnitude and directionality influence the biological responses elicited in endothelial cells. Though our data indicate that flow is important for activating Notch, the differential roles of shear stress magnitude and flow directionality are unclear. In zebrafish, shear stress and retrograde flow at 2 dpf can be manipulated through knockdown of *gata1a* and *gata2a*—two transcription factor genes important for hematopoiesis (Vermot et al., 2009). Interestingly, reducing hematocrit to reduce shear stress and altering retrograde flow fraction in this manner lead to neither reduced Notch reporter expression at 48 hpf nor loss of trabeculation by 80 hpf (Fig. 24A-M). Increasing retrograde flow fraction by knocking down *gata2a*, with or without co-knockdown of *gata1a* slightly increased Notch activation in the ventricle, though reduced ventricle size could also contribute to this phenotype (Fig. 24E-F). Since we see Notch activation as early as 28 hpf, which is before the hematocrit comprises a large fraction of blood volume, we suggest that these results support a role for low levels of flow in Notch activation and cardiac trabeculation.

Since contraction and flow cannot be decoupled in the developing zebrafish ventricle by existing genetic means, we used an *in vitro* model of shear stress to directly assess the role of primary cilia shear stress detection in regulating *Notch1* expression. We used immortalized mouse embryonic endothelial cells (MLECs), which are known to upregulate Notch pathway genes in response to shear stress, to model endocardial cilia-dependent flow responses (Sweet et al., 2013). MLECs were pretreated with either DMSO as vehicle control or CBD to inhibit primary cilia formation and exposed for 0 or 4 hours to low magnitude shear stress (<2 dynes/cm²) comparable to the fluid forces exposed to endocardial cells in early heart development (Goetz et al., 2014). We observed significant elevation in *Notch1*, *Efnb2*, and *Nrg1* in DMSO treated MLECs compared to static controls. Interestingly, this upregulation was inhibited by CBD treatment (Fig. 20J-L). MLECs pre-treated with either DMSO or CBD demonstrated dynamic regulation of the flow-response gene, *Krüppel-like factor 2* (*Klf2*), suggesting that some non-cilia based flow detection mechanisms are not perturbed by CBD treatment (Fig. 25 A-B). Interestingly, *klf2a* was also required for endocardial Notch activation and trabeculation (Fig. 26 A-G). Thus, shear stress stimulates endothelial cells to increase expression of *Notch1*, *EphrinB2*, and *Nrg1* in a myocardium-

independent manner. Combined, these data indicate that primary cilia are important mediators of shear stress to regulate endocardial Notch signaling prior to trabeculation.

Together, our data support a model in which cardiac contraction initiates flow, which is detected by primary cilia on endocardial cells to activate a regulatory *notch1/efnb2a/nrg1* pathway and promote cardiac trabeculation (Fig. 27).

Discussion

Trabeculation, the formation of muscular protrusions which increase myocardial mass prior to coronary vascularization, is an essential aspect of ventricle maturation (Liu et al., 2010; Moorman and Christoffels, 2003; Samsa et al., 2013; Sedmera et al., 2000). Though previous work clearly demonstrated the utility of zebrafish embryo in studying cardiac morphogenesis, mechanistic detail has been lacking to describe how mechanical forces guide the cellular changes that execute heart chamber maturation in zebrafish. In this study, we present evidence supporting a model in which flow, caused by cardiac contraction, is detected by primary cilia on endocardial cells to stimulate *notch1b* expression and regulate trabeculation through *notch1b/efnb2a/nrg1* epistasis. Thus, our study reveals a molecular mechanism that links flow sensing and cell signaling to ventricular maturation in the developing heart.

Our previous work demonstrated that ErbB2 is required to initiate trabeculation in the heart at 2 dpf (Liu et al., 2010). Examining this phenotype further, we found that eliminating cardiac contraction by injection of *tnt2a* morpholino prevented trabeculation and endocardial Notch activation, but did not affect *erbb2* expression levels in the heart. Thus, we hypothesized that cardiac contraction controls expression of the *erbb2/erbb4* ligand, *nrg1* to modulate trabeculation. Previous studies in mouse indicate a critical role of an endocardial *Notch1/EphrinB2/Nrg1* regulatory pathway in cardiac trabecular formation (Grego-Bessa et al., 2007). We asked whether these genes are required downstream of cardiac contraction for zebrafish cardiac trabeculation. Indeed, *notch1b* and *efnb2a* morphants lacked cardiac trabeculae at 3 dpf, and gene expression analysis confirmed epistasis of *notch1b/efnb2/nrg1* with respect to cardiac contraction. Although the potential off-target effects of morpholinos could limit our interpretation of the morphant phenotypes, the fact that *notch1b* morphants and *mib1* mutants exhibit a similar trabecular defect supports a role of Notch signaling in cardiac trabeculation. In addition, our data are also supported by the work from the de la Pompa group showing that *Efnb2* acts directly downstream of *Notch1* to

regulate trabeculation (Grego-Bessa et al., 2007). In addition to the trabeculation defect, we noticed separation of the endocardium and myocardium. This separation is also evident in sections and SEM of mouse embryos with genetic deletion of *Notch1*, *Efnb2*, *Nrg1*, and *Bmp10* (Grego-Bessa et al., 2007). Whether this is due to failure of the cardiac jelly to degrade or detachment of the endocardium remains to be determined, but it appears to be a defect common to many trabeculation phenotypes.

Notch signaling plays many roles in heart development. In zebrafish, we had the opportunity to directly observe the pattern of Notch activation with fine spatial and temporal resolution. The highly stereotyped spatiotemporal distribution of Notch signaling that we observed (Fig. 10A-F) is interesting for several reasons. First, though our data reaffirm the importance of Notch in vertebrate trabeculation, our study indicates a somewhat different pattern of Notch activation in zebrafish heart development. In zebrafish, Notch is active shortly after initiation of blood flow and is not active in the ventricular endocardium during trabeculation. In mice, the NICD is localized in the nucleus of endocardial cells from E8.5-9.5 during the first stages of trabeculation, and subsequently is preferentially localized in the nuclei of endocardial cells at the base of trabeculae (Grego-Bessa et al., 2007). This might reflect differential roles of Notch signaling in zebrafish versus mouse heart development, possibly due to differences in heart size and timing of major morphogenic processes. Second, the spatial segregation of Notch activation between ventricle, atrium, and AVC endocardium from 1-3 dpf suggests that there are previously underappreciated, underlying differences between endocardial cells in these spatially distinct regions, leading to different roles in the maturing heart. Whether their difference in Notch activation are intrinsic properties or due to differential cues derived from the overlying myocardium remains to be seen.

In this study, we also provided evidence suggesting that functional primary cilia are required at the onset of flow for *notch1b* expression in the ventricular endocardium of the developing heart. This expression is important for Notch activation and cardiac trabeculation. Cardiac contraction and blood flow are intimately associated and cannot be easily decoupled in the developing zebrafish ventricle by genetic means. Though endocardial cells may arise from either vascular endothelial cells or cardiac progenitors, they are a type of endothelial cell and are highly sensitive to flow (Bussmann et al., 2007; Kattman et al., 2006; Milgrom-Hoffman et al., 2011; Moretti et al., 2006; Vermot et al., 2009). We used an *in vitro* system to apply low magnitude flow to endothelial cells to model endocardial, cilia-dependent flow responses and

found that flow stimulated *Notch1*, *Efnb2*, and *Nrg1* expression in the absence of myocardial-derived factors or circulating factors in the bloodstream. This upregulation was blocked by pretreating cells with ciliobrevin D (CBD), a small molecule which inhibits the dynein motor protein responsible for trafficking microtubules to primary cilia (Firestone et al., 2012). Notably, though CBD treatment reduces the size and number of primary cilia, it also regulates mitotic spindle formation and organelle transport (Firestone et al., 2012). Thus, our interpretation does not account for the possibility that our observed effects may be due to non-specific effects of CBD.

Though our data showed that a *notch1b/ephrinb2a/nrg1* pathway is required for cardiac chamber maturation, it is not the only genetic network activated by cardiac contraction and involved in trabeculation. Trabeculation is a complex morphogenic event that requires precise coordination of molecular and cellular events in both myocardial and endocardial cells. We found that, though forced NICD expression was sufficient to upregulate *efnb2a* and *nrg1* in *tnnt2a* morphants, it did not induce trabeculation. Curiously, it was also insufficient to rescue trabeculation in *ift88* morphants (unpublished data). Since NICD was overexpressed in all tissues, we suspect that the lack of trabeculation may be due to an inhibitory role of myocardial Notch1 signaling in cardiac trabeculation as well as a loss of other primary cilia downstream signaling. It will be interesting to use separate myocardial and endocardial Gal4 lines to investigate the precise spatiotemporal role of Notch activation in regulating chamber morphogenesis. Additionally, deficiencies in the luminal protrusions extended by cardiomyocytes during trabeculation, which are unstable in *tnnt2a* morphants, could limit trabeculation in *tnnt2a* morphants (Staudt et al., 2014).

Our work prompts many important questions about primary cilia and the role of hemodynamics in cardiac morphogenesis. Much of the work on the role of hemodynamics in endocardial morphogenesis has focused on valvulogenesis. Owing to its position in the heart, the AVC is exposed to an extremely dynamic flow environment in the embryo. Since primary cilia disassemble in high shear stress environments (Iomini et al., 2004) and Notch activity becomes restricted to the AVC after 3 dpf, it will be interesting to explore the differential role of primary cilia for Notch activation in AVC and ventricular endocardium. Others have found that modifying the hemodynamic environment in the heart can alter the position of trabeculae, suggesting that other mechanosensors may be involved in later cardiac

morphogenesis (Peshkovsky et al., 2011). Interestingly, the flow response gene *klf2a* is upstream of *notch1b* (Vermot et al., 2009) and is required for Notch activation and cardiac trabeculation. However, neither lowering the magnitude of shear stress nor altering the retrograde flow fraction using *gata 1a*, *gata2a*, or *gata 1a/2a* morpholinos, as described in Vermot et al. (2009) was capable of preventing endocardial Notch activation or trabeculation; thus, much work remains to be done in order to define the precise hemodynamic cues involved in endocardial Notch activation.

Our work, combined with a recent study showing that primary cilia bending in response to blood flow is a major regulator of vascular development from 24-28 hpf (Goetz et al., 2014), strongly suggest that primary cilia are involved in sensing low magnitude shear stress *in vivo* to regulated cardiovascular morphogenesis. The precise mechanism by which primary cilia detect flow is an area of active research. One theory suggests that stretch-activated TRP channels coupled to primary cilia at the membrane are activated when primary cilia bend, leading to increased intracellular calcium and intracellular signaling (Goetz et al., 2014; Yoshida et al., 2012). Interestingly, mutations in mechanosensitive TRP family demonstrate major valve defects, and TRP channel activity appears to depend on an oscillatory flow pattern (Heckel et al., 2015).

Overall, our data support a model in which endocardial primary cilia are the physical mechanism by which endothelial cells detect low flow to stimulate endocardial *notch1b* expression in the zebrafish heart to promote ventricle chamber maturation. Future studies are needed to determine the precise role of primary cilia in detecting flow in the developing heart.

Materials and methods

Zebrafish husbandry and stocks

All animals were maintained at the UNC-CH aquaculture facility in accordance with IACUC approved protocols (Westerfield, 2000). The zebrafish lines used in this study are as follows: *tnnt2a*^{b109} (Sehnert et al., 2002), *mib*^{ta52b} (Itoh et al., 2003; Jiang et al., 1996; van Eeden et al., 1996), *Tg(myI7:GFP)*^{twu26} (Huang et al., 2003), *Tg(myI7:dsRed)*^{vc6} (Rothschild et al., 2009), *Tg(myI7:mkateCAAX)*^{sd11} (Lin et al., 2012), *Tg(kdrl:EGFP)*^{s843} (Jinn et al., 2005), *Tg(kdrl:mCherry)*^{s896} (Bertrand et al., 2010), *Tg(tp1:EGFP)*^{um14} (Parsons et al., 2009), *Tg(tp1:VenusPest)*^{s940} (Ninov et al., 2012), *Tg(-1.5hsp70l:Gal4)*^{kca4} (Scheer and Campos-Ortega, 1999), *Tg(UAS:notch1a-intra ICD)*^{kca3}

(Scheer et al., 2001) and *Tg(actb2:Arl13b-GFP)^{hsc5Tg}* (Borovina et al., 2010). In all studies, embryos were maintained at 28.5° in either embryo water or system water and treated continuously with 0.003% 1-phenyl 2-thiourea (PTU) starting at 20-24 hpf.

Morpholino injections

Morpholino oligonucleotides (see Table 1) were diluted in 5mM HEPES containing 0.05% phenol red and 1 nl injected into a minimum of 100 embryos at the one cell stage.

Drug treatments

For pharmacological inhibitor studies, dechorinated embryos were treated in 4 ml of 6 μM blebbistatin (Cell Signaling) in embryo water or 200 μg/mL verapamil (Sigma) in 1% DMSO containing embryo medium (5 mM NaCl, 0.17 mM KCl, 0.33 mM CaCl₂, and 0.33 mM MgSO₄, pH 6.8–6.9).

Microscopy imaging and processing

Anesthetized embryos were mounted with 1% low-melt agarose (Sigma) in embryo medium or system water and manually oriented for optimal visual access to the heart. Epifluorescence images were collected on a Leica M205C fluorescence stereoscope. For live epifluorescence imaging, agarose-mounted embryos were submerged in system water and examined at 100X magnification on a Leica M205C fluorescence stereoscope equipped with a high speed monochrome camera. The heart was filmed for 15-30 seconds at 30 frames per second, with 10-75 ms exposure for bright field and fluorescence. After live imaging, embryos were either euthanized or used for confocal imaging (see below). Movies were decompressed and exported as single frames using VirtualDub Program (GNU licensed, available at <http://www.virtualdub.org>). ImageJ (Schneider et al., 2012) was used to select frames and overlay channels representative of end diastole (images) and to quantify mean fluorescence intensity in the ventricle at end systole (quantification). Data was collected for a minimum of 10 embryos and quantified using ImageJ. Imaging was performed as described above with the following modifications. Embryos imaging for Notch reporter quantifications in Figures 12, 22, and 23 were anesthetized and imaged directly in system water rather than mounted in low-melt agarose.

For confocal imaging, agarose-mounted embryos were euthanized with 5-10X Tricaine and imaged after cessation of cardiac contraction. Confocal z-stacks were collected using an Olympus

Fluoview 1000MPE equipped with a 20X XLPlan water immersion objective (NA 1.0) with 2.5X optical zoom. Fluoview software was used to collect images through the top 75% of heart with a minimum of 512x512 pixels resolution and 1-2 μm spacing between z-slices. Fluoview's brightness correction algorithm was used to account for signal attenuation with increasing depth. ImageJ (Schneider et al., 2012) was used to process images. For each Z-stack, we selected either a maximum projection image of the whole stack or a representative mid-chambers slice for the appropriate analysis. Confocal data was collected for a minimum of 3 embryos for each condition, with matching controls for each experiment, where the N>3 embryos were selected as the representative samples from a pool of a minimum of N>12 embryos which were visually inspected for phenotype. To accommodate relatively low expression levels of Arl13b-GFP in *Tg(actb:Arl13b-GFP)* endocardial cells, Figures 19, 20, and 21 confocal images were collected with a wider pinhole for a 2.0 μm optimal z-slice.

In situ hybridization

In situ hybridization was performed as previously described (Liu and Stainier, 2010). *In situ* hybridization probe for *notch1b* was prepared as previously described (Milan et al., 2006) and synthesized from pGEMT vector (Promega) using the DIG RNA labeling kit (Roche). Whole-mount embryo imaging was performed on a Leica MZ16F fluorescence stereomicroscope.

Heart isolation

Hearts were manually isolated from euthanized embryos at 48-72 hpf using a Leica M205C fluorescence stereomicroscope and visualizing cardiac tissue using *Tg(my17:EGFP)* signal, then trimmed free of non-cardiac tissue and transferred to ice-cold lysis buffer. Tissue was homogenized and RNA was isolated from the homogenate using the Qiagen RNeasy Micro kit (Qiagen). Single-strand complement DNA synthesis was performed on freshly isolated RNA using BioRad's iScript cDNA synthesis kit. At least 10 hearts were pooled for each condition.

Cell culture

MLEC (immortalized mouse lung endothelial cells) were prepared as described previously (Sweet et al., 2012). MLECs passage 38-45 were cultured on gelatin-coated plastic tissue culture plates and

maintained in DMEM (Gibco, 11995), 10% FBS (Sigma), 1% penicillin/streptomycin (Gibco), 1% non-essential amino acids (Gibco), and 0.009% β -mercaptoethanol.

In vitro shear stress

Confluent, cobblestone stage MLECs were starved for 12-16 hours in culture media (above) containing 1% FBS then pre-treated with DMSO or 50 μ M ciliobrevin D (Millipore) for 2 hours prior to administration of flow. Shear stress, 2 dynes/cm², was generated using a previously described cone and plate viscometer (Sorescu et al., 2004). After 0, 1, or 4 hr exposure to shear stress, cells were washed with ice-cold PBS then lysed and RNA extracted using Trizol (Invitrogen) according to manufacturer's instructions. RNA was reverse-transcribed using Superscript III First-Strand Synthesis Supermix (Invitrogen) and gene expression assessed as described below.

Expression analysis

For qRT-PCR, NCBI's Primer-BLAST was used to design exon-spanning, gene-specific SybrGreen primers. All primers were validated by high resolution melt analysis, size confirmation, RNA-only, and no-template controls. See Table 2 for primer sequences. SybrGreen real-time PCR was performed in triplicate using Viia7 real-time PCR system (Invitrogen). For quantification, we used the $\Delta\Delta$ CT method in which raw CT values were normalized to *actb* as a housekeeping gene and appropriate baseline condition, then calculated fold-change as $2^{\Delta\Delta CT}$.

Isolation and imaging juvenile hearts

Hearts were dissected from euthanized fish at 4 weeks post-fertilization, and were then fixed in ice-cold 4% paraformaldehyde for 2 hrs on ice. Hearts were mounted in low-melt agarose as described in the Methods section of the accompanying manuscript. Confocal z-stacks were collected using an Olympus Fluoview 1000MPE equipped with a 20X XLPlan water immersion objective (NA 1.0) with 2.5X optical zoom. Fluoview software was used to collect images through the top 75% of heart at 512x512 pixels resolution with 2.5 μ m spacing between z-slices. Fluoview's brightness correction algorithm was used to account for signal attenuation with increasing depth. ImageJ (Schneider et al., 2012) was used to process images and create maximum projection images. N \geq 3 hearts were examined.

Drug treatments

For pharmacological inhibitor studies, embryos were treated with drugs as described below in embryo water (5 mM NaCl, 0.17 mM KCl, 0.33 mM CaCl₂, and 0.33 mM MgSO₄, pH 6.8–6.9) at 28.5°. Figure 7—embryo water was supplemented with 0.003% 1-phenyl 2-thiourea (PTU) and 200 µg/mL verapamil (Sigma) or vehicle (ddH₂O). Figure S2—embryo water was supplemented with PTU at 6 µM blebbistatin (Cell Signaling) and DMSO to 1% final or 1% DMSO vehicle. Figure 9—embryo water was supplemented with PTU and 5 µM PTK787 (Cell Signaling), also known as vatalanib, or vehicle (ddH₂O). Figure 22—ciliobrevinD (CBD) was purchased from Tocris and dissolved in DMSO at 10 mM and stored at -20 until use. Embryos 18-24 hpf were anesthetized with Tricaine and 3-5 nL of CBD or DMSO was injected directly into the yolk as described previously (Milan et al. 2003). Embryos that survived injection were raised in embryo water supplemented with PTU. Figure 23—embryo water was supplemented with 50 µM cyclopamine (Cayman Chemical) diluted in EtOH to 0.2% final or 0.2% EtOH vehicle.

Statistical analysis

Values are presented as means ± s.e.m. Statistical significance was determined by one-sample T-test (between one group and a reference value) or Student's T-test (between two groups).

Chapter 2.2 Figures

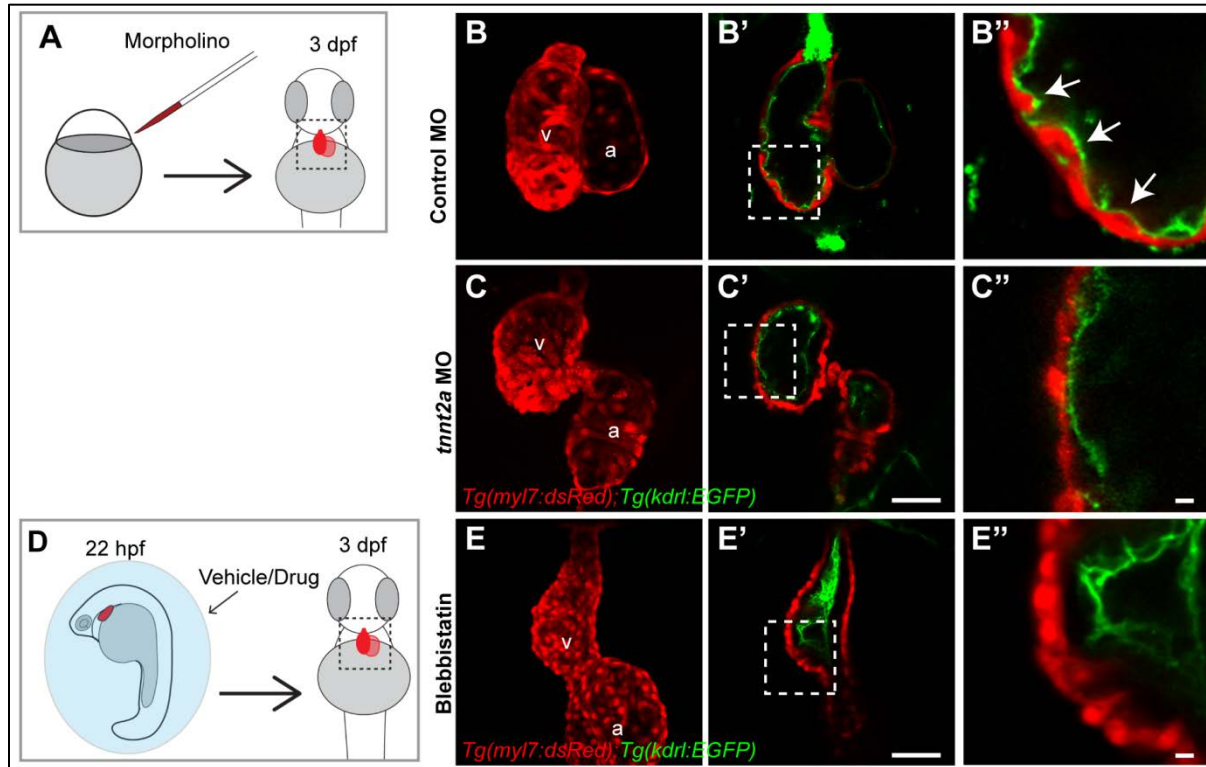


Figure 6 Cardiac contraction is required for myocardial trabeculation

(A) Schematic of morpholino injection at one cell stage or (D) pharmacological inhibition of cardiac contraction (6 μ M blebbistatin) from 22 hpf. The morpholino injected or chemical treated *Tg(kdrl:EGFP);Tg(myI7:dsRed)* double transgenic embryos were allowed to develop further and examined for cardiac trabecular phenotypes at 3 dpf. (B,C,E) Maximum projection of confocal z-stacks reveals the overall shape of the heart. (B',C',E') Mid-chamber confocal optical section of the same hearts shown in (B,C,E). (B'',C'',E'') Magnified high resolution images of the cardiac regions marked by dotted lines in (B',C',E'). White arrows point to trabeculae, a = atrium, v = ventricle. Scale bars (E') 50 μ m and (E'') 10 μ m.

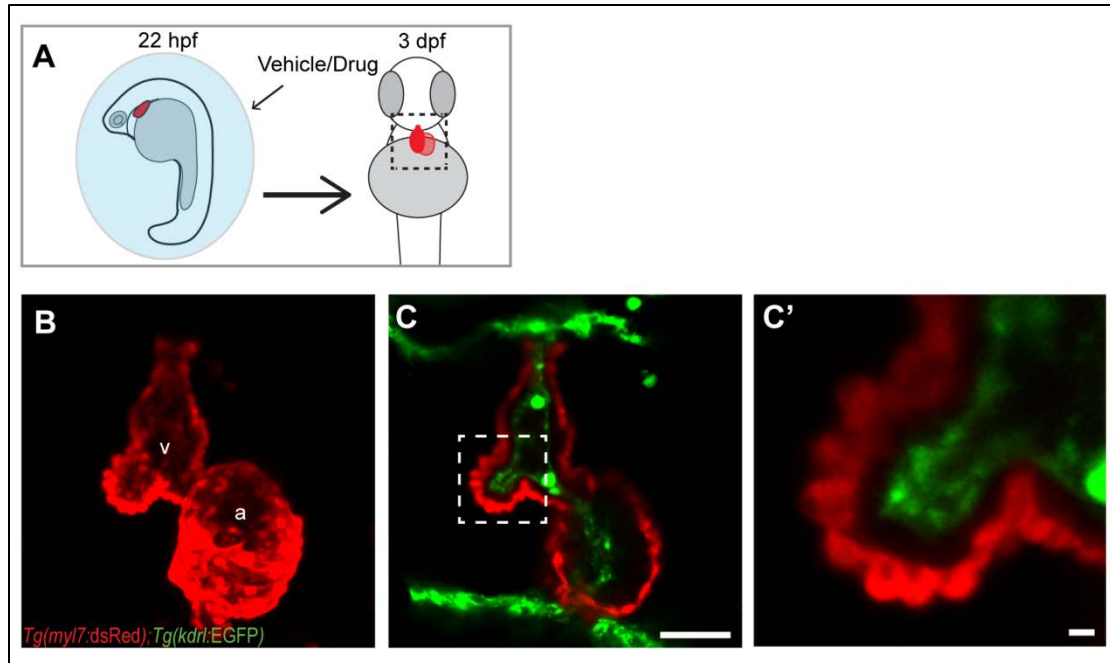


Figure 7 Verapamil treated embryos do not form trabeculae

(A) Experiment schematic. (B-D) *Tg(myI7:dsRed); Tg(kdrl:EGFP)* double transgenic embryos were bathed in 250 $\mu\text{g}/\text{mL}$ verapamil or vehicle from 22 hpf to 3 dpf and the hearts were imaged by confocal microscopy. (B) Confocal z-projection, (C) mid-chamber section, and (C') magnified view of representative verapamil-treated heart. Scale bars (B) 50 μm (C) 10 μm . v=ventricle, a=atrium.

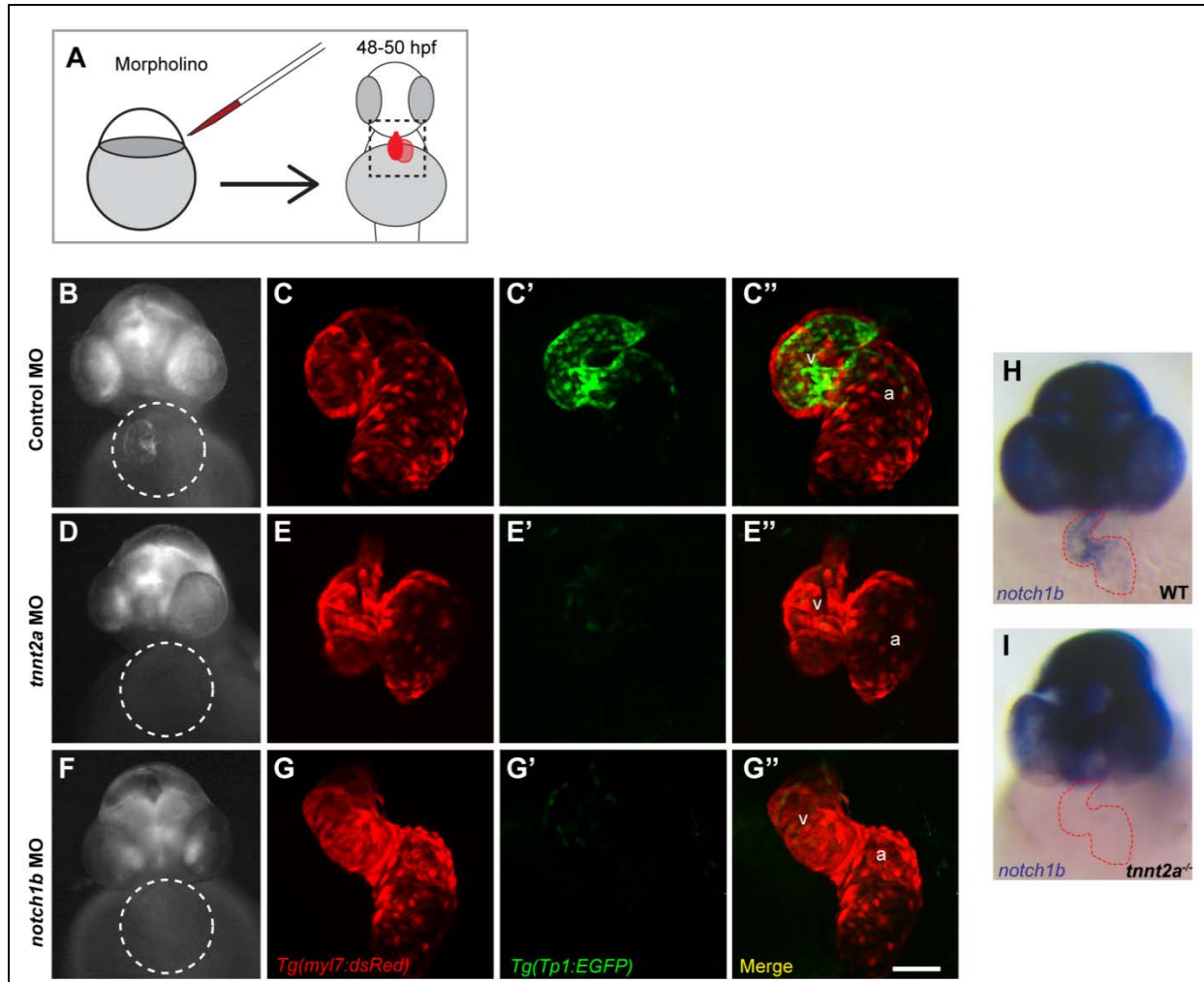


Figure 8 Cardiac contraction is required for endocardial Notch activation and *notch1b* transcription

(A) Morpholino gene knock-down experiment schematic where double transgenic *Tg(tp1:EGFP);Tg(myI7:dsRed)* embryos were injected with (B,C) control, (D,E) *tnnt2a*, or (F,G) *notch1b* morpholinos and imaged at 48-50hpf. (B,D,F) Representative whole mount images of Notch reporter with cardiac regions highlighted by circles. (C,E,G) Confocal maximum intensity projections of the hearts shown in (B,D,F) with cardiomyocytes labeled in red, (C',E',G') Notch reporters in green, and (C'',E'',G'') colocalized signal in yellow. Minimal colocalization indicates Notch activation is in endocardial cells. (H, I) Whole mount *notch1b* riboprobe hybridization in (H) control (I) and *tnnt2a*^{-/-} embryos with the heart outlined in red. Scale bar is 50 μ m, a = atrium, and v = ventricle.

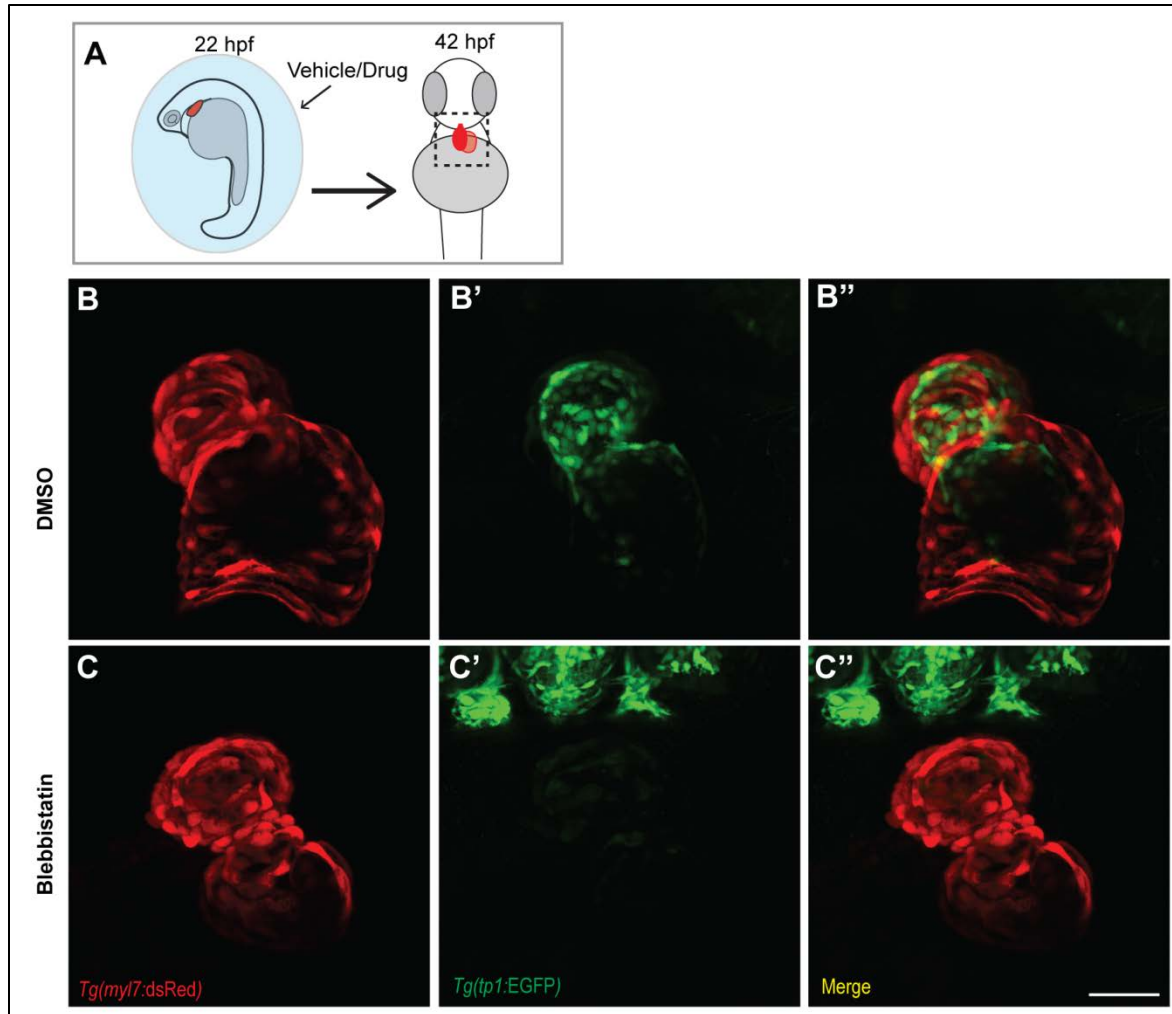


Figure 9 Notch signaling is not active in the hearts of blebbistatin treated embryos

(A) Experiment schematic where zebrafish embryos were bathed in DMSO or 6 μ M blebbistatin from 22 hpf to 42 hpf. (B-C) The hearts of *Tg(myf7:dsRed)*; *Tg(tp1:EGFP)* double-transgenic embryos treated with DMSO (B) or blebbistatin (C) were imaged by confocal microscopy. (B',C') Confocal z-projection of cardiomyocyte marker, (B'',C'') confocal z-projection of Notch reporter signal and (B'',C'') merged signals. Scale bar 50 μ m

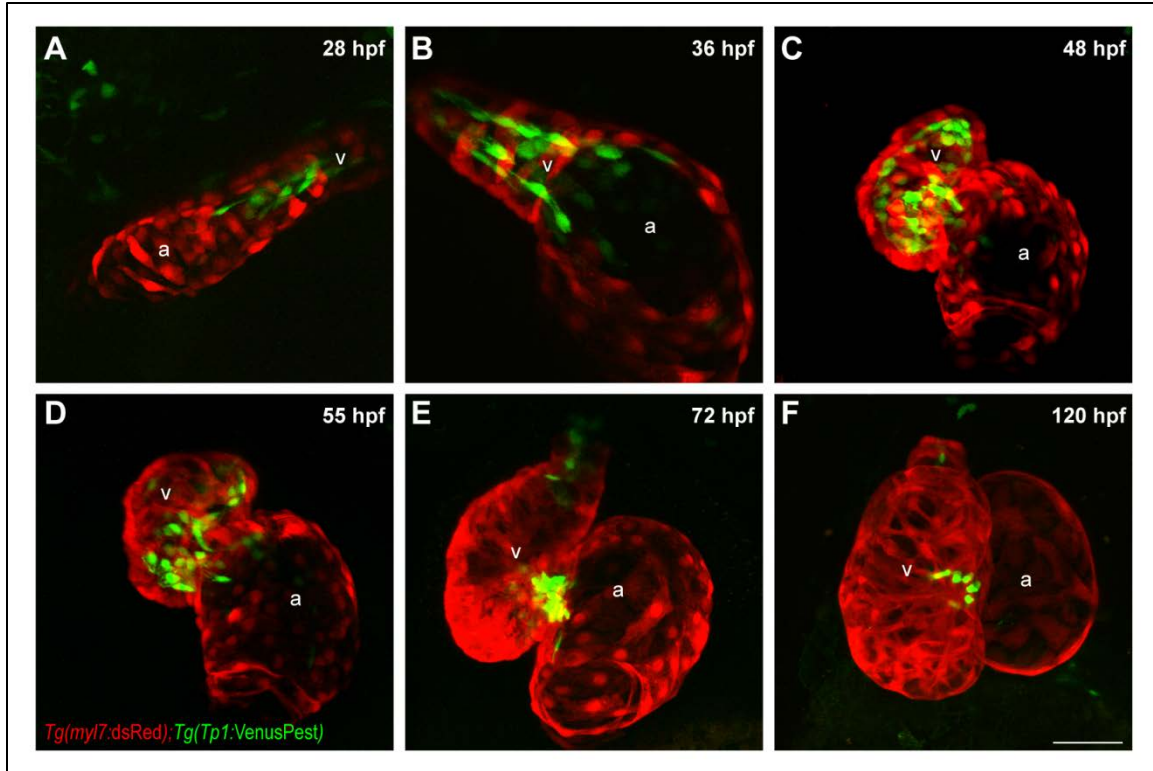


Figure 10 Notch activation in the ventricular endocardium

(A-F) Confocal z-stack maximum intensity projection of hearts from double transgenic *Tg(tp1:VenusPest);Tg(myI7:dsRed)* embryos at designated time points with *Tp1:VenusPest* expression in green and cardiomyocytes marked in red. Scale bar is 50 μ m, a = atrium, and v = ventricle.

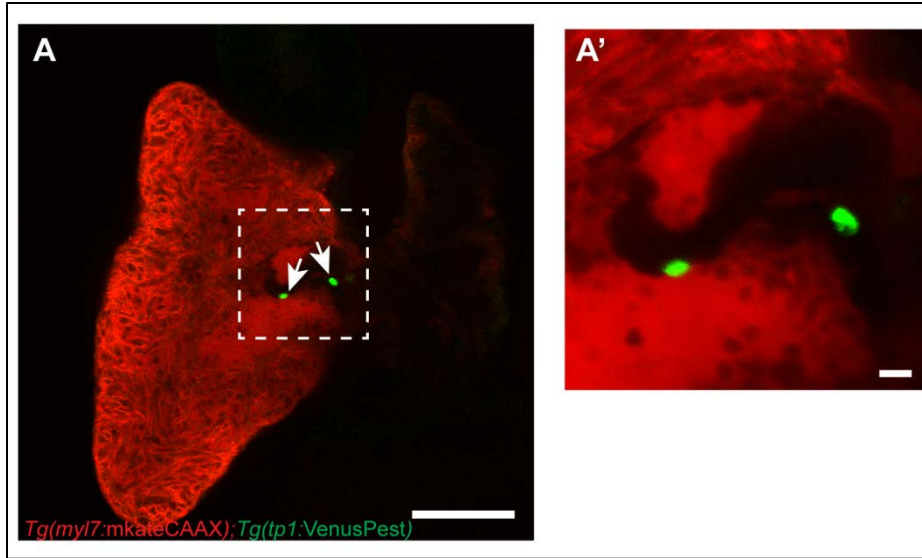


Figure 11 Notch activation at 4 weeks post-fertilization

(A) Representative maximum projection of ventricle isolated from *Tg(myl7:mkateCAAX); Tg(tp1:VenusPest)* larva at 4 weeks post-fertilization. The inset marked by dotted lines is magnified in (B). Arrow points to Notch reporter expression. Scale bar 100 μ m.

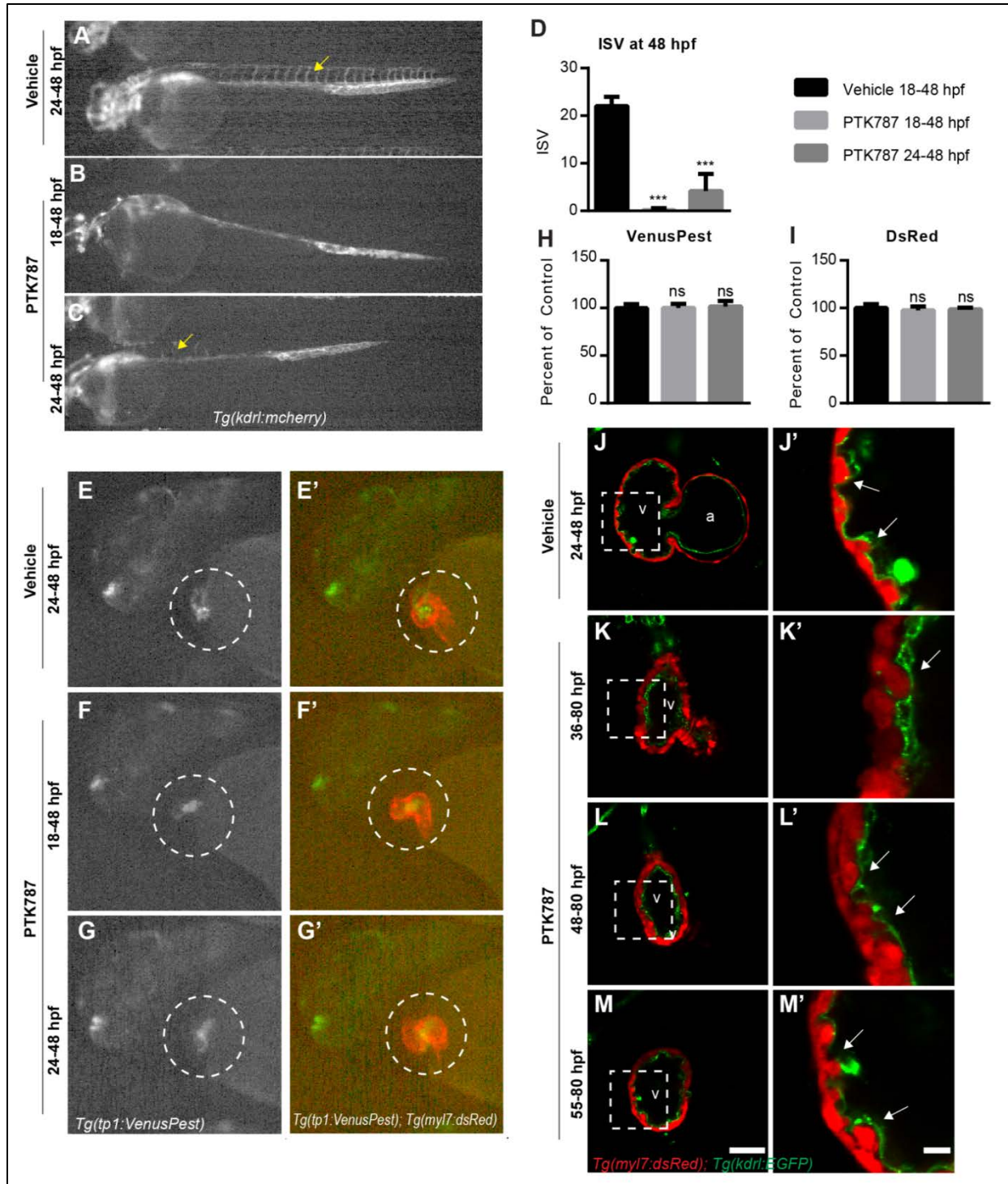


Figure 12 Notch activation in the developing endocardium is not inhibited by PTK787

(A-C, E-G) Representative images of whole mounted embryos carrying *Tg(kdrl:mcherry)* or *Tg(tp1:VenusPest)*; *Tg(myf7:dsRed)* transgenes treated with (A,E) vehicle from 24-48hpf, or 5 μ M PTK787 from (B,F) 18-48 hpf or (C,G) 24-48 hpf. (A-C) Lateral view of endothelial cell marker. Yellow arrows point to representative intersegmental vessels. (D) Average number of intersegmental vessels detected at 48 hpf. (E-G) Representative images of Notch reporter signal in gray and (E'-G') Notch reporter signal in green merged with cardiomyocyte signal in red where white circles designate cardiac region. (H) Mean fluorescence intensity of VenusPest Notch reporter and (I) DsRed cardiomyocyte

reporter mean fluorescence levels in the ventricle. (J-M) Mid-chamber confocal optical section showing cardiomyocytes (red) and endocardial cells (green) in *Tg(myh7:dsRed); Tg(kdrl:EGFP)* embryos treated with (J) vehicle from 24-48 hpf or 5 μ M PTK787 from (K) 36-80 hpf, (L) 48-80 hpf, or (M) 55-80 hpf. (J',K',L', M') The cardiac regions highlighted by dotted lines are shown as magnified high resolution images. White arrows point to trabeculae, ISV = intersegmental vessel, a = atrium, v = ventricle. Scale bars are (M) 50 μ m and (M') 10 μ m. Error bars are s.e.m. Students T-test compared to vehicle control. N=6-12 embryos.

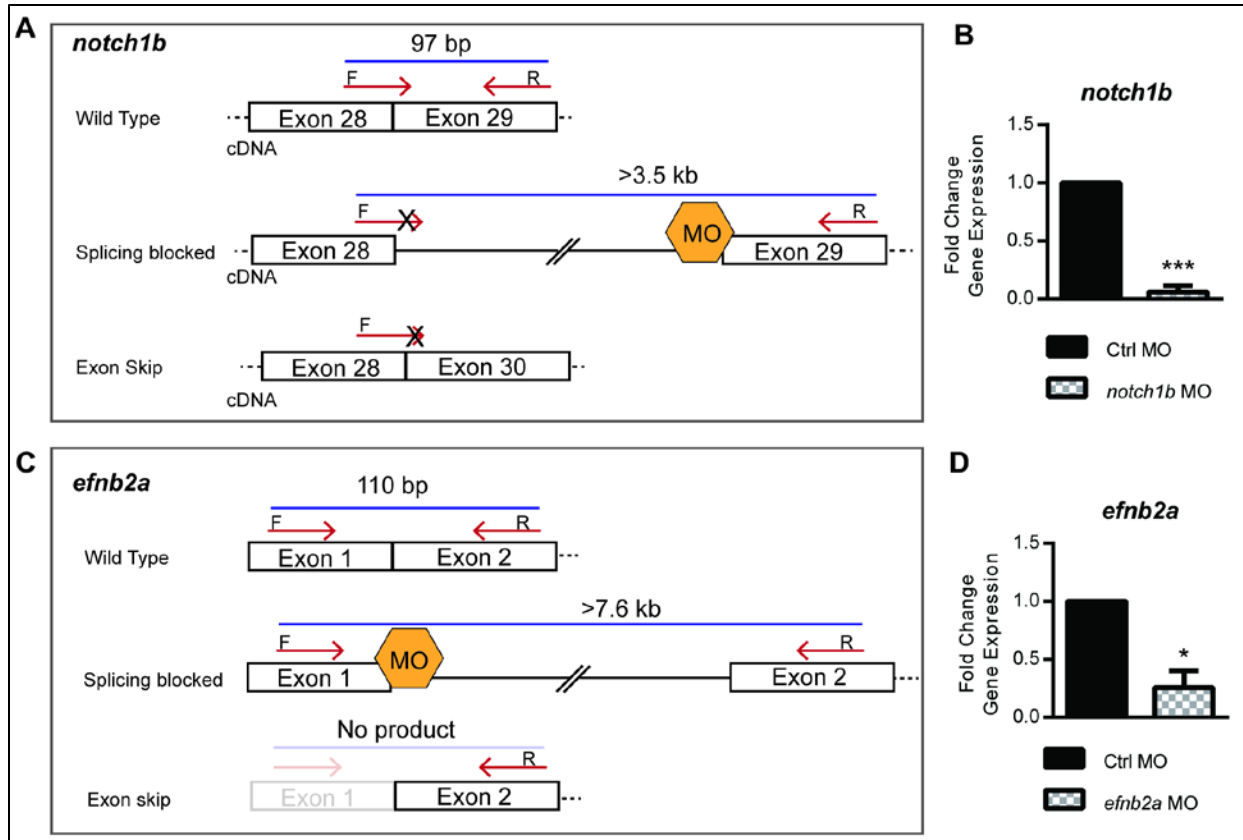


Figure 13 *Notch1b* and *efnb2a* splice blocking MO gene expression quantification

(A,C) Schematic of (A) *notch1b* (B) *efnb2a* cDNA demonstrating expected qRT-PCR products for wild type splicing, splice blocking from morpholino interference, and exon skipping. Forward and reverse primers are indicated with red arrows. Blue line shows expected product with annotated size. Morpholino recognition site is marked with yellow symbol. (B) Relative expression of wild type spliced *notch1b* mRNA in control morphant and *notch1b* morphant hearts by qRT-PCR using primers designated in (A). (D) Relative expression of wild type spliced *efnb2a* mRNA in control morphant and *efnb2a* morphant hearts by qRT-PCR using primers designated in (C). MO = morpholino. Error bars are s.e.m. One-sample T-test compared to normalized control value = 1. N=3-5 biological replicates.

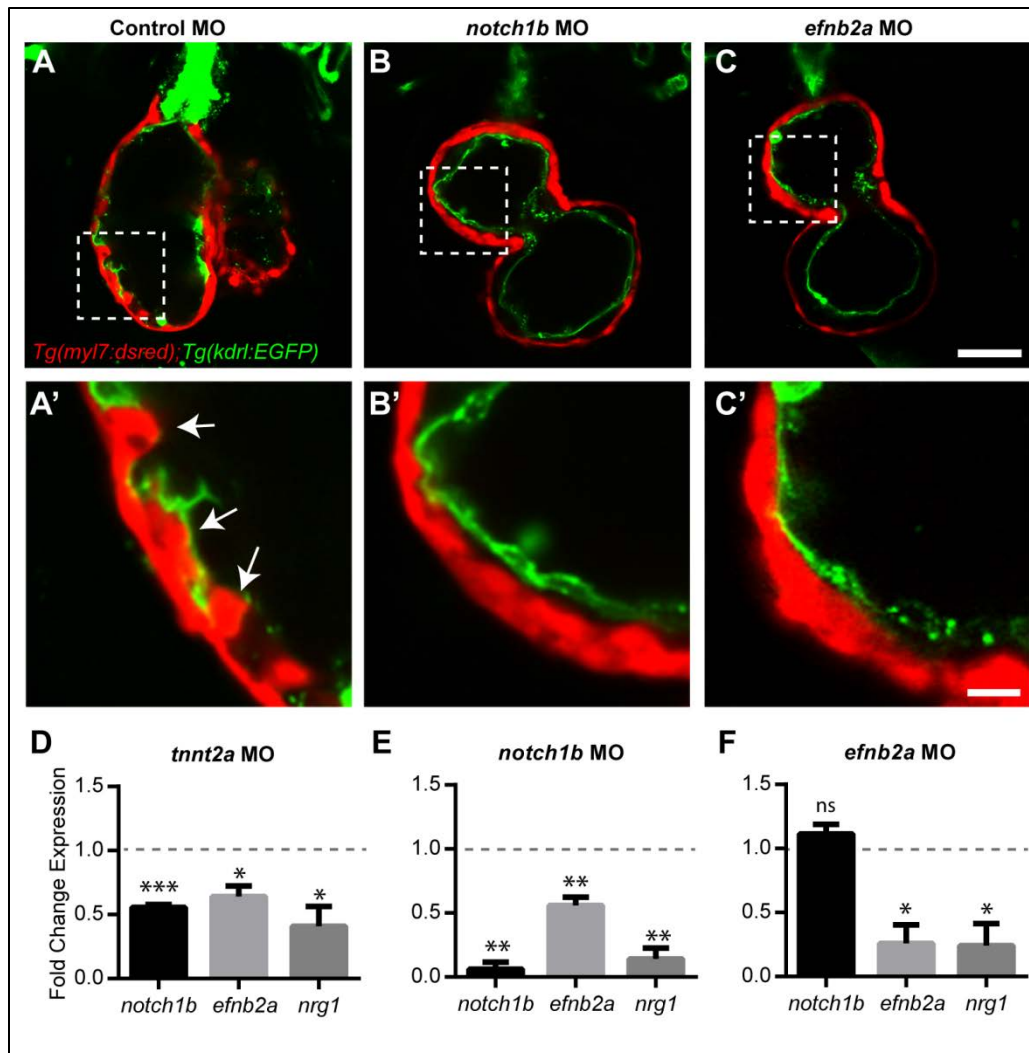


Figure 14 Cardiac contraction promotes trabeculation through *notch1b/efnb2a/nrg1* epistasis

(A,B,C,D) Mid-chamber confocal optical section of *Tg(myI7:dsRED);Tg(kdrl:EGFP)* double transgenic (A) control, (B) *notch1b*, and (C) *efnb2a* morphant hearts showing cardiomyocytes in red and endocardial cells in green. (A',B',C') Magnified high resolution images of the cardiac regions highlighted by dotted lines in (A,B,C). Expression of *notch1b*, *efnb2a*, and *nrg1* in hearts isolated from (D) *tnnt2a*, (E) *notch1b*, and (F) *efnb2a* morphants compared normalized to expression in control morphant hearts (dotted line). * $p \leq 0.05-0.01$, ** $p \leq 0.01-0.001$, *** $p < 0.001$ compared to control morphants (one-sample T-test compared to control morpholino fold change = 1). Error bars are s.e.m. White arrows point to trabeculae. Scale bars are (D) 50 μm and (D') 10 μm .

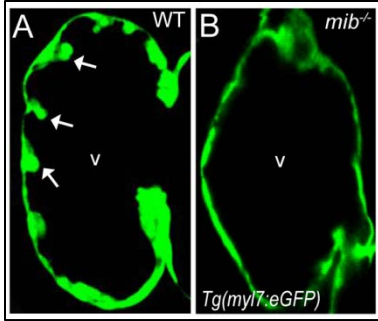


Figure 15 Trabeculation in *mib1* mutant embryos

(A,B) Representative confocal mid-chamber section of the ventricle of (A) WT and (B) *mib1* mutant embryos carrying *Tg(myl7:eGFP)* cardiomyocyte reporter at 3 dpf. White arrows point to trabeculae; v=ventricle.

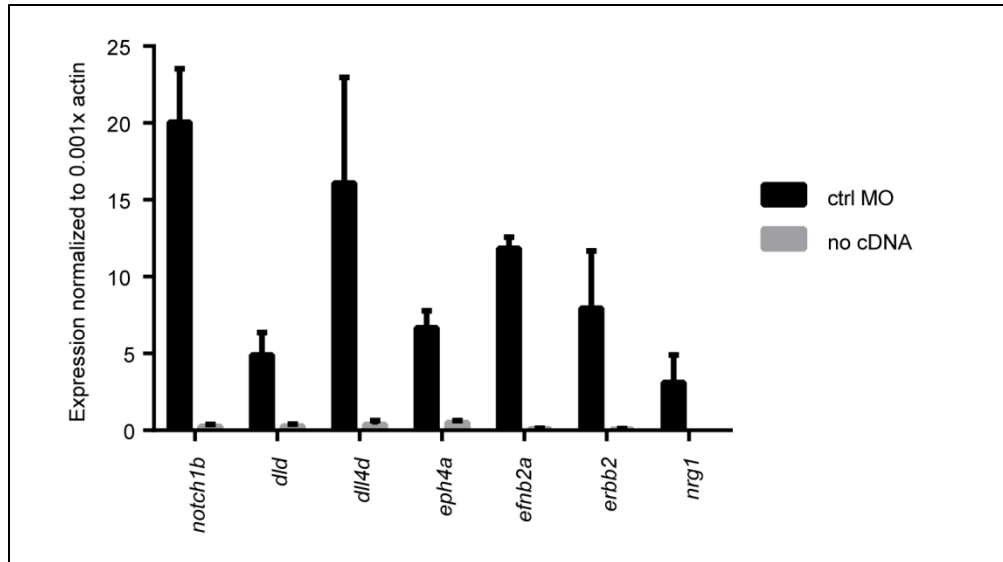


Figure 16 Gene expression at 48hpf

(A) Gene expression in control morphant hearts isolated from *Tg(myI7:EGFP)* embryos at 48 hpf. Expression is relative to 0.001x actin by the Δ CT method and reported as fold change by $2^{\Delta(\Delta$ CT). No-template control is normalized to average actin CT. MO = morpholino, *dld* = *deltaD*, *dll4* = *delta-like 4*, *eph4a* = *eph receptor A4a*, *efnb2a* = *ephrin-B2a*, *erbb2* = *erb-b2 receptor tyrosine kinase 2*, *nrg1* = *neuregulin 1*. Error bars are s.e.m. Students T-test. N=3-5 biological replicates.

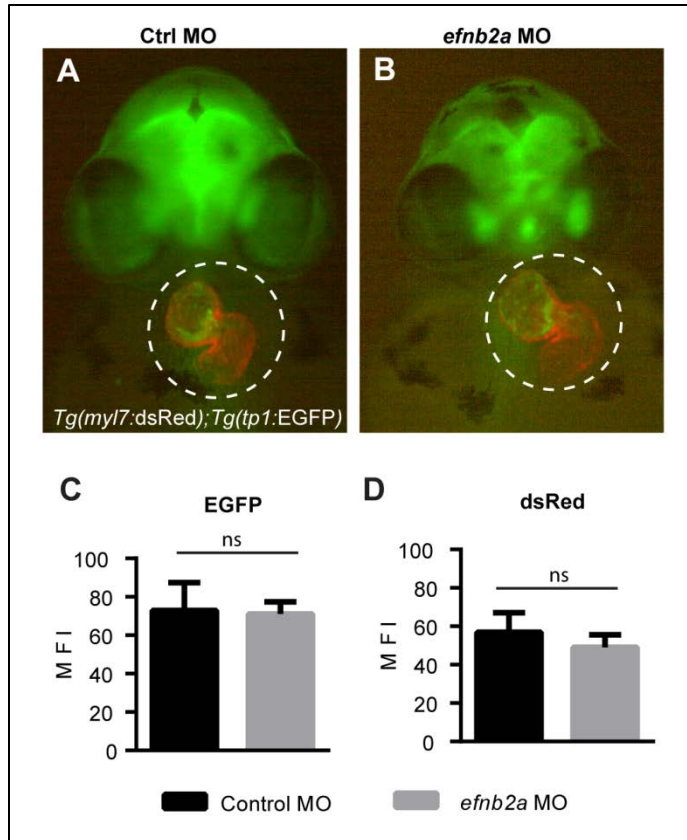


Figure 17 Notch activation pattern in *efnb2a* morphants

(A-B) Representative images of Notch reporter (green) and cardiomyocytes (red) of whole mount embryos injected with (A) control or (B) *efnb2a* morpholinos. Dotted lines note cardiac region. (C and D) Quantification of EGFP (C) Notch reporter signal and (D) cardiomyocyte dsRed mean fluorescence intensity (MFI) in the ventricle of N=8 hearts. Error bars are s.d. Students T-test, ns = $p > 0.05$.

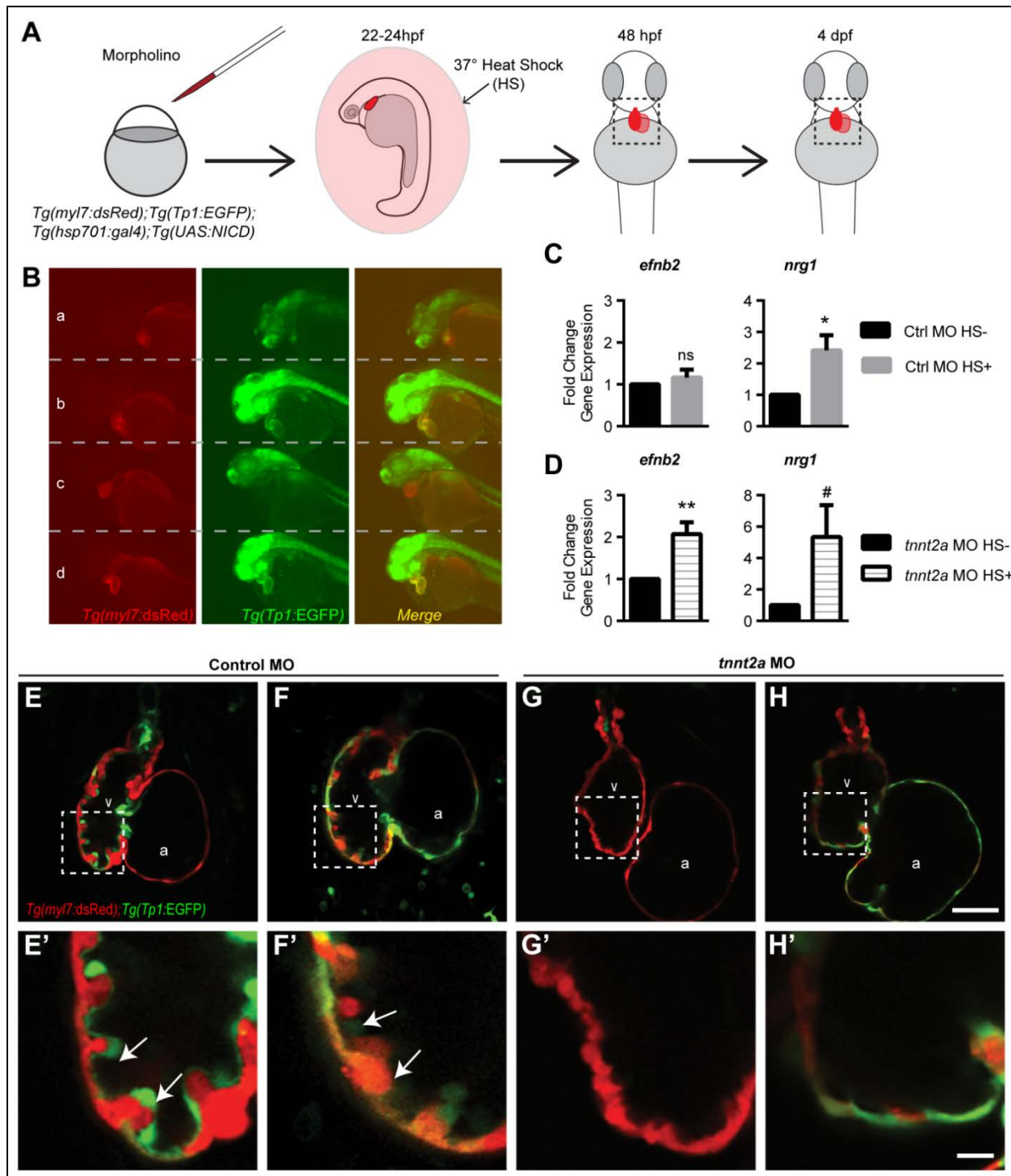


Figure 18 Notch1 activation rescues *efnb2a* and *nrg1* expression in non-contractile hearts

(A) Experimental schematic of morpholino injection and heat-shock overexpression of NICD. qRT-PCR and imaging were performed to examine gene expression and trabecular phenotype at 2-3dpf and 4 dpf, respectively. (B) Representative whole mount images of cardiomyocytes (red) and Notch reporter (green) in (1,2) control and (3,4) *tnnt2a* morphants at 48hpf (1,3) without or (2,4) with NICD overexpression. (C,D) Expression of *efnb2a* and *nrg1* in hearts isolated from (C) control morphants and (D) *tnnt2a* morphants comparing gene expression in embryos with or without NICD overexpression. (E-H) Confocal mid-chamber optical section of 4 dpf hearts with dotted lines marking

the inset magnified in (E'-H'). # $p \leq 0.075-0.05$, * $p \leq 0.05-0.01$, ** $p \leq 0.01-0.001$, *** $p < 0.001$ compared to control morphants (one-sample T-test compared to control morpholino fold change = 1). Error bars are s.e.m. White arrows highlight trabeculae. HS- = heat shock control without NICD overexpression. HS+ = heat shock control with NICD overexpression, a = atrium, and v = ventricle, NICD = Notch intracellular domain. Scale bars are (H) 50 μm and (H') 10 μm .

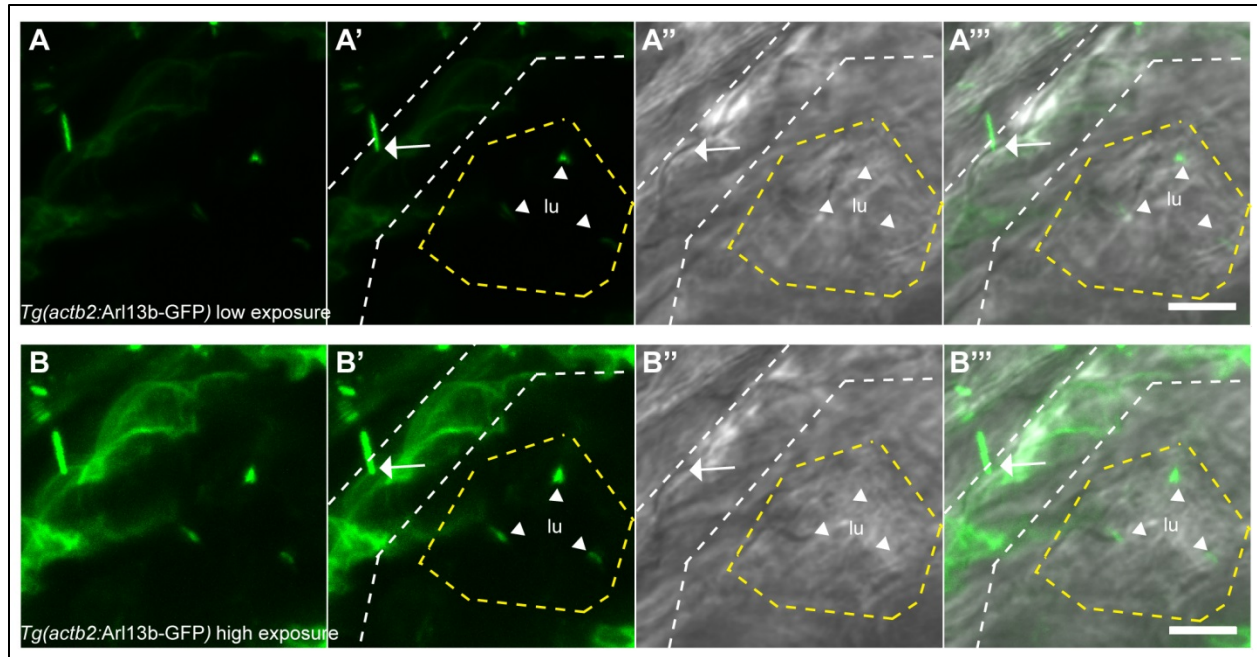


Figure 19 Primary cilia are detectable in myocardium and endocardium

(A-B) Representative confocal images of *Tg(actb2:Ar13b-GFP)* and brightfield images of a single heart at 30hpf using (A) low and (B) high exposures to emphasize primary cilia on myocardial and endocardial cells, respectively. (A'-A''', B'-B''') Boundaries of the myocardial layers are noted by white dotted lines and endocardial boundaries by yellow dotted lines. The white arrow points to a primary cilium protruding from a myocardial cell. White arrowheads point to endocardial primary cilia identified in B. Lu=lumen. Labels are overlaid on (A',B') Ar13b-GFP images, (A'',B'') brightfield image, and (A''',B''') merged Ar13b-GFP and brightfield views. Scale bar is 5 μ m.

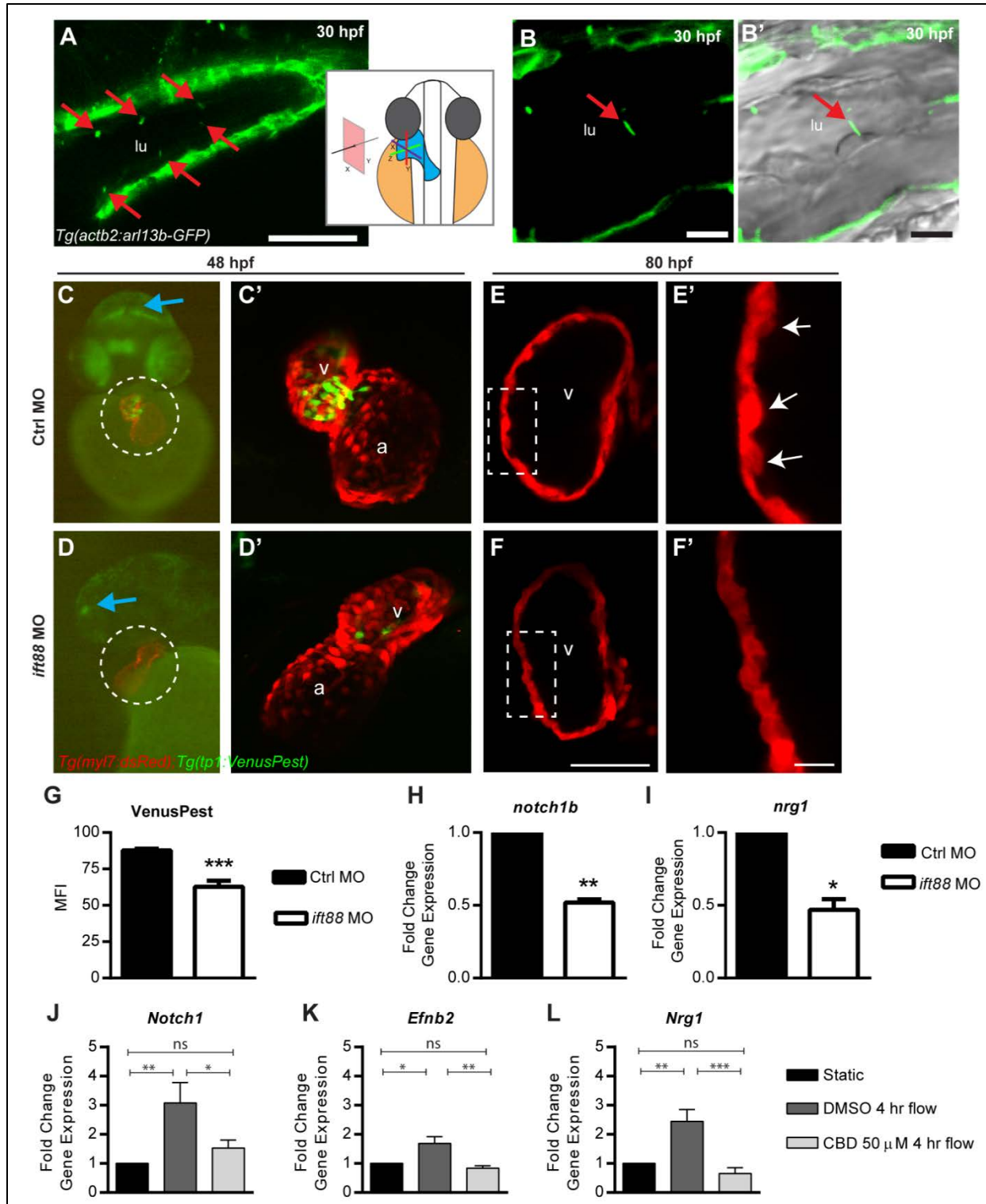


Figure 20 Shear stress promotes *notch1* expression in a primary-cilia dependent manner

(A-B') The hearts of *Tg(actb2:Ar13b-GFP)* embryos were examined by confocal microscopy to assess primary cilia localization in the endocardium. (A) *Tg(actb2:Ar13b-GFP)* reporter expression in the heart. Lower bottom, schematic indicates orientation of the heart and confocal section relative to the whole embryo at 30 hpf. (B) High resolution view of *Ar13b-GFP* merged with (B') bright field image demonstrating colocalization of the primary cilium base with an

endocardial cell. (C,D) Whole mount *Tg(myI7:dsRed); Tg(tp1:VenusPest)* double transgenic (C) control and (D) *ift88* morphants at 48hpf. The hearts are marked with dashed circles. (C',D') Confocal maximum projection of the heart from the individual embryos shown in (C) and (D) overlaying cardiomyocytes (red) and Notch reporter (green). (E,F) Confocal optical section of the (E) control and (F) *ift88* morphant embryo cardiomyocytes (red) at 80 hpf. The insets marked by dotted line were magnified in (E',F'). (G) Quantification of ventricular Notch reporter (EGFP) mean fluorescence intensity (MFI) from whole mount embryos at 48 hpf. (H-I) Relative expression of (H) *notch1b* and (I) *nrg1* in control and *ift88* morphant hearts. (J-L) Expression of (J) *Notch1*, (K) *Efnb2*, and (L) *Nrg1* in DMSO or 50 μ M CBD treated MLECs that were exposed to 2 dynes/cm² shear stress for 4 hours compared to static DMSO and CBD treated controls. Red arrows highlight *Ar13b-GFP* in the endocardium. Blue arrows highlight Notch reporter signal in neural tissue. White arrows highlight trabeculae. *p \leq 0.05-0.01, **p \leq 0.01-0.001, ***p $<$ 0.001 compared to control morphants (one-sample T-Test compared to 1.0 fold change or Student's T-test). Error bars are s.e.m. Scale bars are (A) 50 μ m, (B, B', F') 10 μ m, and (F) 100 μ m. LU = lumen, a = atrium, v = ventricle, MFI = mean fluorescence intensity, MLEC = mouse lung endothelial cell, CBD = ciliobrevin D

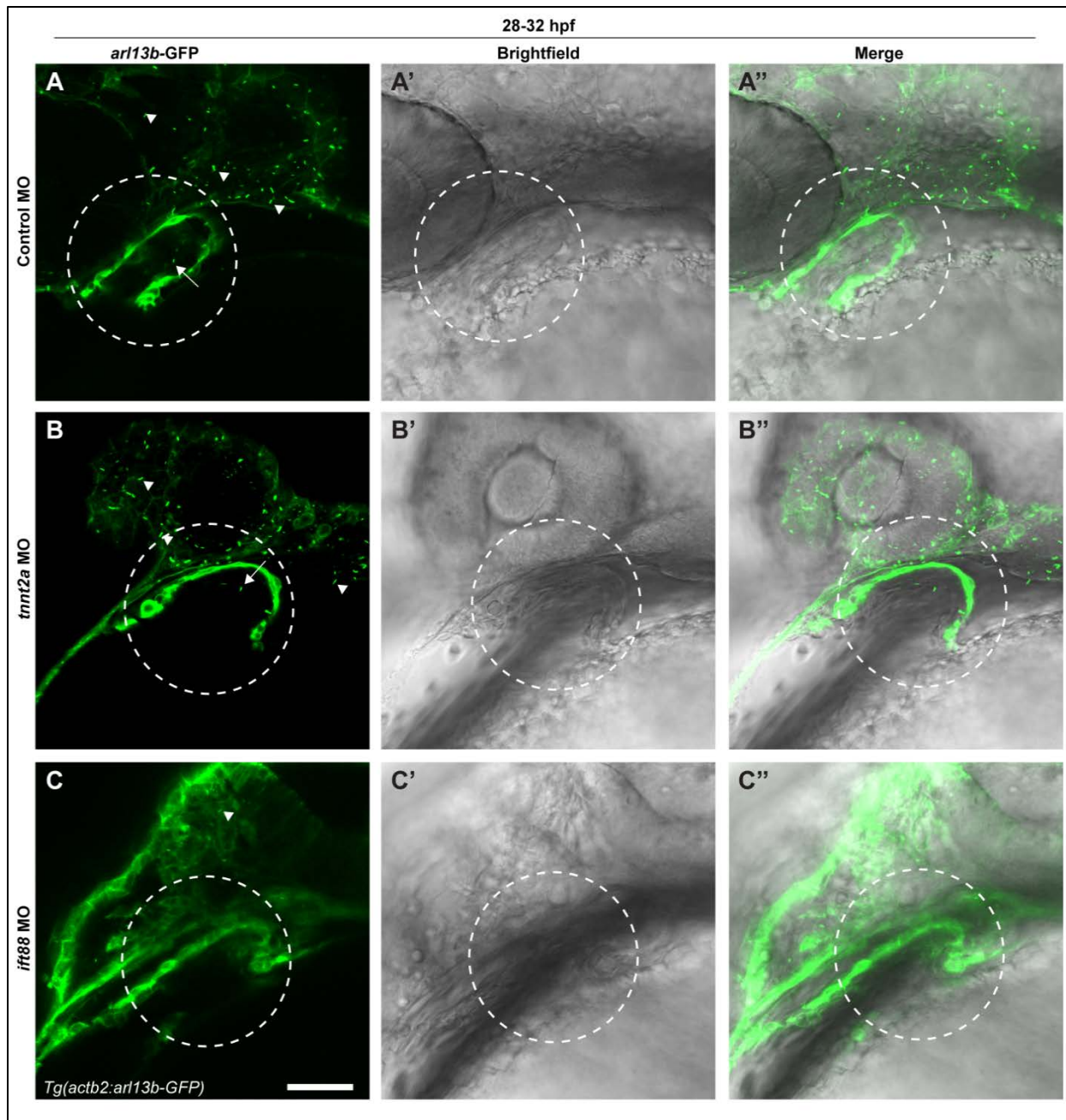


Figure 21 Control and *tnnt2a* morphants have endocardial primary cilia

(A-C) The hearts of homozygous-transgenic embryos carrying *Tg(actb2:arl13b-GFP)* to mark primary cilia were injected with (A) standard control, (B) *tnnt2a*, or (C) *ift88* morpholinos and imaged by confocal microscopy at 28-32 hpf. (A-C) Representative 2 μ m optical section showing Arl13b-GFP expression, (A'-C') brightfield image, and (A''-C'') merged images. White arrow heads point to extra-cardiac primary cilia. White arrows point to endocardial primary cilia. MO = morpholino. Scale bar 50 μ m. N=3-6 embryos.

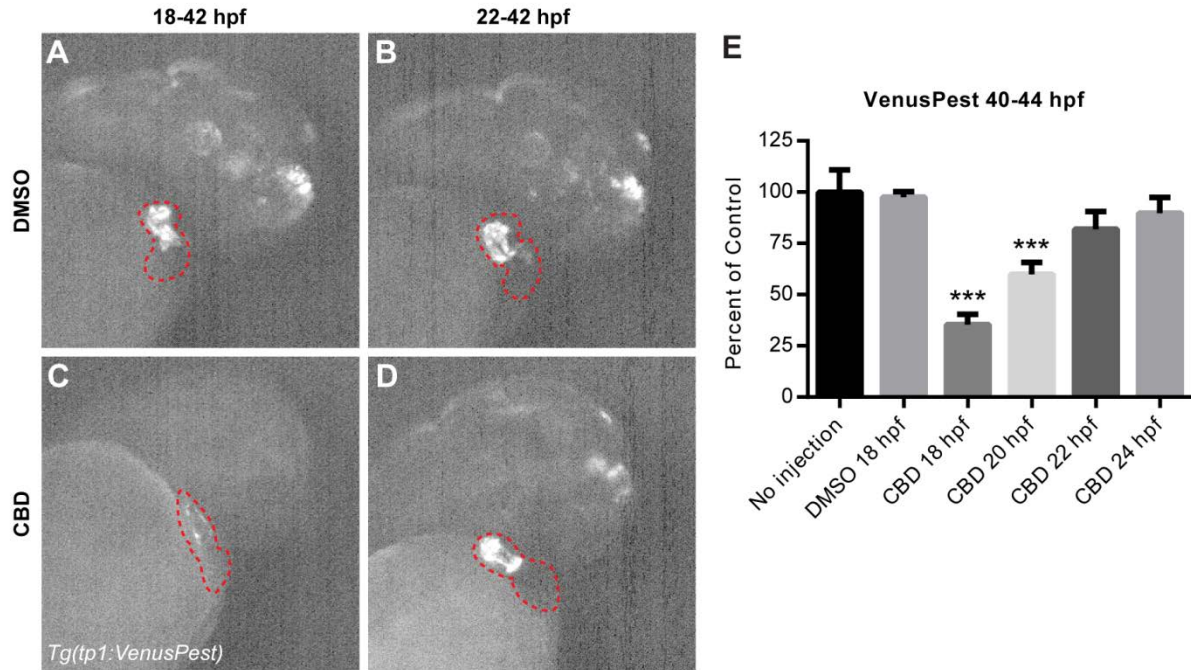


Figure 22 Ciliobrevin D treatment within a short time window prevents Notch activation

(A-D) Representative images of Notch reporter of whole mount *Tg(tp1:VenusPest)* embryos at 42 hpf injected with (A,B) DMSO or (C,D) Ciliobrevin D at (A,C) 18hpf or (B,D) 22 hpf. (E) Quantification of VenusPest Notch reporter mean fluorescence intensity in the ventricle. Minimum N=8 embryos quantified. Error bars are s.e.m. Students T-test compared to DMSO 18hpf.

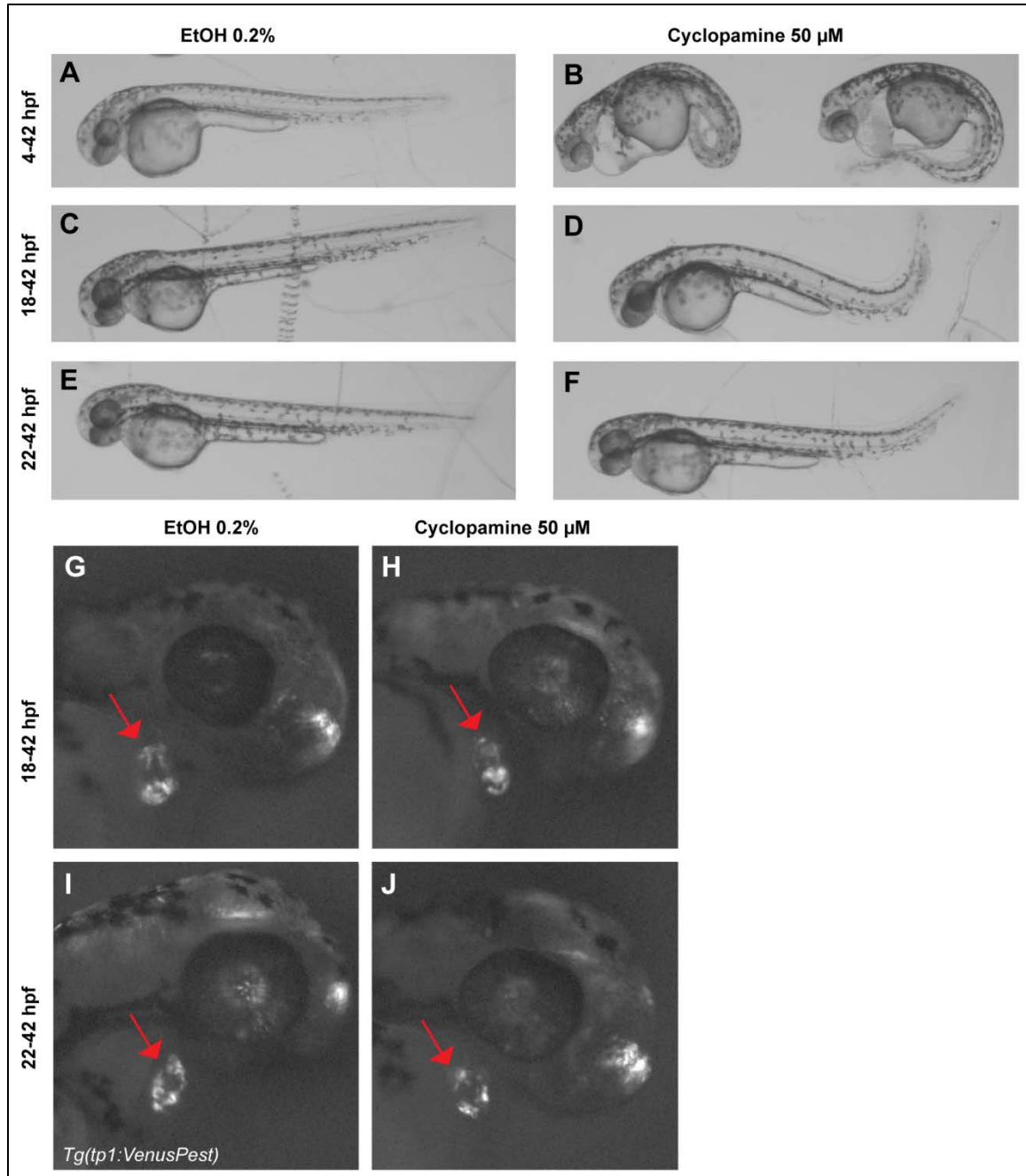


Figure 23 Cyclopamine treatment does not inhibit Notch activation in the endocardium

(A-F) Representative whole mount embryos treated by aqueous delivery with (A,C,E) EtOH 0.2% or (B,D,F) 50 μM cyclopamine in 0.2% EtOH from (A,B) 4-42 hpf, (C-D) 18-42 hpf, or (E-F) 22-42 hpf. (G-J) Representative images of Notch reporter of whole mount *Tg(tp1:VenusPest)* embryos at 42 hpf treated as described above. Minimum N=5 embryos examined per condition.

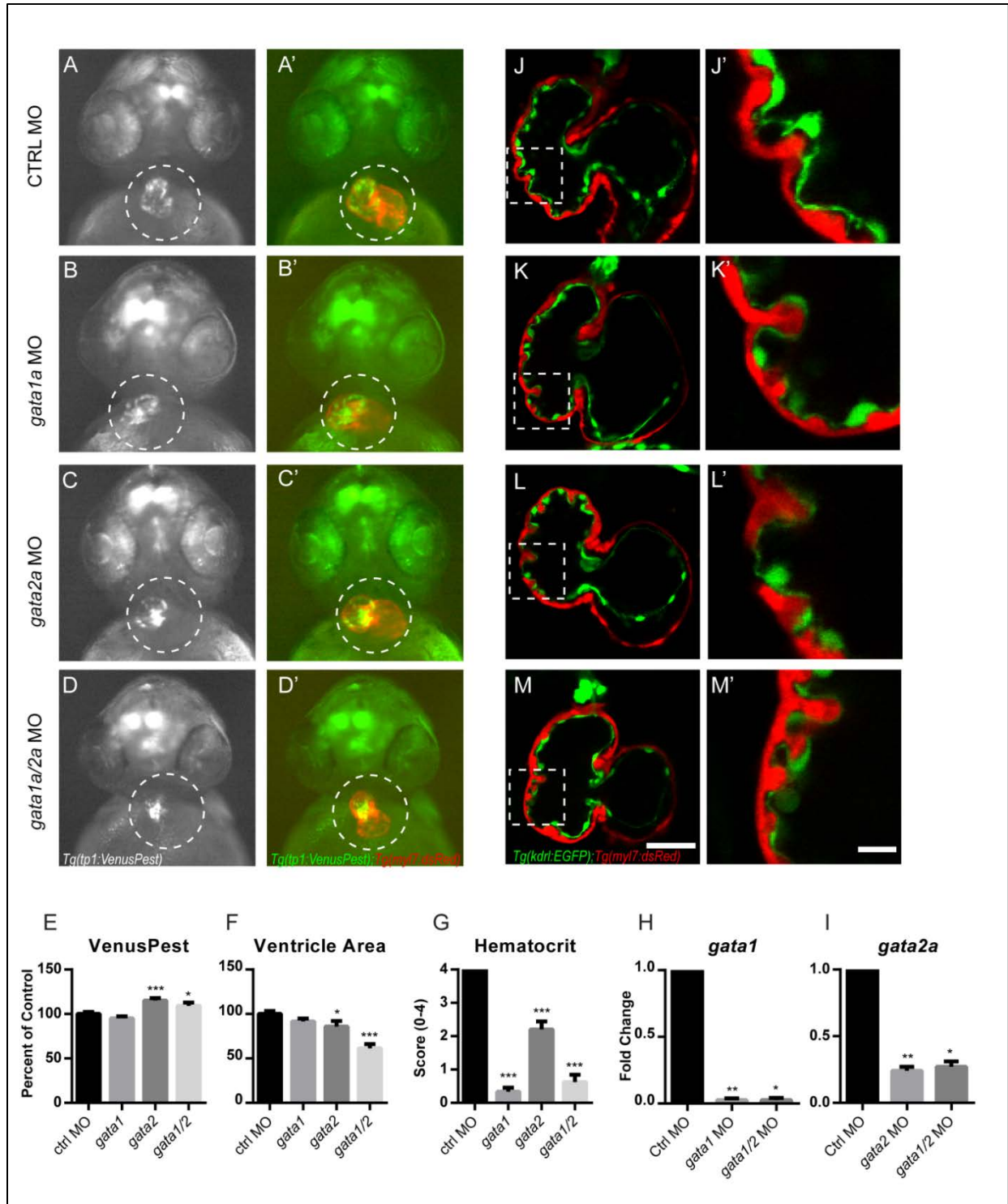


Figure 24 Reducing shear stress or retrograde flow fraction via *gata1a*, *gata2a*, and *gata1a/2a* knockdown does not prevent Notch activation or trabeculation

(A-D) Morpholino gene knock-down experiment where double transgenic *Tg(tp1:VenusPest);Tg(myf7:dsRed)* embryos were injected with (A) control, (B) *gata1a*, (C) *gata2a*, or (D) *gata1a/2a* morpholinos and imaged at 48-50hpf. (A-D) Representative whole mount images of Notch reporter and (A'-D') Notch reporter overlaid with cardiomyocyte reporter with cardiac regions highlighted by circles. (E) Quantification of mean VenusPest intensity in

the ventricle and (F) ventricle area. (G) Mean hematocrit score from 15 second videos where 0 = no hematocrit, 1 = very little, 2 = dramatically reduced, 3 = reduced, 4 = normal levels of hematocrit. (H-I) Gene expression of *gata1a* and *gata2a* in whole embryos at 48 hpf where primers span exons blocked by *gata1a* and *gata2a* splice-blocking morpholinos. (J-M) Mid-chamber confocal optical section showing cardiomyocytes (red) and endocardial cells (green) of (J) control, (K) *gata1a* (L) *gata2a*, (M) *gata1a/2a* morphants hearts carrying *Tg(myl7:dsRed); Tg(kdrl:EGFP)* transgenes. The cardiac regions highlighted by dotted lines are shown as magnified high resolution images in (J'-M'). Error bars are s.e.m. * $p \leq 0.05$ -0.01, ** $p \leq 0.01$ -0.001, *** $p < 0.001$ compared to control morphants. (E-G) Student's T-test for each morphant compared to control morphant. (H-I) One-sample T-test compared to control morpholino fold change = 1. Scale bars are (M) 50 μm and (M') 10 μm .

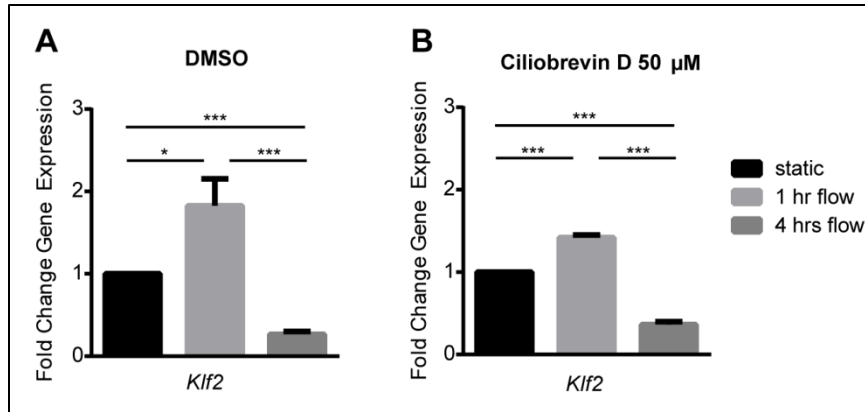


Figure 25 *Klf2* expression in MLECs after 1 and 4 hrs flow

(A,B) *Klf2* expression in MLECs treated with (A) DMSO or (B) Ciliobrevin D and exposed to static media, 1 hr flow, or 4 hrs flow with cone-in-plate viscometer. * $p \leq 0.05-0.01$, ** $p \leq 0.01-0.001$, *** $p < 0.001$, Student's T-test. Error bars are SEM. *Klf2* = Krüppel-like Factor 2.

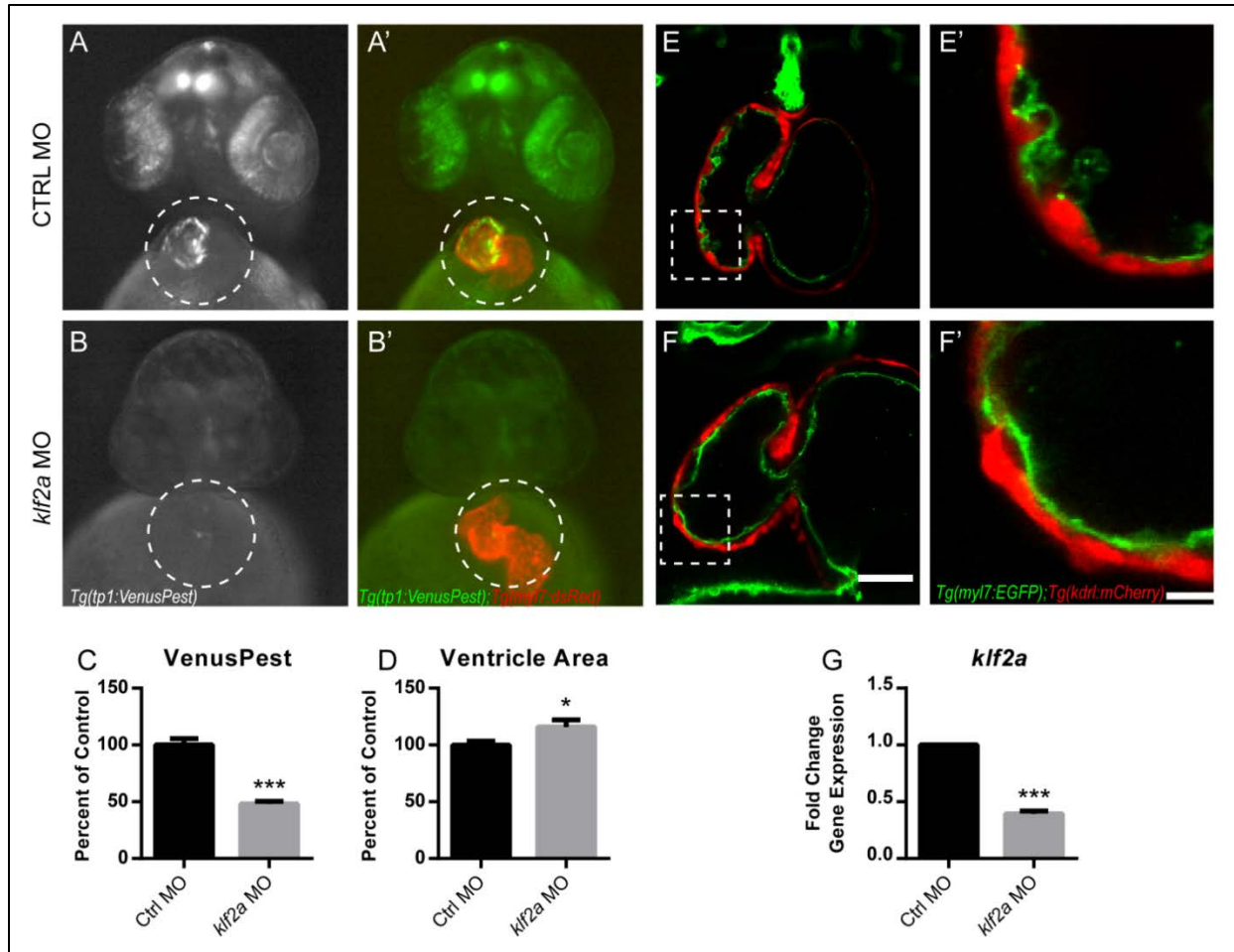


Figure 26 Notch activation requires *klf2a*.

(A-B) Morpholino gene knock-down experiment where double transgenic *Tg(tp1:VenusPest); Tg(myI7:dsRed)* embryos were injected with (A) control or (B) *klf2a* MOs and imaged at 48-50hpf. (A,B) Representative whole mount images of Notch reporter and (A',B') Notch reporter overlaid with cardiomyocyte reporter with cardiac regions highlighted by circles. (C) Quantification of mean VenusPest intensity in the ventricle and (D) ventricle area. Student's T-test for each morphant compared to control morphant. (E-F) Mid-chamber confocal optical section showing cardiomyocytes (red) and endocardial cells (green) of (E) control or (F) *klf2a* morphant hearts carrying *Tg(myI7:dsRed); Tg(kdrl:EGFP)* transgenes. The cardiac regions highlighted by dotted lines are shown as magnified high resolution images in (E',F'). (G) Gene expression of *klf2a* in whole embryos at 48hpf where primers span exons blocked by *klf2a* splice-blocking morpholino. One-sample T-test compared to control morpholino fold change = 1. Error bars are s.e.m. * $p \leq 0.05-0.01$, ** $p \leq 0.01-0.001$, *** $p < 0.001$

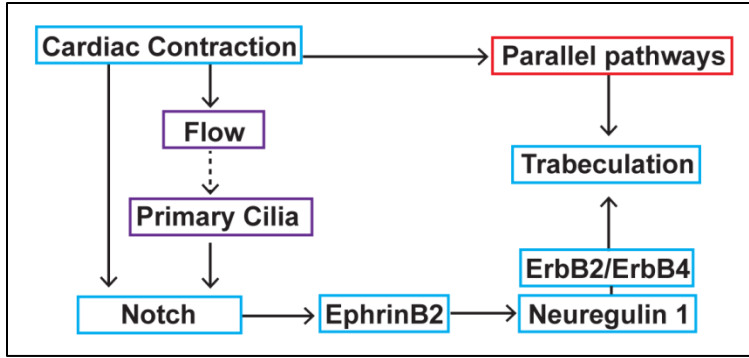


Figure 27 Cardiac contraction activates endocardial Notch signaling in a primary cilia-dependent manner to regulate trabeculation.

Schematic: (Blue boxes) Cardiac contraction activates a regulatory Notch-EphrinB2a-Neuregulin 1 pathway in endocardial cells to activate ErbB2 signaling in cardiomyocytes to promote trabeculation. (Red boxes) Since Notch activation in non-contractile hearts is not sufficient for trabeculation, cardiac contraction also stimulates parallel pathways to promote trabeculation. (Purple box) Cardiac contraction causes blood flow which is likely detected by primary cilia to activate *Notch1*.

Table 1 Chapter 2 Morpholino validation

Gene	Morpholino sequence (5'-3')	Morpholino Type	Dose	Reference	Phenocopied by non-overlapping morpholino	Reduced protein expression	Four-base mismatch control morpholino	Altered splicing demonstrated by RT-PCR	Phenotype rescued by co-injection with mRNA	Phenocopies known mutant	Morpholinos targeting gene in ZFIN database
<i>tnnt2a</i>	CATGTTTGCTCTGAT CTGACACGCA	translation	1.0 ng	Sehnert et al. (2002)		X				X	4
<i>notch1b</i>	AATCTCAAACCTGACC TCAAACCGAC	splice	3.2 ng	Milan et al. (2006)	X		X	X			7
<i>efnb2a</i>	TTGCCGCCTCGCGC ACTTACTTGGT	splice	6.4 ng	Wang et al. (2010)	X	X					5
<i>ift88</i>	CTGGGACAAGATGC ACATTCTCCAT	translation	3.2 ng	Kramer-Zucker et al. (2005)	X					X	6
<i>ift88</i>	GCCTTATTAACAGA AATACTCCCA	translation	3.2 ng	Tsujikawa and Malicki (2004)	X				X	X	6
<i>gata1a</i>	GTTTGGACTCACCTG GACTGTGTCT	splice	6.4 ng	Galloway et al. (2005)			X			X	4
<i>gata2a</i>	CATCTACTCACCAGT CTGCGCTTTG	splice	4.8 ng	Galloway et al. (2005)			X			X	4
<i>klf2a</i>	CTCGCCTATGAAAGA AGAGAGGATT	splice	2-3.0 ng	Nicoli et al (2010)	X			X			6
Control*	CCTCTTACCTCAGTT ACAATTTATA	N/A	1-6.4 ng	Gene Tools, LLC							N/A

*This oligo is reported to have no target and no significant biological activity (in zebrafish). Embryos injected with 1-8 ng of this morpholino were indistinguishable from wild type.

Table 2 Chapter 2 Oligonucleotide sequences

Species	Gene	F	R
zebrafish	<i>actin</i>	CTATGAGCTGCCTGACGGTCA	GTGGTCTCGTGGATACCGCAA
	<i>notch1b</i>	TGCGAGAACAACACACCTGA	CTGGCAGTAGTTGCCAGTGA
	<i>notch1b MO validation</i>	ATTCAGTCGGTTTGAGGCCA	TTGCTGTCGGACTGTTCCCTC
	<i>efnb2a</i>	ACCCTACCAGTTACCCTCCC	CCATCTCCCTTATCTTCCCCA
	<i>efnb2a MO validation</i>	TGATCGCGTGCAAGGTGAA	CTGCGGATACAGCACCAGAC
	<i>nrg1</i>	TGCATCATGGCTGAGGTGAA	TTAACTTCGGTTCCGCTTGC
	<i>gata1a MO validation</i>	TAGACACAGTCCAGTTCCCC	TGGATGTGGGGTTGTAGGGA
	<i>gata2a MO validation</i>	GGCCAGAACAGACCCCTTAT	AGGGTGGTCGTGGTTGTCT
	<i>klf2a MO validation</i>	GCGACTCACACTTGCACTTTT	GATAGGGCTTCTCGCCTGTG
mouse	<i>Gapdh</i>	CATCTTCCAGGAGCGAGACC	CCTTCAAGTGGGCCCCG
	<i>Notch1</i>	ACAGTGCAACCCCTGTATG	TCTAGGCCATCCCACCTCACA
	<i>Efnb2</i>	GGTTTTGTGCAGAACTGCGAT	TGTCCGGGTAGAAATTTGGAGT
	<i>Nrg1</i>	ATGGAGATTTATCCCCCAGACA	GTTGAGGCACCCTCTGAGAC

2.3 Significance and Future Directions

Significance

Early studies of zebrafish embryos lacking endothelial cells (*cloche* mutants), demonstrated the necessity of endocardium in chamber maturation (Stainier et al., 1995), and recently, there has been an increased appreciation for the importance both endocardial-myocardial crosstalk and biomechanical forces in regulating in heart development (Granados-Riveron and Brook, 2012; Tian and Morrisey, 2012). The study described in Chapter 2.2 represents one of the most comprehensive descriptions, to date, of functional crosstalk between these cell layers and biomechanical cues. Our data supports a model in which bending of luminal, protruding primary cilia on endocardial cells leads to activation of Notch signaling and ultimately regulates myocardial trabeculation. However, by necessity, this model is not comprehensive, and additional studies are necessary to further define these relationships (Fig. 27 model). Specifically, it would benefit from additional work to 1) identify the mechanism by which endocardial primary cilia detect low flow, 2) define the epistatic relationship between primary cilia, *klf2*, and Notch in the developing embryo, 3) characterize relationships between fluid dynamics and Notch activity in endocardial cell sub-populations, and 4) identify parallel, contraction-dependent pathways necessary for trabeculation.

Future directions

1) Identify how endocardial primary cilia detect low flow

A key area for future exploration is to identify the mechanism by which primary cilia on endocardial cells detect shear stress flow. Morpholino knockdown of *ift88* inhibits cilia formation, Notch activation through the embryo, and formation of myocardial trabeculae (Fig. 20). Similarly, inhibition of cilia formation via administration of the dynein ATPase inhibitor ciliobrevinD prevents Notch activation in endocardial cells and downstream gene expression both in endocardial cells and in cultured endothelial cells exposed to low magnitude shear stress (Fig. 20, Fig. 22) However, the precise mechanism by which primary cilia detect flow in this developmental context is unknown.

The leading theory for how flow, as a biomechanical cue, is detected by protruding primary cilia suggests that the physical bending of primary cilia exposed to shear stress activates mechanically-gated transient receptor potential (TRP) cation channels. When tethered to a primary cilium plasma membrane

and internal microtubules, cilium bending applies stretch forces to open the TRP channels, leading to transient voltage potential changes which stimulate release of intracellular calcium. This, in turn, activates downstream intracellular signaling cascades to ultimately regulate gene expression (Goetz et al., 2014; Yoshida et al., 2012). Interestingly, mutations in mechanosensitive TRP family genes lead to major valve defects, and TRP channel activity responds to an oscillatory flow pattern *in vivo* (Heckel et al., 2015). In a developmental context, endocardial calcium levels are correlated with the presence of primary cilia, flow bending, and TRP gene expression (Goetz et al., 2014). Thus, we suggest that endocardial cells likely utilize TRP channels on primary cilia in the cilia-bending response to flow. In support of this hypothesis, 3 dpf endocardial cells express transcripts encoding TRP channels *trpp2* and *trpv4* (data not shown). One approach to further evaluate this hypothesis would be to knockout TRP gene expression, then measure calcium levels and Notch activation in endocardial cells. To this end, CRISPR/Cas9 targeting gene editing could be used to induce frameshift mutations in TRP genes. The generated mutant fish which could then be bred onto *Tg(Tp1:EGFP)* Notch reporter and *Tg(fli1:gcamp3.0); Tg(flk1:mcherry)* endothelial-specific calcium reporter backgrounds (Goetz et al., 2014). Based on the above model, we expect that loss of certain TRP channels will reduce blood-flow dependent elevations in endocardial calcium levels and Notch activity.

2) Define the epistatic relationship between primary cilia, *klf2*, and Notch in the developing embryo

Primary cilia are multifunctional organelles. Though their functions are typically described as 1) to mediate the Hedgehog (Hh) signaling pathway and 2) to detect flow, as reviewed by Egorova et al. (2012) and (Van der Heiden et al., 2011), this categorization may be incomplete. In Chapter 2.1, a previously undefined relationship between primary cilia, the flow-responsive transcription factor *klf2a*, and Notch signaling, was observed not just in the heart, but throughout the developing zebrafish embryo (Fig. 26). Specifically, in wildtype embryos, from 24-48 hpf, the *Tg(Tp1:VenusPest)* reporter is detectable in the ventricular endocardium, portions of the arterial vasculature, developing fins, and throughout developing brain (Fig. 10). Using *Tg(actb:Ar13b-GFP)* reporter fish to label primary cilia, we observed primary cilia in nearly all cell types, including these tissues (data not shown). Reducing primary cilia formation using *ift88* morpholinos and knocking down *klf2a* expression led to significant reduction in *Tg(Tp1:VenusPest)* Notch

reporter signal intensity throughout the whole embryo and dramatically in the brain (Fig. 20, Fig. 27). In contrast, inhibiting Hh signaling with cyclopamine had little or no effect on Notch activity (Fig. 23). Though one report indicates that *klf2a* is upstream of *notch1b* and important for valve development (Just et al., 2011), this suggests that there is a previously undescribed relationship between primary cilia, Klf2a, and Notch signaling in multiple cell types in the embryo.

Klf2 is best known for its role as a flow-response transcription factor, so the possibility of other functions in non-vascular tissues is novel and intriguing (Novodvorsky and Chico, 2014). Since primary cilia and Notch are both important for neuronal progenitor differentiation (Kong et al., 2015), an important first step to explore the relationship between Klf2a and these components is to define the epistasis of *klf2a* and *notch1b* in neurons. To this end, *in situ* hybridization for *notch1b* and *klf2a* in *ift88*, *notch1b*, and *klf2a* morphants could explore epistasis at the transcriptional level. If regulation does not occur at the transcriptional level, the effects of gene depletion on early neuronal progenitor differentiation could also help define their inter-relationships. As a caveat, it is also possible that, in neuronal cell populations, Klf2a does act as a flow response gene and is activated in response to the very low magnitude flow caused by motion of extracellular fluid through intracellular space (Novodvorsky and Chico, 2014).

Interestingly, *klf2a* morphants have larger hearts than control morphants clutch mates. Whether this is due to an increase in the number of myocardial cells or increased myocardial cell size remains to be seen, but could be rapidly evaluated in *Tg(myI7:nucDsRed);Tg(myI7:rasGFP)* morphant embryos by counting nucDsRed+ myocardial nuclei and measuring rasGFP surface area (D'Amico et al., 2007; Mably et al., 2003). If the number of cardiomyocytes is elevated in *klf2a* morphants, then *in situ* hybridization studies using heart field markers, such as *hand2*, and proliferation assays, such as nucleotide analog incorporation assays, could be used to explore whether this is due to a larger myocardial progenitor pool or enhanced proliferation (Yelon, 2001). If myocardial surface area is increased, 3D volume rendering could be used to explore whether this reflects hypertrophic growth or atypical distribution or arrangement of myocardial cell mass.

3) Define the relationship between fluid dynamics and Notch activity

Chapter 2.2 supports a pathway in which primary cilia on endocardial cells are activated by low magnitude flow at the onset of heartbeat to activate Notch in the endocardium. However, cardiac Notch

activity is primarily restricted to first the ventricular endocardium from 28-55 hpf, then to the AVC through larval stages (Fig. 10). Using *Tg(actb:arl13b-EGFP)* to label primary cilia, a single cilium is detectable on most endocardial cells in atrium and ventricle from 28-32 hpf. However, these cilia appear to disassemble at higher levels of shear stress. At 48 hpf, primary cilia are detectable on most endocardial cells in *tnnt2a* morphants, but are largely absent in control morphant endocardium (data not shown). This disassembly is consistent with previous descriptions of primary cilia behaviors *in vitro* and observations of the intravascular restriction of endothelial primary cilia to areas of low net flow (Iomini et al., 2004; Van der Heiden et al., 2006). Owing to their position within the heart, during the cardiac cycle, endocardial cells lining the AVC are exposed to dramatic changes in the magnitude and directionality of fluid flow. Notch activity and *notch1b* expression in the valve endocardium is highly responsive to fluid dynamics (Vermot et al., 2009). Overall, this spatiotemporal patterning suggests both that there may be underlying differences in atrial and ventricular endocardial cells and that primary cilia may be dispensable for Notch activity in valve.

Define the relationship between flow directionality and Notch activity: Though primary cilia are important for detecting low flow to activate Notch in the ventricle endocardium, prominent, protruding primary cilia were not observed on valve endocardial cells at 48 hpf (data not shown). In combination with Figure 20, this suggests that other mechanosensors mediate Notch responsiveness responses to high magnitude, dynamic fluid patterns in the valve endocardium. Disrupted, reversing flow patterns lead to inflammatory signaling in endothelial cells and can serve as an important biomechanical cue to regulate many aspects of endothelial cell function (Hahn and Schwartz, 2009). Previous studies have implicated shear stress and reversing flows as major regulators of *notch1b* expression in the valve endocardium (Heckel et al., 2015; Vermot et al., 2009). Intracardiac shear stress levels is lowered *in vivo* by using morpholinos to knock down *gata1* and/or *gata2*. These genes code for transcription factors important for regulating blood cell development, so knocking them down lowers the relative hematocrit fraction, decreasing blood viscosity and shear stress. Morphants deficient in *gata2* display major defects in valvulogenesis that are attributable to decreased retrograde flow fraction through the AVC at 2-4 dpf (Vermot et al., 2009). We found that Notch activity in *gata2* and *gata1/2* morphants is higher than control morphants (Fig. 24). Together, these this suggests that reversing flow patterns may play a primary cilia-

independent role in maintaining active Notch signaling. Testing this model in the zebrafish heart, *in vivo*, could be extremely technically challenging due to lack of methods for decoupling cardiac contraction and flow within the heart. However, several groups are studying the molecular mechanisms of endothelial cell responses fluid dynamics, as reviewed in Baeyens and Schwartz (2016) and other groups are developing or have developed quantitative models of fluid dynamics within the zebrafish heart (Lee et al., 2013). Careful combination of these bodies of work could lead to identification of candidate mechanisms for a hypothesis-driven approach that could address this question in zebrafish

Characterize heterogeneity in atrial and ventricular endocardial cells: From 28 to ~55 hpf, Notch1 in the heart is restricted to endocardial cells lining the ventricle (Fig 10). Though there is dramatic heterogeneity within endothelial cell populations (Aird, 2012), to our knowledge this is the first report of functional heterogeneity in endocardial cells outside of cardiac valves. We suggest a model where differential gene regulatory networks inherent to ventricular and atrial endocardial cells enable transcription of *notch1b* only in the ventricle. Lack of specific markers for endocardial subpopulations precludes experimental approaches to define the gene regulatory network differences in these subpopulations. However, standard molecular cell biology approaches may be used to further characterize the *notch1b* promoter to begin to address how primary cilia-based low flow detection on ventricular endocardial cells leads to *notch1b* transcription. Though a large body of literature has explored regulation of Notch target gene transcription (Borggreffe et al., 2016; Borggreffe and Oswald, 2009; Palermo et al., 2014; Wang et al., 2015), we are not aware of any reports describing the *notch1b* promoter in zebrafish, or Notch1 or NOTCH1 in mouse and human, respectively. CRISPR/Cas9 gene editing, in combination with Notch reporter transgenes, could be used to identify the region of the *notch1b* promoter required for *notch1b* expression in zebrafish by targeted deletion of large stretches of DNA in the promoter region and observing Notch reporter expression level. Identification of the minimal promoter region would lead to identification of putative transcription factor-binding sites, which could be in turn, confirmed by CHIPseq if adequate antibodies are available. Once the transcription factor(s) necessary for *notch1b* expression is identified, as a first step, expression can be evaluated in ventricular and atrial endocardial cells. This would determine if differential expression of these factors (or their binding partners) could explain our observations of differential Notch activation.

4) Identify additional pathways activated by cardiac contraction and required for trabeculation

Although Notch activity stimulated by heartbeat is required for trabeculation, ectopic activation of Notch signaling is not sufficient to stimulate trabeculation in the absence of heartbeat (Fig. 18).

Furthermore, NICD overexpression in cilia-deficient *ift88* morphants was not sufficient to stimulate trabeculation (data not shown). This suggests that heartbeat activates additional, parallel pathways essential for regulating trabeculation. Cardiac contraction exerts stretch and cyclic strain forces on the heart. These forces regulate gene expression in culture models (Shojaei et al., 2015; Wang et al., 2013) and are important for trabeculation (Samsa et al., 2015; Sehnert et al., 2002; Staudt et al., 2014). A recent report combined live, time-lapse imaging and spinning-disc confocal, or single plan illumination microscopy (SPIM) to demonstrate that myocardial cells produce luminal projections when forming trabeculae and that, *tnnta*^{-/-} embryos (which have non-contractile hearts), display a significant reductions in these protrusions (Staudt et al., 2014).

Together, these studies suggest that myocardial contractions stretch and strain forces may be necessary to stimulate trabeculation independent of flow responsive signals from the endocardium. This hypothesis is technically challenging to address due to lack of methods to decouple contraction and flow within the heart. Ideally, trabeculation would be evaluated in mosaic hearts composed of contractile and non-contractile (*tnnt2a*^{-/-}) cardiomyocytes. However, the biomechanical forces within these mosaic hearts are dramatically disrupted, and the non-contractile cardiomyocytes detach or are extruded from the heart (unpublished data, Jiandong Liu). In an alternative approach, differential expression of ventricular and atrial myosin heavy chain genes may be used to differentially manipulate contractility in these chambers. Since embryos with genetic deficiencies in *amhc* (atrial myosin heavy chain C) have weak or absent contractions, embryos deficient in *vmhc* (ventricular myosin heavy chain C) may lack contractile properties in the ventricle (Berdougo et al., 2003). This would allow for evaluation of trabeculation in the ventricle in the presence of flow but absence of contraction. In preliminary experiments, morpholino knockdown of *vmhc* led to reduced ventricular contractility, but atrial contractions exerted cyclic stretch and strain on the ventricle, eventually leading to ventricular collapse, and making this approach unfeasible (data not shown).

Future studies aiming to understand how myocardial contraction regulates trabeculation may begin with RNAseq analysis of gene expression changes that occur in the myocardium in contractile and non-contractile hearts as the heart develops, incorporating time points prior to and after initiation of blood flow. We have established methodology for FACS purification of myocardial cells from zebrafish embryos suitable for use in Fluidigm C1 platforms (Samsa et al., 2016). This could be used to purify populations for RNAseq or for microarray analyses. Comparative transcriptomics between these conditions could lead to identification of candidate signaling pathways activated in the myocardium correlated with contraction. Morpholino and CRISPR/Cas9-based mutagenesis studies could be applied in combination with *in vitro* cell biology studies of cardiomyocyte stretch and strain responses to further define how contraction-response genes may regulate trabeculation.

Alternatively, failure of ectopic Notch activation to stimulate trabeculation could be due, at least in part, to inhibitory roles of Notch signaling in other cell types. Under homeostatic conditions, Notch signaling is involved in fate determination through lateral inhibition (Kageyama et al., 2008). In the developing heart, Notch activity is largely confined to the endocardium (Fig. 10), but it is plausible that, Notch plays an inhibitory role within myocardial cells. This could be tested after development of genetic models capable of inducible, myocardium and endocardium-specific activation of the Notch intracellular domain. If Notch plays an inhibitory role in the myocardium with respect to trabeculation, and cardiac contraction is not required for activation of other trabeculation-required signaling pathways, then ectopic NICD expression in the endocardium, but not the myocardium, may promote trabeculation in non-contractile hearts.

CHAPTER 3 ISOFORM-SPECIFIC MUTAGENESIS INDICATES MULTIPLE ROLES FOR NEUREGULIN 1 IN ZEBRAFISH CARDIAC MATURATION

3.1 Historical Context

Though best known for its role in the nervous system, the Nrg1-ErbB2/ErbB4 signaling pathway came to prominence in the cardiovascular system when key studies demonstrated that each component is essential for cardiac development during mouse embryogenesis (Gassmann et al., 1995; Kramer et al., 1996; Lee et al., 1995; Meyer and Birchmeier, 1995). This pathway's relevance to human heart disease was established when an association between ErbB2 and anthracyclines sensitivity was identified in a subset of breast cancer patients which developed dilated cardiomyopathy during chemotherapy (Vasti and Hertig, 2014).

The Nrg-1/ErbB2/ErbB4 pathway has been implicated in many aspects of cardiovascular development and homeostasis including cardiac trabeculation, conduction system differentiation, and cardiomyocyte metabolism (Rupert and Coulombe, 2015). Furthermore, Nrg1 was recently shown to have a protective effect in animal models of myocardial infarction and chronic heart failure (Fang et al., 2010; Formiga et al., 2014; Guo et al., 2012; Hill et al., 2013; Li et al., 2011; Liu et al., 2006; Xiao et al., 2012). Recombinant, secreted Nrg1 is currently showing promising results in clinical trials as a therapeutic for chronic heart failure (Gao et al., 2010; Jabbour et al., 2011). However, the precise mechanism by which Nrg1 provides these protective effects is unknown (Rupert and Coulombe, 2015).

Since cardiac regeneration and repair mechanisms are thought to involve re-activation of developmental paradigms, understanding role of the Nrg1-ErbB2/ErbB4 signaling pathway in the developmental context could lead to important insights as to the mechanisms by which Nrg1 treatment may lead to improvements in therapeutic outcomes. Owing to their optical transparency and genetic tractability, zebrafish are an advantageous vertebrate model for exploring the molecular regulation of development, and previous work has demonstrated that *erbb2* is essential for cardiac trabeculation in zebrafish, (Brown et al., 2016; Liu et al., 2010). However, the role of *nrg1* in zebrafish heart development is unknown. Data presented in Chapter 3.2, below, describes the first phenotypic analysis of full ablation

of *nrg1* in zebrafish. It reveals that *nrg1* is completely dispensable during development, but is essential in later life, likely through the role of the type III isoform in establishing the ventricular nerve plexus. These findings suggest that there are previously unappreciated, cross-species differences in ErbB2 receptor activation in the developing heart.

3.2 Isoform-Specific Mutagenesis Indicates Multiple Roles for Neuregulin-1 in Zebrafish Cardiac Maturation⁴

Introduction

Congenital heart diseases (CHD) are highly prevalent birth defects (Mozaffarian et al., 2015) and often feature perturbations in cardiac morphogenesis that arise from dysregulated cell function during development (Chin et al., 2012; Samsa et al., 2013). Little is known about the genetic, molecular, and cellular defects underlying most CHDs. Thus, understanding the genetic regulation of heart developmental could lead to important therapeutic insights. Owing to their rapid development, optical clarity, and ease of genetic manipulation, zebrafish have emerged as a premier model organism for understanding the molecular and genetic regulation of heart development, (Brown et al., 2016). Zebrafish embryos are small enough to meet oxygen needs by diffusion alone and can survive for weeks with severe heart malformations (Bang et al., 2004; Chen et al., 1996; Sehnert et al., 2002; Stainier et al., 1996; Strecker et al., 2011). Likewise, adult zebrafish survive with a wide range of cardiac malformations and are relatively tolerant of hypoxia, making them an attractive model for studying progressive sequelae of CHD (Abdallah et al., 2015; Rees et al., 2001).

The Nrg1-ErbB2/ErbB4 signaling pathway is implicated in many aspects of vertebrate heart development and is currently under development as a therapeutic target for heart disease (Harvey et al., 2016; Odiete et al., 2012; Rupert and Coulombe, 2015). Transmembrane pro-Nrg1 expressed on endocardial, microvascular endothelial cells, and/or pericytes is cleaved by proteases to release active Nrg1. Nrg1 binds via its EGF domain to ErbB4 expressed on cardiomyocytes, promoting dimerization with the essential co-receptor ErbB2 (Gemberling et al., 2015; Meyer and Birchmeier, 1995; Milan et al., 2006; Montero et al., 2000; Vermot et al., 2009; Yarden and Sliwkowski, 2001; Yokozeki et al., 2007). While ErbB4 has limited tyrosine kinase activity, ErbB2 has no ligand binding activity, but kinase activity is necessary to modulate cardiomyocyte gene expression (D'Uva et al., 2015; Fuller et al., 2008; Kochupurakkal et al., 2005; Lee et al., 1995).

Early studies demonstrated that Nrg1, ErbB2 and ErbB4 are each required for embryonic formation of highly organized, luminal, myocardial protrusions called trabeculae in mice (Gassmann et al.,

⁴ This part of chapter 3 is in preparation with the expected citation of Brown, D.A. Samsa, L.A., Ito, C.E., Ma, H., Qian, L., and Liu, J. (2016) Isoform-specific mutagenesis indicates multiple roles for Neuregulin1 in zebrafish cardiac maturation. *Manuscript in preparation*

1995; Kramer et al., 1996; Lee et al., 1995; Meyer and Birchmeier, 1995). Likewise, our previous work demonstrates that ErbB2 plays a conserved role in zebrafish cardiac trabeculation (Liu et al., 2010). In zebrafish, trabeculae continue developing through adulthood, and the adult myocardium is comprised primarily of an expanded and remodeled meshwork of trabeculae (Sedmera, 2011; Sedmera et al., 2000). Failure to initiate trabeculation is lethal in vertebrates, and trabeculation defects are often associated with CHDs (Jenni et al., 1999; Samsa et al., 2013). However, requirement for the Nrg1 in zebrafish cardiac development is unknown. Since its expression in the developing zebrafish heart is regulated by components upstream of cardiac trabeculation including blood flow, *notch1b*, and *efnb2*, we reasoned that that Nrg1 may play an important role in trabeculation (Samsa et al., 2015).

Zebrafish *nrg1* produces three major isoforms by alternative splicing, *nrg1-I*, *nrg1-IIa-c*, and *nrg1-III*, and *nrg1-I* is the primary isoform expressed in the heart (Gemberling et al., 2015; Perlin et al., 2011; Vermot et al., 2009). To determine the genetic requirement for Nrg1 in zebrafish trabeculation, we used CRISPR/Cas9 targeted nuclease activity to generate a series of allelic mutations to examine the isoform-specific roles for *nrg1* in the heart. To this end, we produced frameshift mutations in all isoforms of Nrg1 (*nrg1^{nc26}*) or Nrg1-I and Nrg1-II (*nrg1^{nc28}*). Surprisingly, we did not observe trabeculation defects in *nrg1^{nc26}* or *nrg1^{nc28}* lines, and *nrg1^{nc28}* mutant fish were indistinguishable from wild type and heterozygous clutch mates. In contrast, *nrg1^{nc26}* die between late juvenile and early adult stages. Histological analysis of *nrg1^{nc26}* mutant hearts suggests that underlying structural defects could contribute to decline. Both *nrg1^{nc26}* and *nrg1^{z26}*, a previously described line that is deficient only in *nrg1-III*, had major deficiencies in the cardiac nerve plexus which emerge during larval stages and juvenile metamorphosis. Together, these findings suggest that in zebrafish, *nrg1-I* is dispensable for heart development and establishes an essential role for *nrg1-III* isoforms in establishing the cardiac nerve plexus.

Results

Zebrafish Neuregulin 1

The zebrafish genome encodes several members of the neuregulin family—*nrg1*, *nrg2a*, *nrg2b*, and *nrg3* (Laisney et al., 2010). Sequence analysis indicates zebrafish Nrg1 is the closest homolog to human NRG1 and mouse Nrg1 (Fig. 28A, Fig. 29). Zebrafish *nrg1* is located on Chromosome 18 where it is comprised of 14 coding exons (Fig. 28B). Through alternative splicing, *nrg1* produces 3 primary

isoforms, *nrg1-I*, *nrg1-IIa-c*, and *nrg1-III*, which differ primarily in their N-terminal sequence (Fig. 28B). Since Nrg1 isoforms may have differential roles in zebrafish, we used qRT-PCR to assess the relative expression levels of *nrg1-I*, *nrg1-II*, and *nrg1-III* in the heart. At 3 dpf, all isoforms were detectable in cDNA generated from whole embryo lysates (data not shown), but only *nrg1-I* was expressed at appreciable levels with cDNA derived from isolated hearts (Fig. 28C). Similarly, *nrg1-I* was the highest expressing isoform detected in adult hearts where very low levels of *nrg1-III* were detectable in some samples, and *nrg1-II* was below detection (Fig. 28D). Previous studies suggest that cardiac *nrg1* expression is confined to endocardial cells in the embryo. We detected *nrg1* by *in situ* hybridization in the heart and brain of embryo and, FACS enrichment confirmed *nrg1-I* expression in endocardial and not myocardial cells from 3 dpf hearts (Fig. 28E, data not shown).

Nrg1 features 5 distinct molecular domains (Fig. 30A). Alternative splicing leads to differential representation of these domains in *nrg1* isoforms (Fig. 30B). Domains include an isoform-specific N-terminal domain, which in *nrg1-I* and *nrg1-II* does not have any readily discernable function, but for *nrg1-III* is a cysteine rich domain that anchors the N-terminus in the cell membrane. The IgG-like domain is found only in *nrg1-I* and *nrg1-II* and is thought to play a role in allowing Nrg1 to bind to extracellular matrix proteins. The EGF-like domain, which has several versions in the type II isoform (a-c), is shared by all isoforms and binds Nrg1 receptors including ErbB4 in the heart. A shared transmembrane domain is important for proper membrane spanning of pro-Nrg1. Function of the C-terminal, shared Neuregulin domain is largely unknown, but defines Neuregulin proteins from other EGF-like ligands, and has been implicated in reverse signaling (Falls, 2003; Pedrique and Fazzari, 2010).

Generation of novel *nrg1* alleles

To investigate the isoform-specific requirements for *nrg1* in heart development, we used CRISPR/Cas9 gene editing to generate frameshift mutations to truncate all *nrg1* isoforms or the *nrg1-I/II* isoforms only (Fig. 30C).

Since targeting the first exon of any transcript is generally discouraged as it can lead to transcription initiation at cryptic start sites rather than the desired frameshift, to produce the *nrg1-I/II* specific mutant, we targeted exon 3 coding for the start of the IgG domain shared by *nrg1-I* and *nrg1-II*. Two alleles, *nrg1^{nc28}* and *nrg1^{nc29}* were isolated (Fig. 30D-E). These alleles are predicted to code for the

Nrg1-I variant truncated within the IgG domain (Fig. 30C). Similarly, to generate a pan-*nrg1* knockout, we targeted Exon 6, the first exon coding for the shared functional EGF domain. Two alleles, *nrg1*^{nc26} and *nrg1*^{nc27} were isolated and which code for truncations in the EGF-like domain (Fig. 30G-H). Nrg1-I variant amino sequences for each novel line are described in Fig. 31 (A-E). Since *nrg1*^{nc28} and *nrg1*^{nc26} mutations were predicted to cause more severe truncations than *nrg1*^{nc29} and *nrg1*^{nc27} alleles (Fig. 30C, Fig. 31B-E), we focused our efforts on assessing the phenotypes of these alleles.

Expression level of *nrg1* transcripts were dramatically reduced in *nrg1*^{nc28} and *nrg1*^{nc26} mutant embryos or adult hearts, suggesting nonsense-mediated decay of early-truncation transcripts (Fig. 30F,I). In-breeding heterozygous fish for all lines produced homozygous and heterozygous offspring at expected Mendelian ratios (data not shown). In this study, we also included a *nrg1-III*-specific loss of function allele, *nrg1*^{z26}, previously isolated from a large scale mutagenesis screen. *Nrg1*^{z26} mutant embryos feature supernumerary neuromasts in the developing lateral line due to impaired Schwann cell migration (Perlin et al., 2011). To verify the functional effect the new mutations on *nrg1-III*, we used a voltage sensitive vital dye (Mitotracker) to label neuromasts in larvae produced from interbreeding *nrg1*^{z26}, *nrg1*^{nc26}, and *nrg1*^{nc28} heterozygous fish (Lopez-Schier and Hudspeth, 2005). Supernumerary neuromasts (>18 neuromasts) were observed at 5 dpf in *nrg1*^{z26} and *nrg1*^{nc26} larvae at Mendelian ratios, but were not observed in wild type (data not shown) or *nrg1*^{nc28} larvae, demonstrating loss of function of the *nrg1-III* isoform in *nrg1*^{z26} and *nrg1*^{nc26} mutants (Fig. 32 A-F). Interbreeding of heterozygous adults carrying *nrg1*^{nc27} and *nrg1*^{nc29} alleles showed Mitotracker neuromast distributions comparable to *nrg1*^{nc26} and *nrg1*^{nc28} alleles, respectively (data not shown).

Nrg1 is dispensable for trabeculation

Our previous studies and others indicate that ErbB2 signaling is necessary to initiate cardiac trabeculation between 60-68 hpf where trabeculae are readily detected by confocal microscopy at 3 dpf (Liu et al., 2010). We crossed *nrg1*^{nc28} and *nrg1*^{nc26} alleles onto transgenic backgrounds to label cardiomyocytes with fluorescent reporters, and examined optical cross sections of the ventricle at 2 and 3 dpf. Interestingly, though trabeculae were undetectable at 60 hpf, by 3 dpf all genotypes had robust trabeculation (data not shown, Fig. 33A-C). To verify that trabeculation in *nrg1* mutants was not due to escape from requirement of ErbB2 signaling, we incubated embryos from 2 to 4 dpf with the ErbB2-

tyrosine kinase specific inhibitor PD16937 and found that all genotypes had substantially reduced trabeculation (Fig. 33D-I). Thus, *nrg1-l* is dispensable for cardiac trabeculation.

Though our findings indicate that *nrg1* is dispensable for cardiac morphogenesis through larval stages, *nrg1* may be involved in other essential cardiovascular functional or developmental processes. In preliminary studies, we interbred heterozygous fish and followed sibling offspring to adulthood. Homozygous mutant *nrg1^{nc28}* fish were indistinguishable from wild type or heterozygous clutch mates at the gross morphological level, and adult hearts were indistinguishable histologically (Fig. 24A-D). Mutants could be interbred to produce viable offspring, allowing ample tissue for further examination of embryonic phenotypes at the transcriptional level. Since *nrg1-l* is dispensable for trabeculation, but trabeculation requires ErbB2 activity, we hypothesized that a different, EGF-like ligand(s) can bind ErbB2/ErbB4 to stimulate trabeculation. To explore this hypothesis, we screened expression of known EGF-like ligands and EGF receptors in *nrg1^{WT/WT}* and *nrg1^{nc28/nc28}* larval hearts at 3 dpf (Fig. 34E-F). ErbB receptors *egfr1* (*erbb1*), *erbb2*, *erbb3b*, and *erbb4* were expressed at comparable levels in all genotypes (Fig. 34E). Five EGF-like ligands, *nrg1-l heparin-binding egf-like receptor a (hb-egfa)*, *neuregulin 2a (nrg2a)*, *betacellulin (btc)* and *epigen (epgn)* were detected (Fig. 34F). In corroboration with Figure 28, *nrg1-l* transcripts were reduced in mutant hearts (Fig. 34F). Interestingly, *btc* was significantly upregulated in *nrg1^{nc28/nc28}* hearts at 3 dpf, respectively (Fig. 34F). Additional studies are necessary to distinguish between an absolute requirement and a compensatory role for each of these ErbB2/ErbB4-activating ligand(s) in trabeculation.

Nrg1-III is required for adult zebrafish to thrive

In contrast to *nrg1^{nc28}*, *nrg1^{nc26}* mutant fish rarely survived to early adult stages. When observed, adult mutants were smaller than wild type or heterozygous clutch mates and appeared sickly. To quantify this survival defect, we raised a cohort of *nrg1^{z26}*, *nrg1^{nc26}* and *nrg1^{nc28}*, with wildtype or heterozygous and mutant larvae in separate tanks, and assessed survival weekly for 3 months. Equivalent survival rates were observed in *nrg1^{nc28}* mutant and wild type fish (Fig. 35A). In contrast, growth defects in *nrg1^{nc26}* and *nrg1^{z26}* mutants were became apparent by 8 wpf. Survival began to significantly decline at 9 weeks post fertilization (wpf) in *nrg1^{nc26}* mutants and, although survival was not significantly reduced during the observation period, juvenile mortality in *nrg1^{z26}* began at 9 wpf (Fig. 35B-C). Gross abnormalities were apparent in *nrg1-III*-deficient lines (*nrg1^{nc26}*, *nrg1^{nc27}* and *nrg1^{z26}* mutants) where individual fish show a

range of pigmentation defects and jaw malformations (Fig. 36A-F). Relative body mass was significantly reduced in *nrg1^{nc26}* and trended lower in *nrg1^{z26}* fish (Fig. 36G-H). Although smaller than controls, some *nrg1^{z26}* mutants show signs of sexual maturation (Fig. 36D), but in our hands, have not successfully interbred to produce viable offspring (data not shown). In contrast, *nrg1^{nc26}* mutants failed to develop outward signs of sexual differentiation that defines zebrafish the adult life stage (Fig. 36B).

Nrg1-III regulates larval cardiac nerve plexus development

Given that *nrg1^{nc26}* mutants often fail to recover from Tricaine anesthesia, and *nrg1-III* is primarily expressed in neuronal tissue with known roles in regulating myelination of long axons during neuromast formation, we hypothesized that *nrg1-III*-deficient mutants may have cardiac nerve plexus defects. Tricaine is structurally similar to benzocaine and blocks sensory and motor neuronal activity. To test this hypothesis, we isolated hearts from juvenile fish at SL5±1, SL10±1, SL15±1, and SL18±1 and visualized axons using an antibody against acetylated α -tubulin (ACT) (Figs. 37-39). These sizes roughly correspond to 2 wpf intervals and encompass late larval, early juvenile, late juvenile, and young adult stages. Owing to challenges in handling hearts from fish smaller than SL10, SL5±1 hearts were stained and imaged *in situ* with overlying tissues removed.

At SL 5±1, *nrg1^{WT}* hearts demonstrated robust atrial innervation and variable indications of ventricular innervation emerging from the AVC (Fig. 37A). In contrast, all atria and ventricles examined from *nrg1^{nc26/nc26}* fish were largely devoid of axons (Fig. 37B). By SL10±1, the whole wild type heart was extensively innervated with a hierarchical plexus of axons (Fig. 37C). Mutant fish at SL10 had some innervation, particularly in the atrium, but the ventricle and bulbous arteriosus (BA) were largely devoid of ACT positive staining (Fig. 37D).

To explore whether this lack of innervation is attributable to loss of *nrg1-III*, and if *nrg1-III*-deficient ventricles ever become properly innervated, we imaged ACT positive axons in *nrg1^{nc26}* and *nrg1^{z26}* mutants starting at SL10±1. Since our preliminary studies indicated that ventricular innervation is limited to the dorsal surface and appears to form from extension of atrial projections, to standardize orientation and we quantified the axonal coverage on the dorsal surface with the atrium removed. Interestingly, though *nrg1^{nc26}* and *nrg1^{z26}* mutants had some ACT positive axons at SL10±1, SL15±1, and SL18±1, these axons rarely extended to cover more than a small fraction of the ventricle surface and were

dramatically reduced compared to size matched controls (Fig. 38A-G). Together, these staining patterns suggest that *nrg1-III* is an essential regulator of cardiac nerve plexus formation.

To further characterize the ventricular nerve plexus, we examined orthogonal views of axons and cardiomyocytes in *Tg(myI7:rasGFP)* hearts where cardiomyocytes are labeled with a membrane targeted GFP (Fig. 39A-C). The nerve plexus was largely superficial in all genotypes (Fig. 39B). Though we did not observe definitive co-localization of acetylated α -tubulin and cardiomyocyte markers, these signals were in close apposition at the distal end of ACT positive projections (Fig. 39B-C).

Cardiovascular malformations in pan-Nrg1 mutants

Given that emergin innervation defects precede increased mortality in *nrg1^{nc26}* fish by a span of weeks (2 wpf to 9 wpf), we hypothesized that lack of innervation has later physiological consequences that ultimately lead to death. Prior to death, deteriorating *nrg1^{nc26}* mutant fish show behavioral indications of cardiovascular distress including gasping, reduced swimming, and emaciation, as well as sensitivity to anesthesia (Fig. 40A-B, data not shown). Since these symptoms are reminiscent of mammalian heart failure, we sacrificed *nrg1^{nc26}* fish showing at least one of these behaviors and examined cross sections of the heart for indications of heart failure SL11-15 (Fig. 40C-D). Hearts from these failing fish had reduced trabecular density and a thinner outer compact myocardial wall compared to controls (Fig. 40E,F). Though this is suggestive of heart failure, functional assays are necessary to confirm reduced cardiac output.

Myocardial thinning also supports the notion that underlying structural defects may contribute to cardiovascular distress in *nrg1^{nc26}* mutants. We examined the heart in H&E stained sections from individual *nrg1^{nc26}* fish and *nrg1^{WT}* clutch mates showing minimal signs of cardiovascular distress at SL16-SL20 (Fig. 41A-B). In mid-chamber lateral sections, the BA was positioned at an excessively acute angle relative to the ventricle, suggesting a possible change in the biomechanics of propulsion into the outflow tract (Fig. 41E). No change in this BA angle was observed in mutant fish from Fig. 40, suggesting this is acquired as mutant fish become larger (data not shown). Though no significant change in compact wall thickness was observed (data not shown), trabecular myocardium area was reduced in mutant fish (Fig. 41D-F). Additionally, we observed derangement of the compact myocardium in *nrg1^{nc26}* mutants, albeit with variable severity and penetrance (N=6 size-matched fish examined) (Fig. 42). Large lumens were

present in the compact wall of some mutant fish (N=4/6). In wild type hearts, open lumens were present near the AV junction, and blood-filled lumens were observed occasionally in the compact myocardium, consistent with cardiac-associated adipose tissue and coronary vasculature, respectively (Fig. 42A-C). In contrast, mutant hearts had large, open lumens both at the AV junction and throughout the outer curvature (N=3/6) (Fig. 42A-C). Additionally, some hearts showed ostensible increased nuclear density in the compact layer of the outer curvature (N=4/6) and thinning in the inner curvature (N=3/6) (Fig. D,E). There were no gross abnormalities in the AV or VB valves (Fig. 42F, and data not shown). Given the variability in observed histological changes in *nrg1^{nc26}* mutant hearts, we suggest that these malformations are secondary to the innervation defect.

Model

Together, these data support a model (Fig. 43) in which *nrg1* is essential for maintaining cardiac output due the role of *nrg1-III* in regulating cardiac nerve plexus formation. Mortality in *nrg1* mutants may involve structural malformations that emerge secondary to cardiac nerve plexus defects. Future studies are necessary to identify the cellular mechanisms underlying this altered plexus formation and further characterize the functional consequences of loss of *nrg1* in zebrafish.

Discussion and future directions

In this study, we used CRISPR/Cas9 gene editing to generate a series of mutations to examine the isoform-specific roles of *nrg1* in zebrafish heart development. The Nrg1-ErbB2/ErbB4 signaling pathway is essential for heart development in mice. In particular, embryos deficient in Nrg1 through truncation at either IgG or EGF-domains fail to develop cardiac trabeculae and die *in utero*. Zebrafish *nrg1* is alternatively spliced to form three main isoforms, of which *nrg1-I* is the primary isoform expressed in the heart. We generated novel *nrg1* mutant alleles that encode frameshift mutations to delete all isoforms of *nrg1* at the EGF-like domain (*nrg1^{nc26}* and *nrg1^{nc27}*) or only isoforms *nrg1-I* and *nrg1-II* by targeting the IgG domain and explored their phenotypes.

Nrg1-I is dispensable for heart development in zebrafish

Interestingly, trabeculae developed in an ErbB2-dependent manner in all our *nrg1* mutants. We explored several potential explanations for this cross-species difference in requirement of Nrg1 in cardiac

trabeculation. Since teleost fish underwent partial genome duplication approximately 300 million years ago, many zebrafish genes have paralogs with compensatory functions (Howe et al., 2013). However, in a preliminary study, BLAST alignment (Altschul et al., 1990) of *nrg1* with the zebrafish genome (GRZ9) identified only known Neuregulin family genes *nrg2a*, *nrg2b*, and *nrg3*, as having with substantial homology to zebrafish *nrg1*, suggesting that the zebrafish genome does not contain a *nrg1* paralog (data not shown). Since homozygous expression of *nrg1^{nc26}* or *nrg1^{nc28}* alleles does not remove requirement for ErbB2 tyrosine kinase activity in cardiac trabeculation (Fig. 33), this raised the question of how the ErbB2/ErbB4 heterodimers is activated in *nrg1* mutant hearts. Promiscuous ligand binding of EGF-like ligands to EGFR family receptors has reported in other contexts (Kochupurakkal et al., 2005; Laisney et al., 2010; Yarden and Sliwkowski, 2001), so we hypothesized that other EGF-like ligands can stimulate ErbB2 kinase activity in the heart, either as a primary role or through gene compensation (Rossi et al., 2015). To evaluate this possibility, we screened 3 dpf hearts for expression of canonical EGF family ligands and receptors. Of the 12 canonical EGF-like ligands screened, 5 were consistently expressed—*nrg1*, *nrg2a*, *hbegf-a*, *btc* and *epgn* (Fig 34F). Though receptor expression levels were largely unchanged, *btc* was upregulated in *nrg1^{nc28}* mutant hearts, suggesting that it may be involved in a compensatory response to loss of *nrg1*. Additional mutagenesis studies will be necessary to determine which factor(s) binds ErbB4 to promote trabeculation, whether such binding serves a primary or compensatory role in *nrg1* mutant hearts.

Previous reports have described a protective role for cardiac Nrg1-ErbB2/ErbB4 signaling in heart disease and a role for Nrg1 in promoting cardiac repair (Bersell et al., 2009; D'Uva et al., 2015; Gao et al., 2010; Gemberling et al., 2015; Harvey et al., 2016; Jabbour et al., 2011; Lai et al., 2010; Mendes-Ferreira et al., 2016; Polizzotti et al., 2015; Rupert and Coulombe, 2015; Yutzey, 2015). In this context, Nrg1 mitogenic activity is through to promote cardiomyocyte gene expression, survival, and proliferation (Bersell et al., 2009; D'Uva et al., 2015; Gemberling et al., 2015; Polizzotti et al., 2015). Given that *nrg1-l* is the primary isoform expressed in the embryonic and adult heart, and its expression is reduced in *nrg1^{nc28}* and *nrg1²⁹* mutants, it would be interesting to explore whether these mutants have deficiencies in injury response and regeneration. It is possible that, though Nrg1 is dispensable under homeostatic

conditions, defects could emerge when challenged by ventricle resection or cryoinjuries (Dickover et al., 2013).

Nrg1-III-deficient fish have similar survival and gross morphological defects

Though all the *nrg1* mutants we examined survived through embryonic and larval stages, *nrg1^{nc26}* and *nrg1^{z26}* mutants displayed gross morphological differences compared to *nrg1^{nc28}* mutants and wildtype or heterozygous siblings. Their altered pigmentation, jaw malformation, reduced body mass, increased mortality during late juvenile and early adult stages suggest a role for *nrg1-III* isoforms in these phenotypes. Comparing, the *nrg1^{nc26}* and *nrg1^{z26}* lines, the *nrg1^{z26}* mutation generated a less severe phenotype—they survived longer, showed signs of sexual differentiation, and had a less severe reduction in body weight compared to sibling controls. Protective effects from *nrg1-III* isoforms or expression of a partially functional protein from the *nrg1^{z26}* allele might explain this difference. Alternatively, these might be attributable to a strain effect. Though both mutations are on TL strains, outbreeding in zebrafish colonies has led to substantial differences between strains at different facilities, and so differences might be attributable to strain differences. Indeed, control sibling *nrg1^{z26}* fish have a higher average ratio of body weight to standard length than *nrg1^{nc26}* fish within the same size range (Fig. 36G,H). To account for this possibility, we plan to intercross the strains for several generations and compare phenotypes in mixed-background offspring.

Cardiac nerve plexus development is impaired in Nrg1-III-deficient fish

Based on several observations, we hypothesized that *nrg1-III*-deficient fish have defects in the cardiac nerve plexus. During routine handling, *nrg1^{nc26}* fish frequently failed to recover from anesthesia with Tricaine (MS-222), a drug structurally similar to benzocaine and which blocks motor and sensory neuronal signaling. Additionally *nrg1-III* is important for peripheral innervation in larvae, as evidenced by supernumerary neuromasts. Also, a recent report showed that cardiac nerves play an important role in cardiac regeneration in mice and zebrafish in a mechanism involving Nrg1. Extrinsic control of cardiac output begins as early as 4-5 dpf as evidenced by change in heart rate in response to adrenergic and cholinergic stimulation or inhibition (Schwerte et al., 2006). The adult zebrafish cardiac nervous system was recently characterized (Stoyek et al., 2015). It features an extensive intrinsic nerve plexus containing cholinergic and adrenergic axons. This plexus is linked to the extrinsic nervous system primarily at the

venous pole via vagal efferents, with a separate trunk innervating the bulbous arteriosus and proximal ventricle (Stoyek et al., 2015).

Here, an axon-specific marker acetylated α -tubulin (ACT) was used to survey intrinsic cardiac innervation in *nrg1-III*-deficient fish. Focusing on early juvenile stages which precede increased mortality in *nrg1^{nc26}* mutants, we found evidence of an emerging ventricular nerve plexus at SL5 \pm 1 (~14 dpf) in fish carrying WT alleles. This plexus was largely absent in *nrg1^{nc26}* mutants at the same length scale. To determine whether this plexus fails to form or if formation is only delayed, we examined the dorsal surface of ventricles from fish from SL10-SL18. Hearts *nrg1^{WT}* and in a *nrg1^{nc28/nc28}* mutant (data not shown) fish, displayed a robust, hierarchical plexus of axons extending from the AVC over the ventral surface of the heart. Interestingly, in *nrg1^{nc26}* mutant fish the ventral surface of the ventricle is essentially devoid of acetylated α -tubulin positive axons (data not shown). Minimal innervation was detected on the dorsal surface near the AVC in *nrg1^{nc26}* and *nrg1^{z26}* mutants (Fig. 37, Fig. 38).

Due to chamber collapse in isolated hearts and limited confocal imaging penetrance, other techniques are necessary to evaluate extrinsic inputs, particularly of vagal projections to the pacemaker and atrium. However, zebrafish with mutations causing a weak or non-contractile atrium can survive to adulthood, suggesting that atrial contractility is dispensable for survival in a laboratory setting (personal communication, Deborah Yelon). Together, these results indicate that *nrg1-III* is essential for establishing the ventricular nerve plexus, and is necessary during adult life stages.

It is unclear whether defects in cardiac innervation are generally associated with lethality, or if a specific role may be ascribed to *nrg1*. Comparative phenotypic analysis could be conducted between of *nrg1^{z26}* and *Tg(my17:sema3aa)* fish, a line previously described to have dramatic reductions in ventricular coverage of the cardiac nerve plexus, would address this question (Mahmoud et al., 2015). Given that *nrg1-III* deficiency appears to inhibit plexus formation, we predict that any physical or genetic lesion leading to a comparable loss of innervation will have similar effects on survival.

Cardiac abnormalities in *nrg1^{nc26}* mutant fish

As the mutant with the most severe phenotype, we focused on characterizing *nrg1^{nc26}* mutants. These fish showed peri-mortem behavioral indications of cardiovascular distress as early as 8 wpf. Since fish survive for weeks with ventricle innervation defects without obvious signs of distress, we were

interested in identifying the cause of decline, and hypothesized that it is due to progressive heart failure. Fish demonstrating at least one of these behavioral symptoms were sacrificed and compared histologically to *nrg1*^{WT} clutch mates. To our knowledge, there are no standardized methods for molecular or structural characterization of heart failure in adult zebrafish. However, heart failure in murine systems is characterized by an initial hypertrophic response, followed by progression to dilated cardiomyopathy featuring a thinned myocardium (Breckenridge, 2010; Patten and Hall-Porter, 2009). Reminiscent of murine heart failure, we observed reduced trabecular density and outer myocardial wall thickness, suggestive of myocardial thinning were reduced in *nrg1*^{nc26} mutants (SL11-15) showing signs of cardiovascular distress. Other measures are necessary to confirm that these fish are indeed undergoing canonical heart failure including cardiovascular function. However, methods for echocardiography in adult zebrafish have been described only recently, lack resolution and are limited to relatively large zebrafish (Hein et al., 2015; Lee et al., 2016). As a surrogate measure of heart failure, total cardiovascular performance and fitness is being evaluated in all *nrg1* mutant lines by evaluating maximal swim performance (Palstra et al., 2010; Pelster et al., 2003; Plaut and Gordon, 1994). Additionally, electrocardiography is being used to explore the effect of *nrg1* mutants on heart rate and the cardiac action potential (Chaudhari et al., 2013).

We also investigated the possibility that underlying structural malformations, which may be dependent on cardiac innervation, contribute to mortality. To this end, whole *nrg1*^{nc26} mutants and size-matched wildtype or heterozygous clutch mates, SL16-20, were sectioned and stained with hematoxylin and eosin. Focusing on mid-ventricle sections, mutant hearts demonstrated morphological changes suggestive of underlying structural malformations that may contribute to impaired heart function. Possibly, due to relative positioning of a malformed jaw, the bulbous arteriosus is at an excessively acute angle relative to the ventricle base in *nrg1*^{nc26} mutants SL16-20. This could alter the biomechanics of systolic contraction and increase the workload necessary to maintain cardiac output.

Additionally, derangement of the myocardium was evident in *nrg1*^{nc26} mutant hearts at SL16-20, suggesting that loss of *nrg1* may lead to defective cardiac maturation. Trabecular density was reduced in mutant fish, which could reflect a lower number of trabecular cardiomyocytes, reduced cardiomyocyte size, or both. Transgenic fish carrying nuclear and membrane bound markers of cardiomyocytes,

Tg(myl7:nuc-dsRed); Tg(myl7:rasGFP), crossed onto the *nrg1^{nc26}* mutant background could be used to clarify the cellular basis of this trabeculation defect. If the average number of cardiomyocyte nuclei per ventricle section is lower in mutant fish, additional stains could be used to explore whether this is attributable to a lower basal proliferation rate or to increased cell death.

Changes in outer wall thickness may reflect either expansion of the primordial layer, defective cortical layer formation, or proliferation of an extra-myocardial tissue such as the epicardium. Lack of specific, validated markers for the primordial and cortical layers preclude definitive characterization of this defect. However, cortical layer defects could be assessed through clonal labeling, as described in (Gupta et al., 2013; Gupta and Poss, 2012). Similarly, epicardial expansion may be tested by lineage tracing approaches with epicardium-specific *Tg(wt1:Cre^{ERT2})* fish (Kikuchi et al., 2011). Additionally, we observed large open or blood filled lumens in some *nrg1^{nc26}* mutant hearts. While *nrg1^{WT}* hearts occasionally had clusters of open lumen structures located near the AVC and ventricle base at the BA junction, consistent with the morphology of cardiac-associated adipocytes, large, lumens were present in the outer myocardium of some *nrg1^{nc26}* fish in atypical locations. Some were open, and are likely to be cardiac-associated adipocytes, while others contained hematocrit. The blood-filled structures are likely part of the coronary vasculature, and in mutants had unexpectedly large diameters. Since cross-sectional analysis is not optimal for studying the coronary plexus, this potential coronary vascular defect is being further characterized by crossing *nrg1* mutant lines onto *fli1a* reporter backgrounds and assessing surface vasculature (Harrison et al., 2015). Interestingly a recent report in mice showed that cardiac nerves follow coronary veins during mouse coronary development (Nam et al., 2013), suggesting there may be a similar relationship between nerves and coronaries in which is perturbed in *nrg1-III*-deficient fish and could contribute to cardiovascular function.

Conclusions

Together, these findings demonstrate that *nrg1-I* is dispensable for zebrafish heart development, and suggest an essential role for *nrg1-III* isoform in establishing the cardiac nerve plexus. Further studies are needed to characterize the cardiovascular capacity of zebrafish lacking a functional ventricular nerve plexus, identify the mechanism by which *nrg1-III* regulates cardiac nerve formation, and determine how ErbB2 signaling is activated in *Nrg1*-deficient hearts.

Materials and methods

Animal lines and care

Embryos and adult fish were raised and maintained at the aquaculture facility of the University of North Carolina at Chapel Hill in accordance with Institutional Animal Care and Use Committee approved protocols (Westerfield, 2000). The zebrafish lines used in this study are as follows: *nrg1*^{z26} (Perlin et al., 2011), *Tg(myI7:dsRed)*^{vc6} (Rothschild et al., 2009), and *Tg(myI7:rasGFP)*^{s883} (D'Amico et al., 2007).

Primer design

NIH Primer Blast was used to design all primers used in this study. Primers were selected for adherence to optimal criteria including melting temperature of 60°C, 20 bp length, minimal off target specificity, and minimal primer dimerization. Table 3, describes all oligonucleotides used in this study.

CRISPR/Cas9 design and injection

Cas9 mRNA was *in vitro* transcribed from using mMessage mMachine kit (Invitrogen) as previously described (Chang et al., 2013). CRISPR/Cas9 target sites in exons 3, 6, and 11 of *nrg1* were identified using ZiFit software and zebrafish genomic sequence build GRCz9. Single stranded oligonucleotides corresponding to the targeting sequence were annealed and cloned into DR274 vector, then transcribed *in vitro* with T7 MaxiScript kit (Invitrogen). Embryos were injected at the one cell stage with 1-2 nl of a mixture containing 1200 ng Cas9, 50-75 ng gRNA, 10 mM MgCl, and 0.01% phenol red. gRNA targeting efficiency was determined by High Resolution Melt Analysis (HRMA) as described below using primers flanking the target site. F1 offspring from F0 founders that carry favorable mutations were raised to adulthood. F1 founders carrying mutant alleles were identified and interbred to produce homozygous wild type, homozygous mutant, and heterozygous mutant offspring.

PCR and qRT-PCR

RNA was isolated from whole embryos using Trizol reagent (Invitrogen) and from embryonic hearts using Qiagen RNeasy Mini Plus Kit according to manufacturer's instructions. Up to 1 ug of cDNA was reverse transcribed using Invitrogen Superscript Master Mix. For PCR, we used GoTaq reagents with 10 ng cDNA template as per manufacturer's instructions. For qRT-PCR, we used Syber Green chemistry on a ViiA7 qPCR machine in 10 µL reactions. Cycle threshold (CT) values were normalized to *ef1a* as a

housekeeping gene and relative expression was calculated comparing average change in CT in wild type and mutant embryos by the $2^{\Delta\Delta CT}$ method (Livak and Schmittgen, 2001).

HRMA

High resolution melt analysis (HRMA) was used to validate CRISPR/Cas9 reagents, identify F1 founders, and genotype *nrg1^{nc28}* and *nrg1^{nc29}* fish. Each 10 ul reaction contained 0.5 ul genomic DNA (see Genotyping, above), 5 ul Syber Green (Invitrogen), and 4.5 ul primer mix (water with mM forward and reverse primers). Fluorescence was measured every 0.025°C in a melt curve 55-95° and HRMA peaks were called from the derivative curve.

Genotyping

Genomic DNA was collected from fin clips or embryos in lysis buffer consisting of 10 mM Tris-HCl PH 8.0, 50 mM KCl, 0.3% Tween-20, lysed at 95° for 10 minutes, and then digested in 0.5 µg/mL Proteinase K (Denville Scientific). *Nrg1^{z26}* fish were genotyped by PCR and enzyme digestion as previously described (Perlin et al., 2011). HRMA was used to genotype wild type, mutant, and heterozygous all novel *nrg1* lines. Heterozygous alleles had multiple peaks in the derivative melt curve. Homozygous wild type and homozygous mutant allele melt temperatures differed by at >1°C. This genotyping method was verified both by enzyme digestion and by sequencing in a subset of samples.

Heart isolations

Heart isolations were performed as previously described (Samsa et al., 2015). Briefly, larvae were euthanized with 5X Tricaine at 3 dpf. Fine forceps were used to manually remove each heart (ventricle, atrium, and bulbous arteriosus) and dissect away non-cardiac tissues. Hearts were transferred to lysis buffer and processed according to manufacturer's instructions for the RNeasy Mini Plus kit (Qiagen). A minimum of 40 hearts were pooled for each gene expression replicate.

In situ hybridization

In situ hybridization was performed as previously described (Liu and Stainier, 2010). *In situ* hybridization probe for *nrg1* was prepared as previously described (Milan et al., 2006) and synthesized from pGEMT vector (Promega) using the DIG RNA labeling kit (Roche). Whole-mount embryo imaging was performed on a Leica MZ16F fluorescence stereomicroscope.

Mitotracker assay

Supernumerary neuromasts were assayed essentially as previously described (Lopez-Schier and Hudspeth, 2005). Briefly, larvae were incubated for 5-30 minutes in fish water containing Mitotracker Red (Invitrogen) at 1:10000 dilution. Larvae were briefly rinsed with system water and anesthetized with 1X Tricaine, then oriented in a lateral position and epifluorescence images were collected on a Leica M205C fluorescence stereoscope. The number of neuromasts on the lateral line were counted for N>25 embryos. Wild type embryos had 8-12 neuromasts, and we considered 18+ neuromasts to be supernumerary.

Confocal microscopy

Anesthetized embryos and larvae were embedded in 1% low melt agarose and oriented for optimal viewing of the heart. Immediately prior to imaging, embryos were euthanized with 5-10X Tricaine. After cessation of heartbeat, confocal z-stacks were collected using an Olympus Fluoview 1000MPE equipped with a 20X XLPlan water immersion objective (NA 1.0) with 2.5X optical zoom. Fluoview software was used to collect sections through the middle 25-50% of the heart at 512x512 or 1024x1024 pixel resolution and 1-2 μm spacing between z-slices. Fluoview's brightness correction algorithm was used to account for signal attenuation with increasing depth. ImageJ (Schneider et al., 2012) was used to process images. For each Z-stack, we selected either a maximum projection image of the whole stack or a representative mid-chambers slice for the appropriate analysis. Confocal data was collected for a minimum of 3 embryos for each condition, with matching controls for each experiment, where the N>3 embryos were selected as the representative samples from a pool of a minimum of N>12 embryos which were visually inspected for phenotype.

Whole fish microscopy

Juvenile and adult fish were anesthetized with Tricaine in system water. Fish were imaged in a minimal volume of water using an Android 13 MP camera. Brightness and contrast were adjusted and images were scaled using ImageJ software.

Histology

Adult fish were euthanized on ice for 20 minutes. To ensure rapid and complete fixation, each fish was gavaged with 4% paraformaldehyde in PBS (PFA), then the abdominal cavity was opened by

anterior-posterior incision and flushed with 4% PFA. After overnight fixation, the fish were de-calcified with 0.5M EDTA for 3-7 days, dehydrated in 70% ethanol, paraffin embedded and sectioned at 5 μ m intervals.

Histology quantification

H&E staining was imaged using a Leica DMIRB inverted microscope equipped with 10X and 20X objectives and Nikon Elements software. To measure trabecular myocardial density, a 0.25-1.0mm box was drawn in the trabecular myocardium from a mid-chamber slice, taking care to exclude the inner lumen. A blinded observer used Adobe Photoshop to generate a mask of the trabecular myocardium, then calculated area fraction covered by trabecular myocardium using Image J. To measure compact wall thickness, ImageJ was used to draw lines perpendicular to the outer wall at 12 locations throughout the inner and outer curvature. Wall regions in the apex and base positions were avoid and only regions where the compact and trabecular myocardium are clearly distinguishable were selected for analysis. Measurements were compared across genotypes using Student's T-Test.

Survival curve

Embryos were obtained from breeding healthy homozygous ($nrg1^{WT/WT}$ and $nrg1^{nc28/nc28}$ clutchmates) or heterozygous ($nrg1^{WT/nc26}$ and $nrg1^{WT/z26}$) adults. At 5 dpf, juvenile $nrg1^{nc26}$ and $nrg1^{z26}$ mutant fish were separated from wild type and heterozygous clutch mates using the Mitotracker screen for supernumerary neuromasts (above). For each genotype, 7 tanks containing 10 fish each were raised under standard husbandry conditions. Tank order was randomized to minimize husbandry position effects. Survival was recorded weekly at 6-8 day intervals through 12 wpf.

Chapter 3.2 Figures

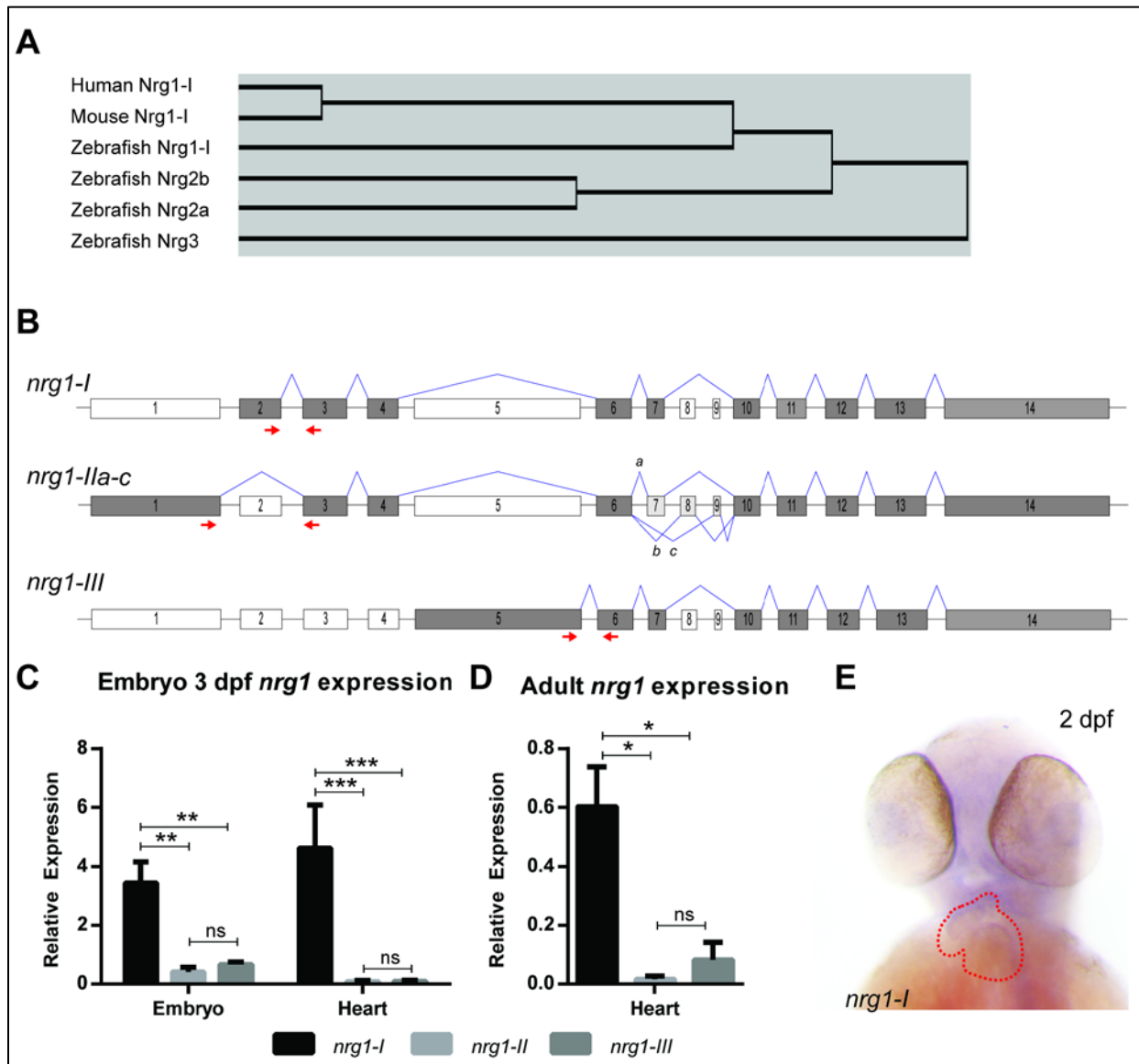


Figure 28 Zebrafish neuregulin 1

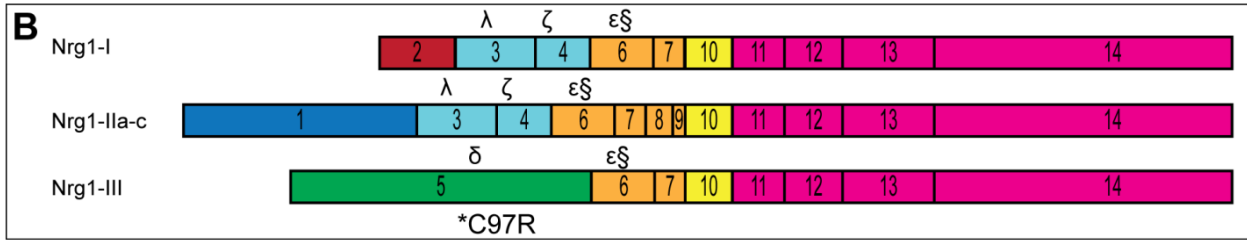
(A) Gene tree from Clustal-Omega multiple alignment comparison. (B) Schematic of *nrg1* gene structure. Exons are to scale; introns are not to scale. Alternative splicing (navy) produces three primary isoforms, *nrg1-I*, *nrg1-IIa-c*, and *nrg1-III*. (C-D) Relative expression of *nrg1* isoforms in (C) 3 dpf embryos and hearts enriched from dissociated 3 dpf embryos or (D) adult zebrafish 1-2 months post-fertilization. (E) *In situ* hybridization of anti-sense riboprobe targeting *nrg1*; representative image from examination of N>6 embryos. Heart is outlined in red. Red arrows in (B) note location of isoform-specific qRT-PCR primers. Student's T-test compared to matched control. Error bars are SEM. N≥3 biological replicates. *p≤0.05-0.01, **p≤0.01-0.001, ***p<0.001

Human Nrg1-I	1	-----
Mouse Nrg1-I	1	-----
Zebrafish Nrg1-I	1	-----
Zebrafish Nrg2b	1	-----
Zebrafish Nrg2a	1	-----
Zebrafish Nrg3	1	MSERTALGATMETMTLEEPGGEQASPRAPGPLRCGPCAIVWPRQQTWLCVVPLLMGFVGLG
Human Nrg1-I	1	-----
Mouse Nrg1-I	1	-----
Zebrafish Nrg1-I	1	-----
Zebrafish Nrg2b	1	-----
Zebrafish Nrg2a	1	-----
Zebrafish Nrg3	61	LSLMLLLKWIIVVGSVQDYVPTDLVDANRIGQDPIFLSKPSSLPGKSDASASTTSTTPSAAP
Human Nrg1-I	1	-----MSEKER-----GRGKGKGGK-KERGSKKPESAAGSQSPAL
Mouse Nrg1-I	1	-----MSEKER-----GRGKGKGGK-KDRGSRGKPAPAEGDPSPAL
Zebrafish Nrg1-I	1	-----MAEVKA-----GKEGKSGDKKKDKES---VRSNKPDNSPQA
Zebrafish Nrg2b	1	-----
Zebrafish Nrg2a	1	-----MREISYRNCGRMRERTT---DRRKKDGL-----REGKKRAS
Zebrafish Nrg3	121	GSATRAAEGTGTVQRTRIGQSSNHTASSSSSSSGGGGG-----LGGGSGNR
IgG domain		
Human Nrg1-I	36	PPRLKEMKSSQESAAGSKLVLRCEETSSEYSSLRFKWFKNGNELNRKKNPQNIKIQKQP--G
Mouse Nrg1-I	36	PPRLKEMKSSQESAAGSKLVLRCEETSSEYSSLRFKWFKNGNELNRRNKPQNVKIQKQP--G
Zebrafish Nrg1-I	34	EPKLNLRSVTVEDGKKTVLKCEILAGNPAPNVKWKYKNGKELTGKKNPKSIKIKKKKQGGK
Zebrafish Nrg2b	1	----MKNPVLADEGSRLLIVKCEAT-GSPAPEYKWKYKDGAEKRSK---EIKIRNNK--K
Zebrafish Nrg2a	34	APKVKPMDSQWLQEGKKTTLKCEAV-GNPSPSFNWYKDGSQLRQKK---TVKIKTNK--K
Zebrafish Nrg3	167	APHLHNRVGRTRVT-----NITTTTRATNPAPP-----GGKEVTP-----RSTTVRKPNI--
Human Nrg1-I	94	KSELRINKASLADSGEYMCKVISKLGNDASASA---NITIVESNEIITGMPASTEGAYVS
Mouse Nrg1-I	94	KSELRINKASLADSGEYMCKVISKLGNDASASA---NITIVESNDLTTGMSASTERPYVS
Zebrafish Nrg1-I	94	ISELLIRKSTEGDAGLYTCEAVNSLGKTNNTA---NLFIIINTA-----
Zebrafish Nrg2b	50	NSKVQIGSAKLEDGNYTCVAENILGKANGTS---TVHVQ-----
Zebrafish Nrg2a	88	NSKLHISKVRLLEDGNYTCVVENSLGRENATS---FVSVQ-----
Zebrafish Nrg3	210	-----GEGGSRASPSARAGPPSPTTTTTTTTITIT-STTTTQAAOPTSTPASP
EGF domain		
Human Nrg1-I	150	SESPIRIS--VSTEG-----ANTSSSTSTSTTGTSHLVKCAE-KEKTFVNGGEC
Mouse Nrg1-I	150	SESPIRIS--VSTEG-----ANTSSSTSTSTTGTSHLIKCAE-KEKTFVNGGEC
Zebrafish Nrg1-I	134	-----TSTTPSAKTSSHVTPCNE-SEKEYCVNHGKC
Zebrafish Nrg2b	87	-----SITTTVSPGSGHARRCND-TEKTYCVNGGDC
Zebrafish Nrg2a	125	-----SITTTLSPGSSHARKCNE-TEKTYCINGGDC
Zebrafish Nrg3	258	SKPGQRWNHGRSSKGPSTKPTRPHRFRTLAPTTSTVRSEFFKPCQDSQEMAFCLNEGEC
Human Nrg1-I	197	FMVKDLNPSRYLCKCPGFTGARCTENVPMK-----VQ-----NQEKAEELYQKRVL
Mouse Nrg1-I	197	FMVKDLNPSRYLCKCPNEFTGDRCONYVMAS-----FYKHLGIEFMEAEELYQKRVL
Zebrafish Nrg1-I	164	FTLEVTGNIIRRLCRCPPGFTGNRCQNRDPVR-----VV-----DHKQAEELYQKRVL
Zebrafish Nrg2b	117	YYIHGI---NQLSCKCPDGYFGPRCLQTEPLR-----LYMP--KPNKAEELYQKRVL
Zebrafish Nrg2a	155	YFIHGI---NQLSCKCPNDYTGERCQTSVMAG-----FYKHLGIEIMEAEELYQKRVL
Zebrafish Nrg3	318	FIIETVAG-VHRHCRCKEGYRGLRCDQFVPKTDSILSDPTADELGLIEFMEAEETYQRQIL
Human Nrg1-I	245	TITGICIALLVGIMCVVAYCKTKKQKQKLDHRLRQSLRSENNMMNIANGPH-HPNPPP
Mouse Nrg1-I	250	TITGICIALLVGIMCVVAYCKTKKQKQKLDHRLRQSLRSENNMMVNIANGPH-HPNPPP
Zebrafish Nrg1-I	212	TITGICIALLVGIMCVVAYCKTKKQKQKLDHRLRQSLRERN---AAAKGPQ-HPHPPP
Zebrafish Nrg2b	165	TITGICVALLVGVVAYCKTKKQKQKMMHNLHQNIYVDHPNR-NLANGPN-HPGGPG
Zebrafish Nrg2a	205	TITGICVALLVGVVAYCKTKKQKQKMMHNLHQNMCAEHPNR-MLANGPN-HPGGPG
Zebrafish Nrg3	377	SIFSIAMGISLLGVACMALYCKNKRQREKHRAHLTEIRNLRDC-TVNA-SGLMSKSSPRL
Human Nrg1-I	304	EN-VQLVNQY--VSKNVISSEHIVEREAET--SFSTSHYTSTAHHSTVTQTPTS-----H
Mouse Nrg1-I	309	EN-VQLVNQY--VSKNVISSEHIVEREVET--SFSTSHYTSTAHHSTVTQTPTS-----H
Zebrafish Nrg1-I	267	EN-LQLVNHY--MPTNPVP-AHMTDKEAET--SLSTNEFTSPTHSTAITHSSS-----Q
Zebrafish Nrg2b	223	EE-IPMVD-Y--ISKNVPATERVIRHGAEA--PFGSRQSSRSHNSSTRA-----
Zebrafish Nrg2a	263	EE-IPMVD-Y--ISKNVPATERVIRHGTETSGNFGSRMSSRSHHTSTASHTSSHRHEER
Zebrafish Nrg3	435	ESSLQLQKSRVHGLSSPQAASIV-----LSSSK-----VSLPNQNR

Human Nrg1-l	354	SWSNGHTESILSESHSVIMSSVENSRRHSPT -GG-PRGRLNGTGGPRECNSFLRHARE-
Mouse Nrg1-l	359	SWSNGHTESIISESHSVIMSSVENSRRHSSPA -GG-PRGRLHGLGGPRECNSFLRHARE-
Zebrafish Nrg1-l	316	CWSNGKAESVVSDSHAVLMKPSAENCQHGTPS ----HRGRLNATGGVHQLNDYLKNSRE-
Zebrafish Nrg2b	267	-----
Zebrafish Nrg2a	319	TWSMERTDSIHSDCQSGALSSSVGTSKCSSPA -CMEARARRAAYCGYPDATQCSLQYGD-
Zebrafish Nrg3	472	SFSMGKRRCRSCSFSSSPALKHKVSNYRAVSKWTPPIPRAGHHLGGSRDSLHSYKHLQEV
Human Nrg1-l	411	-----TPDSYRDSPHSERYV-----S-----AMTTPARMSPV
Mouse Nrg1-l	416	-----TPDSYRDSPHSERYV-----S-----AMTTPARMSPV
Zebrafish Nrg1-l	371	-----AQGSNRDSPYSERYV-----S-----AMTTPTRLSPV
Zebrafish Nrg2b	267	-----HSSTHRYV-----S-----ALTTPARLSPV
Zebrafish Nrg2a	377	-----SYDSL RDSPHSDRYV-----S-----ALTTPARLSPV
Zebrafish Nrg3	532	EVNDVMPQALRRCQSHLDSNQNRCLNMQIMLSAHSKGMSTYDVPCTRLDQGMTFPPP
Human Nrg1-l	438	DFHTPSSPKSPPSEM----SPPVSSMTVSMPSMAV----SPF-MEEERPLLLVTPPRLR
Mouse Nrg1-l	443	DFHTPSSPKSPPSEM----SPPVSSMTVSMPSVAV----SPF-VEEERPLLLVTPPRLR
Zebrafish Nrg1-l	398	GLLSPVTPSSPPSEM----SAPLSSLATSVPSMLT----SPS-GEEERPLLFRTPPILR
Zebrafish Nrg2b	287	DFHYSLPPQVPTFQI----TSPNASHAMSLPPAAH----APYPPEEDQPLRRYQVPLH
Zebrafish Nrg2a	404	DFHSSLPPQVPTFQI----TTPNASHALSLPPAASAIAMAAYSPPDDQPLLYRYR----
Zebrafish Nrg3	592	SFRAHSVPIIPSVQGPDFGGGGGNKLHNVGMGSSSY----NPINP-----
Human Nrg1-l	488	EKKFDHHPQQF----SSFHHPAHDSNSLPASPLRIVEDEEYETTQEYEPAQEPVKKL-
Mouse Nrg1-l	493	EKKYDHHPQQQL----NSFHHPAHQSTSLPPSPLRIVEDEEYETTQEYEPQEPKVV-
Zebrafish Nrg1-l	448	DKSASTQGRKSGHNLNSAHYHGLDIPSPPPSPLHIEEEI--DCLEQYKSTSVPS--A-
Zebrafish Nrg2b	338	EARGHEPYR----QQQRGSYL RDS TGS LPS SPYRLAQE DEYESTQEYLLSMEQPKRS-
Zebrafish Nrg2a	455	-----RSRRPYAAESTGSLPSSPYRFVDEDEYETTQEYSSREQPKKS-
Zebrafish Nrg3	633	-----ETESVANSRSLASSSATVQEPQTLTCSESALMSRGIKHS
Human Nrg1-l	542	-----ANSRRAKR -TKPNGHIANRLEVD-SNTSSQSSNSESETEDE-----
Mouse Nrg1-l	547	-----TNSRRAKR -TKPNGHIANRLEMD-SNPSSVSSNSESETEDE-----
Zebrafish Nrg1-l	504	-----PHSPSAAR -TQPSGQAAPEQAV--SGSNSESSSESETEDE-----
Zebrafish Nrg2b	391	-----SRRWRR -SRLNGHVAPRGYQPSRDLGSRSLSDSDSEE-----
Zebrafish Nrg2a	499	-----SGSRRWRRSRINGHTPG-----PRNYSSQSCLS DSEWEDE---EVG--
Zebrafish Nrg3	675	LVTYTTALGSGTSSRAKT--VISMTVLGTGVKT-TQY-AASLLSKTTAGREEHSAFEEV
Human Nrg1-l	581	--RVGEDTPFLGIQNPLAASLEATPAFRLADSRTN---PAGRFSTQEEIQ-ARLSSVI--
Mouse Nrg1-l	586	--RVGEDTPFLGIQNPLAASLEVAPAFRLAESRTN---PAGRFSTQEEIQ-ARLSSVI--
Zebrafish Nrg1-l	542	--RVGEDTPFLGLQNPAAAGSLVLD--GLEGSRTN---PALHLSPOHELQ-NRLTAVM--
Zebrafish Nrg2b	428	--EEGESTPFLSMQNMNAEPSAL--YRPVPDTRTSHAQSGRHGSRANTQ-TRLTHSRSK
Zebrafish Nrg2a	538	DLGHGESTPFLSMQNMNATEPATI--YRPNDTRT--FSNTGRSGSRPNVQANKLTQSRFR
Zebrafish Nrg3	731	KQGDGLQTSFTGDEKDSFSSGVRGETSLDHPKS-----
Human Nrg1-l	542	-----ANSRRAKR -TKPNGHIANRLEVD-SNTSSQSSNSESETEDE-----
Mouse Nrg1-l	547	-----TNSRRAKR -TKPNGHIANRLEMD-SNPSSVSSNSESETEDE-----
Zebrafish Nrg1-l	504	-----PHSPSAAR -TQPSGQAAPEQAV--SGSNSESSSESETEDE-----
Zebrafish Nrg2b	391	-----SRRWRR -SRLNGHVAPRGYQPSRDLGSRSLSDSDSEE-----
Zebrafish Nrg2a	499	-----SGSRRWRRSRINGHTPG-----PRNYSSQSCLS DSEWEDE---EVG--
Zebrafish Nrg3	675	LVTYTTALGSGTSSRAKT--VISMTVLGTGVKT-TQY-AASLLSKTTAGREEHSAFEEV
Human Nrg1-l	581	--RVGEDTPFLGIQNPLAASLEATPAFRLADSRTN---PAGRFSTQEEIQ-ARLSSVI--
Mouse Nrg1-l	586	--RVGEDTPFLGIQNPLAASLEVAPAFRLAESRTN---PAGRFSTQEEIQ-ARLSSVI--
Zebrafish Nrg1-l	542	--RVGEDTPFLGLQNPAAAGSLVLD--GLEGSRTN---PALHLSPOHELQ-NRLTAVM--
Zebrafish Nrg2b	428	--EEGESTPFLSMQNMNAEPSAL--YRPVPDTRTSHAQSGRHGSRANTQ-TRLTHSRSK
Zebrafish Nrg2a	538	DLGHGESTPFLSMQNMNATEPATI--YRPNDTRT--FSNTGRSGSRPNVQANKLTQSRFR
Zebrafish Nrg3	731	KQGDGLQTSFTGDEKDSFSSGVRGETSLDHPKS-----
Human Nrg1-l	633	ANQDPIAV
Mouse Nrg1-l	638	ANQDPIAV
Zebrafish Nrg1-l	592	ANQDPIAV
Zebrafish Nrg2b	483	PDNAPH--
Zebrafish Nrg2a	594	PDNAPL--
Zebrafish Nrg3	765	-----

Figure 29 Cross-species comparison Nrg1

Clustal-Omega multiple alignment comparing all zebrafish Nrg1 genes to Human and Mouse Nrg1-I. IgG and EGF-like domains are highlighted in yellow.



C

	<i>nrg1^{WT}</i>	<i>λ nrg1^{nc28}</i>	<i>ζ nrg1^{nc29}</i>	<i>ε nrg1^{nc26}</i>	<i>§ nrg1^{nc27}</i>	<i>δ nrg1z26</i>
Nrg1-I	599	55	99	144	147	599
Nrg1-II	722-730	176	214	270	273	722-730
Nrg1-III	687	687	687	232	235	687*

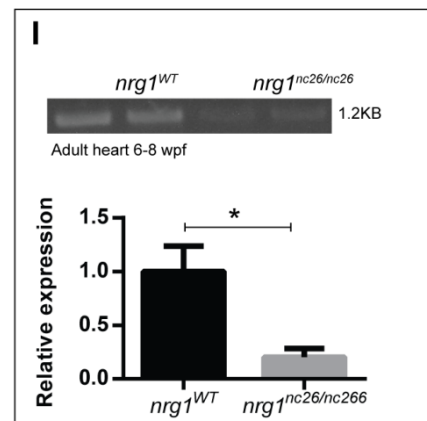
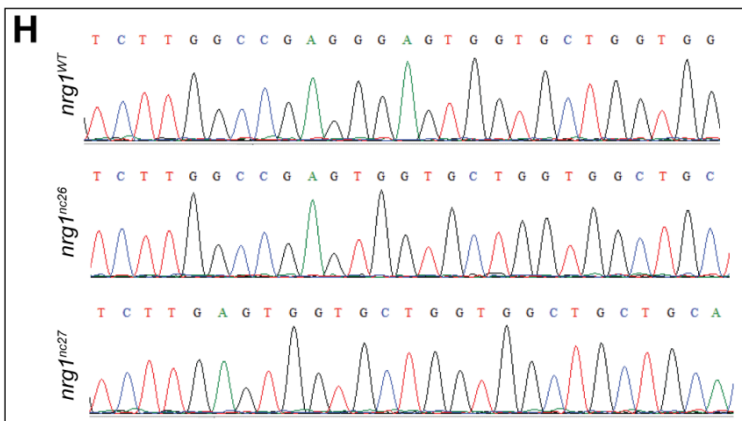
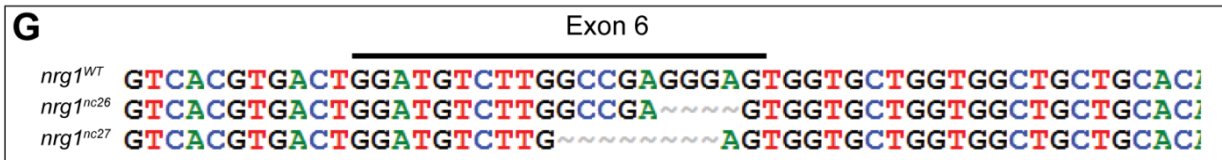
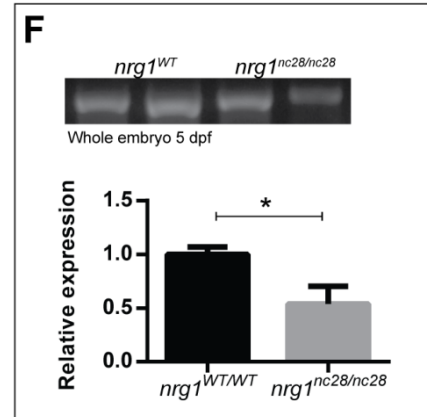
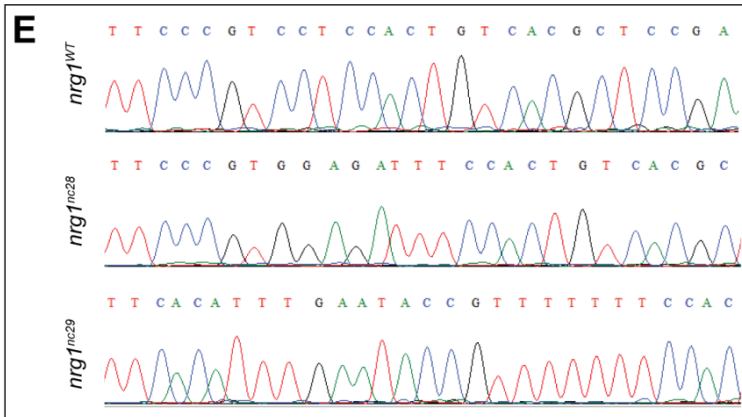
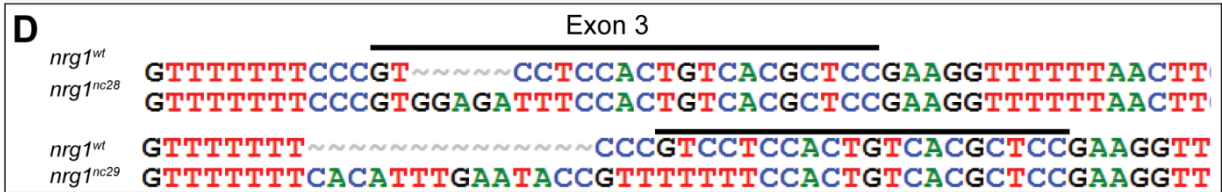


Figure 30 Nrg1 alleles

(A) Schematic of Nrg1 exons and protein domains including an immunoglobulin domain (IgG) coded by exons 3 and 4, a cysteine-rich domain (CRD) coded by exon 5, EGF domain encoded by exons 6-9, a transmembrane (TM) domain in exon 10 and the Neuregulin 1 C-terminal domain. The epidermal growth factor (EGF) domain is essential for binding to epidermal growth factor receptors. (B) Schematic of spliced products of Nrg1-I, Nrg1-IIa-c, and Nrg1-III (note, Nrg1-IIa-c is drawn with all possible EGF-domain modifiers. Greek symbols annotate location of predicted truncation of alleles listed in (C)). (C) Predicted effect of mutations on Nrg1 isoform products. *Note $nrg1^{z26}$ allele codes for a loss of function amino acid substitution C97R in the CRD domain (D) CRISPR/Cas9 gene targeting and validation of $nrg1^{nc28}$ and $nrg1^{nc29}$ alleles showing target site and mutations. (F) Gel electrophoresis and quantification of $nrg1$ amplified from 10ng cDNA derived from $nrg1^{WT}$ or $nrg1^{nc28/nc28}$ embryos at 5 dpf. or (H) hearts of adult $nrg1^{WT}$ or $nrg1^{nc26/nc26}$ fish. (G) Sanger sequence of $nrg1^{WT}$, $nrg1^{nc28}$ and $nrg1^{nc29}$ alleles spanning target site in Exon 3. (E) CRISPR/Cas9 gene targeting and validation of $nrg1^{nc26}$ and $nrg1^{nc27}$ alleles showing target site and mutations. (H) Sanger sequence of $nrg1^{WT}$, $nrg1^{nc26}$ and $nrg1^{nc27}$ alleles spanning target site in Exon 6. (I) Gel electrophoresis and quantification of $nrg1$ amplified from 10ng cDNA derived from adult $nrg1^{WT}$ or $nrg1^{nc26/nc26}$ fish. Student's T-test compared to matched control. Error bars are SEM. N=3 biological replicates. * $p \leq 0.05-0.01$.

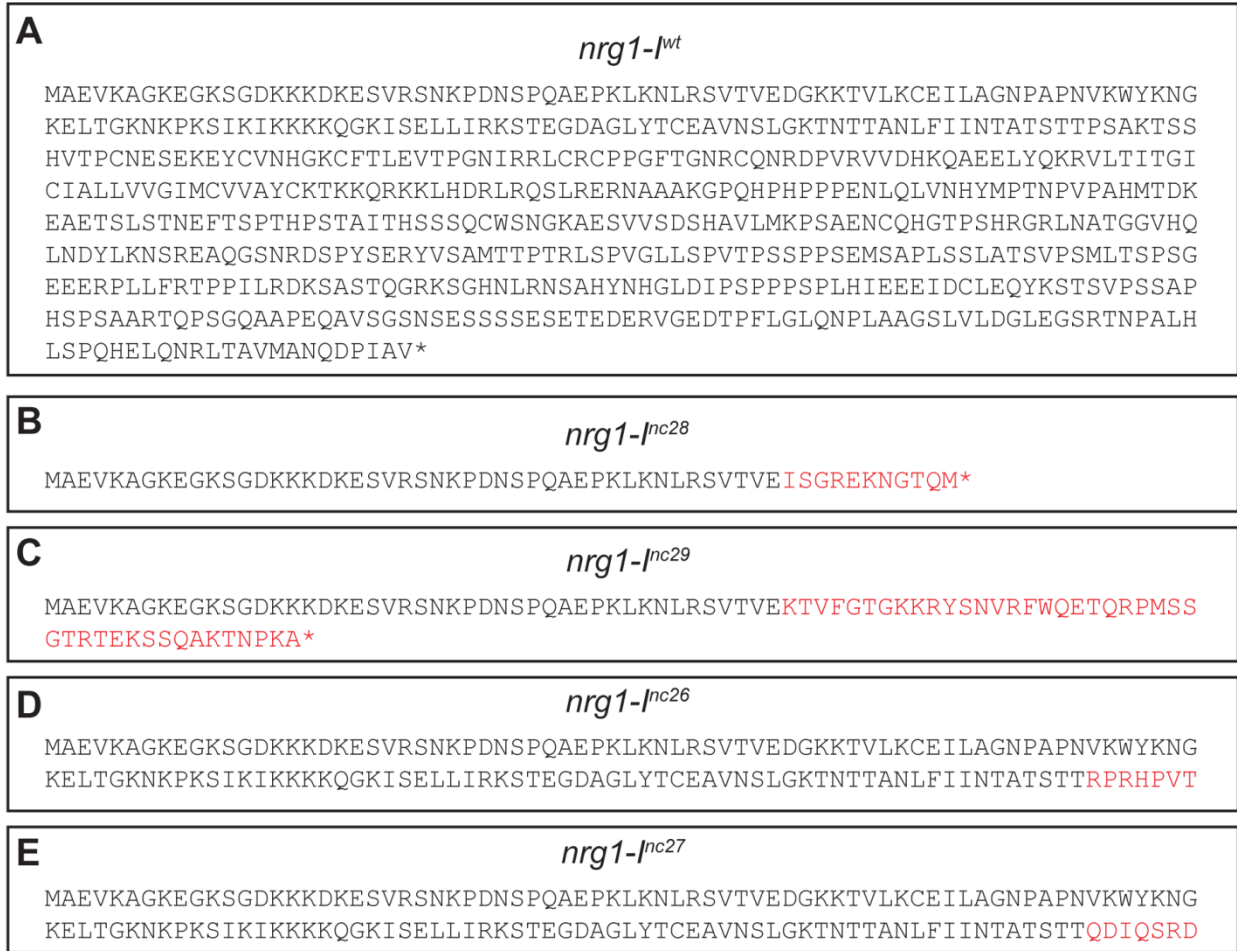


Figure 31 Predicted translations Nrg1-I mutant alleles

(A-E) Nrg1-I wild type and mutant alleles were translated in frame; (A) *nrg1-1^{WT}* allele is translated into 599 aa, (B) *nrg1-1^{nc28}* into 55 aa, (C) *nrg1-1^{nc29}* into 99 aa, (D) *nrg1-1^{nc26}* into 144 aa, and (E) *nrg1-1^{nc27}* into 147aa. (B-E) Amino acids that differ from wild type are in red. Asterisk indicates stop codon.

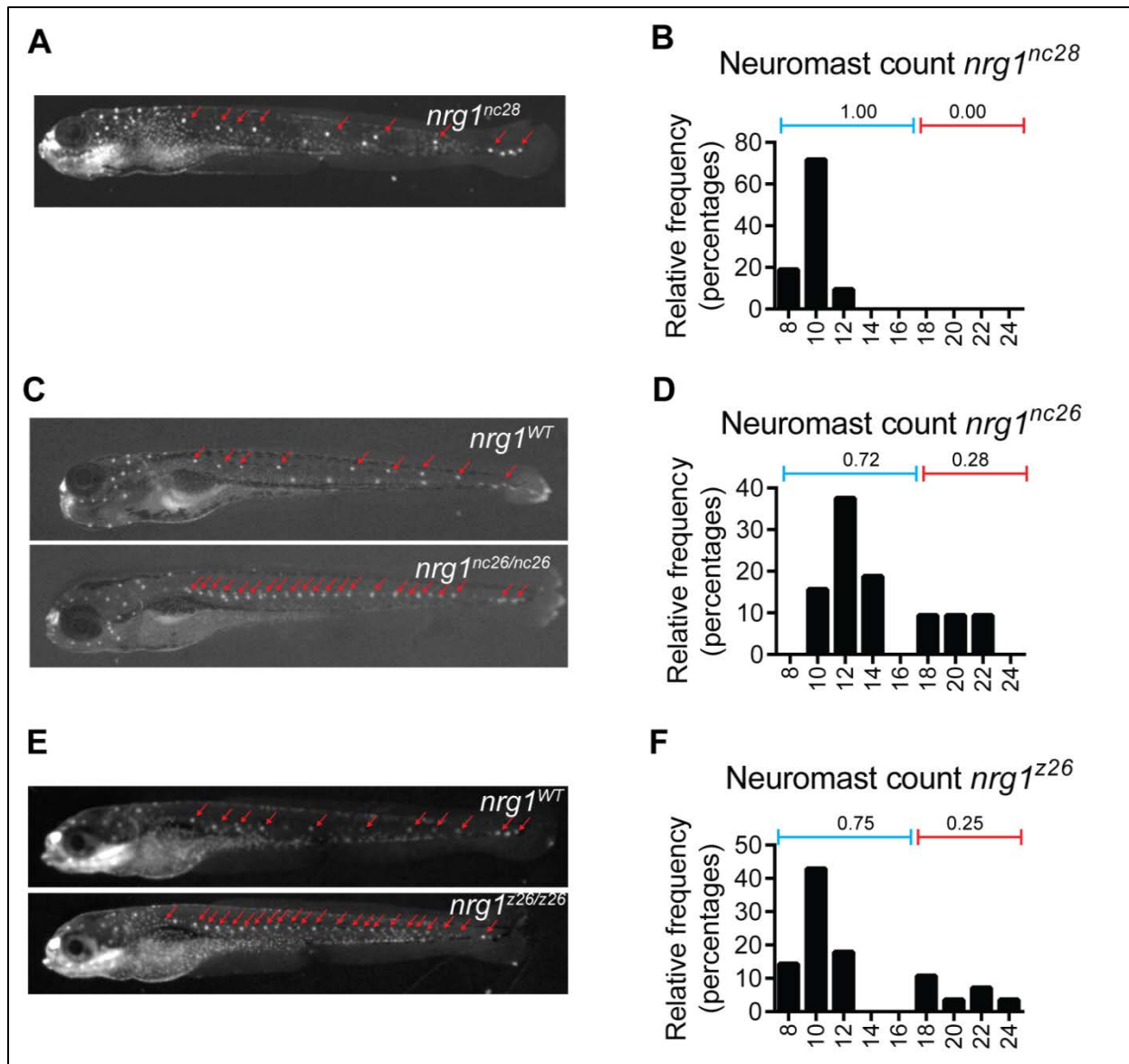


Figure 32 Supernumerary neuromasts in Nrg1-III deficient mutants

(A-F) Heterozygous adult fish carrying (A-B) *nrg1^{WT/nc28}*, (C-D) *nrg1^{WT/nc26}*, or (E-F) *nrg1^{WT/z26}* alleles were inbred, and resulting offspring were evaluated. (A,C,E) Larvae at 5 dpf were stained with Mitotracker, a voltage sensitive vital dye to mark neuromasts (red arrows). (B,D,F) Frequency distribution of the number of neuromasts per embryo. Blue bar marks range of neuromasts found in wild type larvae; red bars mark supernumerary neuromasts. Similar results were obtained with *nrg1^{nc29}* and *nrg1^{nc27}* lines (data not shown). N=15-20 embryos imaged per pairing; N=2 biological replicates.

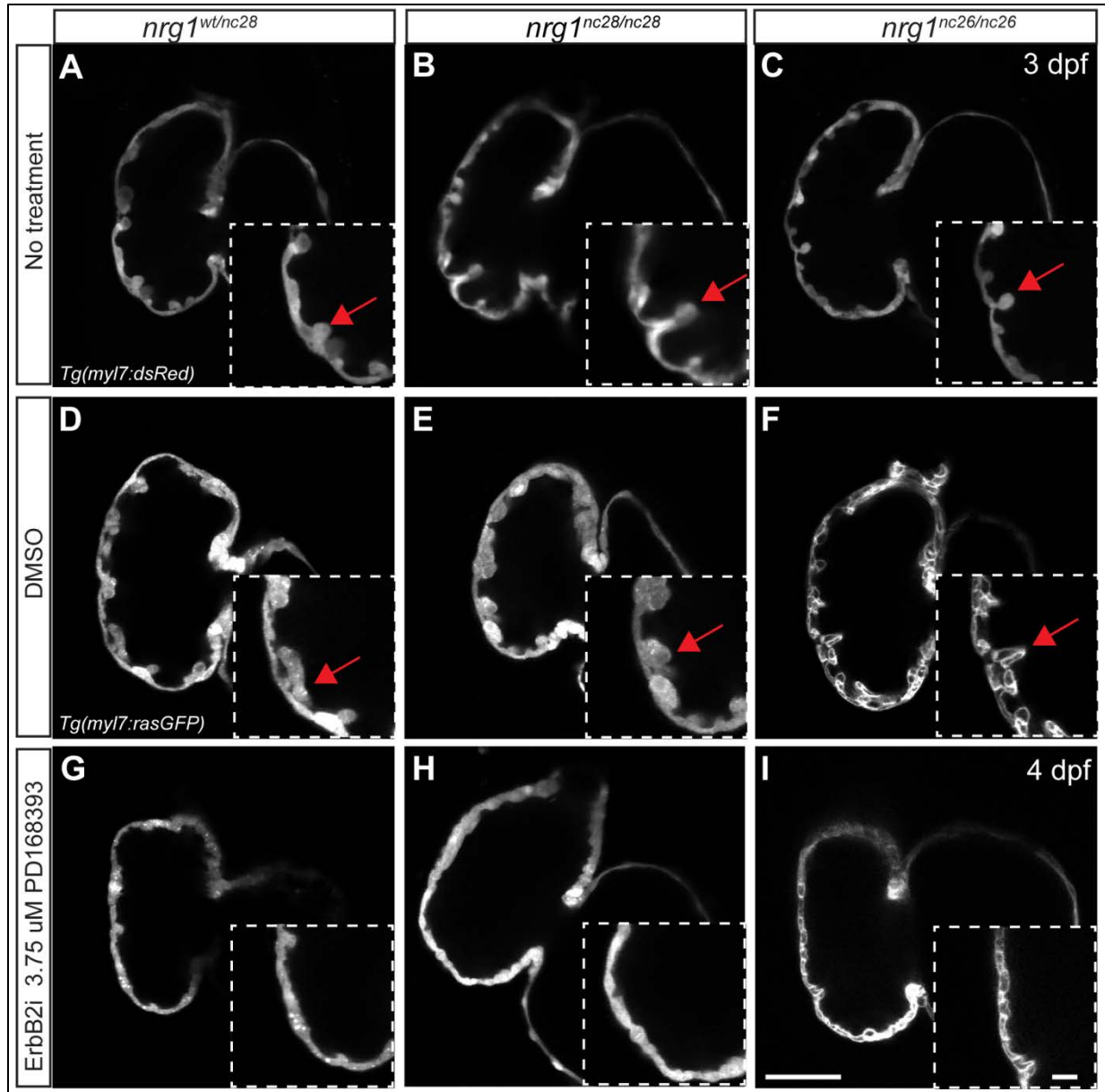


Figure 33 Nrg1 mutants require ErbB2 tyrosine kinase activity to form trabeculae

Adult fish heterozygous for *nrg1*^{nc28} or *nrg1*^{nc26} carrying a fluorescent cardiomyocyte reporter were inbred, and trabeculation was evaluated in the resulting offspring. (A-L) Representative confocal optical mid-chamber slice of the ventricle at 3-4 dpf in larvae carrying *Tg(myI7:dsRed)* or *Tg(myI7:rasGFP)* cardiomyocyte reporters. Boxes include high resolution image of the outer curvature. Larvae were examined at (A-C) 3 dpf or treated from 2-4 dpf with (D-F) 1% DMSO or (G-I) 3.75 μ M PD168393 a specific ErbB2 tyrosine kinase inhibitor (Calbiochem). Larvae were genotyped after imaging. Red arrows point to representative trabeculae. $N \geq 4$ larvae for each condition and genotype. Scale bars are 50 and 10 μ m for figure and inset, respectively.

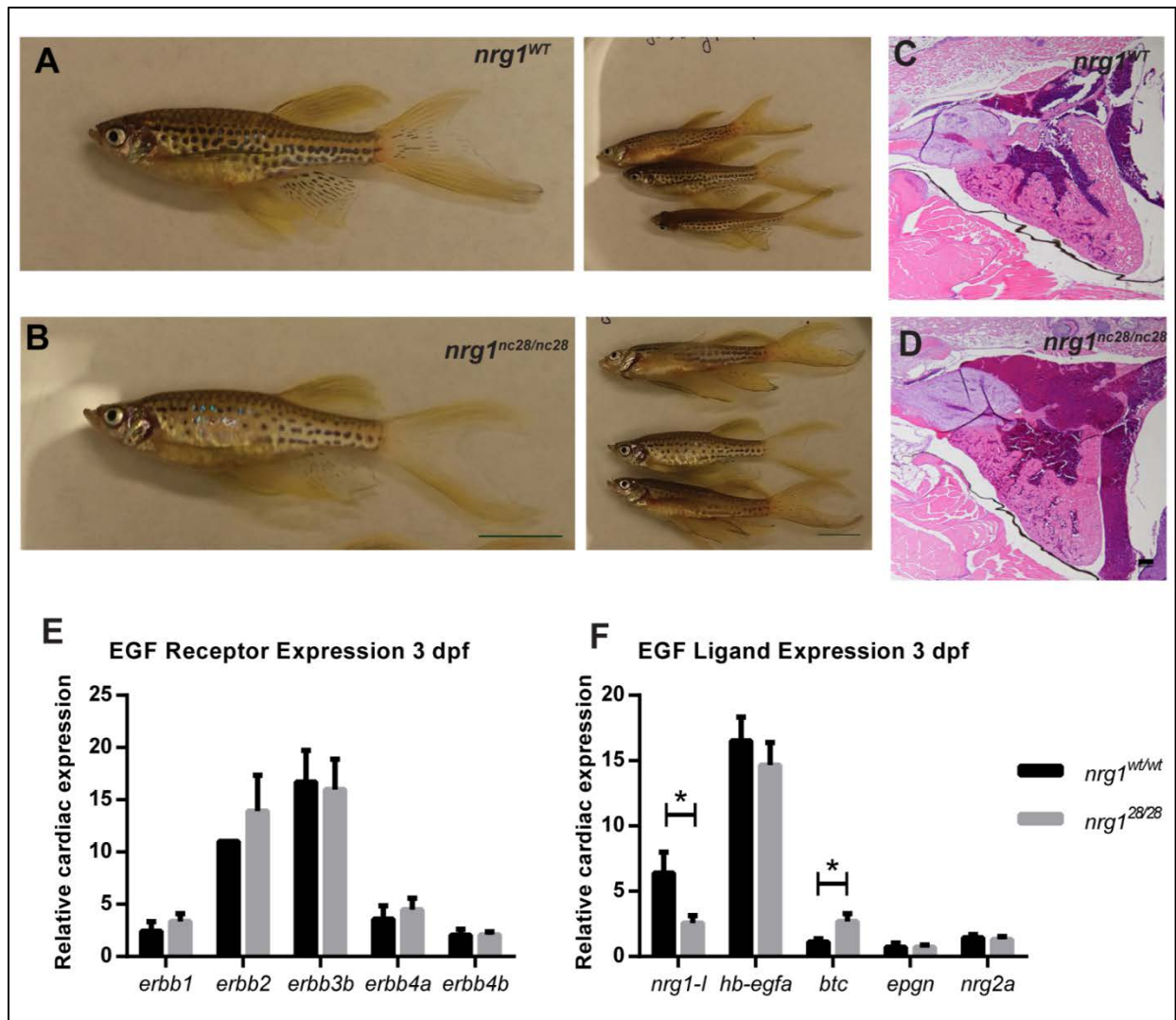


Figure 34 Adult *nrg1^{nc28}* mutant phenotype

(A-B) Representative gross morphology of age-matched (A) *nrg1^{WT/WT}* or (B) *nrg1^{nc28/nc28}* clutch mates, SL25-SL30. Scale bar is 10mm. (C-D) Representative cross section of the heart in H&E stained section of formaldehyde-fixed, paraffin embedded (C) *nrg1^{WT/WT}* and (D) *nrg1^{nc28/nc28}* adult fish. N=3 fish per genotype. Scale bar 100 μ m. (E-F) EGF family (E,F) receptor and (G,H) and gene expression in hearts isolated from *nrg1^{WT/WT}* and *nrg1^{nc28/nc28}* larvae at 3 dpf. Abbreviations: *nrg1-1*, neuregulin1 isoform 1; *hb-egf*, heparin-binding EGF-like growth factor, *btc*, betacellulin; *epgn*, epigen; *nrg2a*, neuregulin 2a; *erb1*, epidermal growth factor (*her1*, *egfr*); *erb2*, *erb-B2* receptor tyrosine kinase 2 (*her2*); *erb3a*, *erb-B2* receptor tyrosine kinase 3a; *erb3b*, *erb-B2* receptor tyrosine kinase 3b; *erb4a*, *erb-B2* receptor tyrosine kinase 4a; *erb4b*, *erb-B2* receptor tyrosine kinase 4b. N=3-5 biological replicates with 30-60 hearts pooled per condition. Student's T-test mutant compared to wild type. Error bars are SEM. N \geq 3 biological replicates. *p \leq 0.05-0.01,

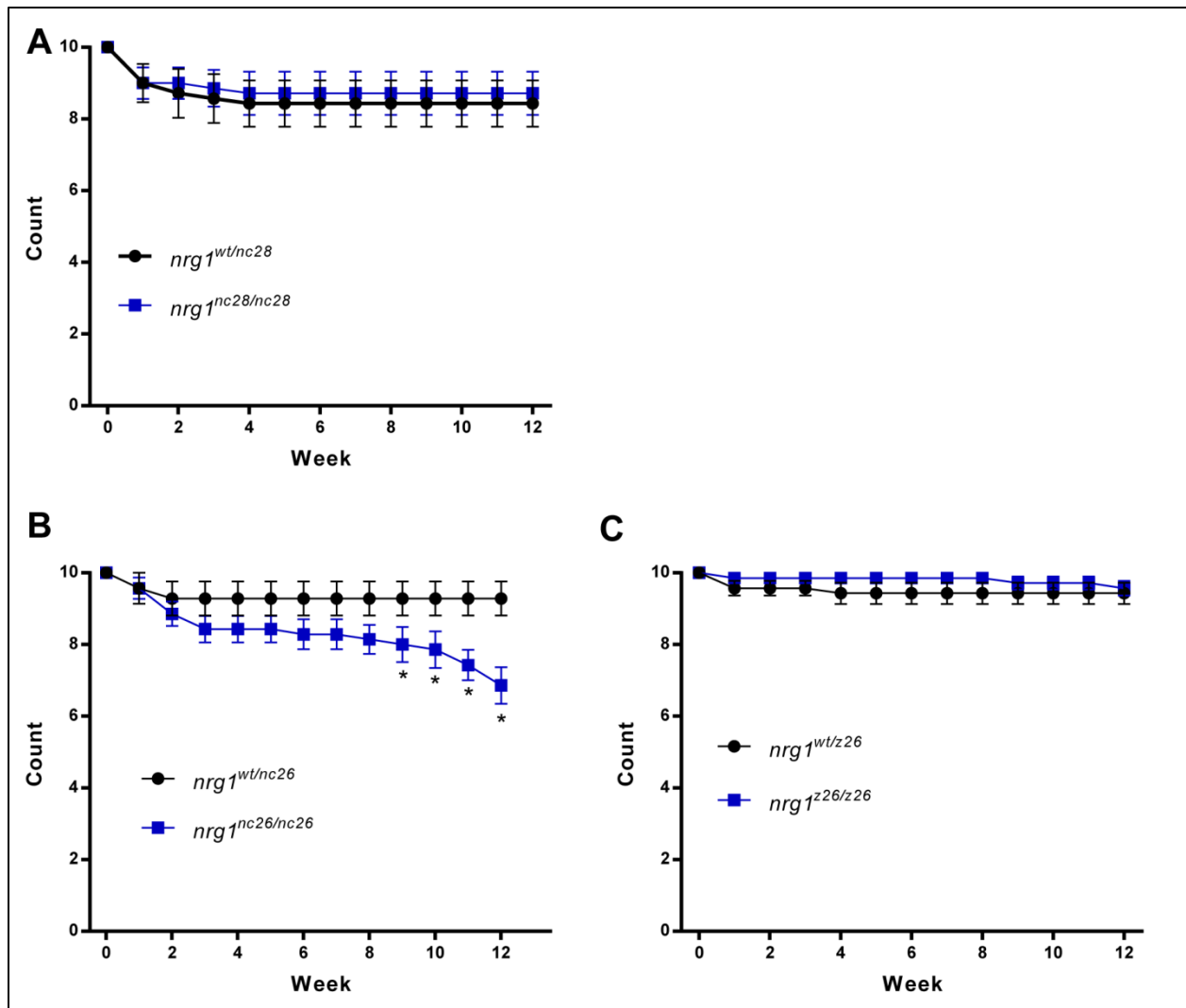


Figure 35 Survival of *nrg1* mutants

(A-C) Average weekly survival of fish from sibling (A) $nrg1^{WT/WT}$ and $nrg1^{nc28/nc28}$ in breeding, (B) clutch mates from $nrg1^{WT/nc26}$ inbreeding and (C) clutch mates from $nrg1^{WT/z26}$ inbreeding. (B-C) Embryos were screened at 5 dpf for presence of supernumerary neuromasts to separate $nrg1^{nc26/nc26}$ and $nrg1^{z26/z26}$ mutants from wild type or heterozygous embryos ($nrg1^{WT/nc26\text{ het}}$ and $nrg1^{WT/z26\text{ het}}$, respectively). Each data point represents the number of fish in each tank, where each tank started with 10 fish per tank. Error bars are SEM. N=7 tanks per genotype, all reared in parallel.

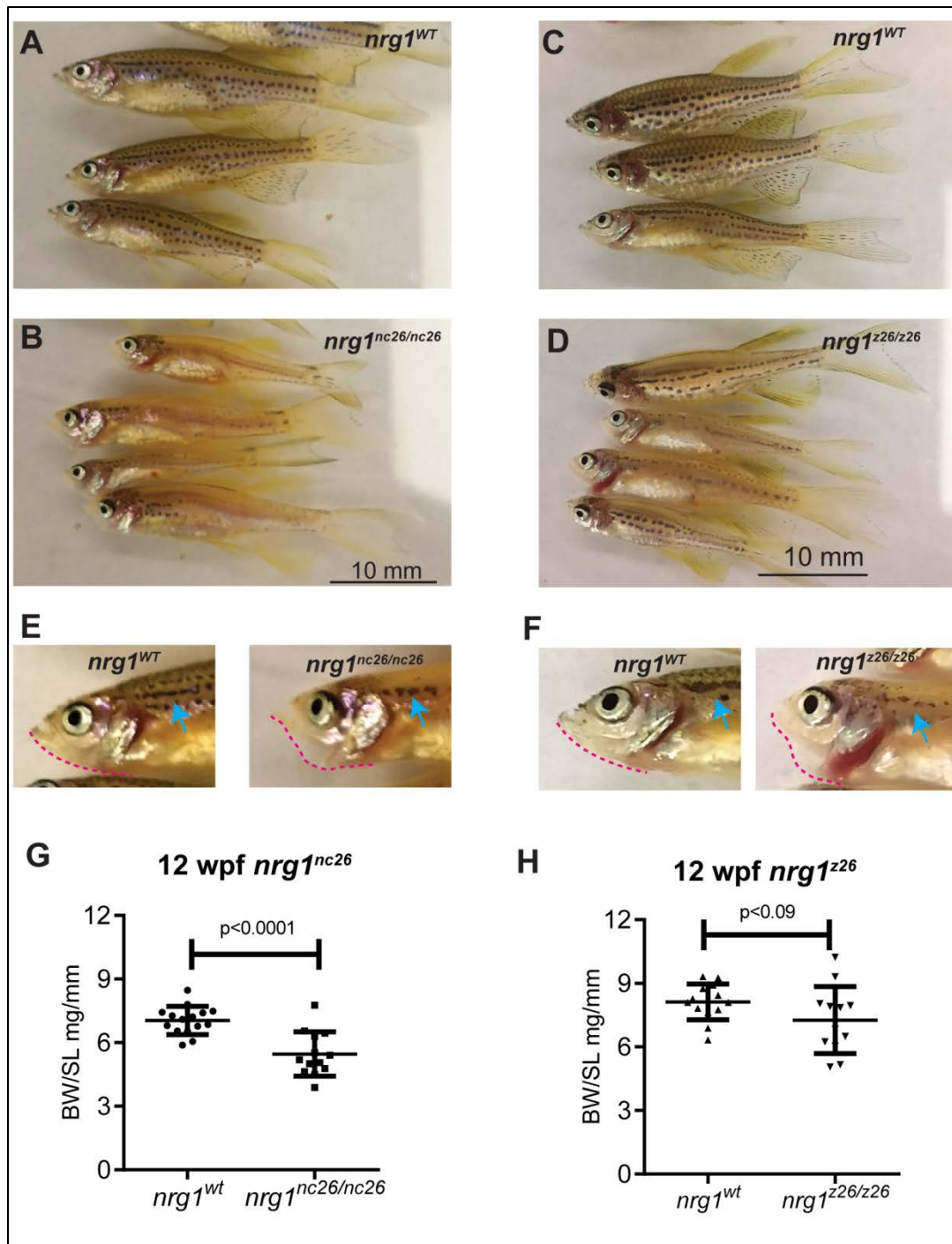


Figure 36 Gross phenotype of *nrg1-III*-deficient mutants

(A-D) Representative gross morphology of age-matched (A-B) *nrg1*^{nc26} or (C-D) *nrg1*^{z26} clutch mates, SL20-SL25. (E-F) Magnified view of pigmentation (blue arrow) and jaw structure (dotted pink line) in (E) *nrg1*^{nc26} or (F) *nrg1*^{z26} mutant fish SL20±2. (G,H) Body mass of wild type or heterozygous and (G) *nrg1*^{nc26} or (H) *nrg1*^{z26} mutant fish normalized to standard length of SL20±2. N=15-20 individuals from N>2 individual clutches.

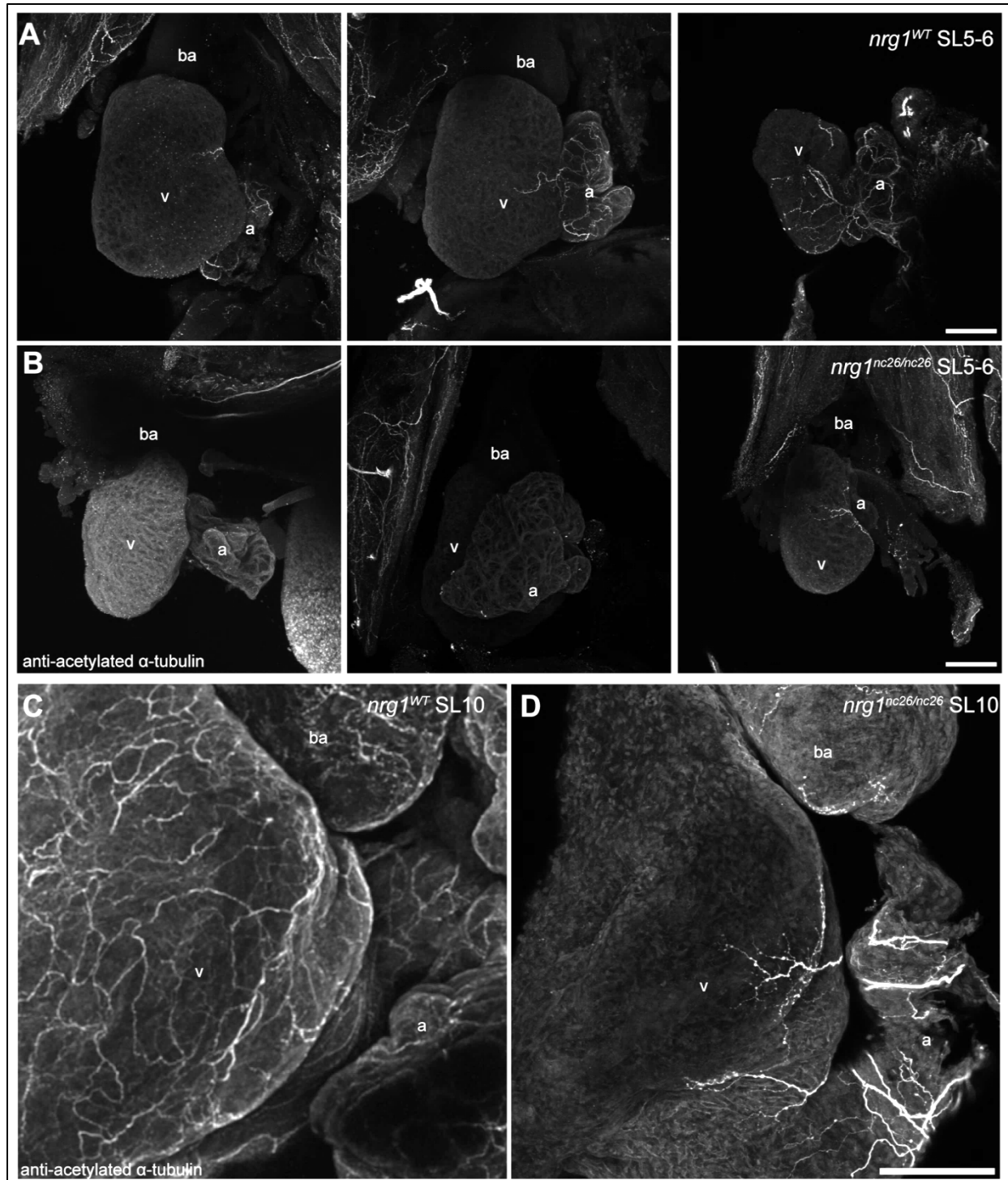


Figure 37 Ventricle surface innervation defect emerges in juvenile stage

(A-D) Z-projection of confocal images of axons stained with anti-acetylated α -tubulin. Images are representative (A,C) $nrg1^{WT}$ and (B,D) $nrg1^{nc26/nc26}$ hearts at (A,B) SL 5-6 and (C,D) SL 10. Abbreviations a=atrium, v=ventricle, ba=bulbous arteriosus. Scale bars are 100 μ m.

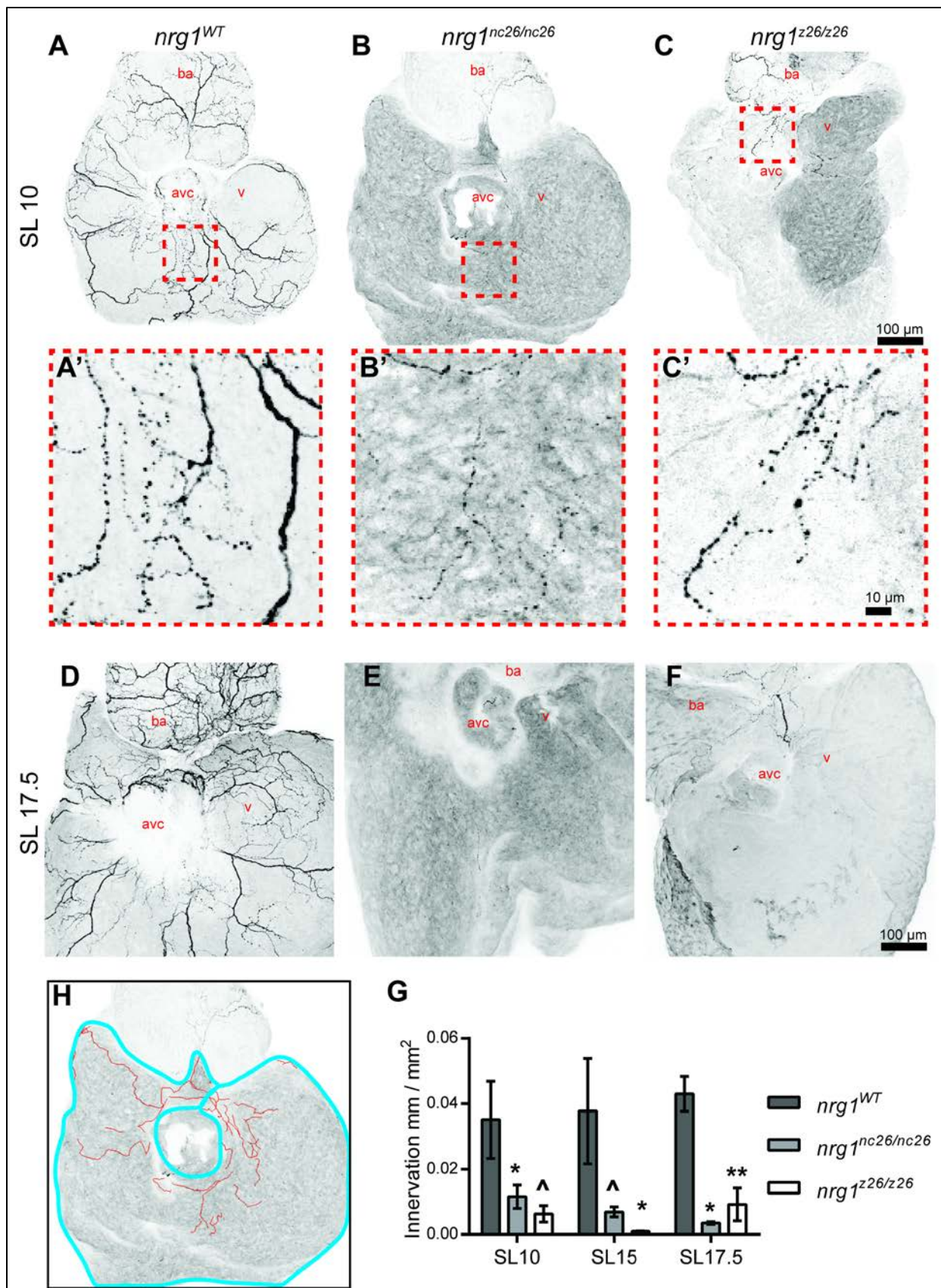


Figure 38 Reduced surface innervation in Nrg1-III-deficient hearts

(A-F) Maximum intensity, z-project of confocal images of dorsal surface of ventricle with atrium removed. Hearts were isolated at (A-C) SL10±1 or (D-F) SL 17.5±1 from (A,D) *nrg1^{WT}*, (B,E) *nrg1^{nc26/nc26}*, or (C,F) *nrg1^{z26/z26}* fish and stained with anti-acetylated α -tubulin to label axons. (A'-C') Magnified view of representative innervated regions. (G-H) Surface innervation was quantified as the quotient of the total length of axons and ventricle surface. Abbreviations a = atrium, avc = atrio-ventricular canal, ba = bulbous arteriosus, and v = ventricle. Student's T-test mutant compared to wild type. Error bars are SEM. N≥2 biological replicates. ^ p=0.05-0.10, * p=0.01-0.05, ** p=0.001-0.01

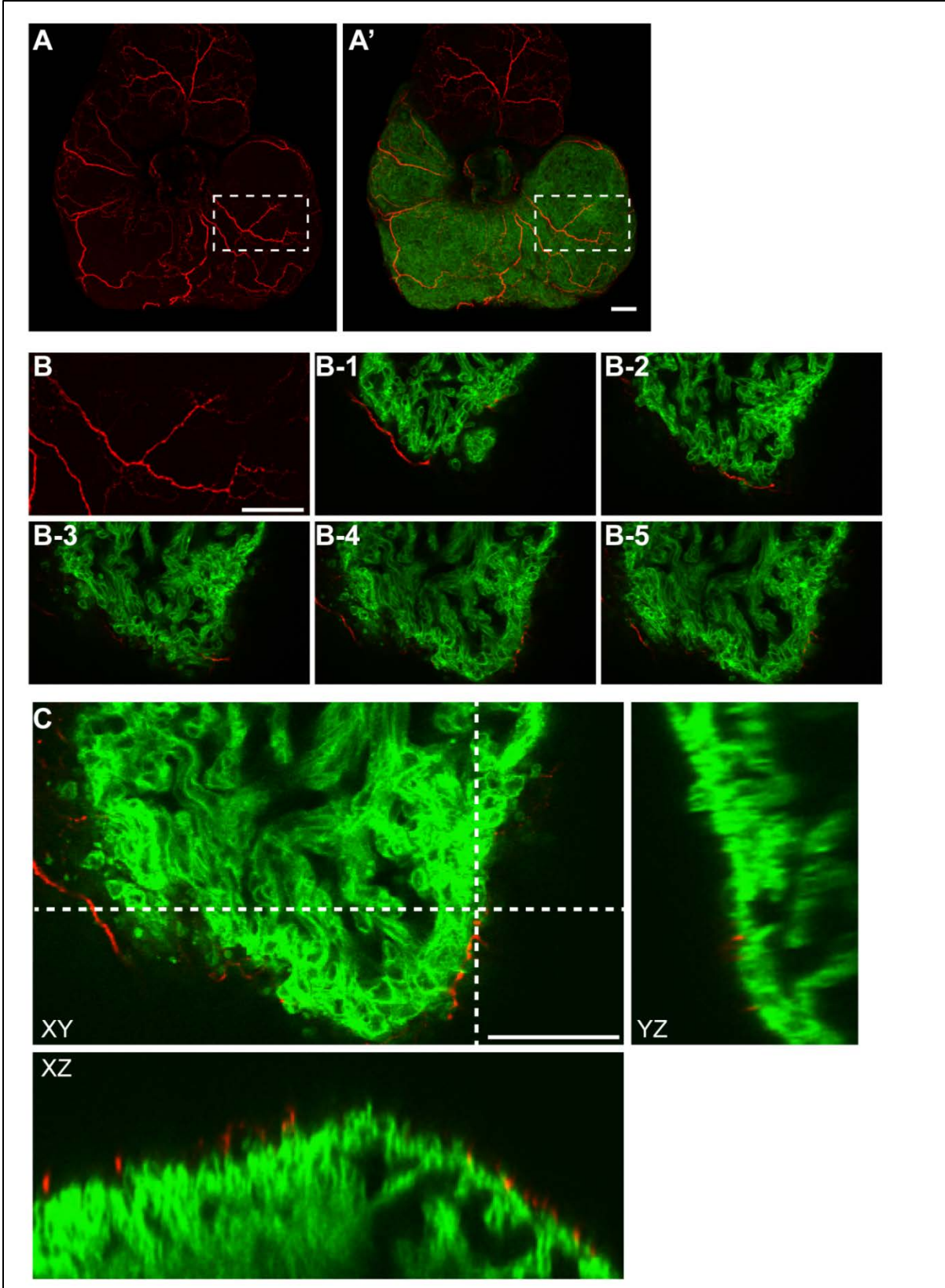


Figure 39 Innervation in the myocardial wall

(A) Z-projection of confocal images from representative *nrg1^{WT}* ventricle carrying *Tg(myI7:rasGFP)* membrane targeted cardiomyocyte reporter and (red) stained for axons with anti-acetylated α -tubulin. (B) Box highlighted in A and A' including axon branches and putative terminal ends. (B-1 to B-5) Single optical sections through z-stack. (C) Orthogonal views showing axons largely on the surface with close apposition to cardiomyocytes at axon terminus. Scale bar is 100 μ m.

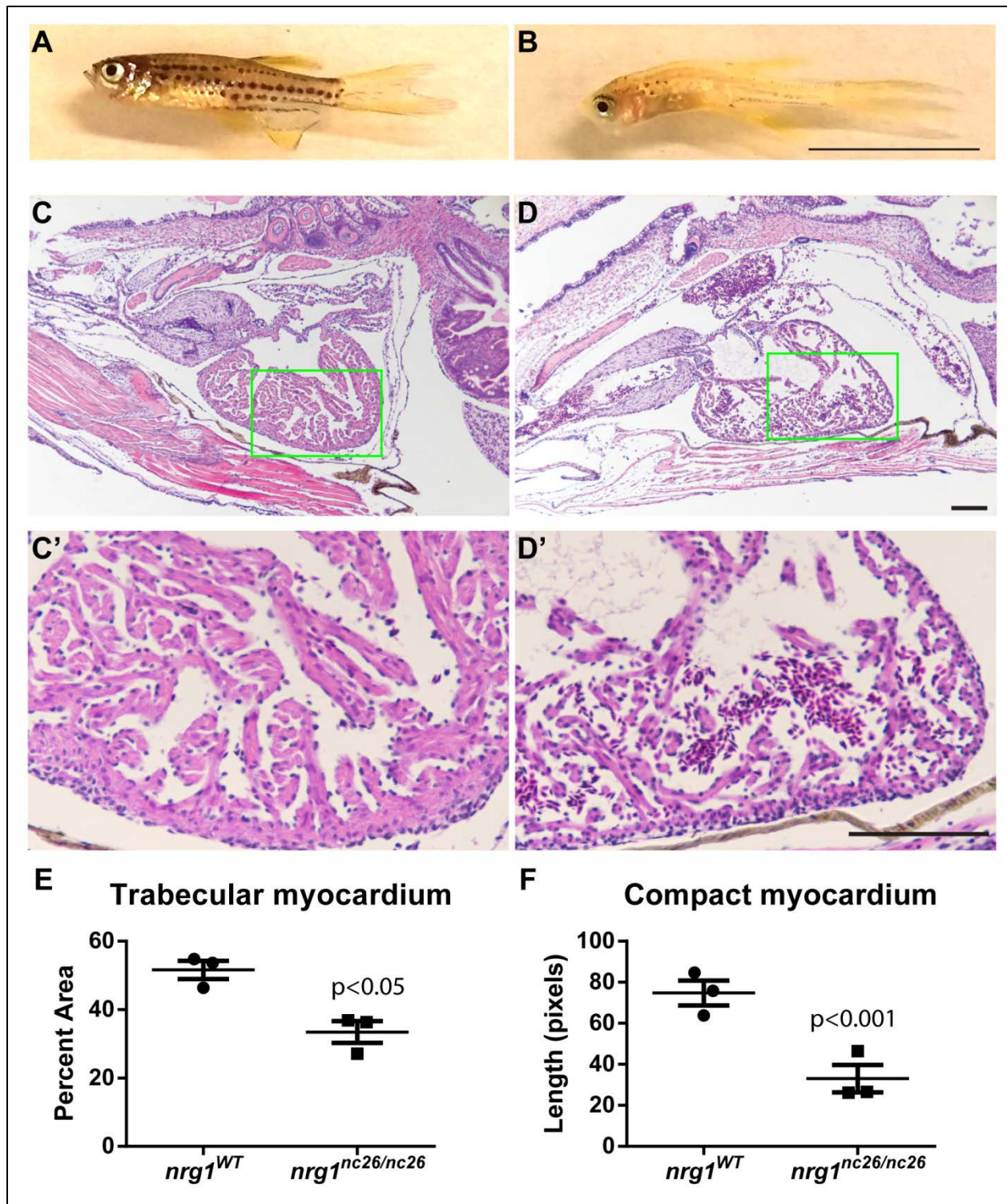


Figure 40 Peri-mortem cardiac morphology of *nrg1*^{nc26} fish

(A-B) Representative gross morphology (A) *nrg1*^{WT} fish and sibling (B) *nrg1*^{nc26/nc26} selected for behavioral indication of cardiovascular failure SL11-SL15. Scale bar is 10 mm (C-D) H&E stained paraffin-embedded sections of *nrg1*^{WT} fish and sibling (B) *nrg1*^{nc26/nc26}. (C'-D') Magnification of apex shown in (C-D) green box. Student's T-test comparing WT and control. N=3 fish per genotype.

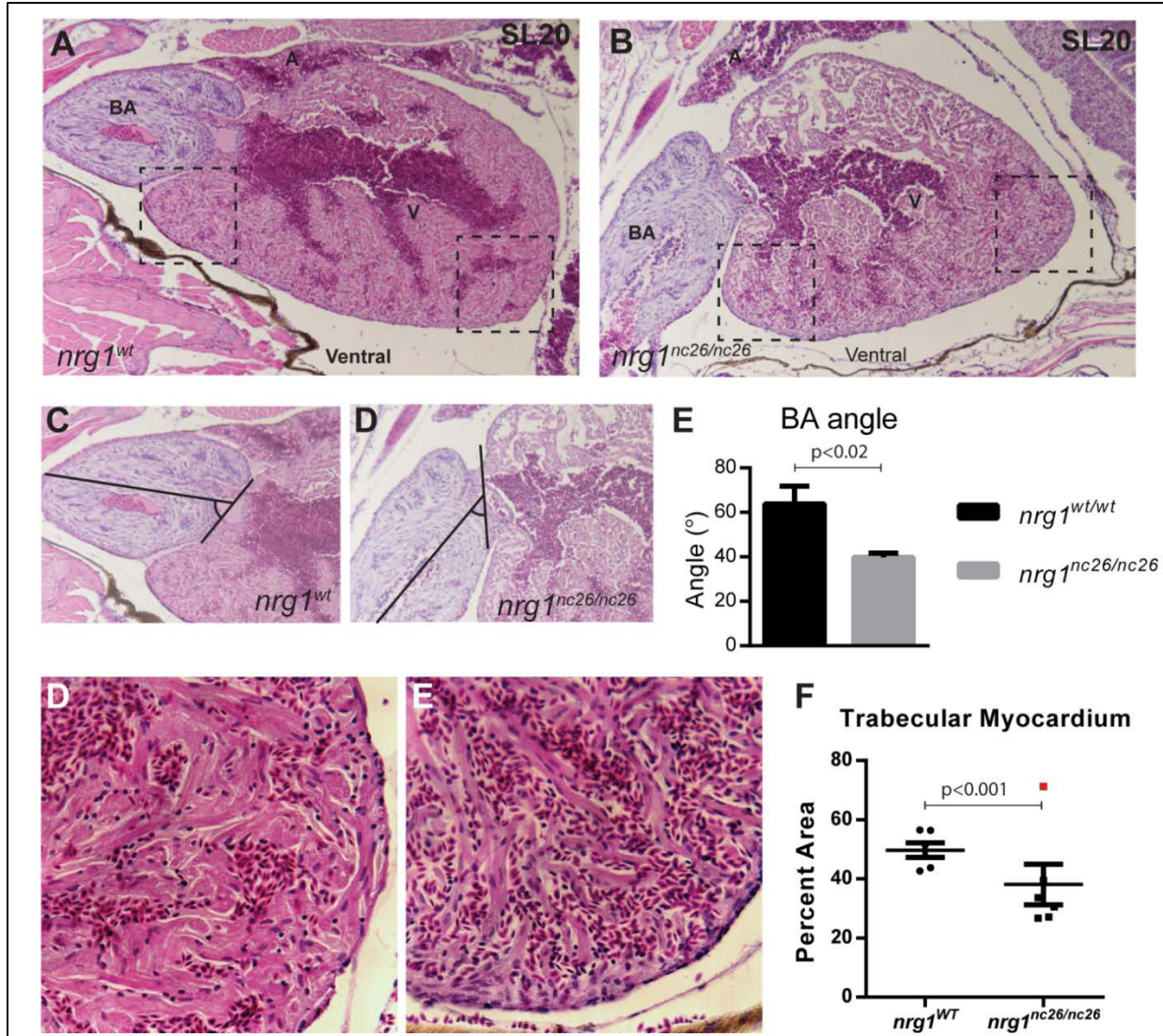


Figure 41 Altered cardiac morphology in *nrg1^{nc26}* mutants

Comparative whole-fish cardiac histology. (A,B,D,E) Representative images of H&E stained hearts from lateral-mounted sections of (A,D) *nrg1^{WT}* and (B,E) *nrg1^{nc26/nc26}* adult fish at SL20. (A-B) Overview of cardiac structure and (C) measurement of the minor angle between the ventricle and bulbous arteriosus is reduced in *nrg1^{nc26/nc26}* fish. (D-E) Representative view of trabecular myocardium in the outer curvature and (F) quantification of trabecular mass. Red square represents excluded outlier. Abbreviations: atrium (a), ventricle (v), and bulbous arteriosus (ba). Student's T-test wild type compared to control. N=5-6 per genotype

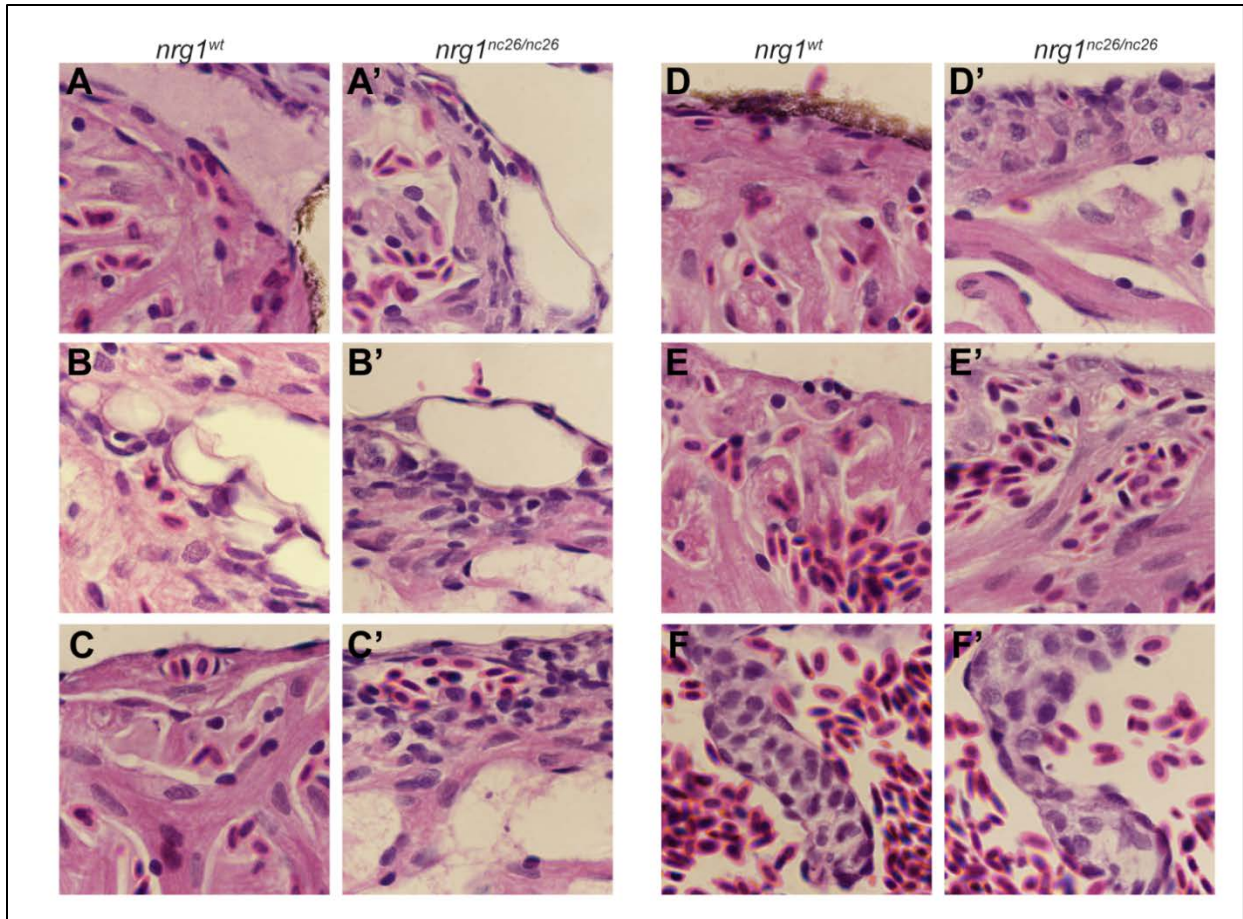


Figure 42 Compact myocardial wall derangements

(A-F) Representative images of myocardial wall in H&E stained hearts from lateral-mounted sections of *nrg1*^{WT} and *nrg1*^{nc26/nc26} adult fish at SL20. (A) Intersection of ventricle base and bulbous arteriosus. (B) Atrioventricular valve leaflet. (C) Compact wall in the inner curvature. (D) Compact wall in the outer curvature. (E) Open lumens present in (left) atrio-ventricular junction in *nrg1*^{WT} and outer curvature in *nrg1*^{nc26/nc26}. (F) Blood-filled lumens present in outer curvature.

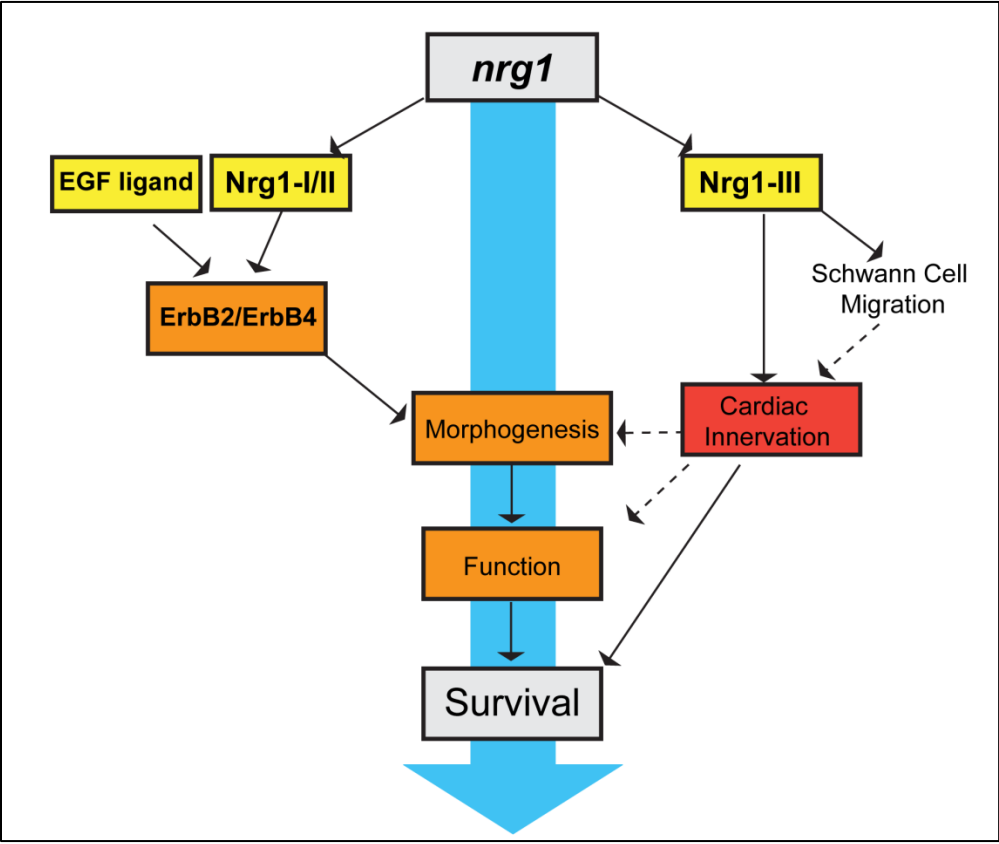


Figure 43 Model

Integrated model for how *nrg1* maintains cardiac output. *Nrg1*-I/II isoforms and other EGF-like ligands in the heart activate ErbB2/ErbB4 signaling in cardiomyocytes to regulate cardiac morphogenesis. *Nrg1*-III is known to regulate Schwann cell migration during neuromast formation, and is important for establishing the ventricular nerve plexus. Defects in cardiac innervation are associated with survival defects through regulating cardiac morphogenesis and/or survival.

Table 3 Chapter 3 Oligonucleotide Sequences

Target	Use	Forward Oligo	Reverse Oligo
<i>nrg1</i> - <i>exon3</i>	HRMA	TTTTCCAGCGGAACCGAAGT	GTACCACTTGACATTGGGCG
<i>nrg1</i> - <i>exon6</i>	HRMA	GTTGTGTTCCCTCTGTGCAGC	TTCTCGCTCTCATTGCAGGG
<i>nrg1</i> - <i>exon11</i>	HRMA	TTTACGAGAGCGAAACGCTG	TGTCTGATCTGTGCAATGACG
<i>nrg1</i> - <i>exon3</i>	PCR and Sequencing	TTTCACCCTTGTGAGCACCG	AATATGCGCGTGTGAGTCTT
<i>nrg1</i> - <i>exon3</i>	Sequencing	TGGGTTTGTTTTTGCCTGTGA	
<i>nrg1</i> - <i>exon6</i>	PCR and sequencing	CACTGCTGCTTTGTTGGACG	TGCTGTTCACTCAGTGGCAA
<i>nrg1</i> - <i>exon11</i>	PCR and sequencing	CTGTGAGTTTGCCTGCTAC	GTCTGATCTGTGCAATGACGA
<i>nrg1</i> - <i>I/II/III</i>	PCR	CCCTCGGCCAAGACATCC	TTGCGGTGAGAGGTGCAG
<i>areg</i>	qRT-PCR	GAACACATCATCGTTCCAGG	AAACCCGTCATCAGTGACTT
<i>btc</i>	qRT-PCR	GGACACTTCTCTGCCTGTCC	TTTTCGCATCTGCATGACGG
<i>egf</i>	qRT-PCR	GTTTCAGCTGTCAAGCAGAGTT	GCACGCCATTTTTGTGTTGC
<i>epgn</i>	qRT-PCR	GTCAGAAAGTACCACCACC	CGTCTCACTTGTGGAGTCGT
<i>hb-egfa</i>	qRT-PCR	TCCTGGCACTCAGTTTTAC	TGGTTTAGTGGTGTGGAGCG
<i>hb-egfb</i>	qRT-PCR	TGCTTTTCTGACAGGTACCAC	TTTTGGCTTTCTTTATCCTTCGTT
<i>nrg1-I</i>	qRT-PCR	GTGAAAGCAGGCAAAGAAGGG	TGTCACGCTCCGAAGTTTT
<i>nrg1-III</i>	qRT-PCR	ACCCACAAATGACACGTCCG	ACTGTCACGCTCCGAAGTT
<i>nrg1-III</i>	qRT-PCR	CAGCCCCAAGAGCACCTTT	GTGACTGGATGTCTTGGCCG
<i>nrg2a</i>	qRT-PCR	GCCGGCAACTGAGAGAGTAAT	CGCTGACACATACCTGTGGG
<i>nrg2b</i>	qRT-PCR	ATCCTGTCTCAGCATGAGGG	TTTGGAGCTGATGCCCTTTTT
<i>nrg3</i>	qRT-PCR	AAAACACGGTAATGCCGAAGC	CAAGACCTCAAGCAAAACAGACA
<i>tgfa</i>	qRT-PCR	TGTATGCCATCCTGGCTTTGT	TCCACCAACAAAACACCAGC
<i>erb1</i>	qRT-PCR	ATGGGCCTTTCTGAACCCAG	CTCTACTGGCATCACGGGAC
<i>erb2</i>	qRT-PCR	GACTTCACTGCTCCACCCAA	CCCAACAACCTGAATCCCCA
<i>erb3a</i>	qRT-PCR	TGAACATTCACTTGGCCCG	TCATCAACATAGAGAATGGCGTGT
<i>erb3b</i>	qRT-PCR	ACCTTGTGGTGAGGCCTGCTC	CGCAAACCCAACCTGCAACC
<i>erb4a</i>	qRT-PCR	ACATCCTGGAGAAAGGCGAACGT	CTCGTGCCATACGGCTGAACTCT
<i>erb4b</i>	qRT-PCR	TGGGTTCCCTGAGGGTGAGACTG	ATGCTGGCCATGATCAGAGCCT

Table 3: Table of oligonucleotides sequence for HRMA, PCR amplification, Sanger sequencing, and qRT-PCR. Abbreviations: *nrg1* (*neuregulin 1*); *areg*, (*amphiregulin*); *btc* (*betacellulin*); *egf* (*epidermal growth factor*); *epgn* (*epigen*); *hb-egfa* (*heparin-binding egf-like protein a*); *hb-egfb* (*heparin-binding egf-like protein b*); *nrg2a* (*neuregulin 2a*); *nrg2b* (*neuregulin 2b*); *nrg3*(*neuregulin 3*); *erb1* (*epidermal growth factor receptor, erb-B2 receptor tyrosine kinase 1*); *erb2* (*erb-B2 receptor tyrosine kinase 2*); *erb3a* (*erb-B2 receptor tyrosine kinase 3a*); *erb3b* (*erb-B2 receptor tyrosine kinase 3b*); *erb4a* (*erb-B2 receptor tyrosine kinase 4a*); and *erb4b* (*erb-B2 receptor tyrosine kinase 4b*).

3.3 Significance and Additional Interpretations

Significance

Though the story is not yet complete, Chapter 3.2 represents the most comprehensive study, to date, of the role of Neuregulin1 in any model organism. Phenotypic analysis of Nrg1 mutants lacking Nrg1-I/II, Nrg1-I/II/II or Nrg1-III isoforms indicates that Nrg1 is dispensable for cardiovascular development and function under homeostatic conditions in zebrafish. However, loss of Nrg1-III causes malformations in the ventricular nerve plexus, which have later cardiovascular consequences, ultimately leading to mortality. In addition to these findings, the novel mutant lines generated in this study are a significant addition to the zebrafish community. Combined with existing lines targeting *nrg1-III* (*nrg1^{z26}*), *erbb2* (*erbb2^{st61}*), *erbb3* (*erbb3b^{st14}*), and *erbb4* (*erbb4b^{sa21550}*), these will be important for deciphering the precise role of *nrg1* gene products during development (Busch-Nentwich, 2013; Lyons et al., 2005; Perlin et al., 2011).

To our knowledge, though the physiological role of cardiac innervation in regulating heart rate and cardiac output has been well-studied historically, and the overall structure of the adult cardiac plexus has been defined, the potential role of non-cell autonomous role of cardiac nerves in regulating heart development has been largely unexplored (Nilsson, 2011; Stoyek et al., 2015). Given that *nrg1^{nc26}* mutants show signs of ventricular plexus malformations as early as SL5-6 (15 dpf) when *nrg1^{WT}* ventricles are just beginning to show signs of intrinsic innervation, and we observed structural changes in the hearts of *nrg1^{nc26}* mutants, there may be previously unappreciated interplay between cardiac-associated nerves and myocardial maturation. Recent work has demonstrated that nerves are involved in regulating cardiomyocyte proliferation and regeneration in mice and zebrafish, but the homeostatic role of interplay between these cells types is unknown (Mahmoud et al., 2015). Our *nrg1* mutants could be a valuable tool for exploring this relationship.

Additional interpretations

As discussed in Chapter 3.2, further studies are necessary to understanding the phenotypes of *nrg1* mutant fish. However, additional interpretations of *nrg1* mutant phenotypes and future directions warrant discussion.

Mechanism of cardiac innervation

How *nrg1-III* regulates formation of the cardiac nerve plexus at the cellular level remains an area of active research. Pigmentation and jaw phenotypes observed in *nrg1-III*-deficient fish are consistent with a defect in neural crest (NC) cell migration, suggesting that a neural crest derived cell is the primary source of *nrg1* mutant phenotypes. During juvenile metamorphosis, neural crest (NC)-derived melanophores migrate to the site of stripe formation where they differentiate and produce pigment (Budi et al., 2008; Parichy and Spiewak, 2015; Parichy et al., 2003). This migration requires ErbB signaling as well as thyroid hormone (Budi et al., 2008; McMenamin et al., 2014; Parichy et al., 2003). Interestingly, zebrafish lacking functional *erbb3b* do not appropriately form trunk dorsal root ganglia (DRG) or sympathetic neurons, both of which originate in the NC (Honjo et al., 2008). Canonically, while these trunk DRG are important for spinal (sympathetic) innervation of the heart, the vagus nerve provides cranial (parasympathetic) innervation, particularly at the pacemaker (Nilsson, 2011). Thus, we suggest NC-derived DRG cells are likely the cell of origin for the innervation phenotypes in *nrg1-III*-deficient fish. However many questions remain as to the cell autonomous and non-autonomous roles for the *nrg1/erbb* in establishing cardiac innervation, particularly in the ventricle.

Previous studies demonstrate that Nrg1-III, which is detected by ErbB3/ErbB2 receptors on Schwann cells, stimulates co-migration of Schwann cells with neurons and myelination of the long axons by Schwann cells (Lyons et al., 2005; Perlin et al., 2011). Reduced Schwann cell migration in *nrg1^{nc26}* or *erbb3b^{st14}* mutant fish leads to an excess of neuromasts at 5 dpf (Lyons et al., 2005; Perlin et al., 2011). Interestingly, ectopic expression of Nrg1-III in neurons can partially rescue Schwann cell migratory defects (Perlin et al., 2011). If outgrowth of DRG axons to form the cardiac plexus employs a comparable molecular mechanism, then we expect that ectopic expression may similarly rescue ventricular plexus formation. This could be tested by crossing the *nrg1^{nc26}* allele onto the *Tg(UAS:hNrg1typeIII)*; *Tg(S1101:Gal4)* transgenic background (Perlin et al., 2011), to produce fish where *nrg1-III* is the only *nrg1* isoform expressed and expression is restricted to neurons. We expect that ventricular coverage of the nerve plexus at SL6-SL10 will be rescued by this genotype. Furthermore, additional studies are required to test the spatiotemporal requirements for *nrg1* in establishing and maintaining the ventricle nerve plexus. Such studies would necessitate development of genetic tools for conditional, tissue-specific

deletion of *nrg1*. By conditionally deleting *nrg1* in neurons, cardiomyocytes, or endothelial cells of adult fish at different zebrafish life stages, the developmental and cell autonomous roles for *nrg1* could be explored.

In support of an essential role of Nrg1-III in neurons, we have produced two additional *nrg1* mutant lines, *nrg1^{nc30}* and *nrg1^{nc31}*, which code for truncation of all isoforms of *nrg1* after the transmembrane domain, have supernumerary neuromasts in the lateral line at 5 dpf (data not shown). The ventricular innervation status of this line is currently under investigation. If membrane targeting is intact, then this mutant produces a partially functional Nrg1 which is predicted to have intact forward signaling but defective reverse signaling. Reverse Nrg1 signaling regulates gene expression in cortical neurons, and could play a similar, cell autonomous role in the neuronal projections which innervate the heart (Pedrique and Fazzari, 2010).

Functional performance

Although cardiac malformations are associated with *nrg1-III*-deficiency in zebrafish, the observed emaciation and impaired innervation phenotypes suggest that metabolic distress could be a factor contributing to decline and mortality. Proper innervation of the myenteric plexus is important for propagating contractile waves to promote bulk transit through the gastrointestinal system. If innervation of this plexus is reduced in a manner similar to the cardiac plexus, these fish may have impaired nutrient absorption. Under standard laboratory rearing conditions, nutrient intake is a major limiting factor for zebrafish growth rates after initial larval stages. When wild type and *nrg1-III*-deficient siblings are reared separately, growth delays between genotypes are not readily observed prior to 6 wpf (~SL15) (unpublished observation). However, when reared together, differential growth is readily observed at 6 wpf (unpublished observation). Combined, this suggests that even if bulk transit is defective in these fish, sufficient nutrients are absorbed for growth during this time range and that *nrg1* mutants are at a competitive disadvantage to *nrg1^{WT}* siblings.

Total metabolic and cardiovascular performance are tested in zebrafish using swim performance assays by measuring peak speed, oxygen consumption, and time to fatigue (Palstra et al., 2010; Pelster et al., 2003; Plaut and Gordon, 1994). Such studies are in progress to compare total cardiovascular efficiency in all *nrg1* lines, and it will be interesting to identify the size range at which *nrg1-III*-deficient fish

begin to demonstrate performance defects. This could lead to insights as to the functional consequences of *nrg1-III*-deficiency.

Potential heart failure model

In mammals, chronic heart failure often features derangements in the neurohormonal system including norepinephrine and adrenergic signaling (Mann and Bristow, 2005; Reed et al., 2014). We suggest that *nrg1^{nc26}* mutants may have utility as a scalable model of heart failure where lack of a ventricular nerve plexus could model deranged neurohormonal inputs. Since most mammalian models of heart failure require labor-intensive surgical or pharmacological treatments, as genetic, aquatic model, *nrg1^{nc26}* zebrafish could be advantageous to rapidly evaluate efficacy of novel therapeutics (Brown et al., 2016). Some necessary early steps in establishing this model would be to explore the manifestation of known signs and symptoms of heart failure in *nrg1^{nc26}* mutants including elevated heart rate, reduced ejection fraction, elevated expression of *nppa* and *nppb*, and elongation of myocardial cells (Mann and Bristow, 2005; Patten and Hall-Porter, 2009). Ultimately, if gold standard therapeutics (such AR1 agonists) are effective at reducing some or all of these indicators, *nrg1^{nc26}* mutant fish could be transitioned into a scalable pre-clinical model. An additional early step to validating this model is to determine whether cardiac arrhythmia accounts for mortality independent of heart failure. As mutant fish age, they show signs of cardiovascular distress, but also demonstrate an increased sensitivity to anesthesia suggestive of a propensity to cardiac arrhythmia. Thus, it is unclear whether mutants die ultimately die from heart failure or from acquisition of fatal arrhythmias. This question could be addressed via thorough characterization of the electrocardiographic profile of mutants.

CHAPTER 4 CONCLUSIONS

Insights into zebrafish chamber maturation

These studies produced specific insights on the molecular regulation of chamber maturation throughout the zebrafish life stages. Below, these contributions are integrated into a model of ventricle chamber maturation at each life stage.

Embryonic: At the time of initiating contraction around 24 hpf, the embryonic heart is a linear tube containing a single layer of myocardial cells separated from endocardial cells by a layer of cardiac jelly. Primary cilia on endocardial cells respond to cardiac contraction, likely by bending to detect flow, to activate Notch signaling. Cardiac looping and constriction of the AVC partition the linear heart tube into the atrium and ventricle, and active Notch is detectable in the ventricular endocardium. Notch activity promotes expression of downstream effectors including *efnb2* and *nrg1*. Notch activity is restricted to the AVC when trabecular ridges begin to form in the outer curvature at around 60 hpf. Trabeculation requires cardiac contraction, primary cilia, Notch and *efnb2*. Although the canonical ErbB4 ligand Nrg1 is dispensable, the ErbB2/ErbB4 receptor heterodimer must be activated for trabeculae to form.

Larval: In the larva, trabeculae continue to expand and remodel into a spongy meshwork. The outermost layer of circumferential cardiomyocytes is called the compact myocardium. Additionally, epicardial cells cover the heart and may begin to contribute epicardial-derived cells to the myocardium. Cardiac valves form to prevent retrograde flow, and the entire heart rotates in the chest cavity to orient the ventricle directly ventral to the atrium. By the end of larval stages, the atrium is extensively innervated while the ventricle and bulbous arteriosus are just beginning to develop a nerve plexus. This innervation is dependent on *nrg1* expression, likely through the role of *nrg1-III*.

Juvenile: Trabeculae continue to expand and remodel. The compact wall thickens either by proliferation, addition of the cortical layer, or both. The cortical layer forms when a small population of trabecular cardiomyocytes breaks through the outer compact wall, and proliferates in a clonal manner over surface of the heart, separating the compact myocardium into cortical and primordial layers.

Additionally, the coronary vasculature forms, originating from a cell source near the AVC. The cardiac nerve plexus expands dramatically to innervate the ventricle in a *nrg1-III*-dependent manner.

Adult: In zebrafish, both the trabecular and compact myocardial layers continue developing through adulthood, and the adult myocardium is comprised primarily of an expanded and remodeled meshwork of trabeculae. Loss of all isoforms of *nrg1* leads to variable changes in trabecular thickness and compact myocardial structure in a *nrg1-III*-independent manner, suggesting an essential role for *nrg1-III* and/or the cardiac nerve plexus in maintaining these structures.

Insights into congenital heart disease modeling

Zebrafish are the least expensive, genetically tractable vertebrate model system currently available. Despite differences in scale and complexity, zebrafish have the potential to offer tremendous insight into the etiology, progression, and treatment of human CHDs. “Congenital heart disease” is a very broad term where the American Heart Association defines congenital cardiovascular defects as “structural problems that arise from abnormal formation of the heart or major blood vessels” (Mozaffarian et al., 2015). This effectively encompasses any heart disease with a genetic association or acquired during heart development that leads to a malformed heart. As a group, CHDs are the most common human birth defect, occurring in nearly 1% of all live births (Mozaffarian et al., 2015). While CHDs may occur in isolation or co-morbid with other defects in specific syndromes, they can all make the heart have to work harder to reach produce adequate cardiac output. Over time, this increased workload can lead to heart failure and ultimately death.

There is a complex, genetic basis for most CHDs. Many different genes are attributable to any single CHD, and the penetrance and severity of CHD varies widely for any single genetic lesion (Fahed et al., 2013). The studies shown in this dissertation support a generalizable model for CHDs in which dysfunction at the cellular level during heart development leads to CHD such that the final structural abnormalities that characterize any particular CHD reflect the timing, location, and severity of these cellular dysfunctions. Thus, the effect of any single gene on cellular function is contingent on the larger genetic context of the individual, explaining the variability in CHD manifestation and penetrance. The emergence of CRISPR/Cas9 gene targeting technologies has enabled the study of virtually any gene and specific genetic lesion, making dramatic progress towards the realization of personalized medicine. Since

the genetic and cellular basis of heart development are largely conserved across species, studies described in Chapter 2 and Chapter 3 lend support to the notion that conserved genes might be tested in zebrafish for capacity to contribute to CHD. Further, zebrafish with CHDs might be used to assess the capacity of small molecule therapeutics in repairing the underlying cellular dysfunctions causing CHDs.

Studies described here further indicate that, during development, cellular dysfunction can be spatially and temporally separate from emergence of a CHD phenotype. Specifically, in Chapter 2, we show that genetic and non-genetic factors influence endocardial gene expression to modulate a later myocardial event. Primary cilia are required during very early heart development to activate Notch and downstream signaling in endocardial cells in a cardiac contraction-dependent manner. Dysfunction in cilia structure, Notch signaling, or these downstream mediators in endocardial cells has dramatic effects the heart, producing a CHD phenotype where the heart lacks trabeculae. Based on the above model of the cellular basis of CHD, any genetic modification that impairs cilia or Notch signaling would have a similar effect on trabeculation. Likewise, mutations in any gene that reduces the capacity of myocardial cells to respond to stimulatory cues from the endocardium could cause trabecular malformations. Data reported in Chapter 3 shows that the cellular defects underlying a CHD can be substantially separated in space and time emergence of the CHD phenotype. Loss of function of a single isoform of *nrg1*, *nrg1-III*, is largely benign until late cardiac maturation stages when structural deficiencies in trabecular density and the superficial cardiac nerve plexus are evident. Since *nrg1-III* is not expressed at appreciable levels in the developing heart and is rarely detected in the adult heart, the cellular defect underlying these malformations is unlikely to originate from a cardiac cell type. Instead, it is likely to involve regulation of Schwann cell migration and myelination of long axons, a process known to be regulated by *nrg1-III* (Perlin et al., 2011). Future studies are necessary to precisely define the relationships between cardiac nerve plexus formation, heart function, and maturation.

In total, the studies described in this dissertation provide support for the necessity of model organisms in understanding CHD. Current trends in biomedical research funding have sought to optimize research investment in part by de-emphasizing use of model organisms, owing to their high cost relative to *in vitro* and “disease in a dish” systems. However, data reported in Chapter 2 and Chapter 3 point to critical roles for the dynamic interplay between cardiac structure, function, and maturation in regulating

heart development. This interplay cannot be recapitulated in an *in vitro* setting, underscoring the importance of *in vivo* models and an approach to understanding CHD etiology that takes into account integrated physiology of the whole organism.

REFERENCES

- Abdallah, S.J., Thomas, B.S., Jonz, M.G., 2015. Aquatic surface respiration and swimming behaviour in adult and developing zebrafish exposed to hypoxia. *The Journal of experimental biology* 218, 1777-1786.
- Aird, W.C., 2012. Endothelial cell heterogeneity. *Cold Spring Harbor perspectives in medicine* 2, a006429.
- Altschul, S.F., Gish, W., Miller, W., Myers, E.W., Lipman, D.J., 1990. Basic local alignment search tool. *J Mol Biol* 215.
- Anderson, K.V., 2006. Cilia and Hedgehog signaling in the mouse embryo. *Harvey lectures* 102, 103-115.
- Angelini, A., Melacini, P., Barbero, F., Thiene, G., 1999. Evolutionary persistence of spongy myocardium in humans. *Circulation* 99, 2475.
- Asnani, A., Peterson, R.T., 2014. The zebrafish as a tool to identify novel therapies for human cardiovascular disease. *Disease models & mechanisms* 7, 763-767.
- Aulehla, A., Wiegraebe, W., Baubet, V., Wahl, M.B., Deng, C., Taketo, M., Lewandoski, M., Pourquie, O., 2008. A beta-catenin gradient links the clock and wavefront systems in mouse embryo segmentation. *Nat Cell Biol* 10, 186-193.
- Auman, H.J., Coleman, H., Riley, H.E., Olale, F., Tsai, H.J., Yelon, D., 2007. Functional modulation of cardiac form through regionally confined cell shape changes. *Plos Biol* 5, 604-615.
- Baeyens, N., Schwartz, M.A., 2016. Biomechanics of vascular mechanosensation and remodeling. *Molecular biology of the cell* 27, 7-11.
- Baker, K., Holtzman, N.G., Burdine, R.D., 2008. Direct and indirect roles for Nodal signaling in two axis conversions during asymmetric morphogenesis of the zebrafish heart. *P Natl Acad Sci USA* 105, 13924-13929.
- Bang, A., Grønkjær, P., Malte, H., 2004. Individual variation in the rate of oxygen consumption by zebrafish embryos. *Journal of Fish Biology* 64, 1285-1296.
- Barros, T.P., Alderton, W.K., Reynolds, H.M., Roach, A.G., Berghmans, S., 2008. Zebrafish: an emerging technology for in vivo pharmacological assessment to identify potential safety liabilities in early drug discovery. *British journal of pharmacology* 154, 1400-1413.
- Bartman, T., Walsh, E.C., Wen, K.K., McKane, M., Ren, J.H., Alexander, J., Rubenstein, P.A., Stainier, D.Y.R., 2004. Early myocardial function affects endocardial cushion development in zebrafish. *Plos Biol* 2, 673-681.
- Beis, D., Bartman, T., Jin, S.W., Scott, I.C., D'Amico, L.A., Ober, E.A., Verkade, H., Frantsve, J., Field, H.A., Wehman, A., Baier, H., Tallafuss, A., Bally-Cuif, L., Chen, J.N., Stainier, D.Y.R., Jungblut, B., 2005. Genetic and cellular analyses of zebrafish atrioventricular cushion and valve development. *Development* 132, 4193-4204.
- Beis, D., Stainier, D.Y., 2006. In vivo cell biology: following the zebrafish trend. *Trends in cell biology* 16, 105-112.
- Benedito, R., Hellström, M., 2013. Notch as a hub for signaling in angiogenesis. *Experimental Cell Research* 319, 1281-1288.

- Berdougo, E., Coleman, H., Lee, D.H., Stainier, D.Y., Yelon, D., 2003. Mutation of weak atrium/atrial myosin heavy chain disrupts atrial function and influences ventricular morphogenesis in zebrafish. *Development* 130, 6121-6129.
- Bersell, K., Arab, S., Haring, B., Kuhn, B., 2009. Neuregulin1/ErbB4 signaling induces cardiomyocyte proliferation and repair of heart injury. *Cell* 138, 257-270.
- Bertrand, J.Y., Chi, N.C., Santoso, B., Teng, S., Stainier, D.Y.R., Traver, D., 2010. Haematopoietic stem cells derive directly from aortic endothelium during development. *Nature* 464, 108-111.
- Bhatia, N.L., Tajik, A.J., Wilansky, S., Steidley, D.E., Mookadam, F., 2011. Isolated noncompaction of the left ventricular myocardium in adults: a systematic overview. *J Card Fail* 17, 771-778.
- Borggreffe, T., Lauth, M., Zwijsen, A., Huylebroeck, D., Oswald, F., Giaimo, B.D., 2016. The Notch intracellular domain integrates signals from Wnt, Hedgehog, TGFbeta/BMP and hypoxia pathways. *Biochimica et biophysica acta* 1863, 303-313.
- Borggreffe, T., Oswald, F., 2009. The Notch signaling pathway: transcriptional regulation at Notch target genes. *Cell Mol Life Sci* 66, 1631-1646.
- Borovina, A., Superina, S., Voskas, D., Ciruna, B., 2010. Vangl2 directs the posterior tilting and asymmetric localization of motile primary cilia. *Nat Cell Biol* 12, 407-412.
- Boselli, F., Freund, J.B., Vermot, J., 2015. Blood flow mechanics in cardiovascular development. *Cell Mol Life Sci* 72, 2545-2559.
- Breckenridge, R., 2010. Heart failure and mouse models. *Disease models & mechanisms* 3, 138-143.
- Breckenridge, R.A., Anderson, R.H., Elliott, P.M., 2007. Isolated left ventricular non-compaction: the case for abnormal myocardial development. *Cardiology in the Young* 17, 124-129.
- Brown, D., Samsa, L., Qian, L., Liu, J., 2016. Advances in the Study of Heart Development and Disease Using Zebrafish. *Journal of Cardiovascular Development and Disease* 3, 13.
- Budi, E.H., Patterson, L.B., Parichy, D.M., 2008. Embryonic requirements for ErbB signaling in neural crest development and adult pigment pattern formation. *Development* 135, 2603-2614.
- Busch-Nentwich, E., Kettleborough, R., Dooley, C. M., Scahill, C., Sealy, I., White, R., Herd, C., Mehroke, S., Wali, N., Carruthers, S., Hall, A., Collins, J., Gibbons, R., Pusztai, Z., Clark, R., and Stemple, D.L. , 2013. Sanger Institute Zebrafish Mutation Project mutant data submission. *ZFIN Direct Data Submission*.
- Bussmann, J., Bakkers, J., Schulte-Merker, S., 2007. Early endocardial morphogenesis requires Scf/Tal1. *Plos Genet* 3, 1425-1437.
- Chang, N., Sun, C., Gao, L., Zhu, D., Xu, X., Zhu, X., Xiong, J.W., Xi, J.J., 2013. Genome editing with RNA-guided Cas9 nuclease in zebrafish embryos. *Cell research* 23, 465-472.
- Chaudhari, G.H., Chennubhotla, K.S., Chatti, K., Kulkarni, P., 2013. Optimization of the adult zebrafish ECG method for assessment of drug-induced QTc prolongation. *Journal of pharmacological and toxicological methods* 67, 115-120.
- Chen, H., Shi, S., Acosta, L., Li, W., Lu, J., Bao, S., Chen, Z., Yang, Z., Schneider, M.D., Chien, K.R., Conway, S.J., Yoder, M.C., Haneline, L.S., Franco, D., Shou, W., 2004. BMP10 is essential for maintaining cardiac growth during murine cardiogenesis. *Development* 131, 2219-2231.

- Chen, J.K., Taipale, J., Cooper, M.K., Beachy, P.A., 2002. Inhibition of Hedgehog signaling by direct binding of cyclopamine to Smoothened. *Gene Dev* 16, 2743-2748.
- Chen, J.N., Haffter, P., Odenthal, J., Vogelsang, E., Brand, M., van Eeden, F.J., Furutani-Seiki, M., Granato, M., Hammerschmidt, M., Heisenberg, C.P., Jiang, Y.J., Kane, D.A., Kelsh, R.N., Mullins, M.C., Nusslein-Volhard, C., 1996. Mutations affecting the cardiovascular system and other internal organs in zebrafish. *Development* 123, 293-302.
- Chen, J.N., vanEeden, F.J.M., Warren, K.S., Chin, A., NussleinVolhard, C., Haffter, P., Fishman, M.C., 1997. Left-right pattern of cardiac BMP4 may drive asymmetry of the heart in zebrafish. *Development* 124, 4373-4382.
- Chi, N.C., Shaw, R.M., Jungblut, B., Huisken, J., Ferrer, T., Arnaout, R., Scott, I., Beis, D., Xiao, T., Baier, H., Jan, L.Y., Tristani-Firouzi, M., Stainier, D.Y., 2008. Genetic and physiologic dissection of the vertebrate cardiac conduction system. *Plos Biol* 6, e109.
- Chin, A.J., Saint-Jeannet, J.P., Lo, C.W., 2012. How insights from cardiovascular developmental biology have impacted the care of infants and children with congenital heart disease. *Mech Dev* 129, 75-97.
- Chin, T.K., Perloff, J.K., Williams, R.G., Jue, K., Mohrmann, R., 1990. Isolated noncompaction of left ventricular myocardium. A study of eight cases. *Circulation* 82, 507-513.
- Christoffels, V.M., Moorman, A.F., 2009. Development of the cardiac conduction system: why are some regions of the heart more arrhythmogenic than others? *Circulation. Arrhythmia and electrophysiology* 2, 195-207.
- Clement, C.A., Kristensen, S.G., Mollgard, K., Pazour, G.J., Yoder, B.K., Larsen, L.A., Christensen, S.T., 2009. The primary cilium coordinates early cardiogenesis and hedgehog signaling in cardiomyocyte differentiation. *Journal of cell science* 122, 3070-3082.
- Cooley, M.A., Fresco, V.M., Durlon, M.E., Twal, W.O., Lee, N.V., Barth, J.L., Kern, C.B., Iruela-Arispe, M.L., Argraves, W.S., 2012. Fibulin-1 is required during cardiac ventricular morphogenesis for versican cleavage, suppression of ErbB2 and Erk1/2 activation, and to attenuate trabecular cardiomyocyte proliferation. *Developmental dynamics : an official publication of the American Association of Anatomists* 241, 303-314.
- Corada, M., Morini, M.F., Dejana, E., 2014. Signaling pathways in the specification of arteries and veins. *Arteriosclerosis, thrombosis, and vascular biology* 34, 2372-2377.
- Culver, J.C., Dickinson, M.E., 2010. The effects of hemodynamic force on embryonic development. *Microcirculation (New York, N.Y. : 1994)* 17, 164-178.
- D'Amico, L., Scott, I.C., Jungblut, B., Stainier, D.Y., 2007. A mutation in zebrafish *hmgcr1b* reveals a role for isoprenoids in vertebrate heart-tube formation. *Curr Biol* 17, 252-259.
- D'Uva, G., Aharonov, A., Lauriola, M., Kain, D., Yahalom-Ronen, Y., Carvalho, S., Weisinger, K., Bassat, E., Rajchman, D., Yifa, O., Lysenko, M., Konfino, T., Hegesh, J., Brenner, O., Neeman, M., Yarden, Y., Leor, J., Sarig, R., Harvey, R.P., Tzahor, E., 2015. ERBB2 triggers mammalian heart regeneration by promoting cardiomyocyte dedifferentiation and proliferation. *Nat Cell Biol* 17, 627-638.
- de la Pompa, J.L., Epstein, J.A., 2012. Coordinating tissue interactions: Notch signaling in cardiac development and disease. *Dev Cell* 22, 244-254.

- de la Pompa, J.L., Timmerman, L.A., Takimoto, H., Yoshida, H., Elia, A.J., Samper, E., Potter, J., Wakeham, A., Marengere, L., Langille, B.L., Crabtree, G.R., Mak, T.W., 1998. Role of the NF-ATc transcription factor in morphogenesis of cardiac valves and septum. *Nature* 392, 182-186.
- de Pater, E., Clijsters, L., Marques, S.R., Lin, Y.F., Garavito-Aguilar, Z.V., Yelon, D., Bakkers, J., 2009. Distinct phases of cardiomyocyte differentiation regulate growth of the zebrafish heart. *Development* 136, 1633-1641.
- Del Amo, F.F., Smith, D.E., Swiatek, P.J., Gendron-Maguire, M., Greenspan, R.J., McMahon, A.P., Gridley, T., 1992. Expression pattern of *Motch*, a mouse homolog of *Drosophila Notch*, suggests an important role in early postimplantation mouse development. *Development* 115, 737-744.
- Delvecchio, C., Tiefenbach, J., Krause, H.M., 2011. The zebrafish: a powerful platform for in vivo, HTS drug discovery. *Assay and drug development technologies* 9, 354-361.
- Dickover, M.S., Zhang, R., Han, P., Chi, N.C., 2013. Zebrafish cardiac injury and regeneration models: a noninvasive and invasive in vivo model of cardiac regeneration. *Methods Mol Biol* 1037, 463-473.
- Dietrich, A.C., Lombardo, V.A., Veerkamp, J., Priller, F., Abdelilah-Seyfried, S., 2014. Blood flow and Bmp signaling control endocardial chamber morphogenesis. *Dev Cell* 30, 367-377.
- Duester, G., 2008. Retinoic acid synthesis and signaling during early organogenesis. *Cell* 134, 921-931.
- Egorova, A.D., van der Heiden, K., Poelmann, R.E., Hierck, B.P., 2012. Primary cilia as biomechanical sensors in regulating endothelial function. *Differentiation; research in biological diversity* 83, S56-61.
- Fahed, A.C., Gelb, B.D., Seidman, J.G., Seidman, C.E., 2013. Genetics of Congenital Heart Disease The Glass Half Empty. *Circ Res* 112, 707-720.
- Falls, D.L., 2003. Neuregulins: functions, forms, and signaling strategies. *Experimental Cell Research* 284, 14-30.
- Fang, S.J., Wu, X.S., Han, Z.H., Zhang, X.X., Wang, C.M., Li, X.Y., Lu, L.Q., Zhang, J.L., 2010. Neuregulin-1 preconditioning protects the heart against ischemia/reperfusion injury through a PI3K/Akt-dependent mechanism. *Chinese medical journal* 123, 3597-3604.
- Firestone, A.J., Weinger, J.S., Maldonado, M., Barlan, K., Langston, L.D., O'Donnell, M., Gelfand, V.I., Kapoor, T.M., Chen, J.K., 2012. Small-molecule inhibitors of the AAA+ ATPase motor cytoplasmic dynein. *Nature* 484, 125-129.
- Fishman, M.C., Chien, K.R., 1997. Fashioning the vertebrate heart: earliest embryonic decisions. *Development* 124, 2099-2117.
- Formiga, F.R., Pelacho, B., Garbayo, E., Imbuluzqueta, I., Diaz-Herraez, P., Abizanda, G., Gavira, J.J., Simon-Yarza, T., Albiasu, E., Tamayo, E., Prosper, F., Blanco-Prieto, M.J., 2014. Controlled delivery of fibroblast growth factor-1 and neuregulin-1 from biodegradable microparticles promotes cardiac repair in a rat myocardial infarction model through activation of endogenous regeneration. *Journal of controlled release : official journal of the Controlled Release Society* 173, 132-139.
- Fuller, S.J., Sivarajah, K., Sugden, P.H., 2008. ErbB receptors, their ligands, and the consequences of their activation and inhibition in the myocardium. *Journal of molecular and cellular cardiology* 44, 831-854.

- Gao, R., Zhang, J., Cheng, L., Wu, X., Dong, W., Yang, X., Li, T., Liu, X., Xu, Y., Li, X., Zhou, M., 2010. A Phase II, randomized, double-blind, multicenter, based on standard therapy, placebo-controlled study of the efficacy and safety of recombinant human neuregulin-1 in patients with chronic heart failure. *Journal of the American College of Cardiology* 55, 1907-1914.
- Garavito-Aguilar, Z.V., Riley, H.E., Yelon, D., 2010. Hand2 ensures an appropriate environment for cardiac fusion by limiting Fibronectin function. *Development* 137, 3215-3220.
- Garita, B., Jenkins, M.W., Han, M., Zhou, C., Vanauker, M., Rollins, A.M., Watanabe, M., Fujimoto, J.G., Linask, K.K., 2011. Blood flow dynamics of one cardiac cycle and relationship to mechanotransduction and trabeculation during heart looping. *American journal of physiology. Heart and circulatory physiology* 300, H879-891.
- Gassmann, M., Casagrande, F., Orioli, D., Simon, H., Lai, C., Klein, R., Lemke, G., 1995. Aberrant neural and cardiac development in mice lacking the ErbB4 neuregulin receptor. *Nature* 378, 390-394.
- Gemberling, M., Karra, R., Dickson, A.L., Poss, K.D., 2015. Nrg1 is an injury-induced cardiomyocyte mitogen for the endogenous heart regeneration program in zebrafish. *eLife* 4.
- Gerdes, J.M., Davis, E.E., Katsanis, N., 2009. The vertebrate primary cilium in development, homeostasis, and disease. *Cell* 137, 32-45.
- Gerety, S.S., Wang, H.U., Chen, Z.F., Anderson, D.J., 1999. Symmetrical mutant phenotypes of the receptor EphB4 and its specific transmembrane ligand ephrin-B2 in cardiovascular development. *Molecular cell* 4, 403-414.
- Go, A.S., Mozaffarian, D., Roger, V.L., Benjamin, E.J., Berry, J.D., Borden, W.B., Bravata, D.M., Dai, S., Ford, E.S., Fox, C.S., Franco, S., Fullerton, H.J., Gillespie, C., Hailpern, S.M., Heit, J.A., Howard, V.J., Huffman, M.D., Kissela, B.M., Kittner, S.J., Lackland, D.T., et al., 2013. Heart disease and stroke statistics--2013 update: a report from the American Heart Association. *Circulation* 127, e6-e245.
- Goetz, J.G., Steed, E., Ferreira, R.R., Roth, S., Ramspacher, C., Boselli, F., Charvin, G., Liebling, M., Wyart, C., Schwab, Y., Vermot, J., 2014. Endothelial cilia mediate low flow sensing during zebrafish vascular development. *Cell reports* 6, 799-808.
- Gonzalez-Rosa, J.M., Peralta, M., Mercader, N., 2012. Pan-epicardial lineage tracing reveals that epicardium derived cells give rise to myofibroblasts and perivascular cells during zebrafish heart regeneration. *Developmental biology* 370, 173-186.
- Gourdie, R.G., Wei, Y., Kim, D., Klatt, S.C., Mikawa, T., 1998. Endothelin-induced conversion of embryonic heart muscle cells into impulse-conducting Purkinje fibers. *P Natl Acad Sci USA* 95, 6815-6818.
- Granados-Riveron, J.T., Brook, J.D., 2012. The impact of mechanical forces in heart morphogenesis. *Circulation. Cardiovascular genetics* 5, 132-142.
- Grego-Bessa, J., Luna-Zurita, L., del Monte, G., Bolos, V., Melgar, P., Arandilla, A., Garratt, A.N., Zang, H., Mukoyama, Y.S., Chen, H., Shou, W., Ballestar, E., Esteller, M., Rojas, A., Perez-Pomares, J.M., de la Pompa, J.L., 2007. Notch signaling is essential for ventricular chamber development. *Dev Cell* 12, 415-429.
- Gridley, T., 2010. Chapter Nine - Notch Signaling in the Vasculature, in: Raphael, K. (Ed.), Current topics in developmental biology. Academic Press, pp. 277-309.

- Grimes, A.C., Kirby, M.L., 2009. The outflow tract of the heart in fishes: anatomy, genes and evolution. *J Fish Biol* 74, 983-1036.
- Guo, Y.F., Zhang, X.X., Liu, Y., Duan, H.Y., Jie, B.Z., Wu, X.S., 2012. Neuregulin-1 attenuates mitochondrial dysfunction in a rat model of heart failure. *Chinese medical journal* 125, 807-814.
- Gupta, V., Gemberling, M., Karra, R., Rosenfeld, G.E., Evans, T., Poss, K.D., 2013. An Injury-Responsive Gata4 Program Shapes the Zebrafish Cardiac Ventricle. *Curr Biol* 23, 1221-1227.
- Gupta, V., Poss, K.D., 2012. Clonally dominant cardiomyocytes direct heart morphogenesis. *Nature* 484, 479-U102.
- Hahn, C., Schwartz, M.A., 2009. Mechanotransduction in vascular physiology and atherogenesis. *Nature reviews. Molecular cell biology* 10, 53-62.
- Hall, C.E., Hurtado, R., Hewett, K.W., Shulimovich, M., Poma, C.P., Reckova, M., Justus, C., Pennisi, D.J., Tobita, K., Sedmera, D., Gourdie, R.G., Mikawa, T., 2004. Hemodynamic-dependent patterning of endothelin converting enzyme 1 expression and differentiation of impulse-conducting Purkinje fibers in the embryonic heart. *Development* 131, 581-592.
- Hami, D., Grimes, A.C., Tsai, H.J., Kirby, M.L., 2011. Zebrafish cardiac development requires a conserved secondary heart field. *Development* 138, 2389-2398.
- Harrison, M.R.M., Bussmann, J., Huang, Y., Zhao, L., Osorio, A., Burns, C.G., Burns, C.E., Sucov, H.M., Siekmann, A.F., Lien, C.L., 2015. Chemokine-Guided Angiogenesis Directs Coronary Vasculature Formation in Zebrafish. *Dev Cell* 33, 442-454.
- Harvey, R.P., 2002. Patterning the vertebrate heart. *Nature reviews. Genetics* 3, 544-556.
- Harvey, R.P., Wystub-Lis, K., del Monte-Nieto, G., Graham, R.M., Tzahor, E., 2016. Cardiac Regeneration Therapies - Targeting Neuregulin 1 Signalling. *Heart, lung & circulation* 25, 4-7.
- Heckel, E., Boselli, F., Roth, S., Krudewig, A., Belting, H.G., Charvin, G., Vermot, J., 2015. Oscillatory Flow Modulates Mechanosensitive klf2a Expression through trpv4 and trpp2 during Heart Valve Development. *Curr Biol* 25, 1354-1361.
- Hein, S.J., Lehmann, L.H., Kossack, M., Juergensen, L., Fuchs, D., Katus, H.A., Hassel, D., 2015. Advanced echocardiography in adult zebrafish reveals delayed recovery of heart function after myocardial cryoinjury. *PloS one* 10, e0122665.
- Hierck, B.P., Van der Heiden, K., Alkemade, F.E., Van de Pas, S., Van Thienen, J.V., Groenendijk, B.C., Bax, W.H., Van der Laarse, A., Deruiter, M.C., Horrevoets, A.J., Poelmann, R.E., 2008. Primary cilia sensitize endothelial cells for fluid shear stress. *Developmental dynamics : an official publication of the American Association of Anatomists* 237, 725-735.
- Hill, M.F., Patel, A.V., Murphy, A., Smith, H.M., Galindo, C.L., Pentassuglia, L., Peng, X., Lenneman, C.G., Odiete, O., Friedman, D.B., Kronenberg, M.W., Zheng, S., Zhao, Z., Song, Y., Harrell, F.E., Jr., Srinivas, M., Ganguly, A., Iaci, J., Parry, T.J., Caggiano, A.O., et al., 2013. Intravenous glial growth factor 2 (GGF2) isoform of neuregulin-1beta improves left ventricular function, gene and protein expression in rats after myocardial infarction. *PloS one* 8, e55741.
- Hofsteen, P., Plavicki, J., Johnson, S.D., Peterson, R.E., Heideman, W., 2013. Sox9b is required for epicardium formation and plays a role in TCDD-induced heart malformation in zebrafish. *Molecular pharmacology* 84, 353-360.

- Hogers, B., DeRuiter, M.C., Gittenberger-de Groot, A.C., Poelmann, R.E., 1997. Unilateral vitelline vein ligation alters intracardiac blood flow patterns and morphogenesis in the chick embryo. *Circ Res* 80, 473-481.
- Holtzman, N.G., Schoenebeck, J.J., Tsai, H.J., Yelon, D., 2007. Endocardium is necessary for cardiomyocyte movement during heart tube assembly. *Development* 134, 2379-2386.
- Honjo, Y., Kniss, J., Eisen, J.S., 2008. Neuregulin-mediated ErbB3 signaling is required for formation of zebrafish dorsal root ganglion neurons. *Development* 135, 2615-2625.
- Hove, J.R., Koster, R.W., Forouhar, A.S., Acevedo-Bolton, G., Fraser, S.E., Gharib, M., 2003. Intracardiac fluid forces are an essential epigenetic factor for embryonic cardiogenesis. *Nature* 421, 172-177.
- Howe, K., Clark, M.D., Torroja, C.F., Torrance, J., Berthelot, C., Muffato, M., Collins, J.E., Humphray, S., McLaren, K., Matthews, L., McLaren, S., Sealy, I., Caccamo, M., Churcher, C., Scott, C., Barrett, J.C., Koch, R., Rauch, G.J., White, S., Chow, W., et al., 2013. The zebrafish reference genome sequence and its relationship to the human genome. *Nature* 496, 498-503.
- Huang, C.J., Tu, C.T., Hsiao, C.D., Hsieh, F.J., Tsai, H.J., 2003. Germ-line transmission of a myocardium-specific GFP transgene reveals critical regulatory elements in the cardiac myosin light chain 2 promoter of zebrafish. *Dev Dynam* 228, 30-40.
- Icardo, J.M., Fernandez-Teran, A., 1987. Morphologic study of ventricular trabeculation in the embryonic chick heart. *Acta anatomica* 130, 264-274.
- Ichida, F., Hamamichi, Y., Miyawaki, T., Ono, Y., Kamiya, T., Akagi, T., Hamada, H., Hirose, O., Isobe, T., Yamada, K., Kurotobi, S., Mito, H., Miyake, T., Murakami, Y., Nishi, T., Shinohara, M., Seguchi, M., Tashiro, S., Tomimatsu, H., 1999. Clinical features of isolated noncompaction of the ventricular myocardium: long-term clinical course, hemodynamic properties, and genetic background. *Journal of the American College of Cardiology* 34, 233-240.
- Iomini, C., Tejada, K., Mo, W., Vaananen, H., Piperno, G., 2004. Primary cilia of human endothelial cells disassemble under laminar shear stress. *The Journal of cell biology* 164, 811-817.
- Itoh, M., Kim, C.H., Palardy, G., Oda, T., Jiang, Y.J., Maust, D., Yeo, S.Y., Lorick, K., Wright, G.J., Ariza-McNaughton, L., Weissman, A.M., Lewis, J., Chandrasekharappa, S.C., Chitnis, A.B., 2003. Mind bomb is a ubiquitin ligase that is essential for efficient activation of Notch signaling by Delta. *Dev Cell* 4, 67-82.
- Jabbour, A., Hayward, C.S., Keogh, A.M., Kotlyar, E., McCrohon, J.A., England, J.F., Amor, R., Liu, X., Li, X.Y., Zhou, M.D., Graham, R.M., Macdonald, P.S., 2011. Parenteral administration of recombinant human neuregulin-1 to patients with stable chronic heart failure produces favourable acute and chronic haemodynamic responses. *European journal of heart failure* 13, 83-92.
- Jenni, R., Oechslin, E., Schneider, J., Attenhofer Jost, C., Kaufmann, P.A., 2001. Echocardiographic and pathoanatomical characteristics of isolated left ventricular non-compaction: a step towards classification as a distinct cardiomyopathy. *Heart (British Cardiac Society)* 86, 666-671.
- Jenni, R., Oechslin, E.N., van der Loo, B., 2007. Isolated ventricular non-compaction of the myocardium in adults. *Heart (British Cardiac Society)* 93, 11-15.
- Jenni, R., Rojas, J., Oechslin, E., 1999. Isolated Noncompaction of the Myocardium. *New England Journal of Medicine* 340, 966-967.

- Jiang, Y.J., Brand, M., Heisenberg, C.P., Beuchle, D., Furutani-Seiki, M., Kelsh, R.N., Warga, R.M., Granato, M., Haffter, P., Hammerschmidt, M., Kane, D.A., Mullins, M.C., Odenthal, J., van Eeden, F.J., Nusslein-Volhard, C., 1996. Mutations affecting neurogenesis and brain morphology in the zebrafish, *Danio rerio*. *Development* 123, 205-216.
- Jinn, S.W., Beisl, D., Mitchell, T., Chen, J.N., Stainier, D.Y.R., 2005. Cellular and molecular analyses of vascular tube and lumen formation in zebrafish. *Development* 132, 5199-5209.
- Just, S., Berger, I.M., Meder, B., Backs, J., Keller, A., Marquart, S., Frese, K., Patzel, E., Rauch, G.J., Katus, H.A., Rottbauer, W., 2011. Protein kinase D2 controls cardiac valve formation in zebrafish by regulating histone deacetylase 5 activity. *Circulation* 124, 324-334.
- Kageyama, R., Ohtsuka, T., Shimojo, H., Imayoshi, I., 2008. Dynamic Notch signaling in neural progenitor cells and a revised view of lateral inhibition. *Nat Neurosci* 11, 1247-1251.
- Kalogirou, S., Malissovass, N., Moro, E., Argenton, F., Stainier, D.Y., Beis, D., 2014. Intracardiac flow dynamics regulate atrioventricular valve morphogenesis. *Cardiovascular research* 104, 49-60.
- Kattman, S.J., Huber, T.L., Keller, G.M., 2006. Multipotent flk-1+ cardiovascular progenitor cells give rise to the cardiomyocyte, endothelial, and vascular smooth muscle lineages. *Dev Cell* 11, 723-732.
- Keegan, B.R., Meyer, D., Yelon, D., 2004. Organization of cardiac chamber progenitors in the zebrafish blastula. *Development* 131, 3081-3091.
- Kessler, M., Rottbauer, W., Just, S., 2015. Recent progress in the use of zebrafish for novel cardiac drug discovery. *Expert opinion on drug discovery* 10, 1231-1241.
- Kikuchi, K., Gupta, V., Wang, J.H., Holdway, J.E., Wills, A.A., Fang, Y., Poss, K.D., 2011. tcf21(+) epicardial cells adopt non-myocardial fates during zebrafish heart development and regeneration. *Development* 138, 2895-2902.
- Kirby, M.L., 2007. Cardiac Development. Oxford University Press, New York.
- Kitambi, S.S., Nilsson, E.S., Sekyrova, P., Ibarra, C., Tekeoh, G.N., Andang, M., Ernfors, P., Uhlen, P., 2012. Small molecule screening platform for assessment of cardiovascular toxicity on adult zebrafish heart. *BMC physiology* 12, 3.
- Kochupurakkal, B.S., Harari, D., Di-Segni, A., Maik-Rachline, G., Lyass, L., Gur, G., Kerber, G., Citri, A., Lavi, S., Eilam, R., Chalifa-Caspi, V., Eshhar, Z., Pikarsky, E., Pinkas-Kramarski, R., Bacus, S.S., Yarden, Y., 2005. Epigen, the last ligand of ErbB receptors, reveals intricate relationships between affinity and mitogenicity. *The Journal of biological chemistry* 280, 8503-8512.
- Kong, J.H., Yang, L., Dessaud, E., Chuang, K., Moore, D.M., Rohatgi, R., Briscoe, J., Novitch, B.G., 2015. Notch activity modulates the responsiveness of neural progenitors to sonic hedgehog signaling. *Dev Cell* 33, 373-387.
- Kramer-Zucker, A.G., Olale, F., Haycraft, C.J., Yoder, B.K., Schier, A.F., Drummond, I.A., 2005. Cilia-driven fluid flow in the zebrafish pronephros, brain and Kupffer's vesicle is required for normal organogenesis. *Development* 132, 1907-1921.
- Kramer, R., Bucay, N., Kane, D.J., Martin, L.E., Tarpley, J.E., Theill, L.E., 1996. Neuregulins with an Ig-like domain are essential for mouse myocardial and neuronal development. *P Natl Acad Sci USA* 93, 4833-4838.

- Krebs, L.T., Xue, Y., Norton, C.R., Shutter, J.R., Maguire, M., Sundberg, J.P., Gallahan, D., Closson, V., Kitajewski, J., Callahan, R., Smith, G.H., Stark, K.L., Gridley, T., 2000. Notch signaling is essential for vascular morphogenesis in mice. *Gene Dev* 14, 1343-1352.
- Lai, D., Liu, X., Forrai, A., Wolstein, O., Michalicek, J., Ahmed, I., Garratt, A.N., Birchmeier, C., Zhou, M., Hartley, L., Robb, L., Feneley, M.P., Fatkin, D., Harvey, R.P., 2010. Neuregulin 1 sustains the gene regulatory network in both trabecular and nontrabecular myocardium. *Circ Res* 107, 715-727.
- Laisney, J.A., Braasch, I., Walter, R.B., Meierjohann, S., Scharf, M., 2010. Lineage-specific co-evolution of the Egf receptor/ligand signaling system. *BMC Evolutionary Biology* 10, 1-16.
- Lavine, K.J., Yu, K., White, A.C., Zhang, X., Smith, C., Partanen, J., Ornitz, D.M., 2005. Endocardial and epicardial derived FGF signals regulate myocardial proliferation and differentiation in vivo. *Dev Cell* 8, 85-95.
- Lazic, S., Scott, I.C., 2011. Mef2cb regulates late myocardial cell addition from a second heart field-like population of progenitors in zebrafish. *Developmental biology* 354, 123-133.
- Lee, J., Moghadam, M.E., Kung, E., Cao, H., Beebe, T., Miller, Y., Roman, B.L., Lien, C.L., Chi, N.C., Marsden, A.L., Hsiai, T.K., 2013. Moving domain computational fluid dynamics to interface with an embryonic model of cardiac morphogenesis. *PloS one* 8, e72924.
- Lee, K.F., Simon, H., Chen, H., Bates, B., Hung, M.C., Hauser, C., 1995. Requirement for neuregulin receptor erbB2 in neural and cardiac development. *Nature* 378, 394-398.
- Lee, L., Genge, C.E., Cua, M., Sheng, X., Rayani, K., Beg, M.F., Sarunic, M.V., Tibbits, G.F., 2016. Functional Assessment of Cardiac Responses of Adult Zebrafish (*Danio rerio*) to Acute and Chronic Temperature Change Using High-Resolution Echocardiography. *PloS one* 11, e0145163.
- Li, B., Zheng, Z., Wei, Y., Wang, M., Peng, J., Kang, T., Huang, X., Xiao, J., Li, Y., Li, Z., 2011. Therapeutic effects of neuregulin-1 in diabetic cardiomyopathy rats. *Cardiovascular diabetology* 10, 69.
- Lin, Y.F., Swinburne, I., Yelon, D., 2012. Multiple influences of blood flow on cardiomyocyte hypertrophy in the embryonic zebrafish heart. *Developmental biology* 362, 242-253.
- Liu, J., Bressan, M., Hassel, D., Huisken, J., Staudt, D., Kikuchi, K., Poss, K.D., Mikawa, T., Stainier, D.Y., 2010. A dual role for ErbB2 signaling in cardiac trabeculation. *Development* 137, 3867-3875.
- Liu, J., Stainier, D.Y., 2010. Tbx5 and Bmp signaling are essential for proepicardium specification in zebrafish. *Circ Res* 106, 1818-1828.
- Liu, J., Stainier, D.Y., 2012. Zebrafish in the study of early cardiac development. *Circ Res* 110, 870-874.
- Liu, X., Gu, X., Li, Z., Li, X., Li, H., Chang, J., Chen, P., Jin, J., Xi, B., Chen, D., Lai, D., Graham, R.M., Zhou, M., 2006. Neuregulin-1/erbB-activation improves cardiac function and survival in models of ischemic, dilated, and viral cardiomyopathy. *Journal of the American College of Cardiology* 48, 1438-1447.
- Livak, K.J., Schmittgen, T.D., 2001. Analysis of relative gene expression data using real-time quantitative PCR and the 2(-Delta Delta C(T)) Method. *Methods* 25.

- Long, Q.M., Meng, A.M., Wang, H., Jessen, J.R., Farrell, M.J., Lin, S., 1997. GATA-1 expression pattern can be recapitulated in living transgenic zebrafish using GFP reporter gene. *Development* 124, 4105-4111.
- Loomes, K.M., Underkoffler, L.A., Morabito, J., Gottlieb, S., Piccoli, D.A., Spinner, N.B., Baldwin, H.S., Oakey, R.J., 1999. The expression of Jagged1 in the developing mammalian heart correlates with cardiovascular disease in Alagille syndrome. *Human molecular genetics* 8, 2443-2449.
- Lopez-Schier, H., Hudspeth, A.J., 2005. Supernumerary neuromasts in the posterior lateral line of zebrafish lacking peripheral glia. *P Natl Acad Sci USA* 102, 1496-1501.
- Lowery, J.W., de Caestecker, M.P., 2010. BMP signaling in vascular development and disease. *Cytokine & growth factor reviews* 21, 287-298.
- Lu, S.Y., Sheikh, F., Sheppard, P.C., Fresnoza, A., Duckworth, M.L., Detillieux, K.A., Cattini, P.A., 2008. FGF-16 is required for embryonic heart development. *Biochem Bioph Res Co* 373, 270-274.
- Lunt, S.C., Haynes, T., Perkins, B.D., 2009. Zebrafish *ift57*, *ift88*, and *ift172* intraflagellar transport mutants disrupt cilia but do not affect hedgehog signaling. *Developmental dynamics : an official publication of the American Association of Anatomists* 238, 1744-1759.
- Lyons, D.A., Pogoda, H.M., Voas, M.G., Woods, I.G., Diamond, B., Nix, R., Arana, N., Jacobs, J., Talbot, W.S., 2005. *erbb3* and *erbb2* are essential for schwann cell migration and myelination in zebrafish. *Curr Biol* 15, 513-524.
- Mably, J.D., Mohideen, M.A., Burns, C.G., Chen, J.N., Fishman, M.C., 2003. heart of glass regulates the concentric growth of the heart in zebrafish. *Curr Biol* 13, 2138-2147.
- MacGrogan, D., Nus, M., de la Pompa, J.L., 2010. Notch signaling in cardiac development and disease. *Current topics in developmental biology* 92, 333-365.
- Mahmoud, A.I., O'Meara, C.C., Gemberling, M., Zhao, L., Bryant, D.M., Zheng, R., Gannon, J.B., Cai, L., Choi, W.Y., Egnaczyk, G.F., Burns, C.E., Burns, C.G., MacRae, C.A., Poss, K.D., Lee, R.T., 2015. Nerves Regulate Cardiomyocyte Proliferation and Heart Regeneration. *Dev Cell* 34, 387-399.
- Mann, D.L., Bristow, M.R., 2005. Mechanisms and Models in Heart Failure: The Biomechanical Model and Beyond. *Circulation* 111, 2837-2849.
- Marchionni, M.A., 1995. Cell-cell signalling. neu tack on neuregulin. *Nature* 378, 334-335.
- Maron, B.J., Towbin, J.A., Thiene, G., Antzelevitch, C., Corrado, D., Arnett, D., Moss, A.J., Seidman, C.E., Young, J.B., 2006. Contemporary definitions and classification of the cardiomyopathies: an American Heart Association Scientific Statement from the Council on Clinical Cardiology, Heart Failure and Transplantation Committee; Quality of Care and Outcomes Research and Functional Genomics and Translational Biology Interdisciplinary Working Groups; and Council on Epidemiology and Prevention. *Circulation* 113, 1807-1816.
- Martin, R.T., Bartman, T., 2009. Analysis of heart valve development in larval zebrafish. *Developmental dynamics : an official publication of the American Association of Anatomists* 238, 1796-1802.
- McCright, B., Lozier, J., Gridley, T., 2002. A mouse model of Alagille syndrome: Notch2 as a genetic modifier of Jag1 haploinsufficiency. *Development* 129, 1075-1082.

- McMenamin, S.K., Bain, E.J., McCann, A.E., Patterson, L.B., Eom, D.S., Waller, Z.P., Hamill, J.C., Kuhlman, J.A., Eisen, J.S., Parichy, D.M., 2014. Thyroid hormone-dependent adult pigment cell lineage and pattern in zebrafish. *Science (New York, N.Y.)* 345, 1358-1361.
- Mendes-Ferreira, P., Maia-Rocha, C., Adao, R., Mendes, M.J., Santos-Ribeiro, D., Alves, B.S., Cerqueira, R.J., Castro-Chaves, P., Lourenco, A.P., De Keulenaer, G.W., Leite-Moreira, A.F., Bras-Silva, C., 2016. Neuregulin-1 improves right ventricular function and attenuates experimental pulmonary arterial hypertension. *Cardiovascular research* 109, 44-54.
- Merki, E., Zamora, M., Raya, A., Kawakami, Y., Wang, J., Zhang, X., Burch, J., Kubalak, S.W., Kaliman, P., Izpisua Belmonte, J.C., Chien, K.R., Ruiz-Lozano, P., 2005. Epicardial retinoid X receptor alpha is required for myocardial growth and coronary artery formation. *P Natl Acad Sci USA* 102, 18455-18460.
- Meyer, D., Birchmeier, C., 1995. Multiple Essential Functions of Neuregulin in Development. *Nature* 378, 386-390.
- Mikawa, T., 1995. Retroviral targeting of FGF and FGFR in cardiomyocytes and coronary vascular cells during heart development. *Annals of the New York Academy of Sciences* 752, 506-516.
- Milan, D.J., Giokas, A.C., Serluca, F.C., Peterson, R.T., MacRae, C.A., 2006. Notch1b and neuregulin are required for specification of central cardiac conduction tissue. *Development* 133, 1125-1132.
- Milgrom-Hoffman, M., Harrelson, Z., Ferrara, N., Zelzer, E., Evans, S.M., Tzahor, E., 2011. The heart endocardium is derived from vascular endothelial progenitors. *Development* 138, 4777-4787.
- Mima, T., Ueno, H., Fischman, D.A., Williams, L.T., Mikawa, T., 1995. Fibroblast growth factor receptor is required for in vivo cardiac myocyte proliferation at early embryonic stages of heart development. *P Natl Acad Sci USA* 92, 467-471.
- Minot, C.S., 1901. On a hitherto unrecognised circulation without capillaries in the organs of Vertebrata. *Proc Boston Soc Nat Hist* 29, 185-215.
- Miquerol, L., Beyer, S., Kelly, R.G., 2011. Establishment of the mouse ventricular conduction system. *Cardiovascular research* 91, 232-242.
- Misfeldt, A.M., Boyle, S.C., Tompkins, K.L., Bautch, V.L., Labosky, P.A., Baldwin, H.S., 2009. Endocardial cells are a distinct endothelial lineage derived from Flk1+ multipotent cardiovascular progenitors. *Developmental biology* 333, 78-89.
- Montero, J.C., Yuste, L., Diaz-Rodriguez, E., Esparis-Ogando, A., Pandiella, A., 2000. Differential shedding of transmembrane neuregulin isoforms by the tumor necrosis factor-alpha-converting enzyme. *Molecular and cellular neurosciences* 16, 631-648.
- Moorman, A.F., Christoffels, V.M., 2003. Cardiac chamber formation: development, genes, and evolution. *Physiological reviews* 83, 1223-1267.
- Moran, A.E., Roth, G.A., Narula, J., Mensah, G.A., 2014. 1990-2010 global cardiovascular disease atlas. *Global heart* 9, 3-16.
- Moretti, A., Caron, L., Nakano, A., Lam, J.T., Bernshausen, A., Chen, Y., Qyang, Y., Bu, L., Sasaki, M., Martin-Puig, S., Sun, Y., Evans, S.M., Laugwitz, K.L., Chien, K.R., 2006. Multipotent embryonic isl1+ progenitor cells lead to cardiac, smooth muscle, and endothelial cell diversification. *Cell* 127, 1151-1165.

- Morriss-Kay, G., 1992. Retinoic Acid and Development. *Pathobiology* 60, 264-270.
- Mozaffarian, D., Benjamin, E.J., Go, A.S., Arnett, D.K., Blaha, M.J., Cushman, M., Das, S.R., de Ferranti, S., Despres, J.P., Fullerton, H.J., Howard, V.J., Huffman, M.D., Isasi, C.R., Jimenez, M.C., Judd, S.E., Kissela, B.M., Lichtman, J.H., Lisabeth, L.D., Liu, S., Mackey, R.H., et al., 2015. Heart Disease and Stroke Statistics-2016 Update: A Report From the American Heart Association. *Circulation*.
- Munshi, N.V., 2012. Gene regulatory networks in cardiac conduction system development. *Circ Res* 110, 1525-1537.
- Murphy, R.T., Thaman, R., Blanes, J.G., Ward, D., Sevdalis, E., Papra, E., Kiotsekoglou, A., Tome, M.T., Pellerin, D., McKenna, W.J., Elliott, P.M., 2005. Natural history and familial characteristics of isolated left ventricular non-compaction. *European heart journal* 26, 187-192.
- Nam, J., Onitsuka, I., Hatch, J., Uchida, Y., Ray, S., Huang, S., Li, W., Zang, H., Ruiz-Lozano, P., Mukoyama, Y.-s., 2013. Coronary veins determine the pattern of sympathetic innervation in the developing heart. *Development* 140, 1475-1485.
- Neugebauer, J.M., Yost, H.J., 2014. FGF signaling is required for brain left-right asymmetry and brain midline formation. *Developmental biology* 386, 123-134.
- Neuhaus, H., Rosen, V., Thies, R.S., 1999. Heart specific expression of mouse BMP-10 a novel member of the TGF-beta superfamily. *Mech Dev* 80, 181-184.
- Nilsson, S., 2011. Comparative anatomy of the autonomic nervous system. *Autonomic neuroscience : basic & clinical* 165, 3-9.
- Ninov, N., Borius, M., Stainier, D.Y., 2012. Different levels of Notch signaling regulate quiescence, renewal and differentiation in pancreatic endocrine progenitors. *Development* 139, 1557-1567.
- Novodvorsky, P., Chico, T.J., 2014. The role of the transcription factor KLF2 in vascular development and disease. *Progress in molecular biology and translational science* 124, 155-188.
- Odiete, O., Hill, M.F., Sawyer, D.B., 2012. Neuregulin in cardiovascular development and disease. *Circ Res* 111, 1376-1385.
- Oechslin, E., Jenni, R., 2011. Left ventricular non-compaction revisited: a distinct phenotype with genetic heterogeneity? *European heart journal* 32, 1446-1456.
- Oechslin, E.N., Attenhofer Jost, C.H., Rojas, J.R., Kaufmann, P.A., Jenni, R., 2000. Long-term follow-up of 34 adults with isolated left ventricular noncompaction: a distinct cardiomyopathy with poor prognosis. *Journal of the American College of Cardiology* 36, 493-500.
- Olson, E.N., Srivastava, D., 1996. Molecular pathways controlling heart development. *Science (New York, N.Y.)* 272, 671-676.
- Palencia-Desai, S., Rost, M.S., Schumacher, J.A., Ton, Q.V., Craig, M.P., Baltrunaite, K., Koenig, A.L., Wang, J., Poss, K.D., Chi, N.C., Stainier, D.Y., Sumanas, S., 2015. Myocardium and BMP signaling are required for endocardial differentiation. *Development* 142, 2304-2315.
- Palermo, R., Checquolo, S., Bellavia, D., Talora, C., Screpanti, I., 2014. The molecular basis of notch signaling regulation: a complex simplicity. *Current molecular medicine* 14, 34-44.

- Palstra, A.P., Tudorache, C., Rovira, M., Brittijn, S.A., Burgerhout, E., van den Thillart, G.E., Spaink, H.P., Planas, J.V., 2010. Establishing zebrafish as a novel exercise model: swimming economy, swimming-enhanced growth and muscle growth marker gene expression. *PLoS one* 5, e14483.
- Parichy, D.M., Spiewak, J.E., 2015. Origins of adult pigmentation: diversity in pigment stem cell lineages and implications for pattern evolution. *Pigment cell & melanoma research* 28, 31-50.
- Parichy, D.M., Turner, J.M., Parker, N.B., 2003. Essential role for puma in development of postembryonic neural crest-derived cell lineages in zebrafish. *Developmental biology* 256, 221-241.
- Parker, S.E., Mai, C.T., Canfield, M.A., Rickard, R., Wang, Y., Meyer, R.E., Anderson, P., Mason, C.A., Collins, J.S., Kirby, R.S., Correa, A., 2010. Updated National Birth Prevalence estimates for selected birth defects in the United States, 2004-2006. *Birth defects research. Part A, Clinical and molecular teratology* 88, 1008-1016.
- Parsons, M.J., Pisharath, H., Yusuff, S., Moore, J.C., Siekmann, A.F., Lawson, N., Leach, S.D., 2009. Notch-responsive cells initiate the secondary transition in larval zebrafish pancreas. *Mech Develop* 126, 898-912.
- Paterick, T.E., Tajik, A.J., 2012. Left ventricular noncompaction: a diagnostically challenging cardiomyopathy. *Circulation journal : official journal of the Japanese Circulation Society* 76, 1556-1562.
- Patra, C., Diehl, F., Ferrazzi, F., van Amerongen, M.J., Novoyatleva, T., Schaefer, L., Muhlfeld, C., Jungblut, B., Engel, F.B., 2011. Nephronectin regulates atrioventricular canal differentiation via Bmp4-Has2 signaling in zebrafish. *Development* 138, 4499-4509.
- Patten, R.D., Hall-Porter, M.R., 2009. Small Animal Models of Heart Failure: Development of Novel Therapies, Past and Present. *Circulation: Heart Failure* 2, 138-144.
- Pedrique, S.P., Fazzari, P., 2010. Nrg1 reverse signaling in cortical pyramidal neurons. *The Journal of neuroscience : the official journal of the Society for Neuroscience* 30, 15005-15006.
- Pelster, B., Sanger, A.M., Siegele, M., Schwerte, T., 2003. Influence of swim training on cardiac activity, tissue capillarization, and mitochondrial density in muscle tissue of zebrafish larvae. *American journal of physiology. Regulatory, integrative and comparative physiology* 285, R339-347.
- Pennisi, D.J., Ballard, V.L., Mikawa, T., 2003. Epicardium is required for the full rate of myocyte proliferation and levels of expression of myocyte mitogenic factors FGF2 and its receptor, FGFR-1, but not for transmural myocardial patterning in the embryonic chick heart. *Developmental dynamics : an official publication of the American Association of Anatomists* 228, 161-172.
- Peralta, M., Gonzalez-Rosa, J.M., Marques, I.J., Mercader, N., 2014. The Epicardium in the Embryonic and Adult Zebrafish. *Journal of developmental biology* 2, 101-116.
- Peralta, M., Steed, E., Harlepp, S., Gonzalez-Rosa, J.M., Monduc, F., Ariza-Cosano, A., Cortes, A., Rayon, T., Gomez-Skarmeta, J.L., Zapata, A., Vermot, J., Mercader, N., 2013. Heartbeat-Driven Pericardial Fluid Forces Contribute to Epicardium Morphogenesis. *Curr Biol* 23, 1726-1735.
- Perlin, J.R., Lush, M.E., Stephens, W.Z., Piotrowski, T., Talbot, W.S., 2011. Neuronal Neuregulin 1 type III directs Schwann cell migration. *Development (Cambridge, England)* 138, 4639-4648.
- Perner, B., Englert, C., Bollig, F., 2007. The Wilms tumor genes wt1a and wt1b control different steps during formation of the zebrafish pronephros. *Developmental biology* 309, 87-96.

- Peshkovsky, C., Totong, R., Yelon, D., 2011. Dependence of cardiac trabeculation on neuregulin signaling and blood flow in zebrafish. *Developmental dynamics : an official publication of the American Association of Anatomists* 240, 446-456.
- Peters, F., Khandheria, B.K., dos Santos, C., Matioda, H., Maharaj, N., Libhaber, E., Mamdoo, F., Essop, M.R., 2012. Isolated left ventricular noncompaction in sub-Saharan Africa: a clinical and echocardiographic perspective. *Circulation. Cardiovascular imaging* 5, 187-193.
- Plaut, I.I., Gordon, M., 1994. SWIMMING METABOLISM OF WILD-TYPE AND CLONED ZEBRAFISH BRACHYDANIO RERIO. *The Journal of experimental biology* 194, 209-223.
- Plavicki, J.S., Hofsteen, P., Yue, M.S., Lanham, K.A., Peterson, R.E., Heideman, W., 2014. Multiple modes of proepicardial cell migration require heartbeat. *Bmc Dev Biol* 14.
- Polizzotti, B.D., Ganapathy, B., Walsh, S., Choudhury, S., Ammanamanchi, N., Bennett, D.G., dos Remedios, C.G., Haubner, B.J., Penninger, J.M., Kuhn, B., 2015. Neuregulin stimulation of cardiomyocyte regeneration in mice and human myocardium reveals a therapeutic window. *Science translational medicine* 7, 281ra245.
- Reed, B.N., Street, S.E., Jensen, B.C., 2014. Time and technology will tell: the pathophysiologic basis of neurohormonal modulation in heart failure. *Heart failure clinics* 10, 543-557.
- Rees, B.B., Sudradjat, F.A., Love, J.W., 2001. Acclimation to hypoxia increases survival time of zebrafish, *Danio rerio*, during lethal hypoxia. *The Journal of experimental zoology* 289, 266-272.
- Risebro, C.A., Riley, P.R., 2006. Formation of the ventricles. *TheScientificWorldJournal* 6, 1862-1880.
- Rohr, S., Otten, C., Abdellilah-Seyfried, S., 2008. Asymmetric involution of the myocardial field drives heart tube formation in zebrafish. *Circ Res* 102, E12-E19.
- Rossi, A., Kontarakis, Z., Gerri, C., Nolte, H., Holper, S., Kruger, M., Stainier, D.Y.R., 2015. Genetic compensation induced by deleterious mutations but not gene knockdowns. *Nature* 524, 230-233.
- Rothschild, S.C., Easley, C.A.t., Francescato, L., Lister, J.A., Garrity, D.M., Tombes, R.M., 2009. Tbx5-mediated expression of Ca(2+)/calmodulin-dependent protein kinase II is necessary for zebrafish cardiac and pectoral fin morphogenesis. *Developmental biology* 330, 175-184.
- Roy, S., 2012. Cilia and Hedgehog: when and how was their marriage solemnized? *Differentiation; research in biological diversity* 83, S43-48.
- Rupert, C.E., Coulombe, K.L., 2015. The roles of neuregulin-1 in cardiac development, homeostasis, and disease. *Biomarker insights* 10, 1-9.
- Ruzicka, L., Bradford, Y.M., Frazer, K., Howe, D.G., Paddock, H., Ramachandran, S., Singer, A., Toro, S., Van Slyke, C.E., Eagle, A.E., Fashena, D., Kalita, P., Knight, J., Mani, P., Martin, R., Moxon, S.A.T., Pich, C., Schaper, K., Shao, X., Westerfield, M., 2015. ZFIN, The zebrafish model organism database: Updates and new directions. *Genesis* 53, 498-509.
- Rychter, Z., Ostadal, B., 1971. Fate of "sinusoidal" intertrabecular spaces of the cardiac wall after development of the coronary vascular bed in chick embryo. *Folia morphologica* 19, 31-44.
- Sabaliauskas, N.A., Foutz, C.A., Mest, J.R., Budgeon, L.R., Sidor, A.T., Gershenson, J.A., Joshi, S.B., Cheng, K.C., 2006. High-throughput zebrafish histology. *Methods* 39, 246-254.

- Salvucci, O., Tosato, G., 2012. Essential roles of EphB receptors and EphrinB ligands in endothelial cell function and angiogenesis. *Advances in cancer research* 114, 21-57.
- Samsa, L.A., Fleming, N., Magness, S., Qian, L., Liu, J., 2016. Isolation and Characterization of Single Cells from Zebrafish Embryos. *Journal of visualized experiments : JoVE*.
- Samsa, L.A., Givens, C., Tzima, E., Stainier, D.Y., Qian, L., Liu, J., 2015. Cardiac contraction activates endocardial Notch signaling to modulate chamber maturation in zebrafish. *Development* 142, 4080-4091.
- Samsa, L.A., Yang, B., Liu, J., 2013. Embryonic cardiac chamber maturation: Trabeculation, conduction, and cardiomyocyte proliferation. *American journal of medical genetics. Part C, Seminars in medical genetics* 163C, 157-168.
- Sankova, B., Machalek, J., Sedmera, D., 2010. Effects of mechanical loading on early conduction system differentiation in the chick. *American journal of physiology. Heart and circulatory physiology* 298, H1571-1576.
- Sasai, N., Briscoe, J., 2012. Primary cilia and graded Sonic Hedgehog signaling. *Wiley interdisciplinary reviews. Developmental biology* 1, 753-772.
- Scheer, N., Campos-Ortega, J.A., 1999. Use of the Gal4-UAS technique for targeted gene expression in the zebrafish. *Mech Dev* 80, 153-158.
- Scheer, N., Groth, A., Hans, S., Campos-Ortega, J.A., 2001. An instructive function for Notch in promoting gliogenesis in the zebrafish retina. *Development* 128, 1099-1107.
- Scherz, P.J., Huiskens, J., Sahai-Hernandez, P., Stainier, D.Y.R., 2008. High-speed imaging of developing heart valves reveals interplay of morphogenesis and function. *Development* 135, 1179-1187.
- Schneider, C.A., Rasband, W.S., Eliceiri, K.W., 2012. NIH Image to ImageJ: 25 years of image analysis. *Nature methods* 9, 671-675.
- Schwerte, T., Prem, C., Mairosi, A., Pelster, B., 2006. Development of the sympatho-vagal balance in the cardiovascular system in zebrafish (*Danio rerio*) characterized by power spectrum and classical signal analysis. *The Journal of experimental biology* 209, 1093-1100.
- Sedmera, D., 2011. Function and form in the developing cardiovascular system. *Cardiovascular research* 91, 252-259.
- Sedmera, D., Pexieder, T., Rychterova, V., Hu, N., Clark, E.B., 1999. Remodeling of chick embryonic ventricular myoarchitecture under experimentally changed loading conditions. *The Anatomical record* 254, 238-252.
- Sedmera, D., Pexieder, T., Vuillemin, M., Thompson, R.P., Anderson, R.H., 2000. Developmental patterning of the myocardium. *The Anatomical record* 258, 319-337.
- Sedmera, D., Thomas, P.S., 1996. Trabeculation in the embryonic heart. *BioEssays : news and reviews in molecular, cellular and developmental biology* 18, 607.
- Sedmera, D., Thompson, R.P., 2011. Myocyte proliferation in the developing heart. *Developmental dynamics : an official publication of the American Association of Anatomists* 240, 1322-1334.
- Sehnert, A.J., Huq, A., Weinstein, B.M., Walker, C., Fishman, M., Stainier, D.Y., 2002. Cardiac troponin T is essential in sarcomere assembly and cardiac contractility. *Nature genetics* 31, 106-110.

- Serluca, F.C., 2008. Development of the proepicardial organ in the zebrafish. *Developmental biology* 315, 18-27.
- Shojaei, S., Tafazzoli-Shahdpour, M., Shokrgozar, M.A., Haghighipour, N., 2015. Comparative analysis of effects of cyclic uniaxial and equiaxial stretches on gene expression of human umbilical vein endothelial cells. *Cell biology international* 39, 741-749.
- Singleman, C., Holtzman, N.G., 2012. Analysis of postembryonic heart development and maturation in the zebrafish, *Danio rerio*. *Developmental dynamics : an official publication of the American Association of Anatomists* 241, 1993-2004.
- Slough, J., Cooney, L., Brueckner, M., 2008. Monocilia in the embryonic mouse heart suggest a direct role for cilia in cardiac morphogenesis. *Developmental dynamics : an official publication of the American Association of Anatomists* 237, 2304-2314.
- Sorescu, G.P., Song, H., Tressel, S.L., Hwang, J., Dikalov, S., Smith, D.A., Boyd, N.L., Platt, M.O., Lassegue, B., Griending, K.K., Jo, H., 2004. Bone morphogenic protein 4 produced in endothelial cells by oscillatory shear stress induces monocyte adhesion by stimulating reactive oxygen species production from a nox1-based NADPH oxidase. *Circ Res* 95, 773-779.
- Stainier, D.Y., Beis, D., Jungblut, B., Bartman, T., 2002. Endocardial cushion formation in zebrafish. *Cold Spring Harbor symposia on quantitative biology* 67, 49-56.
- Stainier, D.Y., Fouquet, B., Chen, J.N., Warren, K.S., Weinstein, B.M., Meiler, S.E., Mohideen, M.A., Neuhauss, S.C., Solnica-Krezel, L., Schier, A.F., Zwartkruis, F., Stemple, D.L., Malicki, J., Driever, W., Fishman, M.C., 1996. Mutations affecting the formation and function of the cardiovascular system in the zebrafish embryo. *Development* 123, 285-292.
- Stainier, D.Y., Lee, R.K., Fishman, M.C., 1993. Cardiovascular development in the zebrafish. I. Myocardial fate map and heart tube formation. *Development* 119, 31-40.
- Stainier, D.Y., Weinstein, B.M., Detrich, H.W., 3rd, Zon, L.I., Fishman, M.C., 1995. Cloche, an early acting zebrafish gene, is required by both the endothelial and hematopoietic lineages. *Development* 121, 3141-3150.
- Stankunas, K., Hang, C.T., Tsun, Z.Y., Chen, H., Lee, N.V., Wu, J.I., Shang, C., Bayle, J.H., Shou, W., Iruela-Arispe, M.L., Chang, C.P., 2008. Endocardial Brg1 represses ADAMTS1 to maintain the microenvironment for myocardial morphogenesis. *Dev Cell* 14, 298-311.
- Stanton, B.Z., Peng, L.F., 2010. Small-molecule modulators of the Sonic Hedgehog signaling pathway. *Molecular bioSystems* 6, 44-54.
- Stanton, C., Bruce, C., Connolly, H., Brady, P., Syed, I., Hodge, D., Asirvatham, S., Friedman, P., 2009. Isolated left ventricular noncompaction syndrome. *The American journal of cardiology* 104, 1135-1138.
- Staudt, D., Stainier, D., 2012. Uncovering the molecular and cellular mechanisms of heart development using the zebrafish. *Annual review of genetics* 46, 397-418.
- Staudt, D.W., Liu, J.D., Thorn, K.S., Stuurman, N., Liebling, M., Stainier, D.Y.R., 2014. High-resolution imaging of cardiomyocyte behavior reveals two distinct steps in ventricular trabeculation. *Development* 141, 585-593.
- Stewart, A.M., Gerlai, R., Kalueff, A.V., 2015. Developing high-throughput zebrafish screens for in-vivo CNS drug discovery. *Frontiers in behavioral neuroscience* 9, 14.

- Stollberger, C., Finsterer, J., 2004. Left ventricular hypertrabeculation/noncompaction. *Journal of the American Society of Echocardiography : official publication of the American Society of Echocardiography* 17, 91-100.
- Stoyek, M.R., Croll, R.P., Smith, F.M., 2015. Intrinsic and extrinsic innervation of the heart in zebrafish (*Danio rerio*). *The Journal of comparative neurology* 523, 1683-1700.
- Strecker, R., Seiler, T.B., Hollert, H., Braunbeck, T., 2011. Oxygen requirements of zebrafish (*Danio rerio*) embryos in embryo toxicity tests with environmental samples. *Comp Biochem Phys C* 153, 318-327.
- Stuckmann, I., Evans, S., Lassar, A.B., 2003. Erythropoietin and retinoic acid, secreted from the epicardium, are required for cardiac myocyte proliferation. *Developmental biology* 255, 334-349.
- Sucov, H.M., Dyson, E., Gumeringer, C.L., Price, J., Chien, K.R., Evans, R.M., 1994. RXR alpha mutant mice establish a genetic basis for vitamin A signaling in heart morphogenesis. *Gene Dev* 8, 1007-1018.
- Sweet, D.T., Chen, Z., Givens, C.S., Owens, A.P., 3rd, Rojas, M., Tzima, E., 2013. Endothelial Shc regulates arteriogenesis through dual control of arterial specification and inflammation via the notch and nuclear factor-kappa-light-chain-enhancer of activated B-cell pathways. *Circ Res* 113, 32-39.
- Sweet, D.T., Chen, Z., Wiley, D.M., Bautch, V.L., Tzima, E., 2012. The adaptor protein Shc integrates growth factor and ECM signaling during postnatal angiogenesis. *Blood* 119, 1946-1955.
- Tahkola, J., Rasanen, J., Sund, M., Makikallio, K., Autio-Harmainen, H., Pihlajaniemi, T., 2008. Cardiac dysfunction in transgenic mouse fetuses overexpressing shortened type XIII collagen. *Cell and tissue research* 333, 61-69.
- Takebayashi-Suzuki, K., Yanagisawa, M., Gourdie, R.G., Kanzawa, N., Mikawa, T., 2000. In vivo induction of cardiac Purkinje fiber differentiation by coexpression of preproendothelin-1 and endothelin converting enzyme-1. *Development* 127, 3523-3532.
- Teekakirikul, P., Kelly, M.A., Rehm, H.L., Lakdawala, N.K., Funke, B.H., 2013. Inherited cardiomyopathies: molecular genetics and clinical genetic testing in the postgenomic era. *The Journal of molecular diagnostics : JMD* 15, 158-170.
- Thavendiranathan, P., Dahiya, A., Phelan, D., Desai, M.Y., Tang, W.H., 2013. Isolated left ventricular non-compaction controversies in diagnostic criteria, adverse outcomes and management. *Heart (British Cardiac Society)* 99, 681-689.
- Tian, Y., Morrisey, E.E., 2012. Importance of myocyte-nonmyocyte interactions in cardiac development and disease. *Circ Res* 110, 1023-1034.
- Timmerman, L.A., Grego-Bessa, J., Raya, A., Bertran, E., Perez-Pomares, J.M., Diez, J., Aranda, S., Palomo, S., McCormick, F., Izpisua-Belmonte, J.C., de la Pompa, J.L., 2004. Notch promotes epithelial-mesenchymal transition during cardiac development and oncogenic transformation. *Gene Dev* 18, 99-115.
- Toyofuku, T., Zhang, H., Kumanogoh, A., Takegahara, N., Suto, F., Kamei, J., Aoki, K., Yabuki, M., Hori, M., Fujisawa, H., Kikutani, H., 2004a. Dual roles of Sema6D in cardiac morphogenesis through region-specific association of its receptor, Plexin-A1, with off-track and vascular endothelial growth factor receptor type 2. *Gene Dev* 18, 435-447.

- Toyofuku, T., Zhang, H., Kumanogoh, A., Takegahara, N., Yabuki, M., Harada, K., Hori, M., Kikutani, H., 2004b. Guidance of myocardial patterning in cardiac development by *Sema6D* reverse signalling. *Nat Cell Biol* 6, 1204-1211.
- Trinh, L.A., Stainier, D.Y.R., 2004. Fibronectin regulates epithelial organization during myocardial migration in zebrafish. *Dev Cell* 6, 371-382.
- Tsao-Wu, G.S., Weber, C.H., Budgeon, L.R., Cheng, K.C., 1998. Agarose-embedded tissue arrays for histologic and genetic analysis. *BioTechniques* 25, 614-618.
- Tsujikawa, M., Malicki, J., 2004. Intraflagellar transport genes are essential for differentiation and survival of vertebrate sensory neurons. *Neuron* 42, 703-716.
- Uyttendaele, H., Marazzi, G., Wu, G., Yan, Q., Sassoon, D., Kitajewski, J., 1996. *Notch4/int-3*, a mammary proto-oncogene, is an endothelial cell-specific mammalian Notch gene. *Development* 122, 2251-2259.
- Van der Heiden, K., Egorova, A.D., Poelmann, R.E., Wentzel, J.J., Hierck, B.P., 2011. Role for primary cilia as flow detectors in the cardiovascular system. *International review of cell and molecular biology* 290, 87-119.
- Van der Heiden, K., Groenendijk, B.C., Hierck, B.P., Hogers, B., Koerten, H.K., Mommaas, A.M., Gittenberger-de Groot, A.C., Poelmann, R.E., 2006. Monocilia on chicken embryonic endocardium in low shear stress areas. *Developmental dynamics : an official publication of the American Association of Anatomists* 235, 19-28.
- van Eeden, F.J., Granato, M., Schach, U., Brand, M., Furutani-Seiki, M., Haffter, P., Hammerschmidt, M., Heisenberg, C.P., Jiang, Y.J., Kane, D.A., Kelsh, R.N., Mullins, M.C., Odenthal, J., Warga, R.M., Allende, M.L., Weinberg, E.S., Nusslein-Volhard, C., 1996. Mutations affecting somite formation and patterning in the zebrafish, *Danio rerio*. *Development* 123, 153-164.
- Vasti, C., Hertig, C.M., 2014. Neuregulin-1/erbB activities with focus on the susceptibility of the heart to anthracyclines. *World journal of cardiology* 6, 653-662.
- Vermot, J., Forouhar, A.S., Liebling, M., Wu, D., Plummer, D., Gharib, M., Fraser, S.E., 2009. Reversing blood flows act through *klf2a* to ensure normal valvulogenesis in the developing heart. *Plos Biol* 7, e1000246.
- Vos, T., Barber, R.M., Bell, B., Bertozzi-Villa, A., Biryukov, S., Bolliger, I., Charlson, F., Davis, A., Degenhardt, L., Dicker, D., Duan, L., Erskine, H., Feigin, V.L., Ferrari, A.J., Fitzmaurice, C., Fleming, T., Graetz, N., Guinovart, C., Haagsma, J., Hansen, G.M., et al., 2015. Global, regional, and national incidence, prevalence, and years lived with disability for 301 acute and chronic diseases and injuries in 188 countries, 1990-2013: a systematic analysis for the Global Burden of Disease Study 2013. *Lancet* 386, 743-800.
- Wagner, M., Siddiqui, M.A., 2007. Signal transduction in early heart development (II): ventricular chamber specification, trabeculation, and heart valve formation. *Experimental biology and medicine (Maywood, N.J.)* 232, 866-880.
- Wang, C., Baker, B.M., Chen, C.S., Schwartz, M.A., 2013. Endothelial cell sensing of flow direction. *Arteriosclerosis, thrombosis, and vascular biology* 33, 2130-2136.
- Wang, H., Zang, C., Liu, X.S., Aster, J.C., 2015. The role of Notch receptors in transcriptional regulation. *Journal of cellular physiology* 230, 982-988.

- Wang, H.U., Chen, Z.F., Anderson, D.J., 1998. Molecular distinction and angiogenic interaction between embryonic arteries and veins revealed by ephrin-B2 and its receptor Eph-B4. *Cell* 93, 741-753.
- Wang, Y., Nakayama, M., Pitulescu, M.E., Schmidt, T.S., Bochenek, M.L., Sakakibara, A., Adams, S., Davy, A., Deutsch, U., Luthi, U., Barberis, A., Benjamin, L.E., Makinen, T., Nobes, C.D., Adams, R.H., 2010. Ephrin-B2 controls VEGF-induced angiogenesis and lymphangiogenesis. *Nature* 465, 483-486.
- Weiford, B.C., Subbarao, V.D., Mulhern, K.M., 2004. Noncompaction of the ventricular myocardium. *Circulation* 109, 2965-2971.
- Wessels, A., Sedmera, D., 2003. Developmental anatomy of the heart: a tale of mice and man. *Physiological genomics* 15, 165-176.
- Westerfield, M., 2000. The zebrafish book. A guide for the laboratory use of zebrafish (*Danio rerio*), 4th ed. ed. Univ. of Oregon Press, Eugene.
- Wilson, C.W., Stainier, D.Y., 2010. Vertebrate Hedgehog signaling: cilia rule. *BMC biology* 8, 102.
- Wilson, J.G., Roth, C.B., Warkany, J., 1953. An analysis of the syndrome of malformations induced by maternal vitamin A deficiency. Effects of restoration of vitamin A at various times during gestation. *The American journal of anatomy* 92, 189-217.
- Wilson, J.G., Warkany, J., 1949. Aortic-arch and cardiac anomalies in the offspring of vitamin A deficient rats. *The American journal of anatomy* 85, 113-155.
- Xiao, J., Li, B., Zheng, Z., Wang, M., Peng, J., Li, Y., Li, Z., 2012. Therapeutic effects of neuregulin-1 gene transduction in rats with myocardial infarction. *Coronary artery disease* 23, 460-468.
- Yang, J., Bucker, S., Jungblut, B., Bottger, T., Cinnamon, Y., Tchorz, J., Muller, M., Bettler, B., Harvey, R., Sun, Q.Y., Schneider, A., Braun, T., 2012. Inhibition of Notch2 by Numb/Numbl-like controls myocardial compaction in the heart. *Cardiovascular research* 96, 276-285.
- Yang, J., Hartjes, K.A., Nelson, T.J., Xu, X., 2014. Cessation of contraction induces cardiomyocyte remodeling during zebrafish cardiogenesis. *American journal of physiology. Heart and circulatory physiology* 306, H382-395.
- Yang, J.T., Rayburn, H., Hynes, R.O., 1995. Cell adhesion events mediated by alpha 4 integrins are essential in placental and cardiac development. *Development* 121, 549-560.
- Yarden, Y., Sliwkowski, M.X., 2001. Untangling the ErbB signalling network. *Nature reviews. Molecular cell biology* 2, 127-137.
- Yelon, D., 2001. Cardiac patterning and morphogenesis in zebrafish. *Developmental dynamics : an official publication of the American Association of Anatomists* 222, 552-563.
- Yelon, D., Horne, S.A., Stainier, D.Y., 1999. Restricted expression of cardiac myosin genes reveals regulated aspects of heart tube assembly in zebrafish. *Developmental biology* 214, 23-37.
- Yokozeki, T., Wakatsuki, S., Hatsuzawa, K., Black, R.A., Wada, I., Sehara-Fujisawa, A., 2007. Meltrin beta (ADAM19) mediates ectodomain shedding of Neuregulin beta1 in the Golgi apparatus: fluorescence correlation spectroscopic observation of the dynamics of ectodomain shedding in living cells. *Genes to cells : devoted to molecular & cellular mechanisms* 12, 329-343.

- Yoshida, S., Shiratori, H., Kuo, I.Y., Kawasumi, A., Shinohara, K., Nonaka, S., Asai, Y., Sasaki, G., Belo, J.A., Sasaki, H., Nakai, J., Dworniczak, B., Ehrlich, B.E., Pennekamp, P., Hamada, H., 2012. Cilia at the node of mouse embryos sense fluid flow for left-right determination via Pkd2. *Science (New York, N.Y.)* 338, 226-231.
- Yozzo, K.L., Isales, G.M., Raftery, T.D., Volz, D.C., 2013. High-Content Screening Assay for Identification of Chemicals Impacting Cardiovascular Function in Zebrafish Embryos. *Environ Sci Technol* 47, 11302-11310.
- Yutzey, K.E., 2015. Regenerative biology: Neuregulin 1 makes heart muscle. *Nature* 520, 445-446.
- Zhang, W., Chen, H., Wang, Y., Yong, W., Zhu, W., Liu, Y., Wagner, G.R., Payne, R.M., Field, L.J., Xin, H., Cai, C.L., Shou, W., 2011. Tbx20 transcription factor is a downstream mediator for bone morphogenetic protein-10 in regulating cardiac ventricular wall development and function. *The Journal of biological chemistry* 286, 36820-36829.
- Zhou, B., von Gise, A., Ma, Q., Rivera-Feliciano, J., Pu, W.T., 2008a. Nkx2-5- and Isl1-expressing cardiac progenitors contribute to proepicardium. *Biochem Biophys Res Commun* 375, 450-453.
- Zhou, Y., Cashman, T.J., Nevis, K.R., Obregon, P., Carney, S.A., Liu, Y., Gu, A., Mosimann, C., Sondalle, S., Peterson, R.E., Heideman, W., Burns, C.E., Burns, C.G., 2011. Latent TGF-beta binding protein 3 identifies a second heart field in zebrafish. *Nature* 474, 645-648.
- Zhou, Y., Gunput, R.A., Pasterkamp, R.J., 2008b. Semaphorin signaling: progress made and promises ahead. *Trends in biochemical sciences* 33, 161-170.